University of Southampton Research Repository
Copyright © and Moral Rights for this thesis and, where applicable, any accompanying data are retained by the author and/or other copyright owners. A copy can be downloaded for personal non-commercial research or study, without prior permission or charge. This thesis and the accompanying data cannot be reproduced or quoted extensively from without first obtaining permission in writing from the copyright holder/s. The content of the thesis and accompanying research data (where applicable) must not be changed in any way or sold commercially in any format or medium without the formal permission of the copyright holder/s.
When referring to this thesis and any accompanying data, full bibliographic details must be given, e.g.
When referring to this thesis and any accompanying data, full bibliographic details must be given, e.g.
Thesis: Author (Year of Submission) "Full thesis title", University of Southampton, name of the University Faculty or School or Department, PhD Thesis, pagination.
Data: Author (Year) Title. URI [dataset]

University of Southampton

Faculty of Environment and Life Sciences

School of Biological Sciences

The Interaction between Plants and Rhizosphere Microbes

by

Pengrui Cai

ORCID ID 0009-0002-3204-2304

Thesis for the degree of Doctor of Philosophy

June 2025

University of Southampton

Abstract

Faculty of Environment and Life Sciences

School of Biological Sciences

Doctor of Philosophy

The Interaction between Plants and Rhizosphere Microbes

by

Pengrui Cai

Specific crops, such as wheat, maize and rice are among the most important crops globally. There are numerous varieties, for example *Triticum aestivum*, is the common wheat that is widely cultivated globally and has more than 20,000 known varieties. Phosphorus and nitrogen fertilisers are commonly used to improve crop yield; however, it is costly and inefficient and can damage the environment. In this circumstance, bio-fertilisers shadow a new future direction for us, which utilise the beneficial relationship between the plants and the microorganisms in the soil. A better understanding of their interaction would give the foundation of sustainable agriculture in the future.

This work investigates the growth and activity of rhizosphere microorganisms. The first results chapter examined the effects of the arbuscular mycorrhizal (AM) fungus *Rhizophagus irregularis* on the hyphosphere microbial community. The relative abundance of fungi (Ascomycota, Basidiomycota, Mucoromycota) was lower in inoculated samples compared to uninoculated controls, suggesting potential competition or inhibition by the AM fungus. The supplementation with nutrients increased hyphae numbers overall, but samples inoculated with *R. irregularis* still had lower hyphae numbers compared to uninoculated controls. Bacterial communities also showed selective enrichment of certain taxa like Alphaproteobacteria and Gammaproteobacteria. Overall, the study highlighted the complex interactions between AM fungi, bacteria, and fungi in the hyphosphere.

The second chapter explored the effects of natural and artificial root exudates on soil bacterial communities. Natural exudates from wheat, sorghum, and chicory shaped distinct microbial profiles compared to artificial exudates. Artificial exudates had dose-dependent impacts, particularly enriching taxa from the phyla Actinobacteria, Firmicutes, and Proteobacteria, with Actinobacteria being most consistently responsive. Enrichment patterns were often treatment-specific across different artificial exudate formulations. The study also revealed that volatile organic compounds (VOCs) produced by soils treated with artificial exudates influenced recipient soil communities. While patterns were less structured, volatiles from lower exudate concentrations produced more consistent changes in ASV abundance.

Work presented in the final chapter isolated and characterised bacteria from different soils and media, assessing their plant growth-promoting traits like phosphate solubilisation and indole-3-acetic acid production. Bacteria from minimal media exhibited greater plant growth promotion abilities compared to those from nutrient-rich media when tested on *Arabidopsis*. Whole genome sequencing revealed the phylogenetic diversity of the isolates, with certain clades like *Streptomyces* and *Mesorhizobium* showing consistent plant growth-promoting effects.

Overall, this research provides insights into the complex interactions between plants, fungi, and bacteria in soil, highlighting the potential of harnessing these relationships to improve plant growth and soil health for sustainable agriculture.

Table of contents

Abstract 2
List of Figures 7
List of Tables 18
Research Thesis: Declaration of Authorship 20
Acknowledgements 21
Definitions and Abbreviations 22
Chapter 1 General introduction 25
1.1 Introduction to crops 25
1.2 Nutrients in soil 27
1.2.1 Macronutrients 27
1.2.2 Micronutrients 28
1.2.3 How do these nutrients get into the soil 28
1.2.4 How plants acquire nutrients from soil 29
1.3 The rhizosphere and microbes 31
1.3.1 Microbes in soil 31
1.3.2 The rhizosphere 31
1.3.3 Rhizosphere microorganisms 32
1.3.4 The mycorrhizal & plant growth-promoting fungi 33
1.3.5 The rhizobacteria 36
1.3.6 The hyphosphere 41
1.4 Phosphorus solubilisation by microbes 44
1.4.1 Inorganic P solubilisation 44
1.4.2 Organic P solubilisation 46
1.5 Nitrogen fixation by microbes 48
1.6 Overview and aims of the thesis 54
Chapter 2 The effects of arbuscular mycorrhizal fungi on the hyphosphere microbial community 57
Abstract 57
2.1 Introduction 58
2.2 Objectives 62
2.3 Materials and methods 63
2.3.1 Experimental setup for growth of wheat and inoculation with *Rhizophagus irregularis* 63
2.3.2 Further study of the inoculation impacts of *R. irregularis* 70

2.3.3 Competition experiment 73
2.3.4 Effects of inoculation and nutrient on soil communities 74
2.3.5 DNA sequence analysis for repeated experiments 76
2.4 Results 77
2.4.1 Principal component analysis (PCA) 78
2.4.2 Heatmap representation of the relative abundance 84
2.4.3 Hyphae counting 92
2.4.4 Competition experiment 93
2.4.5 Effects of inoculation and nutrient on soil communities 95
2.5 Discussion 99
Chapter 3 Effect of root exudates on microbial growth in soil 105
Abstract 105
3.1 Introduction 106
3.1.1 Root exudates and the rhizosphere 106
3.1.2 The soil microbial communities 106
3.1.3 Plant root exudates: wheat, sorghum, and chicory 107
3.1.4 Natural vs. artificial exudates 109
3.1.5 Volatile Organic Compounds (VOCs) produced by soil microbes 110
3.2 Objectives 111
3.3 Materials and methods 111
3.3.1 Plant growth 111
3.3.2 Extraction of root exudates 112
3.3.3 Preparation of natural exudates (wheat, sorghum and chicory) 113
3.3.4 Preparation of artificial exudates 113
3.3.5 Application of exudates to the soil 114
3.3.6 Volatile organic compound (VOC) production 114
3.3.7 DNA sequencing of 16S rRNA genes 115
3.3.8 Data analysis 116
3.4 Results 117
3.4.1 Effects of artificial exudates (AE, AEM & ACM) 117
3.4.2 Effects of natural exudates 125
3.4.3 Effects of volatiles 132
3.5 Discussion 135
3.5.1 Dose-dependent effects of artificial exudates 136
3.5.2 Effects of MBOA 137
3.5.3 Effects of natural exudates 139

3.5.4 Effects of VOCs 140
3.5.5 Conclusions 142
3.5.6 Future directions 143
Chapter 4 Isolation, identification, characterisation of plant growth-promoting bacteria and their impacts on *Arabidopsis thaliana* growth 145
Abstract 145
4.1 Introduction 146
4.1.1 Background 146
4.1.2 Selection of culture medium 147
4.1.3 Selection of soil samples 148
4.1.4 Aims & objectives 148
4.2 Materials and methods 149
4.2.1 Construction of biobank 149
4.2.2 Phosphorus solubilisation assay of the isolates 151
4.2.3 Screening and quantification of Indole-3-acetic Acid (IAA) from isolates using Salkowski reagent 151
4.2.4 Bacterial plant growth promotion assay 152
4.2.5 Whole genome sequencing (WGS) of isolates 153
4.2.6 Data analysis 154
4.3 Results 155
4.3.1 Isolation of bacteria 155
4.3.2 Phosphate solubilisation assay 156
4.3.3 Colorimetric assay to detect the IAA using Salkowski reagent 158
4.3.4 Plant growth promotion assay 160
4.3.5 Classification of isolates 163
4.4 Discussion 168
4.4.1 Summary of findings 168
4.4.2 Effects of different media in isolating PGPB 169
4.4.3 Impacts on *Arabidopsis thaliana* growth 169
4.4.4 Co-existing effects of bacteria 171
4.4.5 Limitations and future directions 172
Chapter 5 General Discussion 175
5.1 Microbial interactions in the rhizosphere: bacteria, fungi, and root exudates 175
5.2 Microbial Consortia 177
5.3 Microbial community network modelling: towards precision agriculture 178
5.4 Concluding remarks 179

Appendix 180
References 205

List of Figures

Figure 1.1 Average yield (metric tons per hectare) (a) and production (million metric tons) (b) of wheat and rice. Modified according to USDA (2021). 26

Figure 1.2. Plate A: Phosphate solubilisation zone on Pikovskaya plates produced by Aspergillus. Plate B(a): Penicillium (1000x magnification), Plate B(b): P solubilisation zone of Penicillium. Figure from Khan et al. (2010). 34

Figure 1.3. Mechanisms in plant growth carried out by phosphate-solubilising fungi. Figure from Khan et al. (2010). 36

Figure 1.4. Direct and indirect mechanisms of plant growth promotion by plant growth-promoting rhizobacteria (PGPR). 40

Figure 1.5 Diagram of rhizosphere, mycorrhizosphere and hyphosphere. Figure from Wang (2014). 43

Figure 1.6. Mechanisms of solubilisation/mineralisation of insoluble soil P by PSM. 48

Figure 1.7 The process of nodulation. (a) Rhizobia attach to root cells. (b) Rhizobia excrete nodulation factors, which causes root hair curl. (c) Rhizobia penetrate root hair and infect/penetrate the cortical cells and form the bacteroid state, thus, nodules are formed. Figure from Ahemad and Kibret (2014). 49

Figure 1.8 Nif genes of Klebsiella pneumoniae. The genes which encode the component proteins of nitrogenase, nifDKH, are highlighted on the left. All the genes are colour coded based on their function in the nitrogen fixation process. Figure from Rubio and Ludden (2008). 53

Figure 1.9 Conceptual overview of the thesis. Wheat plants (top) interact with mycorrhizal fungi (left), which influences the hyphosphere community (bottom); these effects are explored in Chapter 2. The wheat plants, through release of exudates, can also influence the diversity of microbes in the rhizosphere, which is investigated in Chapter 3. Among these organisms are plant growth-promoting bacteria (PGPB), which can be cultivated (image right, and performed in Chapter 4). PGPB can be inoculated into soil systems, which may result in either successful or unsuccessful establishment partly because of the microbiome interactions investigated in Chapters 2 and 3. Long-term goals will be to inoculate the PGPB isolated in this study into crop systems to investigate their interaction with microbiomes and ability to promote crop health. Figure was made using Biorender. 56

Figure 2.1 A CAD rendering of the growth chamber design (a), the final fabricated version (b), a single chamber assembly in the experiment (c). From Keyes et al. (2022). 65

Figure 2.2 Side view of the root and hyphal chamber assembly (only the side-arm hyphal chamber in d1 position is shown here as example). d = the height of the side-arm centroid from the top of the root chamber, h = the distance in the hyphal chamber, away from the barrier mesh. ROI (Region of Interest) refers to the specific area within the side chamber from which soil samples were collected for sequencing. From Keyes et al. (2022). 65

Figure 2.3 Completed hyphal chambers with carrier tubes holding the glass-fibre wicks. Ready to be attached to the root chambers. From Keyes et al. (2022). 67

Figure 2.4 Adapted setup for growing wheat. 71

Figure 2.5 Staining of wheat roots. Left: inoculated. Right: uninoculated. Observed under 80x magnification. 78

Figure 2.6 Stacked bar chart showing the relative abundance of bacterial phyla across different treatment groups. Only taxa with >1% relative abundance are shown; taxa with <1% relative abundance are grouped into “Other”. T = inoculated with *R. irregularis*, C = uninoculated, with P = with phosphorus addition, without P = without phosphorus addition. Original soil = untreated natural soil. 80

Figure 2.7 Principal component analysis (PCA) plot of samples from 16S (a)/18S (b) rRNA sequencing. Different colours (inner fill) denote whether the samples were inoculated with R. irregularis or not. The shapes of the dots (i.e., square, circle) represent the time point: 2 weeks or 4 weeks. The colours of the borders indicate whether phosphorus was added. Note: One inoculated P+ sample was excluded from the 18S analysis due to low read count and missing ASVs, suggesting sequencing failure. 82

Figure 2.8 Principal component analysis (PCA) plot of samples from 16S (a,b)/18S (c,d) rRNA sequencing. Different colours (inner fill) denote whether the samples were inoculated with R. irregularis or not. The shapes of the dots (i.e., square, circle) represent the time point: 2 weeks or 4 weeks. Ellipses were drawn based on 95% confidence interval. (a) & (c): P+. (b) &(d): P−. Note: One inoculated P+ sample was excluded from the 18S analysis due to low read count and missing ASVs, suggesting sequencing failure. 83

Figure 2.9 Heatmap showing the relative abundance of ASVs (16S rRNA with P addition), selected by indicator species analysis ($p < 0.05$). Samples and ASVs are clustered by Manhattan distance. Cell colours represent row-normalised z-scores (–2 to 2), where 0 is the mean abundance across samples. Positive values indicate higher-than-average abundance; negative values indicate lower. The coloured sidebar on the left indicates the phylum assignment of each ASV. Abbreviations indicate: p=phylum, c=class, o=order, f=family, g=genus. 87

Figure 2.10 Heatmap showing the relative abundance of ASVs (16S rRNA without P addition), selected by indicator species analysis ($p < 0.05$). Samples and ASVs are clustered by Manhattan distance. Cell colours represent row-normalised z-scores (–2 to 2), where 0 is the mean abundance across samples. Positive values indicate higher-than-average abundance;negative values indicate lower. The coloured sidebar on the left indicates the phylum assignment of each ASV. Abbreviations indicate: p=phylum, c=class, o=order, f=family, g=genus. 88

Figure 2.11 Heatmap showing the relative abundance of ASVs (18S rRNA with P addition), selected by indicator species analysis ($p < 0.05$). Samples and ASVs are clustered by Manhattan distance. Cell colours represent row-normalised z-scores (–3 to 3), where 0 is the mean abundance across samples. Positive values indicate higher-than-average abundance;negative values indicate lower. The coloured sidebar on the left indicates the phylum assignment of each ASV. For simplicity, only ASVs belonging to Ascomycota, Basidiomycota, and Mucoromycota were explicitly labelled. Abbreviations indicate: p=phylum, c=class, o=order, f=family, g=genus. Note: One inoculated P+ sample was excluded from the 18S analysis due to low read count and missing ASVs, suggesting sequencing failure. 90

Figure 2.12 Heatmap showing the relative abundance ASVs (18S rRNA without P addition), selected by indicator species analysis ($p < 0.05$). Samples and ASVs are clustered by Manhattan distance. Cell colours represent row-normalised z-scores (–3 to 3), where 0 is the mean abundance across samples. Positive values indicate higher-than-average abundance;negative values indicate lower. The coloured sidebar on the left indicates the phylum assignment of each ASV. For simplicity, only ASVs belonging to Ascomycota, Basidiomycota, and Mucoromycota were explicitly labelled. Abbreviations indicate: p=phylum, c=class, o=order, f=family, g=genus. 92

Figure 2.13 Hyphae counting of different samples. Different letters indicate statistically significant differences (Tukey's Multiple Comparisons test, $p \leq 0.05$). Bars represent the mean values (n=3). Error bars represent the standard error of the mean (SEM)..... 93

Figure 2.14 Competition experiment. (a) Time series on hyphae counting to decide until when the hyphae numbers will reach a plateau. T0, T3, T6, T9: start day, day 3, day 6, day 9 of counting. Error bars represent the standard error of the mean (SEM; n = 3). (b): Hyphae count in the competition experiment. MS: Murashige & Skoog Modified Basal Medium with Gamborg Vitamins. All counting were done under 40x magnification. The y-axis represents the number of hyphae per gram of soil, and the x-axis categorises different nutrition conditions applied. Different colours indicate different treatment groups. Bars represent the mean values (n=3). Error bars represent the standard error of the mean (SEM). Different letters indicate statistically

significant differences based on two-way ANOVA followed by Tukey's Multiple Comparisons test ($p \leq 0.05$)..... 94

Figure 2.15 Principal Coordinates Analysis (PCoA) plots of microbial community composition based on 16S rRNA gene sequencing (left) and ITS sequencing (right), using Bray-Curtis dissimilarity matrices. Points represent individual samples, with colours indicating different sample groups..... 96

Figure 2.16 Venn diagrams comparing bacterial families associated with inoculated and uninoculated treatments under MS+/MS- and P+/P- conditions. Families were grouped based on indicator ASVs identified using indicator species analysis ($p < 0.05$) in 16S rRNA data. Each panel shows the number of shared and unique bacterial families between matching conditions: (a) Inoculated with P vs. Inoculated with MS; (b) Inoculated without P vs. Inoculated without MS; (c) Uninoculated with P vs. Uninoculated with MS; (d) Uninoculated without P vs. Uninoculated without MS..... 96

Figure 2.17 Venn diagrams comparing fungal families associated with inoculated and uninoculated treatments under MS+/MS- (ITS data) and P+/P- (18S data) conditions. Families were grouped based on fungal ASVs identified through indicator species analysis ($p < 0.05$), using the ITS dataset for MS+/MS- comparisons and the 18S rRNA dataset (fungal subset only) for P+/P- comparisons. Each panel shows the number of shared and unique fungal families between corresponding conditions: (a) Inoculated with P (18S) vs. Inoculated with MS (ITS); (b) Inoculated without P vs. Inoculated without MS; (c) Uninoculated with P vs. Uninoculated with MS; (d) Uninoculated without P vs. Uninoculated without MS. 97

Figure 2.18 Quantitative PCR (qPCR) analysis showing the 16S rRNA gene copy numbers across different sample groups. M: Murashige & Skoog Modified Basal Medium with Gamborg Vitamins. The y-axis represents the 16S rRNA gene copy number per gram of soil, and the x-axis categorises different nutrition conditions applied. I: inoculated, U: uninoculated, M-: without MS medium added, M+: with MS medium added. Different colours indicate different treatment groups. Bars represent the mean values (n=3), Error bars represent the standard error of the mean (SEM). Different letters indicate statistically significant differences (Tukey's Multiple Comparisons test, $p \leq 0.05$)..... 99

Figure 3.1 Root exudate collection process. a: hydroponic recovery; b: hydroponic collection; c: exudate collected in CellStar Falcon tubes. 113

Figure 3.2 Experimental setup for VOC producing. (a): Treatment. Three caps with more soil added were used for producing VOCs, the fourth cap served as recipient (b): Control. Soil was only added to recipient cap, the other 3 were filled with milli-Q water. 115

Figure 3.3 Principal Coordinates Analysis (PCoA) plots of microbial community composition based on 16S rRNA gene sequencing, using Bray-Curtis dissimilarity matrices. Points represent individual samples, with colours indicating different artificial exudate treatments. AE: artificial exudate only. AEM: AE+MBOA (MBOA diluted together with AE through the concentration gradients). ACM: AE+MBOA (MBOA in constant concentration; only AE diluted through the concentration gradients). 100, 60, 25, 8, 0: concentration gradients of AE (100%, 60%, 25%, 8%, and 0%). (a): PCoA of all artificial exudate treatments combined. (b): PCoA for AEM treatments only. (c): PCoA for ACM treatments only. (d): PCoA for AE treatments only. 118

Figure 3.4 Heatmap showing the relative abundance of ASVs across samples treated with artificial exudates (AE), selected by indicator species analysis ($p < 0.01$), comparing all AE treatments combined against the AE0 control. The ASVs shown were identified as indicators in the combined comparison and are present across all AE samples (excluding AE0), though their relative abundances vary between treatments. Rows (ASVs) are clustered by Manhattan distance. Cell colours represent row-normalised z-scores (–3 to 3), where 0 is the mean abundance across samples. Positive values indicate higher-than-average abundance; negative values indicate lower. The coloured sidebar on the left indicates the phylum assignment of each ASV; the top sidebar indicates different treatment concentrations. Abbreviations indicate: p=phylum, c=class, o=order, f=family, g=genus. 119

Figure 3.5 Heatmap showing the relative abundance of ASVs across samples treated with artificial exudates (ACM), selected by indicator species analysis ($p < 0.01$), comparing all ACM treatments combined against the ACM0 control. The ASVs shown were identified as indicators in the combined comparison and are present across all ACM samples (excluding ACM0), though their relative abundances vary between treatments. Rows (ASVs) are clustered by Manhattan distance. Cell colours represent row-normalised z-scores (–3 to 3), where 0 is the mean abundance across samples. Positive values indicate higher-than-average abundance; negative values indicate lower. The coloured sidebar on the left indicates the phylum assignment of each ASV; the top sidebar indicates different treatment concentrations. Abbreviations indicate: p=phylum, c=class, o=order, f=family, g=genus. 121

Figure 3.6 Heatmap showing the relative abundance of ASVs across samples treated with artificial exudates (AEM), selected by indicator species analysis ($p < 0.01$), comparing all AEM treatments combined against the AEM0 control. The ASVs shown were identified as indicators in the combined comparison and are present across all AEM samples (excluding AEM0), though their relative abundances vary between treatments. Rows (ASVs) are clustered by Manhattan distance. Cell colours represent row-normalised z-scores (–2 to 2), where 0 is the mean abundance across samples. Positive values indicate

higher-than-average abundance; negative values indicate lower. The coloured sidebar on the left indicates the phylum assignment of each ASV; the top sidebar indicates different treatment concentrations. Abbreviations indicate: p=phylum, c=class, o=order, f=family, g=genus. 123

Figure 3.7 Venn diagram showing the overlap of bacterial ASVs identified in the indicator species analysis in response to three artificial exudate treatments: AE, ACM, and AEM. The diagram illustrates the number of ASVs uniquely associated with each treatment, as well as those shared between two or all three treatments. 125

Figure 3.8 Principal Coordinates Analysis (PCoA) plots of microbial community composition based on 16S rRNA gene sequencing, using Bray-Curtis dissimilarity matrices. Points represent individual samples, with colours indicating different treatment groups of natural exudates. 126

Figure 3.9 Principal Coordinates Analysis (PCoA) plots comparing natural and artificial exudate microbial communities' composition based on 16S rRNA gene sequencing, using Bray-Curtis dissimilarity matrices. Points represent individual samples, with colours indicating different treatment groups of exudates. AE: artificial exudate only. 100,60,25,8,0: concentration gradients of AE: 100%, 60%, 25%, 8%, 0%. 127

Figure 3.10. Heatmap showing the relative abundance of ASVs across samples treated with natural root exudates from wheat, sorghum, and chicory. ASVs were selected by indicator species analysis ($p < 0.05$), using the three natural exudate treatments as distinct groups to identify ASVs significantly associated with each plant type. The heatmap also includes their relative abundance in AE0 and AE8 for reference. Rows (ASVs) are clustered by Manhattan distance. Cell colours represent row-normalised z-scores (–3 to 3), where 0 is the mean abundance across samples. Positive values indicate higher-than-average abundance; negative values indicate lower. The coloured sidebar on the left indicates the phylum assignment of each ASV; the top sidebar indicates different treatment concentrations and natural exudate types. Abbreviations indicate: p=phylum, c=class, o=order, f=family, g=genus..... 129

Figure 3.11 Heatmap showing the relative abundance of ASVs across samples treated with natural exudates, selected by indicator species analysis ($p < 0.01$), comparing all natural exudate treatments combined against the AE0 control. The ASVs shown were identified as indicators in the combined comparison and are present across all wheat, sorghum, and chicory samples, though their relative abundances vary between treatments. Rows (ASVs) are clustered by Manhattan distance. Cell colours represent row-normalised z-scores (–3 to 3), where 0 is the mean abundance across samples. Positive values indicate higher-than-average abundance; negative values indicate lower. The coloured sidebar on the left indicates the phylum assignment of

each ASV. Abbreviations indicate: p=phylum, c=class, o=order, f=family, g=genus. 130

Figure 3.12 Principal Coordinates Analysis (PCoA) plots of microbial community composition based on 16S rRNA gene sequencing, using Bray-Curtis dissimilarity matrices. Points represent individual samples, with colours indicating different treatments of soil to produce volatiles. 100,60,25,8,0: concentration gradients of AE: 100%, 60%, 25%, 8%, 0% added to soil to produce volatiles. VC refers to the control setup, in which only recipient soil was included. No VOC-producing soil was added; instead, Milli-Q water was applied to the empty caps to match the volume used in treatment conditions. VC samples were incubated under the same conditions as the treatments but kept in a separate box. 133

Figure 3.13 Heatmap showing the relative abundance of ASVs across recipient soil samples exposed to volatiles produced by soils treated with different concentrations of AE. ASVs were selected by indicator species analysis ($p < 0.01$), comparing all AV treatments combined against the VC control. The ASVs shown were identified as indicators in the combined comparison and are present across all AV samples (excluding VC), though their relative abundances vary between treatments. VC is the control with no volatiles produced. Rows (ASVs) are clustered by Manhattan distance. Cell colours represent row-normalised z-scores (–3 to 3), where 0 is the mean abundance across samples. Positive values indicate higher-than-average abundance; negative values indicate lower. The coloured sidebar on the left indicates the phylum assignment of each ASV; the top sidebar indicates the concentration used to treat the volatile-producing soil. Abbreviations indicate: p=phylum, c=class, o=order, f=family, g=genus. 134

Figure 4.1 Selection of isolates from different media. B, C and R stand for the locations from where the bacteria were isolated, Boxworth, Chilworth and Rosemaund, respectively. “-55”,”-70”: the isolates were obtained from VL55 or VL70 medium. 156

Figure 4.2 Results of P solubilisation assay. Halos were observed around bacteria that grew and solubilised the calcium phosphate in the medium (a, b). For bacteria that could not solubilise the calcium phosphate, no halos were found (c). 157

Figure 4.3 Results of colorimetric assay using Salkowski reagent. Error bars indicate standard error of the mean (SEM) calculated based on technical replicates (n=3). (a): IAA concentration of selected isolates from Vegitone medium. (b): IAA concentration of selected isolates from VL55 medium. (c): IAA concentration of selected isolates from VL70 medium. (d): An example of pink colour development in the colorimetric reaction. 159

Figure 4.4 The effects of the Vegitone bacteria inoculation on the root traits of the *Arabidopsis* seedlings in the plant growth promotion assay. (a) Total fresh weight, (b) primary root length, and (c) lateral root number were measured 14 days after inoculation. Bars represent the mean values (n=3), Error bars represent the standard error of the mean (SEM). Different letters indicate statistically significant differences (Tukey's Multiple Comparisons test, $p \leq 0.05$). 160

Figure 4.5 The effects of the VL55 bacteria inoculation on the root traits of the *Arabidopsis* seedlings in the plant growth promotion assay. (a) Total fresh weight, (b) primary root length, and (c) lateral root number were measured 14 days after inoculation. Bars represent the mean values (n=3), Error bars represent the standard error of the mean (SEM). Different letters indicate statistically significant differences (Tukey's Multiple Comparisons test, $p \leq 0.05$). 161

Figure 4.6 The effects of the VL70 bacteria inoculation on the root traits of the *Arabidopsis* seedlings in the plant growth promotion assay. (a) Total fresh weight, (b) primary root length, and (c) lateral root number were measured 14 days after inoculation. Bars represent the mean values (n=3), Error bars represent the standard error of the mean (SEM). Different letters indicate statistically significant differences (Tukey's Multiple Comparisons test, $p \leq 0.05$). 162

Figure 4.7 Phylogenetic tree of isolates and enrichments. The tree was built from 49 core, universal genes, using SpeciesTree - v2.2.0 within KBase. Organisms from this study are highlighted in yellow. Reference sequences of closely related organisms were selected from the public KBase genomes from RefSeq. The names of enrichments are indicated as "bins", whereas those names without "bin" are presumed to be pure cultures. The effect of the enrichments/isolates on Arabidopsis growth are indicated with circles (blue circle: positive effect relative to control ($p<0.05$); red circle: negative effect relative to the control ($p<0.05$); open circle: no effect). The medium used for cultivation is indicated with squares. 167

Figure S 1 Complete heatmap showing the relative abundance of ASVs (16S with P addition), selected by indicator species analysis ($p < 0.05$). Samples and ASVs are clustered by Manhattan distance. Cell colours represent row-normalised z-scores (–2 to 2), where 0 is the mean abundance across samples. Positive values indicate higher-than-average abundance; negative values indicate lower.The taxonomy of each ASV is labelled to the lowest level that could be obtained during the classification. Abbreviations indicate: k=kingdom, p=phylum, c=class, o=order, f=family, g=genus. 180

Figure S 2 Complete heatmap showing the relative abundance of ASVs (16S without P addition), selected by indicator species analysis ($p < 0.05$). Samples and ASVs are clustered by Manhattan distance. Cell colours represent row-normalised z-scores (–2 to 2), where 0 is the mean abundance across samples. Positive values indicate higher-than-average abundance; negative values indicate lower.The taxonomy of each ASV is labelled to the lowest level that could be obtained during the classification. Abbreviations indicate: k=kingdom, p=phylum, c=class, o=order, f=family, g=genus. 181

Figure S 3 Complete heatmap showing the relative abundance of ASVs (18S with P addition), selected by indicator species analysis ($p < 0.05$). Samples and ASVs are clustered by Manhattan distance. Cell colours represent row-normalised z-scores (–3 to 3), where 0 is the mean abundance across samples. Positive values indicate higher-than-average abundance;negative values indicate lower.The taxonomy of each ASV is labelled to the lowest level that could be obtained during the classification. Abbreviations indicate: k=kingdom, p=phylum, c=class, o=order, f=family, g=genus. Note: One inoculated P+ sample was excluded from the 18S analysis due to low read count and missing ASVs, suggesting sequencing failure. 183

Figure S 4 Complete heatmap showing the relative abundance of ASVs (18S without P addition), selected by indicator species analysis ($p < 0.05$). Samples and ASVs are clustered by Manhattan distance. Cell colours represent row-normalised z-scores (–3 to 3), where 0 is the mean abundance across samples. Positive values indicate higher-than-average abundance; negative values indicate lower.The taxonomy of each ASV is labelled to the lowest level that could be obtained during the classification. Abbreviations indicate: k=kingdom, p=phylum, c=class, o=order, f=family, g=genus. 185

Figure S5 Complete heatmap showing the relative abundance of ASVs across samples treated with artificial exudtes (AE), selected by indicator species analysis ($p < 0.01$), comparing all AE treatments combined against the AE0 control. The ASVs shown were identified as indicators in the combined comparison and are present across all AE samples (excluding AE0), though their relative abundances vary between treatments. Rows (ASVs) are clustered by Manhattan distance. Cell colours represent row-normalised z-scores (–3 to 3), where 0 is the mean abundance across samples. Positive values indicate higher-than-average abundance; negative values indicate lower. The top sidebar indicates different treatment concentrations. Abbreviations indicate: k=kingdom,p=phylum, c=class, o=order, f=family, g=genus. 186

Figure S6 Complete heatmap showing the relative abundance of ASVs across samples treated with artificial exudates (ACM), selected by indicator species analysis ($p < 0.01$), comparing all ACM treatments combined against the ACM0 control. The ASVs shown were identified as indicators in the combined

comparison and are present across all ACM samples (excluding ACM0), though their relative abundances vary between treatments. Rows (ASVs) are clustered by Manhattan distance. Cell colours represent row-normalised z-scores (–3 to 3), where 0 is the mean abundance across samples. Positive values indicate higher-than-average abundance; negative values indicate lower. The top sidebar indicates different treatment concentrations. Abbreviations indicate: k=kingdom,p=phylum, c=class, o=order, f=family, g=genus. 187

Figure S7 Complete heatmap showing the relative abundance of ASVs across samples treated with artificial exudates (AEM), selected by indicator species analysis ($p < 0.01$), comparing all AEM treatments combined against the AEM0 control. The ASVs shown were identified as indicators in the combined comparison and are present across all AEM samples (excluding AEM0), though their relative abundances vary between treatments. Rows (ASVs) are clustered by Manhattan distance. Cell colours represent row-normalised z-scores (–2 to 2), where 0 is the mean abundance across samples. Positive values indicate higher-than-average abundance; negative values indicate lower. The top sidebar indicates different treatment concentrations. Abbreviations indicate: k=kingdom, p=phylum, c=class, o=order, f=family, g=genus. 189

Figure S8 Complete heatmap showing the relative abundance of ASVs across samples treated with natural root exudates from wheat, sorghum, and chicory. ASVs were selected by indicator species analysis ($p < 0.05$), using the three natural exudate treatments as distinct groups to identify ASVs significantly associated with each plant type. The heatmap also includes their relative abundance in AE0 and AE8 for reference. Rows (ASVs) are clustered by Manhattan distance. Cell colours represent row-normalised z-scores (–3 to 3), where 0 is the mean abundance across samples. Positive values indicate higher-than-average abundance; negative values indicate lower. The top sidebar indicates different treatment concentrations and natural exudate types. Abbreviations indicate: k=kingdom, p=phylum, c=class, o=order, f=family, g=genus. 190

Figure S 9 Complete heatmap showing the relative abundance of ASVs across samples treated with natural exudates, selected by indicator species analysis ($p < 0.01$), comparing all natural exudate treatments combined against the AE0 control. The ASVs shown were identified as indicators in the combined comparison and are present across all wheat, sorghum, and chicory samples, though their relative abundances vary between treatments. Rows (ASVs) are clustered by Manhattan distance. Cell colours represent row-normalised z-scores (–3 to 3), where 0 is the mean abundance across samples. Positive values indicate higher-than-average abundance; negative values indicate

lower. Abbreviations indicate: k=kingdom, p=phylum, c=class, o=order, f=family, g=genus. 192

Figure S10. Complete heatmap showing the relative abundance of ASVs across recipient soil samples exposed to volatiles produced by soils treated with different concentrations of AE. ASVs were selected by indicator species analysis ($p < 0.01$), comparing all AV treatments combined against the VC control. The ASVs shown were identified as indicators in the combined comparison and are present across all AV samples (excluding VC), though their relative abundances vary between treatments. VC is the control with no volatiles produced. Rows (ASVs) are clustered by Manhattan distance. Cell colours represent row-normalised z-scores (–3 to 3), where 0 is the mean abundance across samples. Positive values indicate higher-than-average abundance; negative values indicate lower. The top sidebar indicates the concentration used to treat the volatile-producing soil. Abbreviations indicate: k=kingdom, p=phylum, c=class, o=order, f=family, g=genus. 193

Figure S 11 BLAST alignments of primer sequences against *Rhizophagus irregularis* (isolate Att690-23 (DAOM197198); GenBank: FM992377.1). Primer sequences (queries) were aligned against the *R. irregularis* 18S/ITS reference sequence (subject) to assess alignment specificity. Panels show matches for each primer used in 18S and ITS amplicon sequencing: (a) 18S forward primer; (b) 18S reverse primer; (c) ITS1 forward primer; (d) ITS1 reverse primer. Bars indicate alignment positions along the *R. irregularis* reference sequence,.. 195

List of Tables

Table 1.1. Common plant growth-promoting rhizobacteria (PGPR) and their associated functions. (N: Nitrogen; P: Phosphorus; IAA: Indole-3-acetic acid). 41

Table 2.1 Overview of experimental treatments. 72

Table 2.2 Combination of inoculation status, phosphorus condition and time points. 78

Table 4.1 IAA production and corresponding effect on *Arabidopsis* lateral root number for bacterial isolates. IAA concentrations were measured using the Salkowski reagent method. Concentrations (µg/mL) are reported as means ± SEM (n=3). Isolates were categorised based on their observed effect on lateral root number in *Arabidopsis*, relative to controls, as Positive (significantly increased), Neutral (no significant change), or Negative (significantly reduced). 162

Table 4.2 Summary of isolates/enrichments, including closest cultivated relative, ANI value, assembly size (bp), and GC content. The names of enrichments are indicated as “bin”, whereas those names without “bin” are presumed to be pure cultures..... 166

Table S1 Summary of isolates from Vegitone agar. B, C, R: locations of the soil from where the bacteria were isolated. 196

Table S2 Summary of isolates from VL55 agar. B, C, R: Locations of the soil from where the bacteria were isolated. 196

Table S3 Summary of isolates from VL70 agar. B, C, R: Locations of the soil from where the bacteria were isolated. 197

Table S4 Summary of genome sequencing results..... 199

Table S 5 Bacterial families significantly enriched in inoculated samples under P+ conditions based on Chi-square tests (*df* = 1 for all). Families are grouped by phylum. Overlapping families between P+ and P- conditions are highlighted in yellow..... 200

Table S 6 Bacterial families significantly enriched in inoculated samples under P- conditions based on Chi-square tests (df = 1 for all). Families are grouped by phylum. Overlapping families between P+ and P- conditions are highlighted in yellow..... 200

Table S 7 Bacterial families significantly enriched in AE-treated samples at different concentrations (AE100, AE60, AE25, and AE8), based on Chi-square tests (df = 1 for all). Families are grouped by phylum. All enrichments shown are significant at $p < 0.0001$. Numbers in each cell represent Chi-square (χ^2) values..... 201

Table S 8 Bacterial families significantly enriched in ACM-treated samples at different concentrations (ACM100, ACM60, ACM25, and ACM8), based on Chi-square tests (df = 1 for all). Families are grouped by phylum. All enrichments shown are significant at $p < 0.0001$. Numbers in each cell represent Chi-square (χ^2) values. 201

Table S 9 Bacterial families significantly enriched in AEM -treated samples at different concentrations (AEM100, AEM60, and AEM8), based on Chi-square tests (df = 1 for all). Families are grouped by phylum. All enrichments shown are significant at $p < 0.0001$ unless otherwise specified. Numbers in each cell represent Chi-square (χ^2) values. 201

Table S 10 Bacterial families significantly enriched in samples treated with natural exudates (wheat, sorghum, and chicory), grouped together during indicator species analysis and compared against the AE0 control. Families are grouped by phylum. All enrichments shown are significant at $p < 0.0001$ based on Chi-square tests (df = 1). Numbers in each cell represent Chi-square (χ^2) values. 202

Table S 11 Bacterial families significantly enriched in samples treated with natural exudates (wheat, sorghum, or chicory), identified by indicator species analysis, where the three exudate treatments were analysed as distinct groups. Families are grouped by phylum. Numbers in each cell represent Chi-square (χ^2) values; corresponding p values are shown in parentheses. All Chi-square tests had df = 1. 202

Table S 12 Bacterial families significantly enriched in samples exposed to volatile organic compounds (VOCs) from AE-treated soils at five concentrations (AV100, AV60, AV25, AV8, and AV0), based on Chi-square tests (df = 1 for all). Families are grouped by phylum. All enrichments shown are significant at $p < 0.0001$ unless otherwise specified. Numbers in each cell represent Chi-square (χ^2) values. 203

Table S 13 Pairwise comparison of Average Nucleotide Identity (ANI) values between closely related bacterial isolates. ANI values ≥99.99% suggest that the isolates are likely the same strain. 203

Table S 14 Presence of IAA biosynthesis-related genes across selected bacterial genomes. Presence of the gene is indicated by “Y”. 204

Research Thesis: Declaration of Authorship

Print name: Pengrui Cai

Title of thesis: The Interaction between Plants and Rhizosphere Microbes

I declare that this thesis and the work presented in it are my own and has been generated by me as the result of my own original research.

I confirm that:

1. This work was done wholly or mainly while in candidature for a research degree at this University.

2. Where any part of this thesis has previously been submitted for a degree or any other qualification at this University or any other institution, this has been clearly stated.

3. Where I have consulted the published work of others, this is always clearly attributed.

4. Where I have quoted from the work of others, the source is always given. With the exception of such quotations, this thesis is entirely my own work.

5. I have acknowledged all main sources of help.

6. Where the thesis is based on work done by myself jointly with others, I have made clear exactly what was done by others and what I have contributed myself.

7. Parts of this work have been published as:

Keyes, S., van Veelen, A., McKay Fletcher, D., Scotson, C., Koebernick, N., Petroselli, C., Williams, K., Ruiz, S., Cooper, L., Mayon, R., Duncan, S., Dumont, M., Jakobsen, I., Oldroyd, G., Tkacz, A., Poole, P., Mosselmans, F., Borca, C., Huthwelker, T., Jones, D. L. & Roose, T. (2022). Multimodal correlative imaging and modelling of phosphorus uptake from soil by hyphae of mycorrhizal fungi. *New Phytologist,* 234(2)**,** pp. 688-703

Signature: Date: 16/06/2025

Acknowledgements

First and foremost, I would like to express my deepest gratitude to my parents for their unwavering financial and emotional support throughout my PhD journey. Without their belief in me, I could not have reached this point.

I owe endless thanks to my wife, Jingmeng Li, whose companionship and constant encouragement kept me grounded and focused, even in the toughest moments. Your patience and understanding were invaluable throughout this journey.

Academically, I am profoundly grateful to my two supervisors, Dr Marc Dumont and Professor Tiina Roose. Their invaluable guidance, insightful feedback, and unwavering support throughout this journey have been pivotal to the successful completion of this thesis. Their expertise was particularly crucial during the experimental stages of my research, where their advice and direction helped me navigate complex challenges and refine my methods. Without their patience, knowledge, and dedication, I would not have been able to achieve the outcomes I present here.

I would like to extend my sincere thanks to PhD students, Miss Kathryn De Abreu, for her valuable help with *Arabidopsis* growth, and Mrs Fardina Rahimi for her assistance with qPCR during the later stages of my research. Your contributions were vital to the success of my experiments. My thanks also go to the lab technicians, whose consistent support over the last five years was indispensable. From maintaining equipment to providing technical assistance and troubleshooting, their skill and consistent support ensured that my experiments ran smoothly and efficiently.

Finally, I want to express my deep appreciation to Southampton Football Club (the Saints). Watching their turbulent 2023-2024 season, filled with setbacks and challenges, resonated deeply with me. Just like my own PhD journey, they experienced many highs and lows, yet their relentless spirit and determination saw them fight their way back to the Premier League through promotion. Their resilience during the season inspired me, and watching their matches gave me the momentum to push through the final, toughest year of my PhD.

Definitions and Abbreviations

ACM ..... Artificial exudate with MBOA in constant concentration across concentration gradients

AE ..... Artificial exudate without MBOA

AEM ..... Artificial exudate with MBOA diluted together with AE

AMF ..... Arbuscular mycorrhizal fungi

ANOVA ..... Analysis of variance

ASV ..... Amplicon sequence variant

ATP ..... Adenosine triphosphate

AV ..... Recipient soil exposed to VOCs produced from soil treated with AE

Al ..... Aluminium

B ..... Boxworth

BNF..... Biological nitrogen fixation

C..... Chilworth

CAS agar ..... Chrome azurol sulphonate agar

Ca..... Calcium

Ct ..... Cycle threshold

Cu..... Copper

DIMBOA ..... 2,4-dihydroxy-7-methoxy-(2H)-1,4-benzoxazin-3(4H)-one

EPS ..... Exopolysaccharide

FAA ..... Formaldehyde, acetic acid, alcohol [ethanol] mixture

Fe ..... Iron

FeMo-co ..... Iron–molybdenum cofactor

IAA ..... Indole-3-acetic acid

ISR ..... Induced systemic resistance

ITS ..... Internal transcribed spacer

K ..... Potassium

LB medium ..... Luria Bertani medium

LPS ..... Lipopolysaccharides

MBOA..... 6-methoxy-benzoxazolin-2-one

MIR ..... Mycorrhizal-induced resistance

MS ..... Murashige & Skoog Modified Basal Medium with Gamborg Vitamins

Mg..... Magnesium

Mn ..... Manganese

Mo ..... Molybdenum

N..... Nitrogen

NSAPs ..... Non-specific acid phosphatases

NH_3 ..... Ammonia

NH_4^+ ..... Ammonium

NO_2^- ..... Nitrite

NO_3^- ..... Nitrate

OD ..... Optical density

P ..... Phosphorus

PCA..... Principal component analysis

PCoA..... Principal coordinates analysis

PERMANOVA ..... Permutational multivariate analysis of variance

PGPB..... Plant growth-promoting bacteria

PGPF..... Plant growth-promoting fungi

PGPM ..... Plant growth-promoting microbe

PGPR ..... Plant growth-promoting rhizobacteria

PSB ..... Phosphate-solubilising bacterium/bacteria

PSM ..... P-solubilizing microorganisms

PVK medium ..... Pikovskaya medium

PVLG ..... Polyvinyl alcohol-lactic acid-glycerol

Pi ..... Inorganic p

Po ..... Organic P

R ..... Rosemaund

S ..... Sulfur

SEM ..... Standard error of the mean

V ..... Vanadium

VC ..... Samples without any VOCs produced in it, only recipient soil alone

VOCs ..... Volatile organic compounds

WGS ..... Whole-genome sequencing

Zn ..... Zinc

qPCR ..... Quantitative polymerase chain reaction

Chapter 1 General introduction

1.1 Introduction to crops

Food production is critical for human civilisation, and the history of growing foods has shaped the development of human societies. From the half a million plant species on the planet, we heavily rely on four major crops: wheat, maize, rice and soybean, which account for more than three-quarters of our plant-based food supply (Von Braun, 2007; Cai et al., 2024). The production of crops is a currently a major concern as their demand is increasing every year due to the rapid global population growth (Chandra et al., 2024b).

Wheat and rice are two of the world's most important staple crops. According to the United States Department of Agriculture (USDA, 2021), both wheat and rice yields and production steadily increased between 2010 and 2020. For wheat, average yield rose by 10.4% from 2010 to 2015 and by 7.3% from 2015 to 2020, while production increased by 11.8% and 4.9% over the same periods. Rice average yield also showed a gradual increase, rising by 4.2% from 2010 to 2015 and 4.5% from 2015 to 2020, accompanied by production increases of 6.5% and 4.0%, respectively (Figure **1**.**1**).

a

b

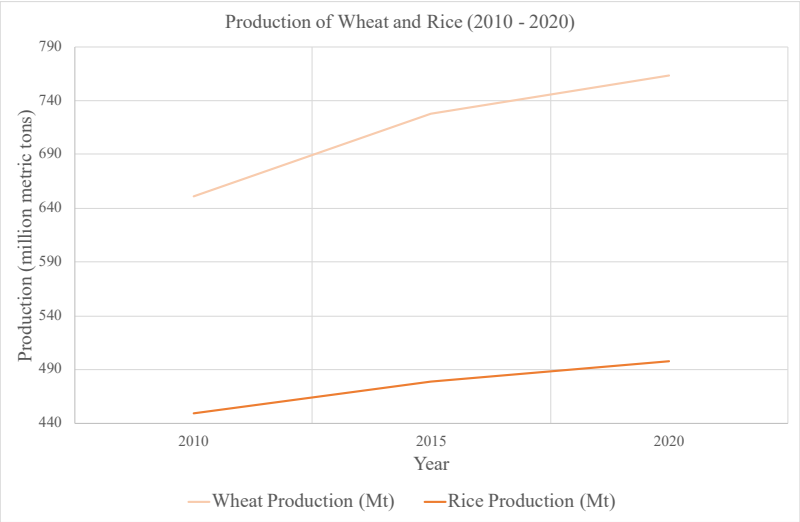

Figure 1.1 Average yield (metric tons per hectare) (a) and production (million metric tons) (b) of wheat and rice. Modified according to USDA (2021).

The global population is expected to reach 8.5 billion in 2030 (United Nations-Department of Economic and Social Affairs-Population Division, 2019); furthermore, it was predicted that population size will exceed 9.7 billion by 2050 (United Nations-Department of Economic and Social Affairs-Population Division, 2019).The human population is increasing in the world every year, yet the growth in crop yields is lagging behind the rising demand for food; thus, it is necessary to increase the yield of food production in order to feed the human population across the world. With the decreased availability of agricultural lands due to factors like urbanisation and environmental degradation, it presents significant challenges for global food security; developing approaches to utilise the remaining lands wisely to increase crop yields is becoming crucial (Fan et al., 2024).

When we consider strategies to optimise land use, in the meantime, it is equally important to recognise the fundamental role of nutrients in supporting plant growth (Uchida, 2000). The main source of nutrients for the crops come from the soil in which they grow.

1.2 Nutrients in soil

The nutrients in the soil boost the growth of the crops, and those needed by the plants to complete their life cycle and maintain normal functions are called essential nutrients (Bakki et al., 2024). Plants uptake nutrients from the soil to grow, and there are more than ten of these needed in the growth of plant species. These nutrients can be divided into two categories: macronutrients and micronutrients (Marschner, 2023).

1.2.1 Macronutrients

Macronutrients are defined as the nutrients needed in the largest quantities by plants. There are six primary macronutrients: Nitrogen (N), Phosphorus (P), Potassium (K), Magnesium (Mg), Sulfur (S), and Calcium (Ca), which are essential for crop growth (Maathuis, 2009; Kumari et al., 2024).

Nitrogen (N) is a key element in crop growth as it is part of nucleic acids and proteins, and also used in the synthesis of some vitamins. It is also involved in chlorophyll production (Bojović and Marković, 2009), which is essential for light harvesting for photosynthesis in plants. **Phosphorus** (P) plays a key part in synthesising phospholipids and nucleic acids. Also, phosphorus forms part of ATP (adenosine triphosphate), which helps the transfer of energy from sunlight to plants through oxidative phosphorylation (light energy to chemical energy). **Potassium** (K) regulates opening and closing of the stomata, which helps maintain the water balance (Hetherington and Woodward, 2003). **Magnesium** (Mg) is also an important component of chlorophyll as well as the green colouring material of plants and is also important for photosynthesis. **Sulfur** (S) is a component of amino acids in the proteins of plants, for example methionine and cysteine and it exists in several coenzymes. During photosynthesis, sulfur plays an important role as part of iron-sulfur (Fe-S) clusters in electron transport chain proteins, such as ferredoxin, which are essential for maintaining the efficiency of electron transfer and energy conversion in plants (Terry, 1976; Watson and Jüttner, 2023). **Calcium** (Ca) is essential for the growth of the roots and the development of leaves (Jiao et al., 2024; White and Broadley, 2003).

1.2.2 Micronutrients

Micronutrients, also called trace elements, are nutrients required in small amounts by plants (Muthulakshmi et al., 2024). The primary micronutrients include iron (Fe), copper (Cu), molybdenum (Mo), zinc (Zn) and manganese (Mn) (Sagwal et al., 2023).

Iron (Fe) is an essential element for the synthesis of chlorophyll (Briat et al., 2015; Katyal and Sharma, 1980). **Copper** (Cu) acts as a cofactor for several plant enzymes, such as Cu/Zn superoxide dismutase (SOD), amino oxidase, laccase, plastocyanin, cytochrome c oxidase and polyphenol oxidase (Yruela, 2005). **Molybdenum** (Mo) is necessary for reducing nitrate, which is crucial for the production of amino acids (Peters and Szilagyi, 2006; Liu et al., 2022b). **Zinc** (Zn) is involved in the plant hormone producing processes that regulate leaf expansion and stem elongation (McCauley et al., 2009; Shehzadi et al., 2024). **Manganese** (Mn) plays an important part in photosynthesis, by activating over 35 different enzymes, some of which are involved in the metabolism of carbohydrate and the formation of chlorophyll, and manganese is also essential for Photosystem II (Mousavi et al., 2011; Alejandro et al., 2020).

1.2.3 How do these nutrients get into the soil

The soil system itself harbours a large supply of a variety of naturally occurring nutrients. These nutrients enter the soil through various pathways, such as the decomposition of the bodies of dead animals, the animal wastes and dead plants; rock weathering; atmospheric deposition, as well as the metabolism of microorganisms (Ohkuma, 2003; Doran and Zeiss, 2000; Fontaine et al., 2023). Besides, nutrients can be artificially added to the soils in the forms of fertilisers, the most common chemical fertilisers used by human are the phosphorus and nitrogen fertilisers (Savci, 2012).

Phosphorus (P) is mostly insoluble in soil. P fertilisers are primarily mined from rock phosphate and used in intensive agricultural activities to address the P deficiency (Richardson et al., 2011). Currently, more than a hundred million tonnes of P are being extracted globally each year, with demand for P-based fertilisers still projected to grow (Gilbert, 2009). However, despite advances in mining industry, the stock of rock phosphate is limited on the planet which poses significant risk of depletion; with some studies indicating that this resource may fall into shortages within the next 70 to 140 years (li et al., 2017).

The use of P fertilisers is expensive for the agricultural industry. There are also harmful environmental consequences to intensive use of P fertilisers (Gyaneshwar et al., 2002). The use of chemical fertilisers that contain P and N in the soil can cause negative environmental impacts like soil degradation. Moreover, use of chemical fertilisers although increases crop productivity by enhancing the fertility of soil, also result in nitrate leaching into the ground water as well as N and P surface run-off. When they enter water body they cause aquatic eutrophication (Ayiti and Babalola, 2022; Adesemoye and Kloepper, 2009). Additionally, the P in the fertilisers is typically immobilised in the soil very quickly by binding with iron, aluminium, or calcium to form insoluble phosphate compounds (Shen et al., 2011). These forms are not readily available to plants, meaning fertiliser input must be increased to ensure that the plants can take up enough nutrients. Fertilisers are also quite inefficient in certain types of soil, particularly acidic soils, alkaline soils (Marschner et al., 2005), and calcareous soils (Tiecher et al., 2023; Khan et al., 2023). Plants and soil microbes can mobilise some of this immobilised P by releasing organic acids and enzymes that help solubilise phosphorus (Wei et al., 2024).

In conclusion, the use of P and N fertilisers, while essential for increasing crop productivity, is associated with significant costs, inefficiencies, and environmental damage. These factors make their long-term use in agricultural practice unsustainable without significant improvements in management practices and the development of more sustainable alternatives.

1.2.4 How plants acquire nutrients from soil

Plants employ several strategies to obtain the essential nutrients needed for growth. Root hairs are particularly important in nutrient acquisition from the soil, with approximately 80% of the total nutrients being absorbed by root hairs. The role of root hair formation in nutrient uptake has been extensively reviewed (Jungk, 2001). Here we mainly focus on P and N.

P is a critical component for plant growth and food production, but its mineral resources are unevenly distributed globally. Around 66% of the world's phosphate reserves are located in Morocco, with smaller percentages in China, Algeria, and Syria, and less than 1% in other countries (Gross, 2017). In soils, P exists in both organic (Po) and inorganic (Pi) forms, primarily in insoluble or poorly soluble inorganic states (Munshi and Dave, 2005). Plants absorb P as orthophosphate anions (mainly HPO_4^{2-} and

$H_2PO_4^-$) from the soil solution (Richardson et al., 2009a), but the concentration of these anions is typically low, ranging from 1 to 5 µM in most soils (Bieleski, 1973). P can become adsorbed onto aluminium (Al), iron (Fe), or calcium (Ca) hydroxides or oxides, forming insoluble compounds that make it inaccessible to plants. Additionally, P can precipitate with metal cations (primarily Al/Fe in acidic soils and Ca in alkaline soils), further reducing its availability (Oburger et al., 2011). Consequently, P is unique among soil nutrients due to its low solubility, low mobility, and rapid immobilization by the soil matrix (Shen et al., 2011).

To overcome these challenges, plants have developed various mechanisms to increase P uptake from the soil. These strategies include altering root growth and architecture, such as modifying root topology, morphology, and distribution patterns (Richardson et al., 2011; Shen et al., 2011). P deficiency has been shown to promote the formation of root clusters, with the proportion of the root system devoted to these clusters decreasing as P availability increases (Dinkelaker et al., 1989; Niu et al., 2013). Moreover, some plant species employ P-mining strategies, such as releasing root exudates containing organic acid anions (e.g., malate, oxalate, and citrate) and phosphatases, which enhance the solubilisation and mineralisation of P in the soil (Richardson et al., 2009a; Hinsinger, 2001; Pantigoso et al., 2020). Organic acid anions, like citrate, can desorb orthophosphate from adsorption sites in the soil matrix, thereby helping to dissolve insoluble Pi. It has been reported that some plants increase citrate release under P-limited conditions (Hunter et al., 2014; Islam et al., 2023). Among these, altering root architecture is considered a more common and widespread strategy across plant species (Chen et al., 2023). However, the capacity to release organic acid anions varies among species, and is particularly notable in plants such as white lupin and members of the Proteaceae family (Zhou et al., 2020; Zhao et al., 2021b).Soil biological processes involving microbes also play a crucial role in phosphorus acquisition, which will be discussed in later sections.

Nitrogen (N) is taken up by plant roots primarily in the forms of ammonium (NH_4^+) and nitrate (NO_3^-), as well as in organic forms such as amino acids, urea, and peptides (Kiba and Krapp, 2016). Studies have shown that organic N forms contribute to plant nutrition in specific ecosystems, such as boreal forests (Jones and Kielland, 2012; Werdin-Pfisterer et al., 2012). However, in most soils, ammonium and nitrate are the predominant forms of nitrogen absorbed by plants.

1.3 The rhizosphere and microbes

1.3.1 Microbes in soil

Soil is home to a diverse array of microorganisms, including bacteria, fungi, protozoa, and nematodes, which coexist within the soil matrix (Ekelund et al., 2009). Among these, certain microbes play a crucial role in enhancing plant growth and are collectively known as plant growth-promoting microbes (PGPMs). The primary categories of these beneficial microbes are plant growth-promoting fungi (PGPF) and plant growth-promoting bacteria (PGPB) (Richardson et al., 2009a; Ku et al., 2024).

To date, mycorrhizal fungi and nitrogen-fixing bacteria—such as those that form root nodules, and free-living bacteria—have been extensively characterized for their contributions to plant health. These microbes contribute to plant health by facilitating nutrient acquisition—particularly N, P and Fe—and by enhancing the plant's resistance to biotic stress (e.g., pathogens) and abiotic stressors (Pineda et al., 2010; Thepbandit and Athinuwat, 2024).

1.3.2 The rhizosphere

The rhizosphere is defined as the soil zone surrounding the root that is directly influenced by the plant (Lynch and Whipps, 1990). This narrow zone, extending just a few millimeters from the plant root, is characterised by significantly higher microbial activity compared to the bulk soil. The microbial population in the rhizosphere can reach up to 1 x 10^{10} - 10^{12} cells per gram rhizosphere soil, which is 10 to 100 times greater than in the surrounding bulk soil (Weller and Thomashow, 1994; McNear, 2013). Additionally, the rhizosphere plays a crucial role in belowground carbon transfer, with research indicating that up to 40% or more of photosynthetically fixed carbon is transported through this zone, including the carbon released by the plant in the form of root exudates (Lynch and Whipps, 1990). Within this process, up to a quarter of a plant's photosynthetically fixed carbon is released into the rhizosphere in a process known as rhizodeposition (Nguyen, 2003; Guyonnet et al., 2018).

Rhizodeposition refers to the loss of plant materials from the roots into the surrounding soil (Whipps and Lynch, 1985; Patra et al., 2021). This process includes the release of various materials such as mucilage, dead epidermal and cortical cells, lysates, root cap and border cells, water-soluble exudates (e.g., malate, oxalate, and citrate), secondary

metabolites (e.g., phenolics, flavonoids, and alkaloids), and gases like CO_2 and ethylene (Hütsch et al., 2002; Mushtaq and Fauconnier, 2024). The organic compounds excreted, such as citrate, can solubilise insoluble inorganic phosphorus in the soil (Hunter et al., 2014). Moreover, the root exudates from rhizodeposition supply carbon and energy for microbial populations in the rhizosphere, significantly contributing to their development and driving microbial colonisation (Whipps, 2001).

Root exudates also contain antimicrobial substances known as phytoanticipins and phytoalexins. Phytoanticipins are "low molecular weight, antimicrobial compounds that are present in plants before challenge by microorganisms or are produced after infection solely from preexisting constituents" (VanEtten et al., 1994), whereas phytoalexins are defined as "low molecular weight, antimicrobial compounds that are both synthesized by and accumulated in plants after exposure to microorganisms". While there are numerous classes of plant antimicrobial compounds (Pedras and Yaya, 2015), their impact on microbial growth in the rhizosphere is still not well characterised. Recent studies have shown that 6-methoxy-benzoxazolin-2-one (MBOA), a common phytoanticipin, shapes the microbial community in the rhizosphere and significantly impacts plant immunity (Hu et al., 2018; Cotton et al., 2019).

1.3.3 Rhizosphere microorganisms

The soil hosts a vast abundance of microbes, with rhizosphere microbial communities being largely shaped by the plants they interact with (Smalla et al., 2001). These microorganisms are often differentiated based on the carbon sources they utilize, such as carboxylic acids, carbohydrates, and amino acids, which are released from plant roots (Grayston et al., 2001; Grayston et al., 1998; Liu et al., 2023). In other words, different types of carbon sources influence the composition of microbial communities.

Rhizosphere microorganisms play crucial roles in promoting plant growth by performing various beneficial processes. These include: the production of phytohormones (by bacteria and fungi), nitrogen fixation (by bacteria), and the solubilisation of inorganic phosphorus and mineralization of organic phosphorus through the release of organic acids, phytase, and phosphatase enzymes (Idriss et al., 2002; Richardson et al., 2009a); Additionally, microorganisms contribute to P supply through cell turnover and siderophore production, which aids in iron acquisition by plants (Glick, 2012).

This chapter focuses particularly on the P-solubilising and nitrogen-fixing microbes. These microorganisms have significant potential to reduce our dependence on chemical fertilisers by enhancing the availability of water-soluble phosphorus and nitrogen that can be readily absorbed by crops (Sharma et al., 2013).

1.3.4 The mycorrhizal & plant growth-promoting fungi

Fungi are one of the most intensively studied groups of rhizosphere microorganisms. In the rhizosphere, fungi and bacteria coexist with plants and supply P and N to the plants. Many plants form symbiotic relationships with fungi to acquire more P from the soil, which are called mycorrhizae (Smith and Read, 2008). It had been reported that mycorrhiza might also play some role in the nitrogen fixation, but there was no correlation found (Richards and Voigt, 1964; Palanisamy et al., 2024); however, Palanisamy et al. (2024) recently suggested that nitrogen-fixing bacteria and mycorrhizal fungi play roles in improving soil structure and fertility, indicating a possible connection. It is estimated that 95% of plant species are mycorrhizal (Tao and Zhao, 2005). Mycorrhizal fungi receive carbon, accounting for 20-40% of the total photosynthate, in exchange for transporting essential nutrients (e.g., phosphorus, nitrogen, zinc, copper) and water from the soil to the plant (Merryweather and Fitter, 1995). Mycorrhizal fungi attach to the surface of plant roots and colonise the root cortex. Subsequently, the external hyphae, or mycelia, develop to connect the root to the surrounding soil (Richardson et al., 2009a). Studies have demonstrated that the hyphae perform a similar function to root hairs in crops for phosphorus acquisition, effectively extending the root surface area (Richardson et al., 2011; Shen et al., 2011).

The mycorrhizal relationship can generally be divided into two types: ectomycorrhizal and endomycorrhizal (which includes arbuscular, orchid, and ericoid mycorrhizae) (Chilvers et al., 1987). The primary difference between these types lies in their interaction with host plants: ectomycorrhizal fungi do not penetrate the cell walls of the host plants, whereas endomycorrhizal fungi do.

Arbuscular mycorrhizal fungi (AMF) are the most common endomycorrhizal associations with plants. arbuscular mycorrhizas form a widespread symbiotic association between fungi from the *Glomeromycota* and the roots of about 70% of land plant species, spanning both herbaceous and woody plants (Shen et al., 2011; Hawkins et al., 2023). AMF transfer the nutrients through the mycelium to the plants and the plants give the

AMF carbon in return. The study of AMF is challenging because these fungi are obligate symbionts; they cannot complete their life cycle or grow well without a host plant. This obligate nature, as highlighted by Bagyaraj (2014), makes it hard to grow and survive well under laboratory conditions, hence limiting the ability to conduct research on them.

While AMF are crucial for nutrient exchange through their symbiotic relationships with plant roots, they represent just one aspect of how fungi within the broader category of plant growth-promoting fungi (PGPF) can enhance plant growth. Beyond these symbiotic interactions, other PGPF also play a significant role in supporting plant health. Unlike AMF, these PGPF include a diverse array of fungi that promote growth through mechanisms such as mineral solubilisation, biological control of pathogens, and the production of secondary metabolites (Khan et al., 2010; Abdenaceur, 2023). One well-studied example is the ability to initiate induced systemic resistance (ISR) in cucumber against *Colletotrichum orbiculare* , thereby promoting plant growth (Koike et al., 2001). Additionally, PGPF from the rhizosphere, such as *Trichoderma* species, can directly suppress pathogens and prevent diseases (Hyakumachi, 1994; Yu et al., 2024). Most importantly, the P-solubilising fungi that utilise the unavailable P forms present a great alternative to chemical fertilisers.

In soil, P-solubilising fungi constitute approximately 0.1–0.5% of the total fungal populations (Kucey, 1983; Zhang et al., 2019; Tariq et al., 2022). Among the fungal species in the rhizosphere, *Aspergillus* and *Penicillium* are among the most frequently reported fungal genera involved in solubilising P (Souchie et al., 2006; Wakelin et al., 2004; Chandra et al., 2024a) (Figure 1.2).

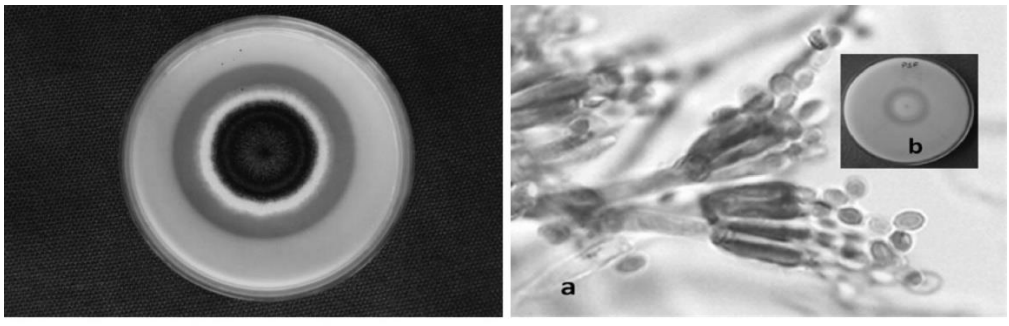

Figure 1.2. Plate A: Phosphate solubilisation zone on Pikovskaya plates produced by *Aspergillus*. Plate B(a): *Penicillium* (1000x magnification), Plate B(b): P solubilisation zone of *Penicillium*. Figure from Khan et al. (2010).

P-solubilising fungi promote plant growth through several mechanisms:

a) They provide essential micronutrients like manganese (Mn), which is crucial for various physiological functions in plants, including photosynthesis, N metabolism (particularly reduction of nitrate), and the synthesis of aromatic ring compounds. Additionally, they facilitate the solubilisation of plant nutrients from solid-phase compounds like Fe_2O_3, MnO_2, and metallic zinc, through the activities of phosphate-solubilising and bio-control fungi like *Trichoderma harzianum* Rifai 1295–22 (T-22), which secrete chemical agents (including organic acids and siderophores) that chemically mobilise metal ions via chelation and reduction. This chemical process occurs in unison with the solubilisation of phosphate ions bound to these metal oxides, leading to enhanced phosphorus availability (Altomare et al., 1999).

b) They synthesize growth-promoting substances such as siderophores, phytohormones and antibiotics, which are important for plant growth (Khan et al., 2010).

c) They protect the plants against soil borne pathogens (bio-control). For instance, it was reported that P-solubilising fungus *Aspergillus awamori* could suppress the severity of wilt (caused by *Fusarium oxysporum f. sp. lycopersici*) in tomatoes *(Lycopersicon esculentum* L.) by 29–37%; moreover, these species had increased the yield of tomato by 22% (Khan et al., 2007).

Mechanisms of plant growth promotion by P-solubilising fungi are shown in

Figure 1.3.

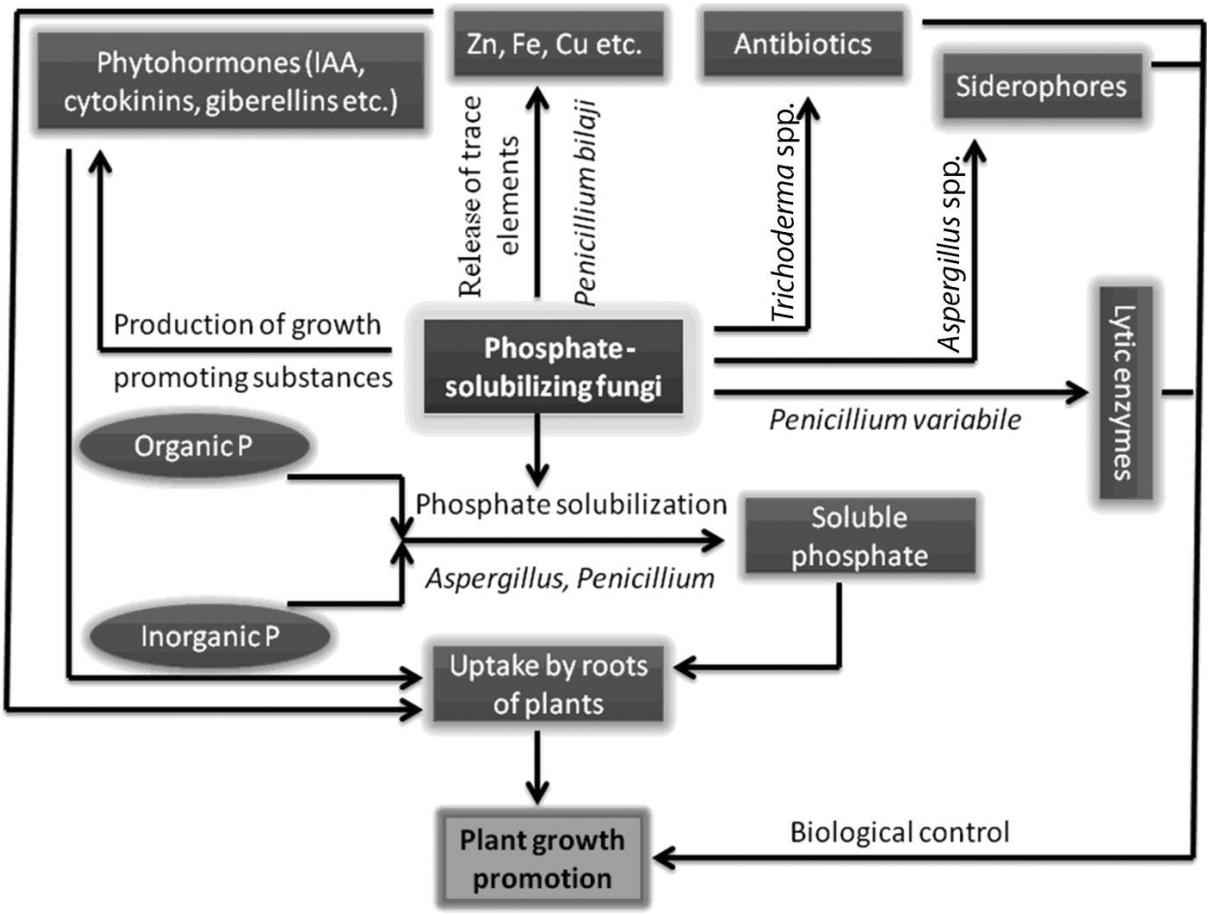

Figure 1.3. Mechanisms in plant growth carried out by phosphate-solubilising fungi. Figure from Khan et al. (2010).

1.3.5 The rhizobacteria

In addition to the benefits provided by mycorrhizal fungi, plant growth-promoting rhizobacteria (PGPR) are equally important in supporting crop growth (Richardson et al., 2009a). Rhizobacteria refers to the bacteria that are adapted to the rhizosphere soil, and PGPR) are a subset of plant growth-promoting bacteria (PGPB) that specifically colonise plant roots and enhance plant growth (Beneduzi et al., 2012; Riaz et al., 2021). The majority of PGPB are found in the rhizosphere. The microbial communities in the rhizosphere are shaped by various plant factors, such as plant species and root exudates, resulting in different plants harbouring distinct bacterial communities in the rhizosphere (Berg and Smalla, 2009). According to Kloepper et al. (1989), these bacteria are also called beneficial soil bacteria. However, bacteria that specifically promote plant growth in the rhizosphere are estimated to constitute only 2%–5% of the total bacteria population in this zone (Antoun and Kloepper, 2001; Beneduzi et al., 2012; Singh et al., 2023).

Different genera of bacteria belong to the PGPR, *Bacillus* and *Pseudomonas spp* are predominant among them (Podile and Kishore, 2006).

In general, PGPR can affect plant growth in direct and indirect ways (Gupta et al., 2015), as outlined in Figure 1.4, and common PGPR are listed in Table 1.1, along with their associated functions.

PGPR can directly enhance plant growth through various mechanisms:

- By providing the plant with specific compounds synthesized by the bacterium (Glick, 1995). For instance, PGPR can produce phytohormones such as auxins (including indole acetic acid [IAA]), ethylene, cytokinins, and gibberellins, which exhibit significant phyto-stimulation activity (Patten and Glick, 2002; Gupta et al., 2015). Among these, IAA is the most well-studied auxin and plays a key role in cell division, extension, and differentiation. Moreover, IAA can stimulate the germination of seeds and tubers, enhances the development rate of xylem and root, and regulates vegetative growth process. It also initiates the formation of lateral and adventitious roots, mediates plant responses to light, gravity and florescence, and influences pigment formation, photosynthesis , the biosynthesis of various metabolites, and resistance to stressful conditions (Spaepen and Vanderleyden, 2011).

  Cytokinins induce cell division and differentiation. They also promote RNA synthesis and stimulate protein and enzyme activities in plant tissues. Gibberellins are often used to induce plantlet formation from adventive embryos. There are several PGPR such as *Azotobacter sp., Bacillus subtilis, Pantoea agglomerans, Rhizobium sp., Rhodospirillum rubrum, Pseudomonas fluorescens* and *Paenibacillus polymyxa* that can produce cytokinins or gibberellins, or both to promote plant growth (Kang et al., 2010).

  Ethylene is well-known for promoting fruit ripening. It also stimulates seed germination and adventitious root initiation; inhibits root elongation at high concentrations; and promotes leaf abscission during plant senescence. Furthermore, ethylene can activate the synthesis of other plant hormones (Glick et al., 2007). PGPR can modulate ethylene levels in plant roots by producing 1-aminocyclopropane-1-carboxylate (ACC) deaminase, which breaks down ACC (the immediate precursor of ethylene) , thereby reducing ethylene biosynthesis in the plant (Glick, 2014).

- Fixing nitrogen (Dobereiner, 1992): PGPR carry out nitrogen fixation by converting atmospheric nitrogen (N_2) into ammonia (NH_3), a form that plants can readily utilise. This process, known as biological nitrogen fixation (BNF), is mediated by the enzyme nitrogenase. The detailed mechanism of this process will be elaborated in later sections.
- Phosphorus solubilisation/mineralisation: P is a key nutrient for plants, essential alongside N. However, more than 80% of soil P exists in immobilised and insoluble forms (Sharma et al., 2013; El Attar et al., 2022). Plants can only absorb P in two soluble forms: monobasic ($H_2PO_4^-$) and dibasic (HPO_4^{2-}) phosphate ions. PGPR apply various strategies to solubilise insoluble inorganic phosphorus and mineralize organic phosphorus compounds, making them available for plant uptake. More detailed mechanisms of phosphorus solubilisation and mineralisation by PGPR are described in later sections.
- Potassium solubilisation: PGPR can solubilise potassium (K) from potassium-bearing rocks by producing organic acids (Han and Lee, 2006; Chieb and Gachomo, 2023).
- Siderophore production: In nature, Fe^{3+} is the predominant form of iron but it is sparingly soluble and insufficient for both bacterial and plant assimilation (Glick, 2012; Wairich et al., 2024). To overcome this, microorganisms have evolved specific mechanisms, including the production of low molecular weight iron-chelating compounds called siderophores. Siderophores have a high affinity for Fe^{3+}, facilitating the transport of iron into cells. Siderophores benefit plants both directly and indirectly. Direct benefits have been demonstrated in studies where radiolabelled ferric siderophores served as the sole source of iron. Plants were able to take up this labelled iron via PGPR such as: *Aeromonas, Azotobacter, Bacillus, Burkholderia, Pseudomonas, Rhizobium, Serratia and Streptomyces sp*., leading to enhanced chlorophyll levels (Sharma et al., 2003; Aioub et al., 2022). The indirect effect of siderophore production by PGPR on plant growth will be discussed in the next section.

PGPR also employ various mechanisms to promote plant growth indirectly:

a) Antibiotic production: One powerful biocontrol mechanism of PGPR is the production of antibiotics, which has been extensively studied. These antibiotics serve as

potent tools against phytopathogens, helping to protect plants from diseases (Gupta et al., 2015).

b) Lytic enzyme production: Some PGPR produce enzymes such as β-glucanase, cellulases, chitinases, dehydrogenase, lipases, phosphatases and proteases, which can lyse the cell walls of phytopathogenic microorganisms (particularly fungi) (Hayat et al., 2010). Through these enzymes, PGPR play a significant role in plant growth by suppressing pathogenic fungi including *Botrytis cinerea, Fusarium oxysporum, Phytophthora sp., Rhizoctonia solani, Sclerotium rolfsiiand,* and *Pythium ultimum* (Nadeem et al., 2013).

c) Siderophore production: In addition to the direct mechanism previously mentioned, siderophore production by PGPR can also benefit plants indirectly. Siderophore-producing PGPR sequester the Fe^{3+} by binding with ferric ions (Fe^{3+}) and forming siderophore-ferric complexes, which bind to bacterial cell surface receptors. This process limits the availability of iron to pathogens, thereby suppressing their growth (Glick, 2012).

d) Induced systemic resistance (ISR): ISR is a phenomenon in which PGPR trigger plant defence mechanisms against pathogens, without the need for direct interaction between the PGPR and the pathogens. The plants respond to ISR are said to be "primed", with ethylene and jasmonate signalling playing key roles in stimulating the plant's defence response against a wide range of pathogens (Yu et al., 2022). Additionally, bacterial molecules like β-glucans, lipopolysaccharides (LPS), chitin, flagellar proteins, siderophores, cyclic lipopeptides, 2, 4-diacetylphloroglucinol, homoserine lactones, and pyoverdine not only activate ISR but also work in tandem with these signaling pathways, ensuring a robust and coordinated defense response throughout the plant (Glick, 2012; Raouani et al., 2022).

e) Exopolysaccharide (EPS) production: EPS can function as active signalling molecules during beneficial interaction with plants and play an important part in forming biofilms that support microbial colonisation and persistence on plant roots. These biofilms help protect plants by stabilising microbial communities in the rhizosphere. During infection processes, EPS aids in plant defence by forming physical barriers against pathogens and altering the microenvironment to benefit beneficial microbes. Moreover, EPS influences root architecture and build up resilience

to stresses for plants. Through these mechanisms, EPS plays a vital, albeit indirect, role in both defence and general health of plants (Parada et al., 2006; Bogino et al., 2013; Srivastava and Sharma, 2023; Ajijah et al., 2023).

There is a growing scientific interest in understanding the mechanisms by which PGPR solubilise insoluble phosphate and fix atmospheric nitrogen, hence making these essential nutrients more available to crops. Although various methods have been explored,the specific biochemical pathways and microbial components related to phosphate solubilisation are still largely unknown, whereas the biochemical pathways of nitrogen fixation are well characterised (Illmer and Schinner, 1995; Vessey, 2003; Richardson and Simpson, 2011; Pan and Cai, 2023). Research on this topic is important due to the need to increase crop yields and promote sustainable agricultural practices. Studies have begun to uncover the roles of organic acids, enzyme secretion, and microbial interactions in these processes, but many areas remain unexplored (Rodríguez and Fraga, 1999; Hariprasad and Niranjana, 2009; Borah et al., 2023; Hasan et al., 2024).

A brief description of the known mechanisms by which PGPR facilitate phosphorus solubilisation and nitrogen fixation are presented in section 1.4 and 1.5.

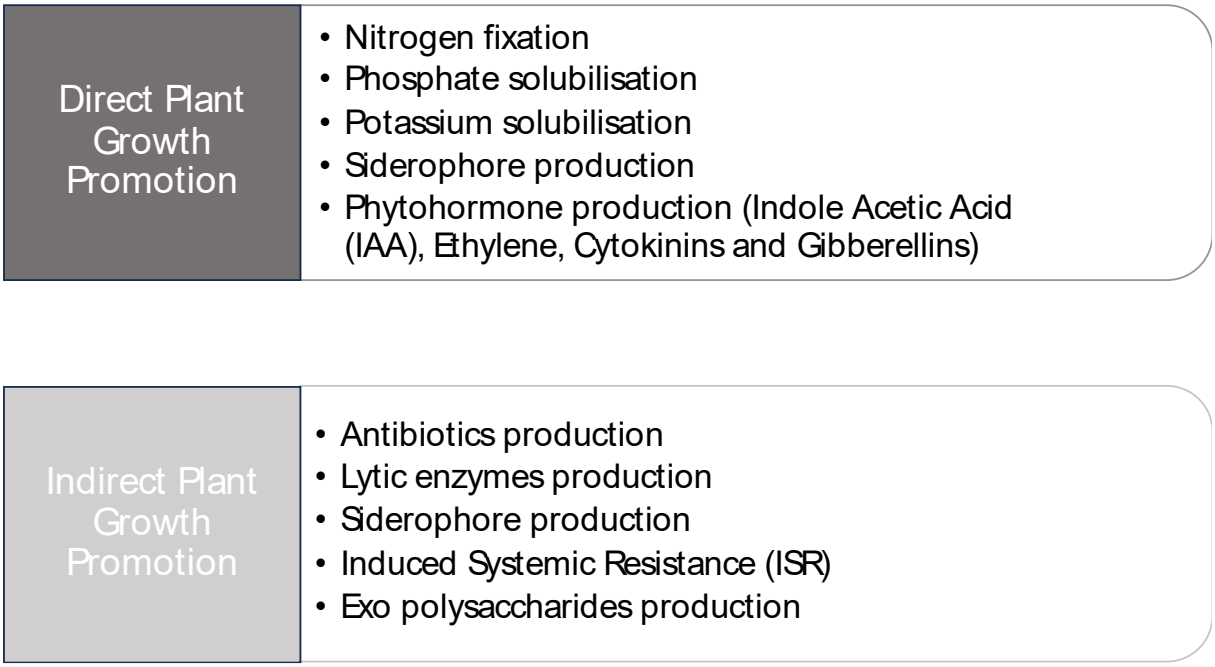

Figure 1.4. Direct and indirect mechanisms of plant growth promotion by plant growth-promoting rhizobacteria (PGPR).

Table 1.1 Common plant growth-promoting rhizobacteria (PGPR) and their associated functions. (N: Nitrogen; P: Phosphorus; IAA: Indole-3-acetic acid).

Genus	Functions	References
Bacillus	Enzyme production, antibiotic production, phytohormone production, biocontrol of pathogens, P solubilisation	(Castaldi et al., 2021; Mahdi et al., 2022)
Pseudomonas	Siderophore production, phytohormone production, biocontrol	(Sah et al., 2021)
Rhizobium	N fixation (symbiotic), particularly with leguminous plants	(Oldroyd et al., 2011)
Azospirillum	N fixation, phytohormone production	(Bashan and de-Bashan, 2010)
Enterobacter	P solubilisation, IAA production	(Jha et al., 2011)
Paenibacillus	P solubilisation, antifungal compound production, phytohormone production	(Khan et al., 2020)
Burkholderia	N fixation, siderophore production, P solubilisation, IAA production	(Elshafie and Camele, 2021)
Serratia	Siderophore production, phytohormone production, biocontrol	(Kalbe et al., 1996; Zaheer et al., 2016)

1.3.6 The hyphosphere

The hyphosphere refers to the specific soil zone that is directly influenced by the hyphae of mycorrhizal fungi (Figure 1.5). Unlike the rhizosphere, which is primarily shaped by the activities of plant roots and their associated microbial interactions, the hyphosphere extends these influences deeper into the soil, particularly through the hyphae of AM fungi like *Rhizophagus irregularis* (Johansson et al., 2004). This region plays a crucial role in soil ecology, particularly in facilitating nutrient cycling. The hyphosphere enables plant roots to access less available nutrients, such as P, from deeper soil layers that roots alone cannot reach, effectively extending the nutrient-absorbing capability of roots (Smith and Read, 2008). Moreover, fungal hyphae contribute to soil structure by promoting the formation and stabilization of soil aggregates, which enhances soil porosity and stability; this process is more pronounced in the hyphosphere compared to the rhizosphere, making it a unique aspect of soil ecology (Rillig and Mummey, 2006).

The microbial community within the hyphosphere is significantly different from that in the bulk soil or even the rhizosphere due to the influence of fungal hyphae. Hyphae release exudates, including organic acids that lower soil pH and mobilise nutrients like P.

This creates a niche that supports microorganisms adapted to lower pH environments, particularly P-solubilising and N-fixing bacteria (Toljander et al., 2007). Mycorrhizal fungi establish symbiotic relationships with these bacteria, enhancing processes such as P solubilisation and N fixation (Artursson et al., 2006). The selective pressures exerted by the hyphae encourage the growth of microbes that either contribute to or benefit from these symbiotic interactions, such as mycorrhizal-helper bacteria and certain fungi involved in nutrient cycling and pathogen suppression. A well-studied example of such interactions is the synergistic relationship between AM fungi and rhizobia, which can significantly enhance plant growth (Frey-Klett et al., 2007).

AM fungi, including *R. irregularis*, are vital for nutrient transport and mobilisation within the hyphosphere. These fungi form a complex mycorrhizal network which significantly extends the root system of plants, greatly enhancing nutrient uptake, especially phosphorus (Gianinazzi et al., 2010). The extension of the root system increases the surface area available for nutrient absorption (Khaliq et al., 2022). The expanded network not only improves nutrient uptake but also enhances plant health by increasing drought tolerance and resistance to pathogens in the soil (Begum et al., 2019). Furthermore, the presence of fungal hyphae contributes to the modification of soil structure by promoting the formation and stabilisation of soil aggregates, which improves soil porosity, water retention, and root penetration;this process is less common in the rhizosphere, which makes AM fungi unique in the soil ecology (Rillig and Mummey, 2006). The structural changes are important for the long-term health of soils and plants.

As an extension to the root system, hyphae of the AM fungi release different kind of exudates and enzymes that play an important role in solubilisation of Pi and mineralisation of Po (Smith et al., 2011). Beyond P cycling, the hyphosphere also impacts the C and N dynamics within the soil. AM fungi interact closely with N-fixing bacteria results in a better N availability, which is also vital for plant growth (Basiru et al., 2023). Additionally, AM fungi contribute to the stabilization of organic C in the soil through processes such as competing with decomposers for C resources, which reduces the decomposition rate of organic matter. They also store C provided by plants within the fungal biomass, which makes it less prone to rapid decomposition compared to other forms of organic matter, hence contributing to longer-term C storage in the soil (Averill et al., 2014). These interactions combined not only enhance soil fertility but also boost plant nutrient uptake, which is particularly important in nutrient-deficient soils.

The hyphosphere is a critical zone within the soil environment, which plays a crucial role in plant-microbe interactions, nutrient cycling and soil structure. A better understanding of the processes occurring within this zone can help researchers develop more effective strategies to maintain soil health and improve crop yields without the excessive use of chemical fertilisers, thereby contributing significantly to sustainable agriculture (Wang et al., 2022).

Among AM fungi, *R . irregularis* is one of the most widely studied species due to its broad host range, ability to form symbioses with many plant species, and the availability of genomic resources. The genome of *R. irregularis* lacks many plant cell wall-degrading enzymes, reflecting its obligate biotrophic lifestyle (Tisserant et al., 2013). It also possesses genes encoding phosphate transporters, lipid metabolism enzymes, and symbiosis-related signaling pathways, making it an ideal model for studying nutrient uptake and symbiotic interactions (Fiorilli et al., 2013; Wewer et al., 2014). Therefore, *R. irregularis* was selected in this study to investigate its interactions with microbes in the hyphosphere.

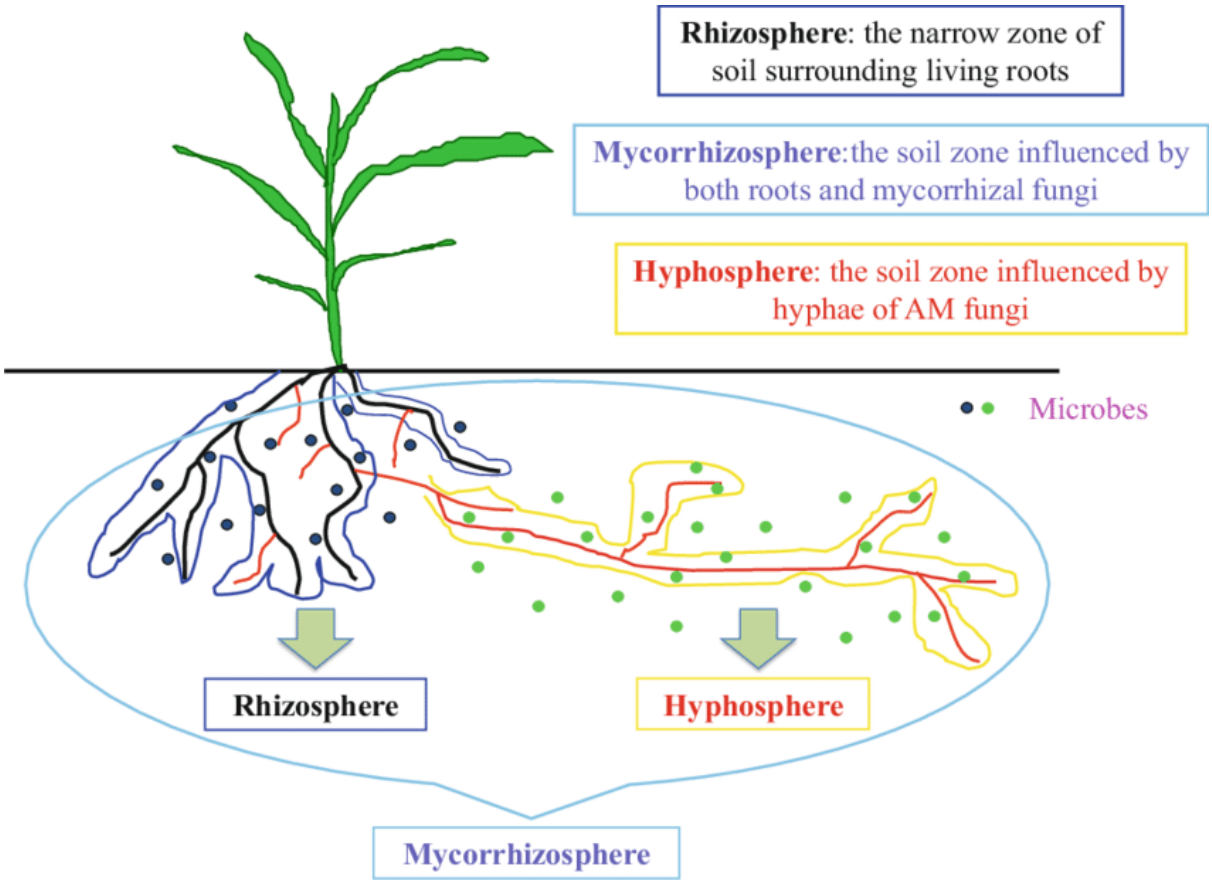

Figure 1.5 Diagram of rhizosphere, mycorrhizosphere and hyphosphere. Figure from Wang (2014).

1.4 Phosphorus solubilisation by microbes

The main processes involved in the soil P release include (1) precipitation-dissolution (Ca, Fe, Al phosphates); (2) sorption-desorption (clays minerals, Al/Fe oxides); and (3) immobilisation-mineralisation (conversions of P between organic and inorganic forms mediated by microorganisms) (Sharma et al., 2013). Microbes enhance P solubilisation through (1) releasing complexing or mineral dissolving compounds such as organic acid anions, siderophores, protons (H^+), hydroxyl ions (OH^-) as well as CO_2; (2) secreting extracellular enzymes like phosphatases that drive biochemical P mineralisation; and (3) releasing P during organic matter decomposition, a process known as biological P mineralisation (McGill and Cole, 1981).

1.4.1 Inorganic P solubilisation

Pi solubilisation by P-solubilizing microorganisms (PSM) primarily occurs through the production of organic acids. Organic acids achieve this by (i) lowering pH, (ii) enhancing chelation of P-bound cations responsible for P precipitation, (iii) competing for adsorption sites on soil particles, and (iv) forming soluble complexes with metal ions associated with insoluble P compounds (e.g., Al, Ca, Fe phosphates), leading to P release (Sharma et al., 2013).

Organic acids: Organic acids are the product of the microbe's metabolism, which mainly comes from the fermentation of organic carbon sources such as glucose or by oxidative respiration (Trolove et al., 2003). Organic acids can chelate the Al, Ca, Fe ions associated with P to release P as well as dissolve the mineral P directly by anion exchange using acid anion (Sharma et al., 2013). Additionally, the monovalent anion phosphate ($H_2PO_4^-$) is the predominant form of soluble inorganic phosphate under low pH conditions. Secretion of organic acids by phosphate-solubilizing microorganisms (PSM) acidifies the surrounding soil environment, results in the release of P from the P mineral by substituting the cation bound to phosphate by H^+ (Goldstein, 1994). The main organic acids involved in the insoluble P solubilisation are aspartic acid, citric acid, gluconic acid, lactic acid, oxalic acid and tartaric acid (Kim et al., 1997). Whitelaw et al. (1999) used gluconic acid and HCl to solubilise P and proved that chelation of Al^{3+} by gluconic acid plays a role in the colloidal Al phosphate solubilisation.

Besides organic acids, inorganic acid can also solubilise the insoluble P. Kim et al. (1997) had reported that adding HCl artificially can also solubilise P from hydroxyapatite; however, it solubilised less P compared to oxalic acid or citric acid under the same pH. Furthermore, Azam and Memon (1996) reported that bacteria from the genera *Nitrosomonas* and *Thiobacillus* can produce nitric and sulfuric acids to dissolve phosphate compounds.

PSM can produce H_2S, which can release phosphate when the H_2S reacts with ferric phosphate ($FePO_4$) to form ferrous sulphate ($FeSO_4$) (Swaby and Sperber, 1958). It was reported that PSM can assimilate/remove the P from the liquid solution, which can cause the indirect dissolution of calcium phosphate ($Ca_3(PO_4)_2$) triggered by P removal (Illmer et al., 1995).

Parks et al. (1990) suggested that proton released (H^+ excretion) from the assimilation of NH_4^+ is another mechanism for solubilising P other than the release of organic acids. Illmer and Schinner (1995) analysed the culture solution of *Penicillium aurantiogriseum* and *Pseudomonas sp.* (PI1889) using HPLC and found that no organic acid was detected while solubilisation of P occurred, they reported that the reason for this was the release of protons following NH_4^+ assimilation or cellular respiration. Furthermore, in an experiment, two fungi, *Penicillium bilaji* and *Penicillium cf.fuscum,* were used to test for the ability of solubilising rock phosphate without N addition or with NH_4^+ present. The result indicated that *P. bilaii* was the only organism which could decrease the pH and mobilise P without N added (Asea et al., 1988). However, in another study, Park et al. (2009) used *Pseudomonas fluorescens* RAF15 to test the ability to solubilise insoluble P under different C supply (glucose/fructose) and N supply (e.g. NH_4^+/ NO_3^-) , and found no clear differences in pH and P solubilisation between the microbes in the glucose-ammonium and glucose-nitrate media, whilst glucose made a greater difference compared to fructose, which indicates that organic acid production is directly correlated with the proton release for the solubilisation of P. Here we have two possible mechanisms: organic acid production (aforementioned) and proton excretion from ammonium assimilation. Thus, different species utilize various mechanisms for proton release, with some depending on the presence of NH_4^+. In fact, both excretion of H^+ originating from assimilation of NH_4^+ and respiratory production of H_2CO_3 has been suggested as metabolic pathway for acid-mediated solubilisation of calcium phosphate (Jurinak et al., 1986).

Siderophores. Siderophores are produced by majority of microorganisms when iron deficiency occurs. PSM have been reported to produce siderophores (Hamdali et al., 2008; Vassilev et al., 2006); however, the production of siderophores is not yet well recognised as a mechanism of P solubilisation. Although the ligand exchange by organic acid anions is the dominant mechanism, potential of siderophore production involved in increasing the solubility of P should be considered in the future.

Exopolysaccharides (EPS). EPSs are polymers which consist of carbohydrates and secreted by bacteria and fungi. The structure and composition of EPS varies, and they can be either homopolysaccharides or heteropolysaccharides; moreover, they may also contain many different organic and inorganic substituents (Sutherland, 2001). Yi et al. (2008) used four bacterial strains: *Enterobacter sp.* (EnHy-401), *Arthrobacter sp.* (ArHy-505), *Azotobacter sp.* (AzHy-510) and *Enterobacter sp.* (EnHy-402) that harbour the ability to solubilise tricalcium phosphate (TCP), to assess the function of EPS in P solubilisation. All the strains demonstrated strong P-solubilising ability and produced a large amount of EPS, so they suggested that EPS has the ability of holding P; however, the correlation between P solubilisation and production of EPS is still unclear, which means further studies are required to fully understand the potential of EPS for phosphorus solubilisation.

It has been suggested that the oxidation of glucose leads to the production of gluconic acid in the periplasmic space, which results in acidification of the surrounding environment. Thus, extracellular acidification via the direct oxidation pathway plays a role in soils where the significant amounts of insoluble calcium phosphate ($Ca_3(PO_4)_2$) exist (Goldstein, 1995).

1.4.2 Organic P solubilisation

Solubilisation of organic P (Po) is also called mineralisation of organic P. Typically, Po accounts for 35% to 65% of the total phosphorus in soils, with this proportion occasionally reaching up to 90% in soils that are managed organically (Khan et al., 2009; Zhang et al., 2024a). Soil Po mineralisation plays an important role in agriculture.

Po in soil can be released by enzymes:

a) **Non-specific acid phosphatases (NSAPs)**: NSAPs can dephosphorylate phosphoester or phosphoranhydride bonds of the organic matter. Phosphomonoesterases, commonly referred to as phosphatases, are the most studied and abundant

enzymes released by PSM for organic P mineralisation (Nannipieri et al., 2011). These enzymes can be classified into acid phosphomonoesterases as well as alkaline phosphomonoesterases, both of which can be produced by PSM depending on the environment (e.g. pH) (Kim et al., 1998). According to Eivazi and Tabatabai (1977), in general, acid phosphatases mainly exist in acidic soils while alkaline phosphatases are predominant in alkaline and neutral soils. Plant roots produce acid phosphatases however they rarely produce alkaline phosphatases. Criquet et al. (2004) suggested that PSM potentially play a role in producing alkaline phosphatases. Also, it is hard to differentiate whether the phosphatases in the soil are produced by PSM or the roots (Richardson et al., 2009a; 2009b). Tarafdar et al. (2001) tested the efficiency of acid phosphatases produced by fungi and plants against Po compounds, the results indicated that acid phosphatase produced by microbes are more efficient than that generated from the plant sources; however, the relationship between PSM in soil and Po mineralisation remains largely unclear.

b) **C–P lyases and phosphonatases,** enzymes which break the C–P bond in the organo-phosphonates (Rodríguez et al., 2006).

c) **Phytases**: Phytases specifically degrade the phytate (inositol hexakisphosphate), which causes the release of Po (Gerke, 2015). Phytate is a major storage form of P in plants (pollen and seeds) and main source of inositol (Skoglund et al., 2009). It is also a major component of Po in the soil (Richardson, 1994). Plants normally do not acquire P from phytate directly because of their limited capability; however, Richardson et al. (2001) found out that the P-nutrition and growth of pasture plants (*Danthonia richardsonii* and *Phalaris aquatica*) supplied with phytate was significantly enhanced when inoculated with either total soil microorganisms or a specific strain, *Pseudomonas sp.* strain CCAR59, that has the ability to release the phosphate from phytate. Hence, microorganisms in the soil are a key driver in mineralising phytate and they can compensate the plants which cannot obtain P directly from phytate (Richardson and Simpson, 2011).

In conclusion, although the solubilisation of P by the PSM has been studied extensively over the decades, many aspects remain inadequately understood. PSM employ various mechanisms to solubilise insoluble P in the soil, and these mechanisms can vary significantly among different species, with some microorganisms utilizing multiple pathways simultaneously. Identifying a single predominant mechanism is challenging because

each plays a crucial role in the overall process of P solubilization and mineralization, as illustrated in Figure 1.6.

Furthermore, PSM act not only as agents of P solubilization but also serve as temporary P sinks. They become a source of P for plants when P is released from their cells due to factors such as environmental changes, predation, or starvation (Sharma et al., 2013). Notably, Butterly et al. (2009) observed significant increases in available P—referred to as flush events—resulting from massive cell lysis triggered by environmental stresses like freezing–thawing and drying–rewetting cycles. These findings highlight the vital role of PSM in soil phosphorus dynamics and emphasize the need for further research to fully clarify their mechanisms—particularly the role of EPS, siderophores, and enzyme-mediated processes—and their contributions to plant nutrition.

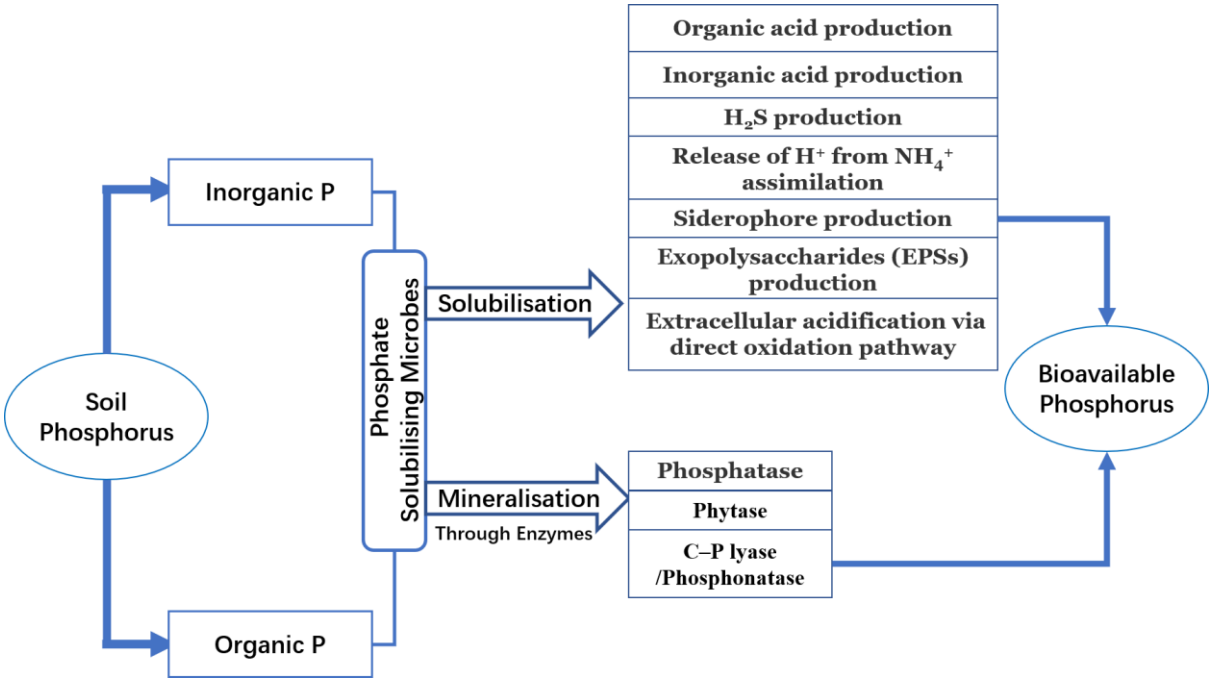

Figure 1.6. Mechanisms of solubilisation/mineralisation of insoluble soil P by PSM.

1.5 Nitrogen fixation by microbes

Nitrogen gas (N_2) makes up around 78 % of the of the Earth's atmosphere, but it is not directly available to plants (Gupta et al., 2015). Plants cannot directly utilise atmospheric N_2 or convert it into ammonia for growth (Gupta et al., 2015). In order to convert the atmospheric N_2 into utilisable form, a biological process called biological nitrogen fixation (BNF) is needed, which converts nitrogen (N_2) to ammonia (NH_3) through nitro-

gen-fixing bacteria using a complex enzyme system called nitrogenase (Gaby and Buckley, 2012). BNF mainly occurs at mild temperatures, and is widespread in natural habitats (Raymond et al., 2004). Moreover, BNF also presents an important role as an alternative of chemical fertilisers (Ladha et al., 1997).

Nitrogen-fixing PGPR can provide fixed nitrogen to plants via two mechanisms: symbiotic and non-symbiotic (Gupta et al., 2015).

Symbiotic nitrogen fixation: Symbiotic nitrogen fixation involves a mutualistic relationship between microbes and plants. In this relationship, the microbes enter the plant roots and form nodules where the nitrogen fixation takes place (Gupta et al., 2015). Symbiotic N_2-fixing bacteria , such as members of the Rhizobiaceae family, form symbioses with leguminous plants (e.g., *Medicago*), while *Frankia* associates with non-leguminous trees (Zahran, 2001). Rhizobia refers to a large group of rhizobacteria that form a symbiotic relationship by the colonisation and formation of root nodules (Figure 1.7) with leguminous plants (Gupta et al., 2015). The PGPR (i.e., root-nodule bacteria), which widely act as symbionts can be classified into four genera: *Rhizobium, Bradyrhizobium, Mesorhizobium and Sinorhizobium* (Zahran, 2001).

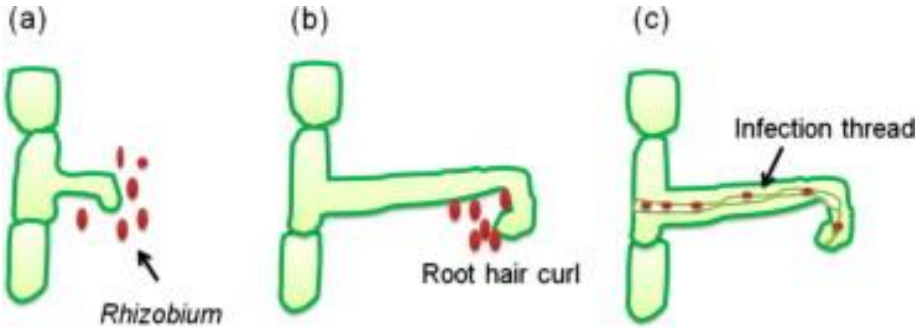

Figure 1.7 The process of nodulation. (a) Rhizobia attach to root cells. (b) Rhizobia excrete nodulation factors, which causes root hair curl. (c) Rhizobia penetrate root hair and infect/penetrate the cortical cells and form the bacteroid state, thus, nodules are formed. Figure from Ahemad and Kibret (2014).

Non-symbiotic nitrogen fixation: Non-symbiotic nitrogen fixation is performed by free-living bacteria that can promote plant growth in various crops, including radishes and rice (Gupta et al., 2015). Free-living PGPR that fix N_2 in non-leguminous plants are known as diazotrophs, which can form non-obligate relationships with their host plants (Glick et al., 1999). The non-symbiotic nitrogen-fixing bacteria come from genera such

as cyanobacteria (e.g. *Anabaena*, *Nostoc*), *Acetobacter*, *Azospirillum*, *Azotobacter*, *Azomonas, Beijerinckia*, *Burkholderia*, *Enterobacter*, *Gluconoacetobacter*, *Pseudomonas* and *Azoarcus*, etc. (Madigan et al., 2008; Gupta et al., 2015; Bhattacharyya and Jha, 2012); however, it was suggested that the non-symbiotic nitrogen-fixing bacteria only provide a small amount of the fixed nitrogen that is required by the host plants (Glick, 2012), Khan et al. (2021); Reed et al. (2011) estimated that free-living nitrogen fixation contributes approximately 1–20 kg N ha^{-1} yr^{-1} at the biome scale. In contrast, symbiotic nitrogen fixation can reach up to 150 kg N ha^{-1} yr^{-1}.

The N_2 fixation is facilitated by the complex enzyme system known as nitrogenase (Kim and Rees, 1994). Nitrogenase is the only enzyme family which is known to catalyse this reaction. According to Hoffman et al. (2014), all the nitrogenases are two-component metalloenzymes. This two-component system consists of **component I**: dinitrogenase which has a metal cofactor and **component II**: dinitrogenase reductase which is a Fe protein. Dinitrogenase reductase transfers the electrons with high reducing power to dinitrogenase, after which, the dinitrogenase would use these electrons for the reduction of N_2 to NH_3 (Ahemad and Kibret, 2014). Three types of nitrogenase have been identified in nitrogen-fixing bacteria, differentiated by the metal cofactors in component I: (a) molybdenum (Mo) nitrogenase, (b) vanadium (V) nitrogenase, and (c) iron-only (Fe) nitrogenase (Peters and Szilagyi, 2006).

The Component I is an MoFe protein in molybdenum nitrogenase, and Hoffman et al. (2014) suggested that two metal clusters are included in MoFe protein: (a) the iron–molybdenum cofactor (FeMo-co), which provides the active site for binding the substrate and reduction, and the (b) P-cluster, which is involved in electron transfer from the Fe protein (component II) to FeMo-co (component I). For vanadium (V-) and iron-only (Fe-) nitrogenases, the Mo in the iron–molybdenum cofactor (FeMo-co) is replaced by V or Fe (only Fe in the iron-only (Fe-) nitrogenases). Different bacterial genera will apply different N_2-fixing systems, either Mo-, V-, or Fe -nitrogenase, molybdenum nitrogenase, among these three, is the one that has been extensively studied and well characterised (Franche et al., 2009). The molybdenum nitrogenase can be found in all diazotrophs (Bishop and Joerger, 1990). In some bacterial species of *Azotobacter*, vanadium nitrogenase and iron-only nitrogenase were also found as an alternative of molybdenum nitrogenase (Franche et al., 2009).

The reaction of nitrogen fixation in molybdenum nitrogenase is highlighted in Equation 1. Sippel and Einsle (2017) proposed another different equation specifically for the vanadium (V) nitrogenase (Equation 2). In here, vanadium (V) nitrogenase drives a bigger portion of the electrons from the Fe protein against the formation of H_2 compared to the molybdenum (Mo) nitrogenase.

$$N_2 + 8\,H^+ + 8\,e^- + 16\,MgATP \rightarrow 2\,NH_3 + H_2 + 16\,MgADP + 16\,Pi$$

Equation 1

$$N_2 + 14\,H^+ + 12\,e^- + 40\,MgATP \rightarrow 2\,NH_4^+ + 3\,H_2 + 40\,MgADP + 40\,Pi$$

Equation 2

The typical nitrogen cycle, which benefits plant growth, involves several transformations. Ammonia (NH_3) is converted into ammonium (NH_4^+) when it mixes with water in the soil, then the nitrifying bacteria convert the ammonium ions (NH_4^+) into nitrites (NO_2^-) and then nitrates (NO_3^-) , which are easier for plants to absorb (Galloway et al., 2004).

Nitrogen fixation genes, known as *nif* genes, are present in both symbiotic and free-living diazotrophic microorganisms (Kim and Rees, 1994; Reed et al., 2011). The main product of the *nif* genes is the nitrogenase enzyme complex. Nitrogenase (*nif)* genes include the structural genes, which are involved in the Fe protein activation, biosynthesis of iron molybdenum cofactor (i.e., FeMo-co) and the donation of electron (Gupta et al., 2015); moreover, the *nif* genes also include the regulatory genes which are required for the synthesis and function of the enzyme (Ahemad and Kibret, 2014; Gupta et al., 2015). The cluster of *nif* genes is normally found to be around 20–24 kb and include seven operons which encode 20 different proteins (Glick, 2012; Ahemad and Kibret, 2014). *Klebsiella pneumoniae* was the first diazotroph in which the *nif* genes had been identified and analysed by combining both genetic and biochemical techniques (Roberts et al., 1978; MacNeil et al., 1978). According to Rubio and Ludden (2008), the twenty *nif* genes, *nifJHDKTYENXUSVWZMFLABQ*, are clustered in a single 23-kb region in the *K. pneumoniae* chromosome, moreover, they are organised in several transcriptional units (Figure 1.8). The structural component proteins of the molybdenum nitrogenase enzyme

complex is encoded by *nifDKH* genes. The functions of each *nif* gene have been described elsewhere (Rubio and Ludden, 2008; Kim and Rees, 1994), whilst this section will only briefly describe some aspects related to the molybdenum nitrogenase enzyme complex.

The MoFe protein is a tetramer (α2β2) protein with a total molecular mass of around 240kDa, which is formed by two αβ dimers. The α and β subunits are encoded by the *nifD* and *nifK* genes, respectively (Kim and Rees, 1994). One iron molybdenum cofactor (FeMo-co) is bound within the active site of each α-subunit (NifD) in the NifDK (Rubio and Ludden, 2008). The Fe protein is a dimeric protein with total molecular mass of around 60kDa, which has two identical subunits encoded by *nifH* gene. Each subunit folds as an α helix or β sheet type as a single domain (Kim and Rees, 1994). According to Rubio and Ludden (2008), the products from at least 12 *nif* genes are required for the catalytically active molybdenum nitrogenase biosynthesis (Figure 1.8) due to the complex and unique structure of FeMo-co and the P-cluster (Rubio and Ludden, 2005). Besides, it was also suggested that some gene products from *nif* genes also provide electrons to nitrogenase. In *K. pneumoniae*, this role is fulfilled by the pyruvate:flavodoxin oxidoreductase (NifJ) and the flavodoxin (NifF) (Shah et al., 1983). Furthermore, *nifA* and *nifL* genes form the products which together act as an activator/antiactivator regulation system, which would control the expression of *nif* gene and ensure that the expression of *nif* gene only occurs when the environmental conditions are physiologically appropriate (Martinez-Argudo et al., 2004).

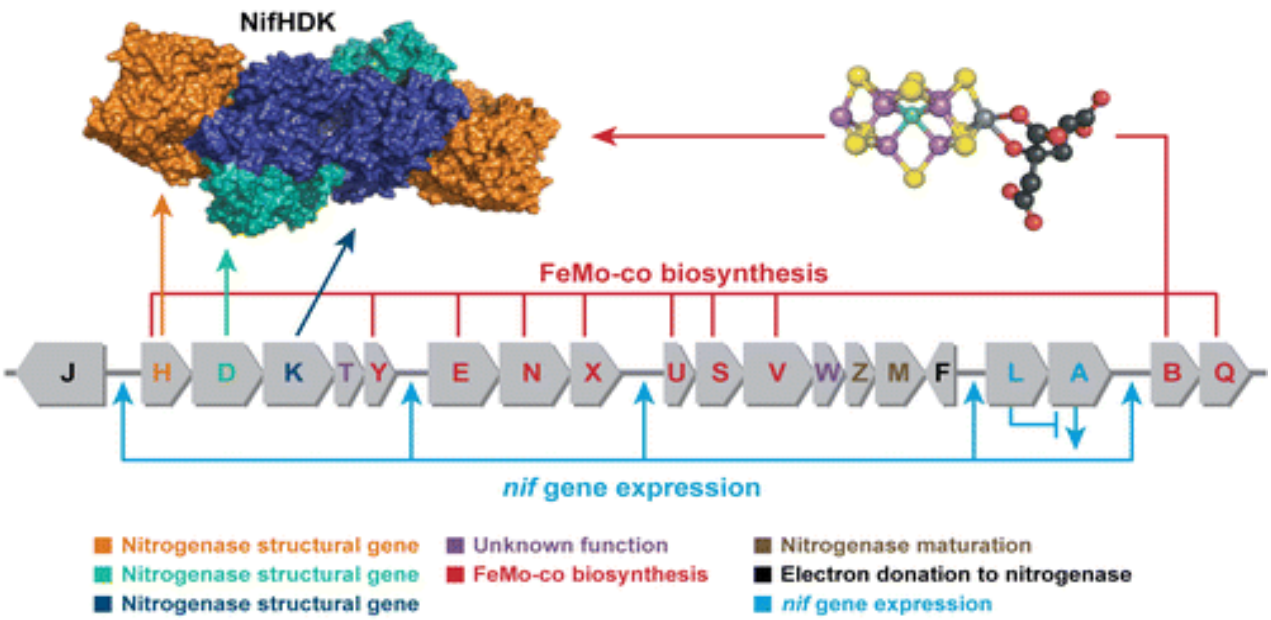

Figure 1.8 *Nif* genes of *Klebsiella pneumoniae*. The genes which encode the component proteins of nitrogenase, *nifDKH*, are highlighted on the left. All the genes are colour coded based on their function in the nitrogen fixation process. Figure from Rubio and Ludden (2008).

Because this system is highly complicated, the genetic strategies to improve nitrogen fixation have not yet been well established. However, scientists believe that once the *nif* genes are well isolated and characterized, is highly possible to improve the nitrogen fixation through genetic engineering (Glick, 2012). It is well known that nitrogen fixation requires at least 16 mol of ATP to reduce each mole of nitrogen (N_2) (Equation 1). Glick (2012) proposed that if the carbon resources of bacteria can be directed toward oxidative phosphorylation, which results in the ATP synthesis, instead of the glycogen synthesis to store the energy in the glycogen form, it would be of great advantage. In a previous study, Marroquí et al. (2001) deleted the gene for glycogen synthase (*glgA*) in one strain of *Rhizobium tropici*, and inoculated this engineered bacterium with legume plants. Results indicated that both the number of nodules formed as well as the plant dry weight were increased compared to the plants treated by wild-type strain. However, although the mutant's nodule number and plant biomass have been increased in the field, it did not seem to grow and survive well in the natural soil environment. This is one of the few examples in which scientists tried to genetically modify a bacterium while also obtaining increased fixed nitrogen levels.

Nitrogenase is highly sensitive to oxygen (O_2), as dinitrogenase reductase can be rapidly and irreversibly inactivated by O_2 (Madigan et al., 2008). Therefore, diazotrophs employ

mechanisms that ensure a sufficient O_2 supply for energy needs while protecting nitrogenase from the negative effects of O_2 (Ahemad and Kibret, 2014). According to Lucía and Baca (2001) and Madigan et al. (2008), they have several strategies to limit O_2 access to nitrogenase: 1) avoid O_2 by living in permanent anoxic environments and growing anaerobically; 2) by forming a physical barrier (O_2-retarding slime layers) around the nitrogenase in order to prevent O_2 from diffusing to the enzyme; 3) reducing the concentration of O_2 in the surrounding of the nitrogenase enzyme by high rates of metabolism (respiration); 4) in aerobic nitrogen fixers like *Azotobacter*, the nitrogenase can be protected from the O_2 by complexing with a specific protein in a process called conformational protection, which is reversible; when the O_2 level is not at inhibitory level the protected nitrogenase would become active once again. In certain cyanobacteria, nitrogenase is compartmentalised in a special type of cell, which is called the heterocyst (Madigan et al., 2008). Moreover, is also possible to introduce bacterial hemoglobin into the *Rhizobium*. Ramírez et al. (1999) transformed the *Rhizobium etli* with the hemoglobin gene, which encodes an oxygen-binding protein, from *Vitreoscilla sp.* (a Gram-negative bacterium), and observed that, at low oxygen levels, bean plants inoculated with the strains with hemoglobin gene had higher nitrogenase activity as well as the total nitrogen content (68% and 14 to 53%, respectively) compared to the plants inoculated with the non-transformed strains; they concluded that the synthesis of hemoglobin in *R. etli* had stimulated the respiratory efficiency of free-living rhizobia, probably also the bacteroids in the nodule, which resulted in higher symbiotic nitrogen fixation levels.

1.6 Overview and aims of the thesis

This thesis aims to investigate the interactions between plants and soil microbes in various contexts, with a particular focus on (1) the impact of fungal inoculation on soil microbial communities; (2) the influence of root exudates on soil microbiomes; and (3) the effect of bacteria on plant growth promotion (Figure 1.9). The research aims to better understand how plants and microbes interact and to help create ways to improve plant growth and soil health for more sustainable agriculture.

The first research chapter (**Chapter 2**) begins with the analysis of the effect of *Rhizophagus irregularis*, an arbuscular mycorrhizal (AM) fungus, on the hyphosphere microbial community. This was part of a larger, collaborative, project with a broader aim to model

P transport by mycorrhiza between the soil and plant, but the focus of this chapter is specifically to study how AM fungi inoculation affects the structure and diversity of microbial communities within the soil. Follow-up experiments are performed to determine whether the observed decrease in fungal abundance following *R. irregularis* inoculation is caused by the production of inhibitory compounds by *R. irregularis* or by competition for nutrients.

Whereas in Chapter 2 the aim is to investigate the role of AM on the hyphosphere community, **Chapter 3** focuses on the effect of root exudates on the microbial community. Here I focus on the effects on the bacterial community and compare artificial root exudates and natural exudates. Natural exudates differ in composition but also contain various compounds that may broadly inhibit microbial activity. The effect of MBOA, a breakdown product of a common allelopathic compound released by plant roots, is tested. Finally, I look at the distance effects of exudates by studying the impact of soil volatiles, produced from the addition of artificial root exudates, on the microbial community.

Finally, **Chapter 4** aims to isolate plant-growth promoting bacteria. These will be selected for plant growth-promoting traits (i.e., P solubilisation, IAA production) followed by tests of their ability to influence *Arabidopsis thaliana* growth, which is a model plant. Their genomes will be sequenced to determine their phylogeny and identify potential functions. The longer-term goal, which was not achieved in this study due to time constraints, is to reintroduce these into the model systems tested in Chapters 2 and 3 to determine how they respond to AM fungal growth, plant root exudates, and how they potentially influence the microbial community.

These points highlight the project's aim to uncover the complex dynamics between plants, fungi, and microbes in the soil environment, with a particular focus on how these interactions can be harnessed to improve plant growth and soil health.

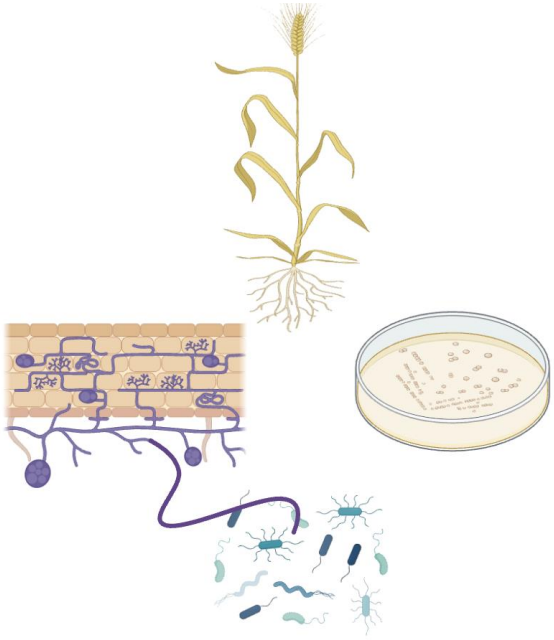

Figure 1.9 Conceptual overview of the thesis. Wheat plants (top) interact with mycorrhizal fungi (left), which influences the hyphosphere community (bottom); these effects are explored in Chapter 2. The wheat plants, through release of exudates, can also influence the diversity of microbes in the rhizosphere, which is investigated in Chapter 3. Among these organisms are plant growth-promoting bacteria (PGPB), which can be cultivated (image right, and performed in Chapter 4). PGPB can be inoculated into soil systems, which may result in either successful or unsuccessful establishment partly because of the microbiome interactions investigated in Chapters 2 and 3. Long-term goals will be to inoculate the PGPB isolated in this study into crop systems to investigate their interaction with microbiomes and ability to promote crop health. Figure was made using Biorender.

Chapter 2 The effects of arbuscular mycorrhizal fungi on the hyphosphere microbial community

Abstract

Arbuscular mycorrhizal fungi (AMF), particularly *Rhizophagus irregularis*, are known to enhance plant nutrient acquisition and influence microbial communities in the soil. However, their effects on the fungal and bacterial composition of the hyphosphere — an extension of the rhizosphere influenced exclusively by AM hyphae — remain insufficiently understood. This chapter aimed to evaluate the impact of *R. irregularis* inoculation and nutrient availability on soil microbial communities associated with wheat (*Triticum aestivum*), focusing on bacterial abundance, fungal suppression, and potential competition with native fungi.

Using a root-hyphal chamber system, wheat was grown under nutrient-rich (P+/MS+) and nutrient-deficient (P−/MS−) conditions with or without AM fungal inoculation. 16S amplicon sequencing and qPCR revealed that *R. irregularis* inoculation significantly altered bacterial community structure without affecting overall bacterial abundance. Proteobacterial taxa such as Sphingomonadaceae and Devosiaceae were enriched, with some families shared between nutrient treatments and others unique to either P+ or P− conditions. Fungal responses were more variable: while ITS sequencing showed little inoculation effect, 18S analysis revealed a significant reduction in the abundance of common soil fungi (Ascomycota, Basidiomycota, and Mucoromycota) following inoculation.

Notably, hyphal counts suggested *R. irregularis* may suppress native fungal growth, potentially through nutrient competition or secretion of inhibitory compounds. Furthermore, *R. irregularis* was undetectable in sequencing datasets despite clear microscopic evidence of colonisation, likely due to primer mismatches and off-target amplification. The broader underrepresentation of Glomeromycota across datasets underscored the limitations of universal primers. Future studies could employ qPCR or metagenomics for improved detection.

Collectively, these findings demonstrate that *R. irregularis* exerts a strong influence on the hyphosphere microbiome. Understanding these interactions is critical for developing AMF-based strategies to enhance soil health and sustainable crop production.

2.1 Introduction

Wheat is considered one of the most important crops around the world (Kavamura et al., 2021), which is among the first batch of domesticated crops between 7000 and 9000 BCE (Bell, 1987). *Triticum aestivum*, which is also known as common wheat or bread wheat, is widely cultivated globally and has more than 20,000 known varieties (Kavamura et al., 2021). Human beings started growing food between 10,000 and 4000 years ago, which directly led to the wild crop domestication and the emergence and early development of agriculture (Taiz, 2013). The progress of agriculture also boosted the growth of global population, which increases every year, although it is slower now than at any time since 1950. From an estimate of 7.7 billion people worldwide in 2019, the global population was expected to grow to around 8.5 billion in 2030 (United Nations-Department of Economic and Social Affairs-Population Division, 2019). Wheat is a major global crop. In order to meet the large food demand of the increasing population, the yield of wheat is required to increase by 11% between 2017 and 2026, but cultivation areas can only be increased by 1.8% (OECD/FAO, 2017). Furthermore, the United Nations predicted that population size will exceed 9.7 billion by 2050 (United Nations-Department of Economic and Social Affairs-Population Division, 2019).

A more sustainable method for agriculture is urgently needed to cope with the fast-growing population. It is well known that plants can be colonised by microorganisms that may bring potential benefits to the host plants (Kavamura et al., 2021). This characteristic can be explored and used to develop bio-fertilizers that provide higher yields at the same time avoid the use of chemical fertilisers (Misra et al., 2020) .

The term arbuscular mycorrhizal fungi (AMF) refers to the fungi that cannot live alone but grow in association with a living plant (Wang and Feng, 2021). In nature, around 80% of terrestrial plant species can be colonised by AM fungi and develop symbioses (Smith and Read, 2008). AM fungi are considered as obligate biotrophs that cannot grow alone without a plant since they need carbon (C) supply through the photosynthates from the host plant (Smith and Read, 2008).

AM colonisation has been studied widely. In order for the AM fungi to colonise plants, strigolactone hormones are exuded from plant roots, which stimulates spore germination, metabolism and hyphal branching of AM fungi (Akiyama et al., 2005; Besserer et

al., 2006). The hormone also stimulates the release of signalling molecules called lipochitooligosaccharide (Genre et al., 2013), which is also known as mycorrhizal (Myc) factors, which are recognised by receptors on the host plant (Kosuta et al., 2003). Signals from the host receptors are transmitted through a transcriptional activation pathway that is common to AM fungi colonization (Stracke et al., 2002). Plant epidermal cells then produce a sub-cellular structure that is called the pre-penetration apparatus (PPA), under the chemical and mechanical stimulation from the hyphopodia of AM fungi (Genre et al., 2005). PPA predicts the entry pathway of fungal hyphae. The hyphae travel through the epidermal cells of roots, then pass between the underlying cells and enter inner cortical cells eventually. After entering cortical cells, the hyphae branch repeatedly and arbuscules are formed, which serve as the structures for nutrient exchange (Smith and Read, 2008; Parniske, 2008)

Colonisation of AM fungi brings up many positive effects, including that it can improve tolerance to many abiotic stress (e.g. salt and drought) (Nelsen and Safir, 1982; Feng et al., 2002) and biotic stresses (mainly soil-borne pathogens) (Sikes, 2010). Improvement in drought tolerance in the colonised plants can be explained by its effects on the plant water relations (Augé, 2001; Ruiz-Lozano et al., 1995) and improved phosphorus nutrition (Nelsen and Safir, 1982). The improved tolerance of AM fungi-colonised plants to salt stress was suggested due to the soluble sugar accumulation in the roots (Feng et al., 2002), maintenance of K/Na ratios (Giri et al., 2007) and enhancement in nutrient (e.g., P, Zn, Cu, Mn, and Fe) uptake (Al-Karaki and Al-Raddad, 1997; Evelin et al., 2009).

Plants colonised with AM fungi were found to have better resistance against a wide range of soil pathogens, particularly root pathogens (Jacott et al., 2017). The mycorrhizal fungi in the root can establish mycorrhizal-induced resistance (MIR), a type of priming that make colonized plants more resistant to soil pathogens. It was shown that AM-colonised plants had reduced disease caused by various pathogens such as *Fusarium, Rhizoctonia, Pythium, Phytophthora*, pathogenic bacteria and parasitic nematodes (Pozo and Azcón-Aguilar, 2007; Sikes, 2010). Besides, AMF-colonised plants change root morphology and secrete root exudates that could decrease pathogen virulence, or alter the soil microbial community and prevent soil pathogens from growing. Lastly, the colonisation of the roots by mycorrhizal fungi could prevent the infection and establishment of other root pathogens.

Most importantly, AM symbiosis can improve nutrient acquisition. AM fungi play an important role in the acquisition of microelements by plants. Previous studies had shown that the acquisition of Cu and Zn by the mycorrhizal (extraradical) hyphae account for 25% of the total Zn uptake in maize in an experiment which used compartmented microcosms and 53–62% of the total Cu uptake in the white clover (Kothari et al., 1991; Li et al., 1991). Moreover, Caris et al. (1998) studied the effect of an AM fungus on iron (Fe) uptake of sorghum (*Sorghum bicolor* L.) using ^{59}Fe and found that the concentration of ^{59}Fe in the shoots of mycorrhizal sorghum plants increased, which proved that inoculation of the AM fungus significantly affected ^{59}Fe concentration in the shoots of sorghum plants. The finding suggested that Fe can be mobilised by the external hyphae of AM fungi from the hyphal compartment and taken by the host plants.

It is well known that AM symbiosis has great contribution in the nitrogen uptake by the plants, ammonium and nitrate ions are easy to get to the root via diffusion compared to phosphate in the soil (Jin et al., 2012; Hodge and Storer, 2015). Studies using ^{15}N-labeled compounds also confirmed that the external hyphae of AM fungi absorb inorganic N in the form of NO_3^- (Tobar et al., 1994) as well as NH_4^+ (Johansen et al., 1994; Toussaint et al., 2004); moreover, it can also absorb organic N as amino acids (Hawkins et al., 2000). The N absorbed by the AM fungi is then transferred to host plants.

Besides, AM fungi are mobilisers of sparingly soluble P, AM fungi can mobilise insoluble P from soil through: (1) releasing protons, organic acids, as well as phosphatases, and (2) extending mycelia (Wang and Feng, 2021). Wang et al. (2013) reported that acidification of the hyphosphere induced by NH_4^+ absorption through the mycelia of AM fungi resulted in the increase of phosphatase activity; the mineralisation of organic phytin-P was also promoted as a result and uptake of P from phytin-P in maize was improved. Another study showed that *Rhizophagus irregularis*, an AM fungus, interacted with a phosphate-solubilising bacterium (PSB), *Pseudomonas alcaligenes,* in the hyphosphere. The interaction increased phosphatase activity and enhanced mineralisation of organic P (Na-phytate) in the soil consequently (Zhang et al., 2014).

With the advances in the studies about AM fungi, the knowledge about rhizosphere has been extended and incorporated with the soil that surround both the root and mycorrhi-

zal fungi, namely “mycorrhizosphere” (Linderman, 1988; Fogel, 1988). Inside the mycorrhizosphere, there is a more specific zone which is influenced only by the hyphae of AM fungi, giving the term “hyphosphere” (Wang and Feng, 2021) (Figure 1.5).

Since the symbiosis between AM fungi and host plants is mutualistic, host plants provide carbon (C) to AM fungi in exchange for nutrients such as phosphorus (P), nitrogen (N), and other minerals (Wang and Feng, 2021). Studies using isotopic ^{14}C as a tracer in cucumber plants showed that AM fungi utilised around 4–20% of photo-assimilated C from the plants (Jakobsen and Rosendahl, 1990)

Similarly to roots, AM also release exudates (e.g., enzymes, protons, carbohydrates) into the soil (hyphosphere) through extraradical hyphae (Wang and Feng, 2021) . Excretion of carbohydrates by the mycelia of AM fungi presents a good source of carbon for the bacteria in the hyphosphere (Zhang et al., 2014). The first study that attempted to detect carbohydrates from the extraradical mycelium of an AM fungus was done by Toljander et al. (2007). Toljander et al. (2007) managed to obtain carbohydrates from the exudate of AM fungus (G*lomus sp.* MUCL 43205) associated with the plant roots of white clover (*Trifolium repens* L.) in a split-dish system and identified them using proton nuclear magnetic resonance (HNMR) spectrometry. Low-molecular-weight compounds were detected such as formate, acetate, glucose and oligosaccharides. Besides, this study also showed that mycelia exudates would change the bacterial community composition and increased growth of bacteria. There are also some unidentified or trace substances in the exudates which may inhibit bacterial activity or growth (Welc et al., 2010; Filion et al., 1999). Moreover, Zhang et al. (2018) investigated the interactions between AM fungus *Rhizophagus irregularis* and the phosphate solubilising bacterium (PSB) *Rahnella aquatilis* under strict in vitro culture conditions, and found that fructose exuded by *R. irregularis* stimulated the expression of genes related to phosphatase in the PSB as well as the rate of phosphatase release. This experiment described for the first time that fructose not only plays the role as carbon source, but also acts as a signal molecule that triggers bacteria-mediated mineralisation of organic P.

Plant roots recruit different microbial communities, influenced by the composition of root exudates, which vary between plant species (Tkacz et al., 2020), and the extraradical hyphae of AM fungi exhibit similar behaviour by releasing their own exudates that influence microbial communities. The bacteria colonising the hyphae (hyphosphere) may

be of equal importance to the AM symbiosis, but little is known about the bacterial community colonising the hyphae of AM fungi (Scheublin et al., 2010b), due to the difficulty of studying bacteria colonising the hyphae in the hyphosphere. Scheublin et al. (2010b) analysed bacterial communities attached to the hyphae of *Glomus intraradices* and *Glomus proliferum* and concluded that bacterial communities attached to the hyphae were different from the non-attached communities. Also, analysis of amplified 16S rRNA genes indicated bacteria from the family Oxalobacteraceae were highly abundant in AM fungi hyphosphere. Moreover, *Rhizophagus irregularis* was found to exert a strong selection and elicited greater enrichment for the class Alphaproteobacteria and Gammaproteobacteria (Emmett et al., 2021).

The interaction between the AM fungi and host plants presents a potential to develop sustainable agriculture to satisfy the large demand of foods by humans. Despite the benefits of AM fungi, such as increased resistance to environmental stress and better nutrient acquisition, there are still many unknown areas about how AM fungi interact with the hyphosphere microbial communities.

First, it is well-known that AM fungi form a mutualistic symbiotic relationship with plants, but the specific effects of AM fungi inoculation on the hyphosphere bacterial and fungal communities are still not well understood, which is a critical area of research, as the interaction between them would affect the success of plant growth promotion using AM fungi (Scheublin et al., 2010a). Second, the effect of nutrient supplementation on the interaction is unclear. Addition of nutrient might impact the community dynamics, but to what extend this will change the dynamics, particularly related to AM fungi inoculation, has not been well-studied (Maitra et al., 2021).

To address these unknown areas, this study aims to investigate the effects of AM fungi (*R. irregularis*) inoculation and nutrient supplementation on microbial communities and hyphal development in the wheat (*Triticum aestivum*) hyphosphere.

2.2 Objectives

The objectives of this chapter are:

1. To assess the impact of AM fungi inoculation on fungal and bacterial communities in the wheat hyphosphere.

2. To determine how nutrient supplementation influences hyphal growth and microbial community structure.
3. To explore potential competition between inoculated AM fungi and native fungal communities.
4. To evaluate the effects of AM fungi inoculation and nutrient supplementation on bacterial abundance.

Disclaimer

Some sections of this work has been published in Keyes et al. (2022) and aspects were performed by other researchers as part of that study. Specifically, the experimental set up (Section 2.3.1) was published and not performed as part of the PhD. The sequence data analysis (e.g., 2.3.1.4 was performed by me as part of the PhD and included in Keyes et al. (2022), for which I was acknowledged in the paper). The follow-up wheat plant experiments (e.g. 2.3.2) were done solely for this PhD and have not been published.

2.3 Materials and methods

2.3.1 Experimental setup for growth of wheat and inoculation with *Rhizophagus irregularis*

The growth medium used in our study was a sand-textured Eutric Cambisol soil, collected in 2015 from a surface plot at Abergwyngregyn (53°14′N, 4°01′W), North Wales, UK, selected to maintain consistency with previous experiments that utilised the same soil as part of an ongoing study. The soil contained 52.7% sand, 32.8% silt and 14.5% clay. The soil was stored in an outdoor pile under ambient conditions until use. For the experiment, it was first sieved using 5mm sieve, then air dried for 3 d at 23±1 °C. The dried soil was then sieved to three different fractions: coarse, passing between 1180 µm and 2 mm; fine, between 1180 and 600 µm and very fine, passing through <600 µm.

The wheat cultivar (*Triticum aestivum* cv. Apache, WBCDB0003-PG-1), sourced from the Germplasm Resources Unit of the John Innes Centre (Norwich, UK), was selected for its known high compatibility with colonisation by AMF (Keyes et al., 2022). The seeds of wheat were first sterilised using milli-Q water containing 2.5% sodium hypochlorite

(50% v/v Domestos) and a single drop of Triton X100 surfactant solution. Seeds were shaken in sterilising solution for 8 minutes, then rinsed five times using sterile pure water. Afterwards, seeds were germinated at 23 ±1 °C for 96h under dark conditions on moist Millipore filter paper (autoclaved) in Petri dishes. After germination, seeds were planted to the root chambers using sterile forceps.

A growth box system was designed to keep the experiment in controlled conditions (Figure 2.1; Figure 2.2). The system consists of hyphal and root chambers. The purpose of the chamber system was to maintain the root and hyphal chambers under stable water potential (applied externally) in dark conditions. The growth box was designed using SolidWorks software (version 2015) (Dassault Systèmes S.A., France) and manufactured using acrylic sheet (3 mm) (Plastock, High Wycombe, UK) as well as 3D printed parts. The 3D printed parts made in ABS (Acrylonitrile butadiene styrene) were printed using UP! BOX printer (Tiertime, Beijing, China).

Root chambers were made from box-section acrylic tubing (inner diameter: 15.9 mm; outer diameter: 19.1 mm) and were attached to the base using 3 mm-thickness laser-cut acrylic tabs. A hole was left at the bottom of each chamber in order to allow the entry of the glass-fibre wick. The glass-fibre wick at the bottom was used to maintain the water content in the soil. Besides, 5mm holes were drilled at d_1, d_2 and d_3 positions in each root chamber (Figure 2.2), which indicated 25 mm, 65 mm and 105 mm respectively from the top opening of the root chamber. A 38 µm rectangular nylon mesh (Normesh, Lancaster, UK) was stretched over the front face of each root chamber and attached using adhesive tape down the side. Down the bottom of each root chamber, a braided glass-fibre wick (5 mm diameter) (Stovax Ltd., Exeter, UK) was introduced, running up the entire height of the root chamber. Around 20 mm of wick was extended above the soil surface and around 200 mm of the wick was extended below each root chamber to allow hydration via capillary rise (Figure 2.2). The wick was held to the back face of the plant chamber using adhesive tape. Distilled water was put in a plastic container in the base of the growth box acting as water reservoir.

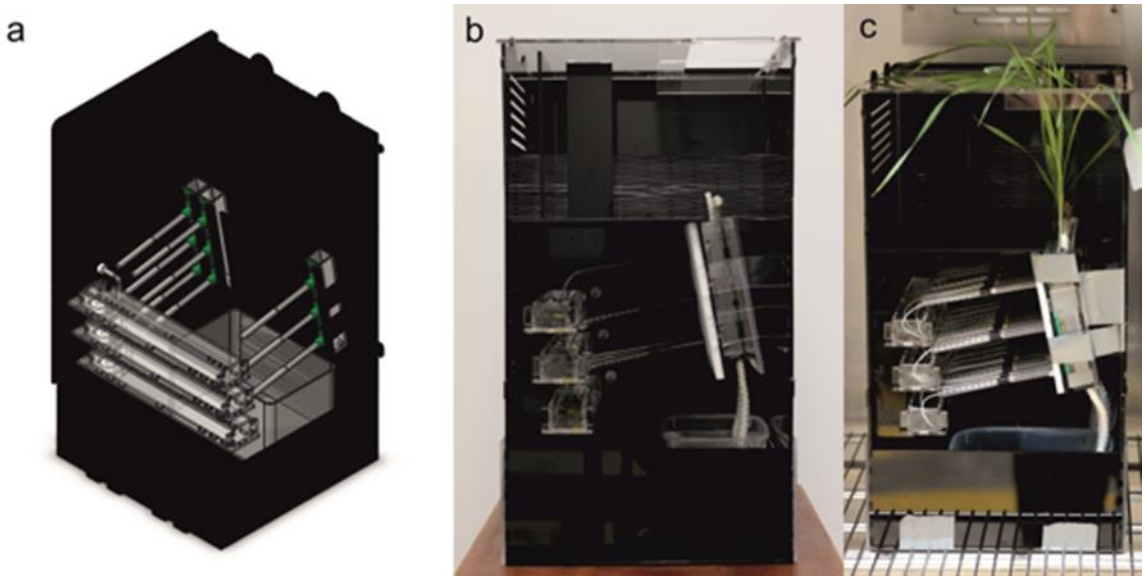

Figure 2.1 A CAD rendering of the growth chamber design (a), the final fabricated version (b), a single chamber assembly in the experiment (c). From Keyes et al. (2022).

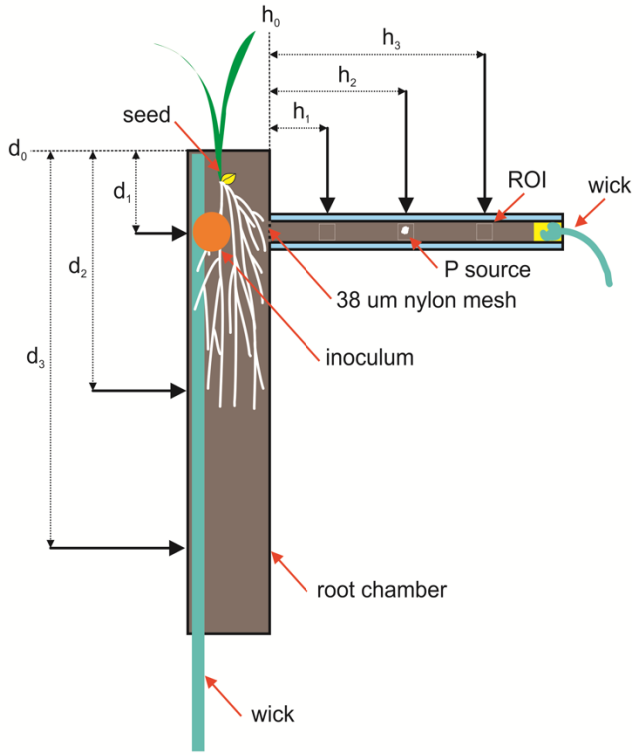

Figure 2.2 Side view of the root and hyphal chamber assembly (only the side-arm hyphal chamber in d1 position is shown here as example). d = the height of the side-arm centroid from the top of the root chamber, h = the distance in the hyphal chamber, away from the barrier mesh. ROI (Region of Interest) refers to the specific area within the side chamber from which soil samples were collected for sequencing. From Keyes et al. (2022).

Hyphal chambers were produced from sterile 1 ml polypropylene syringes (BD Plastipak). 1 ml of working volume was given to each chamber by cutting the syringes down to the 1 ml gradation using a scalpel. A braided 1 mm diameter glass-fibre wick (The Mesh

Company, Warrington, UK) was introduced to the bottom of each hyphal chamber and knotted. Fine sand (British Standard Fraction D) was put into the hyphal chamber to surround the knotted wick to improve the hydraulic conductivity between the soil and the knotted wick. Sand was first sterilised by heating to 130°C for 24 h in the oven prior to putting inside the hyphal chamber. Each chamber was filled up to the 0.15 ml line by the sand, sand was later pressed down to the 0.1 ml line by a syringe plunger.

A tube was fitted to the free end of the glass-fibre wick as a holder and attached to the base of the hyphal chamber using adhesive tape (Figure 2.3). The carrier tubes were made of sterile 1 ml syringes as mentioned before. A scalpel was used to cut at the 0 ml and 1 ml gradations to form an open tube. Soil was filled up to the 0.6 ml line in each hyphal chamber, and the chambers were tapped until soil settled back to around 0.55 ml (Gregory et al., 2003). In the P+ (with P added) groups, a small pellet of triple super-phosphate (TSP) fertiliser (a highly concentrated phosphorus fertiliser containing about 46% P_2O_5;mean mass 0.0757 g, SD = 0.007 g) was added at the point of P source as indicated in Figure 2.2, using forceps. Afterwards, each hyphal chamber was filled with the soil up to the 1 ml line, then tapped to consolidate, the vacant space was then re-filled up to 1 ml mark.

Each hyphal chamber was fastened to the plant root chamber at the position d_1, d_2 and d_3 (Figure 2.2) using adhesive tape, which wrapped around the entire root chamber. Hyphal chambers were angled downwards at 10 degrees to horizontal, hydration racks were built opposite to the hyphal chamber (Figure 2.1). Root chambers were filled with the coarse soil stock (< 2mm fraction).

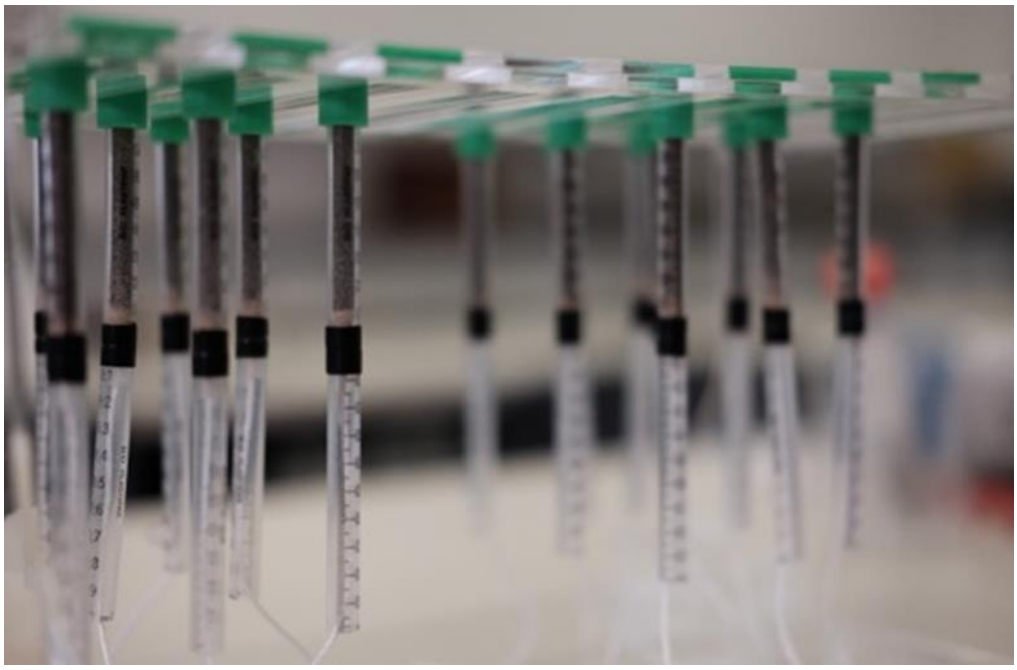

Figure 2.3 Completed hyphal chambers with carrier tubes holding the glass-fibre wicks. Ready to be attached to the root chambers. From Keyes et al. (2022).

2.3.1.1 *Rhizophagus irregularis* inoculation and non-mycorrhizal controls

A single-strain inoculum was used (BEG72, PlantWorks Ltd., UK) for the inoculation of samples with *Rhizophagus irregularis*. The inoculum supplied by the manufacturer contained hyphae, spores and colonised root fragments in an inert carrier media which is made of zeolite granules sieved between 3 and 1 mm.

In order to produce a uniform inoculating mixture, the media was concentrated as recommended by the manufacturer. Briefly, 300-ml volume of the inoculum was placed in a 750 µm sieve, the 750 µm sieve was stacked over a 53-µm sieve. The inoculum was washed vigorously under a water jet for 2 minutes. The material that remained in the 53 µm sieve, consisting of AM fungal spores and hyphae, was gently decanted into a Petri dish, and soil stock (very fine fraction, <600 µm) was added along with pure water to produce 30 g of stiff paste-like media. During inoculation of each root chamber, 1.5 g of inoculating paste and 0.5 g of raw inoculum were added together at each of the positions where the hyphal chambers were mounted (i.e., d_1, d_2 and d_3) using spatula. Gentle tapping was applied during filling in order to consolidate the soil.

For the controls, due to the nature of the soil, it contained naturally occurring fungal spores (including mycorrhizas), making it difficult to attain and maintain full sterilisa-

tion. There was also an increased likelihood of opportunistic, non-mycorrhizal fungi rapidly dominating colonisation of a sterilised soil, which should be avoided. Therefore, unsterilised soil was used throughout the experiment.

Because the soil was non-sterile, it would contain mycorrhizal spores, to avoid the development of symbiosis and mycorrhizal mycelium, it was necessary to keep the non-mycorrhizal controls plant-unassociated. Therefore, it was decided to keep the control samples (non-mycorrhizal control) unplanted.

2.3.1.2 Plant growth conditions

The set up involved inoculating strain (*Rhizophagus irregularis*/non-mycorrhizal control), phosphorus condition (P+/P-) and time (2/4 weeks). Three replicate samples were prepared for each combination.

Each assembly (a single root chamber, three hyphal chambers) was put into the growth box (Figure 2.1). The maximum capacity of each growth box was nine assemblies. The growth boxes were put in a growth chamber under controlled environmental conditions (Conviron A1000). Under an inverse diurnal cycle (where light and dark periods are reversed compared to natural daylight), the light period was set for 14 h at 23°C with 75% humidity under full light (700 µmol.m^{-2}. s^{-1}), and the dark period was set for 10 h at 18°C with 75% humidity. An inverse diurnal cycle was used to align the plants' daytime with laboratory working hours, ensuring easier access for sampling and monitoring.

2.3.1.3 16S rRNA and 18S rRNA amplicon sequencing

For sequencing, three biological replicate soil samples from the d1 position were collected, frozen using liquid nitrogen, and stored at -80°C. Soil DNA was extracted from 0.5 g of soil (wet weight) from each replicate. Soil was taken from the uppermost part of each hyphal chamber. DNA was extracted using a Zymo D6003 soil dsDNA extraction kit (Zymo Research, Orange, CA, USA) according to the instruction provided. Samples were kept on ice during the process. Illumina sequencing was carried out for the 16S rRNA gene (targeting bacteria) and the 18S rRNA gene (targeting eukaryotes, including fungi). The sequencing was done in Environmental Sequencing Facility at the University of Southampton.

Primers F515 Modified (5'- GTGYCAGCMGCCGCGGTAA – 3') (Parada et al., 2016) and R806 Modified (5'- GGACTACNVGGGTWTCTAAT - 3') (Apprill et al., 2015) were used for the amplification of 16S rRNA genes. Primers F574 (5'- GCGGTAATTCCAGCTCCAA- 3') and R952 (5'- TTGGCAAATGCTTTCGC -3') were used for the amplification of 18S rRNA genes (Hadziavdic et al., 2014).

2.3.1.4 DNA sequence analysis

Quality filtering and trimming of the sequence reads was performed using the package DADA2 (Callahan et al., 2016),with forward and reverse reads merged by using the DADA2 mergePairs command. Downstream processing was performed by using DADA2 makeSequenceTable command to construct a table with amplicon sequence variant (ASV), and function removeBimeraDenovo to remove chimeric sequences. ASV can be regarded as a higher-resolution version of the traditional OTU table, which can identify more variants than other methods (Callahan et al., 2016). Sequences shorter than 320 bp were discarded. Unlike the traditional OTU table, in an ASV table, the number of times each exact amplicon sequence variant (ASV) is observed in each sample is recorded (Callahan et al., 2017). ASVs were classified using the Wang Bayesian classifier in DADA2 (Callahan et al., 2016; Wang et al., 2007) and the Silva taxonomy (Quast et al., 2013) . The taxonomy of selected ASVs that could not be identified using the classifier were individually analysed by BLAST against the non-redundant (nr) NCBI database; the taxonomy of closest BLAST of a type strain match was used as an indication of the identity of the ASV.

A heatmap representation of the relative abundance of ASVs between inoculated and uninoculated samples was constructed using the R programme (version 4.3.0) (http://www.r-project.org/). The ASV counts were first subjected to a Hellinger transformation with the decostand function in the vegan package (version 2.5-6) (Oksanen et al., 2019). Principal components analysis (PCA) was then performed using the R function prcomp, which showed that the inoculated and uninoculated samples were separated along the first two axes. To identify ASVs that best explained the differences between inoculated and uninoculated samples, indicator species analysis was performed separately for 16S and 18S rRNA datasets using the multipatt function in the indicspecies package (version 1.7.15) in R based on the approach described by De Cáceres and

Legendre (2009), with a significance threshold of α = 0.05. This method statistically assesses the association of each ASV with a treatment group by combining its relative abundance and frequency of occurrence. ASVs with significant indicator values ($p < 0.05$) were selected as representative of either the inoculated or uninoculated group.The relative abundance of these ASVs was calculated and visualised in heatmaps, using the pheatmap function in the pheatmap package (version 1.0.12) (Kolde, 2019).

To test whether bacterial families associated with the inoculated treatment were significantly enriched, a chi-square (χ^2) test was performed on ASVs identified by indicator species analysis ($p < 0.05$) under both P+ and P- conditions. ASVs were grouped by family, and the observed frequency of each family in the indicator subset was compared to its expected frequency based on its proportion in the full ASV dataset. Families with $p < 0.05$ were considered significantly enriched, indicating a non-random association between specific families and the inoculated treatment. Chi-square tests were performed using GraphPad Prism version 10 (GraphPad Software, California, USA).

Shannon diversity indexes of the inoculated and non-mycorrhizal (uninoculated) control samples were calculated. In addition, the relative abundances of selected taxa between inoculated and uninoculated samples were also calculated. Student's t-tests were used to compare both the Shannon diversity and the relative abundance between inoculated samples and non-mycorrhizal controls at a 95% confidence level. $P < 0.05$ was considered statistically significant.

2.3.2 Further study of the inoculation impacts of *R. irregularis*

2.3.2.1 Root chamber setup

To further study the impact of the inoculation of *R. irregularis*, a simplified version of the setup illustrated in Figure 2.4 was adapted from the design mentioned in Figure 2.1. In this new growth setup, 50-ml CELLSTAR tubes (Greiner Bio-one, Gloucester, UK) replaced the wheat chamber, while the setting for the hyphal chamber remained the same.

A 5-mm diameter hole was drilled in the front face of each plant chamber, positioned 25 mm from the upper opening of the plant root compartment, according to the experiment

described by Keyes et al. (2022). Nylon mesh (Normesh, Lancaster, UK) with a 38-µm aperture size was gently stretched over the front face of each root compartment and affixed using a strip of adhesive tape along each side. A 5-mm diameter fibreglass rope (Stovax Ltd., Exeter, UK) was introduced through the base of each root chamber, extending the entire height. Approximately 10 cm of wick extended vertically below the root compartment, and about 20 mm extended above the soil surface, held in place against the back of the root chamber using adhesive tape. Each root chamber was filled with 66 grams of soil, and a reservoir was set up at the bottom to supply water to the root chambers.

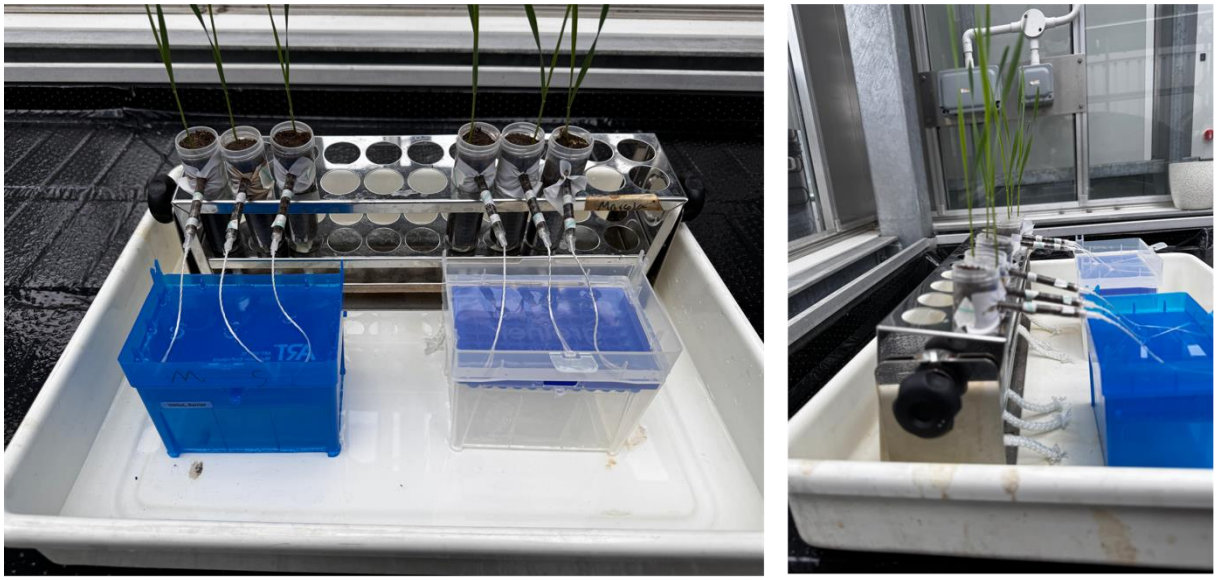

Figure 2.4 Adapted setup for growing wheat.

2.3.2.2 Hyphal chamber setup

In the hyphal chamber setup, sterile 1-ml polypropylene syringes (BD Plastipak) were used as hyphal compartments, as previously described by Keyes et al. (2022). The syringes were cut down to the 1 ml line with a scalpel, resulting in a working volume of 1 ml in each chamber.

A 1-mm diameter silica wick (JAG Hilly Trading, Fareham, UK) was knotted and introduced to the base of each chamber, with the excess part of the knot trimmed by scissors. The knot was gently pulled to the base of the syringe, and wicks were extended horizontally, approximately 90 mm at the end of each hyphal compartment. Each hyphal chamber was filled with 1 gram of soil, and then mounted onto the root chambers

through the drilled holes, secured using tape. Hydration racks were placed opposite the chambers to maintain water supply.

2.3.2.3 Preparation of wheat seeds and the inoculum

For the preparation of wheat seeds and inoculum, the same procedures described in previous sections were followed. After planting the seeds, the setup was placed in a glasshouse for growth, with daytime temperatures of 23°C, nighttime temperatures of 18°C, and 16 hours of daylight at 55% humidity. The plants were grown in the glasshouse for 2 weeks.

2.3.2.4 Control setup

Control setups included the same "inoculated" ("plant + inoculant") and "uninoculated" ("soil alone") controls from Keyes et al. (2022), as well as new controls such as samples with sterile inoculant ("plant + sterile inoculant" and "soil + sterile inoculant"), and samples with plant but no inoculant ("Plant alone"). The treatment groups are illustrated in Table 2.1, and triplicates were prepared for each treatment.

Table 2.1 Overview of experimental treatments.

Treatment group	Description
Plant + inoculant	Plant + live inoculant
Soil + inoculant	Soil + live inoculant
Plant + sterile inoculant	Plant + sterilised inoculant
Soil + sterile inoculant	Soil only + sterilised inoculant
Plant alone	Plant only (no inoculant)
Soil alone	Soil only (no plant, no inoculant)

2.3.2.5 Hyphal counting

After 2 weeks, hyphal numbers in the samples were counted using a modified protocol from Dodd et al. (2001).

Briefly, soil samples from each hyphal chamber were collected individually into 500 ml beakers and suspended in 250 ml of pure water. The soil-water mixture was blended using a Waring 8011ES 2-speed laboratory blender with stainless steel blades (Waring Commercial, USA) for 30 seconds at high speed (22000 rpm). The blended mixture was then filtered through a 210-µm mesh sieve, transferred to a flask, agitated, and allowed

to stand at room temperature for 1 minute. A 6-ml aliquot of the soil suspension was then placed onto a 1.0 µm Millipore filter and filtered under vacuum. After filtration, the vacuum was turned off and the filter was stained with 1 ml of 10% Sheaffer blue in 25% acetic acid for 3 minutes. The remaining stain was then removed, and the filter was rinsed with 1 ml of pure water. The filter was placed on a microscope slide for drying, after which one drop of glycerol was added, and a cover slip was placed over the filter. The slide was examined under a light microscope for hyphal counting, with one slide prepared from each hyphal chamber. Five random fields were selected from each slide for counting under 40x magnification.

2.3.2.6 Root staining

Roots from inoculated samples were stained to confirm the successful colonisation of *R. irregularis* using a modified method from Wilkes et al. (2020).

Briefly, fresh roots were first rinsed with water and fixed in FAA (formaldehyde, acetic acid, alcohol [ethanol], and deionized water solution, 10:5:50:35) for 24 hours. The roots were then heated at 90°C for approximately 1 hour in 10% w/v KOH (a clearing step to remove cellular contents and pigments, facilitating better visualisation of fungal structures) (Phillips and Hayman, 1970), and then rinsed in water. After clearing, roots were submerged in 5% hydrochloric acid (HCl) for 30 minutes and incubated at 60°C in a water bath (acidification). After cooling to room temperature, the roots were dissected into 1 cm pieces and stained with 10% Sheaffer blue ink in 25% glacial acetic acid (Vierheilig et al., 1998) for 3 minutes at room temperature. The stains were then poured away, and root samples were de-stained using 25% acetic acid. The samples were mounted on slides using polyvinyl alcohol-lactic acid-glycerol (PVLG) and observed under 80x magnification.

2.3.3 Competition experiment

A competition experiment was conducted to determine if competition existed between *R. irregularis* and indigenous fungi in the hyphal chamber. Murashige & Skoog Modified Basal Medium with Gamborg Vitamins (MS) (Product ID: M404; PhytoTech Labs, U.S.) was used as a nutrient source. The duration of plant growth was determined by setting

up different individual samples and counting the hyphal numbers in the individual hyphal chambers on days 0, 3, 6, and 9 after wetting to observe when the hyphal numbers reached a plateau. Ultimately, a 14-day growing period was chosen for this experiment.

Using the same plant-growing setup as illustrated in Figure 2.4, additional controls were created, with or without nutrient supplementation, on top of the inoculation groups: inoculated (MS+), inoculated (MS-), uninoculated (MS+), and uninoculated (MS-). Triplicate samples were prepared for each treatment. The hyphal chambers were pre-wetted with 1 ml of either MS ("MS+" treatments) or pure water ("MS-" treatments) before being attached to the root chambers. The setup was placed in the glasshouse and grown for 14 days, with the hyphal chambers re-wetted halfway through the experiment by adding 200 µl of either MS or pure water, depending on the treatments, to prevent the soil from drying out. Hyphal numbers were counted using the steps mentioned in the previous section.

2.3.4 Effects of inoculation and nutrient on soil communities

The same settings as the competition experiment were applied to study the impact of both *R. irregularis* inoculation and MS supplementation on both the bacterial and fungal communities in the soil of the hyphosphere. After the 14-day growing period, DNA was extracted from the soil using the NucleoSpin® Soil kit (MACHEREY-NAGEL GmbH & Co. KG, Düren, Germany) according to the manufacturer's standard protocol. A different kit was used from the previous extraction because this was the kit available in our laboratory at the time of the experiment, and it is also widely used for reliable soil DNA extraction. DNA concentration (ng/µL) of each sample was determined using a BioDrop Duo+ Spectrophotometer (Biochrom Ltd, Cambridge, UK). The samples were then stored at -80°C until further analysis.

2.3.4.1 Amplicon sequencing

Amplicon sequencing was performed targeting the V4 region of the 16S rRNA gene for the bacterial community (as described in Section 2.3.1.3) and the internal transcribed spacer (ITS) 1 region for the fungal community using primers ITS1-F (5'-CTTGGTCATTTAGAGGAAGTAA-3') and ITS1-R (5'-GCTGCGTTCTTCATCGATGC-3'). The ITS region was

chosen instead of the 18S rRNA gene (used previously) to more specifically target fungal taxa and avoid amplifying unrelated eukaryotic sequences such as plants and protozoa. Sequencing was done at Biomarker Technologies (BMK) GmbH.

2.3.4.2 Quantitative polymerase chain reaction (qPCR)

To determine whether inoculation also affected the number of bacteria in the soil, quantitative polymerase chain reaction (qPCR) was conducted. This was done to assess the impact of inoculation and nutrient supplementation on the bacterial community by quantifying the 16S gene copy numbers across samples. qPCR was performed using a StepOnePlus instrument with StepOne software v2.3 (Applied Biosystems) to quantify bacterial concentrations. Reactions were carried out in a 96-well qPCR plate using TaqMan Fast Advanced Master Mix (Thermo Fisher Scientific). The assay was done according to the steps described by Vera-Gargallo et al. (2023). A purified PCR product of a 16S rRNA gene was used as a DNA standard. The concentration of the DNA standard was determined using a Qubit Fluorometer (Thermo Fisher Scientific). A single-use aliquots of $1x10^6$ molecules μl^{-1} was prepared. Bacterial DNA was targeted using primers BAC338F (5' ACT CCT ACG GGA GGC AG 3') and BAC805R (5' GAC TAC CAG GGT ATC TAA TC 3') with the corresponding TaqMan probe BAC516P (5' TGC CAG CAG CCG CGG TAA TA 3'), which was labelled with 6-carboxyfluorescein (6-FAM) on the 5' end and Black Hole Quencher 1 (BHQ1) on the 3'end (Sigma-Aldrich). The primer/probe mix was prepared by combining 18 µl of forward primer (0.9 µM), 18 µl of reverse primer (0.9 µM), 5 µl of probe (0.25 µM), and 59 µl of TE buffer (Sigma-Aldrich) to achieve the desired working concentrations.

To prepare the qPCR reactions, a 10-fold serial dilution of the DNA standard was carried out to obtain a concentration range from 10^1 to 10^6 molecules μl^{-1} in nuclease-free water. The qPCR master mix was prepared as follows for each reaction: 5 µl of 2 x TaqMan Fast Advanced Master Mix, 0.5 µl of the primer/probe mix, 3.5 µl of nuclease-free water. The master mix was briefly vortexed to ensure complete mixing. A total of 9 µl of this master mix was added into each well of the 96-well qPCR plate. Subsequently, 1 µl of the DNA template (standard, sample, or nuclease-free water for blanks) was added to each well, resulting in a final reaction volume of 10 µl per well.

The qPCR was conducted under the following thermal cycling conditions: initial denaturation at 95°C for 5 minutes, followed by 35 cycles of denaturation at 95°C for 30 seconds, and annealing/extension at 62°C for 60 seconds.

Fluorescence data were collected at the end of each cycle during the extension phase, and threshold cycle (Ct) values were calculated using StepOne software. The obtained Ct values were used to deduce the DNA concentration in the samples based on the standard curve generated from the DNA standards.

2.3.5 DNA sequence analysis for repeated experiments

R software version 4.3.2 (http://www.r-project.org/) was used for processing the sequencing data. The data were analysed using the DADA2 pipelines as mentioned in previous section(2.3.1.4). ASVs were classified using the Wang Bayesian classifier in DADA2 (Callahan et al., 2016; Wang et al., 2007) , referencing the Silva taxonomy database for 16S sequencing (Quast et al., 2013) and the UNITE ITS database (Abarenkov et al., 2024) for ITS sequencing. The ASV counts were subjected to a Hellinger transformation using the decostand function in the vegan package (version 2.5-6) (Oksanen et al., 2019) in R. Bray-Curtis dissimilarity matrix was calculated and Principal Coordinates Analysis (PCoA) was then performed using the R function pcoa. To determine whether inoculation or nutrient supplementation had a significant impact on soil communities ($P<0.05$), Permutational Multivariate Analysis of Variance (PERMANOVA) was conducted using the adonis2 function in the vegan package.

The same indicator species analysis approach was applied to the repeat experiment, performed separately for 16S and ITS datasets under MS+ and MS- conditions, using the multipatt function from the indicspecies package (De Cáceres and Legendre, 2009), as described above (Section 2.3.1.4). ASVs significantly associated with either the inoculated or uninoculated groups ($p < 0.05$) were identified. The sets of ASVs identified under MS+ and MS- conditions were then compared to those identified under P+ and P- conditions (Section 2.4.2), and visualised using Venn diagrams generated with the draw.pairwise.venn() function from the VennDiagram package (version 1.7.3) (Chen and Boutros, 2011) in R.

Data from hyphal counting and qPCR were analysed using analysis of variance (ANOVA) followed by Tukey's Multiple Comparisons test, implemented in GraphPad Prism version 10 (GraphPad Software, California USA). The results were then visualised using the same software.

2.4 Results

Wheat was grown with or without arbuscular mycorrhizal (AM) fungi *R. irregularis* under two different phosphorus conditions (with P added: P+; without P added: P-) and two time points (2 and 4 weeks). In both P+ and P- conditions, *R. irregularis* successfully colonised wheat roots, but hyphal growth patterns differed: P+ samples had greater hyphal length density (total length of observed hyphae per unit volume of soil) at 2 weeks, while P– samples showed more hyphal growth near roots by 4 weeks. Hyphal tortuosity (the degree of twisting and turning of hyphae, reflecting their exploratory growth) was higher in P+ treatments. Plant growth also reflected phosphorus availability, with P+ treatments showing significantly higher root and shoot biomass and phosphorus content than P–, particularly at 2 weeks (Keyes et al., 2022).

The full set of treatment combinations is summarised below (Table 2.2) (Keyes et al., 2022). All treatments were prepared in triplicate, except for the original soil treatment, which included four replicates. 28 samples in total were sequenced using Illumina sequence for 16S rRNA (bacteria) and 18S rRNA (eukaryotes). Original soil is the natural soil collected from the field that was not put in the controlled growth condition like other samples.

To confirm that the inoculation of *R. irregularis* actually worked, representative images of root colonisation for hyphal counts are shown in Figure 2.5. Although these results are from a later experiment (Section 2.4.3), they serve as an early visual validation that the inoculation approach was successful.

Table 2.2 Combination of inoculation status, phosphorus condition and time points.

Treatment group	Inoculation status (T/C)	Duration (2/4)	Phosphorus condition (P+/P-)
T4P+	Inoculated	4 weeks	with P addition
T4P-	Inoculated	4 weeks	without P addition
T2P+	Inoculated	2 weeks	with P addition
T2P-	Inoculated	2 weeks	without P addition
C4P+	Uninoculated	4 weeks	with P addition
C4P-	Uninoculated	4 weeks	without P addition
C2P+	Uninoculated	2 weeks	with P addition
C2P-	Uninoculated	2 weeks	without P addition
Original soil	Soil without any treatment		

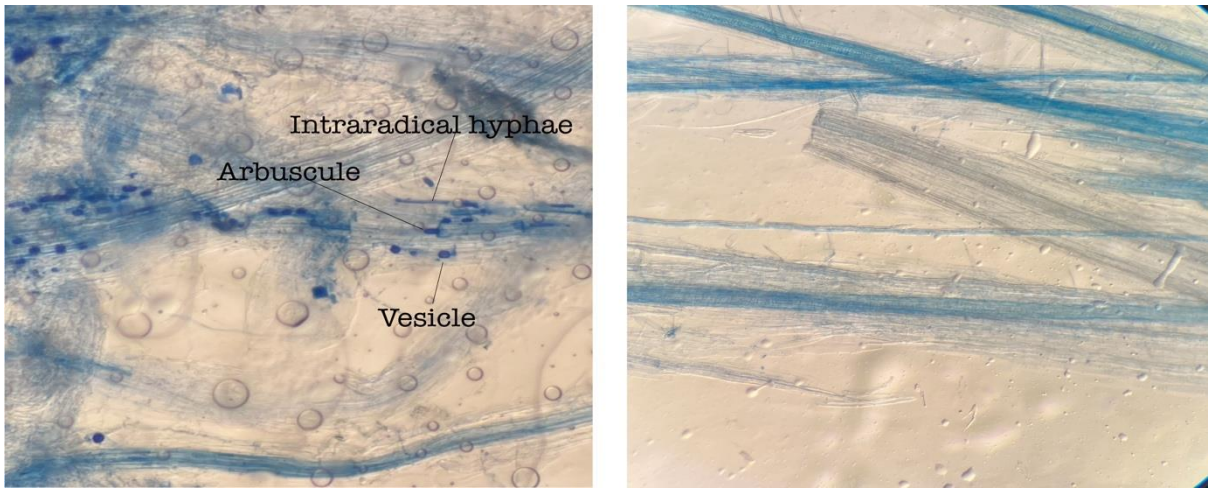

Figure 2.5 Staining of wheat roots. Left: inoculated. Right: uninoculated. Observed under 80x magnification.

This chapter reports the key finding that inoculation with *R. irregularis* led to a significant reduction in fungal abundance in the hyphosphere, despite no significant changes in fungal community structure. Inoculation also caused shifts in bacterial community structure without affecting bacterial abundance. The following sections present these findings in detail.

2.4.1 Principal component analysis (PCA)

To provide an overview of the bacterial community composition across all treatments, the relative abundance of major bacterial phyla (>1%) was visualised using a stacked

bar chart (Figure 2.6). The dominant phyla across all treatment groups are Proteobacteria (approximately 26–31%), Firmicutes (approximately 22-40%), and Actinobacteria (approximately 16-20%). Other phyla such as Acidobacteria, Chloroflexi, Planctomycetes, and Verrucomicrobia were also consistently detected across all samples, generally contributing between 3% and 7% of the total community composition. Compared to the original untreated soil, experimental groups (T & C) show noticeable shifts in phylum-level composition. For instance, Proteobacteria and Firmicutes are more abundant in experimental groups, while Acidobacteria and Planctomycetes are reduced.

In both P+ and P− conditions, Firmicutes are consistently more abundant in uninoculated treatments, while Planctomycetes and Verrucomicrobia are more abundant in inoculated groups. Other phyla, including Acidobacteria, Actinobacteria, Chloroflexi, and Proteobacteria, show relatively stable abundances across inoculated and uninoculated treatments. When comparing phosphorus treatments, Firmicutes are consistently more abundant in P+ treatments than in P− treatments across both inoculated and uninoculated groups, while Acidobacteria, Actinobacteria, Chloroflexi, and Planctomycetes generally show reduced relative abundances. Other phyla, such as Proteobacteria and Verrucomicrobia, show no clear or consistent pattern between P+ and P− treatments across both inoculated and uninoculated samples.

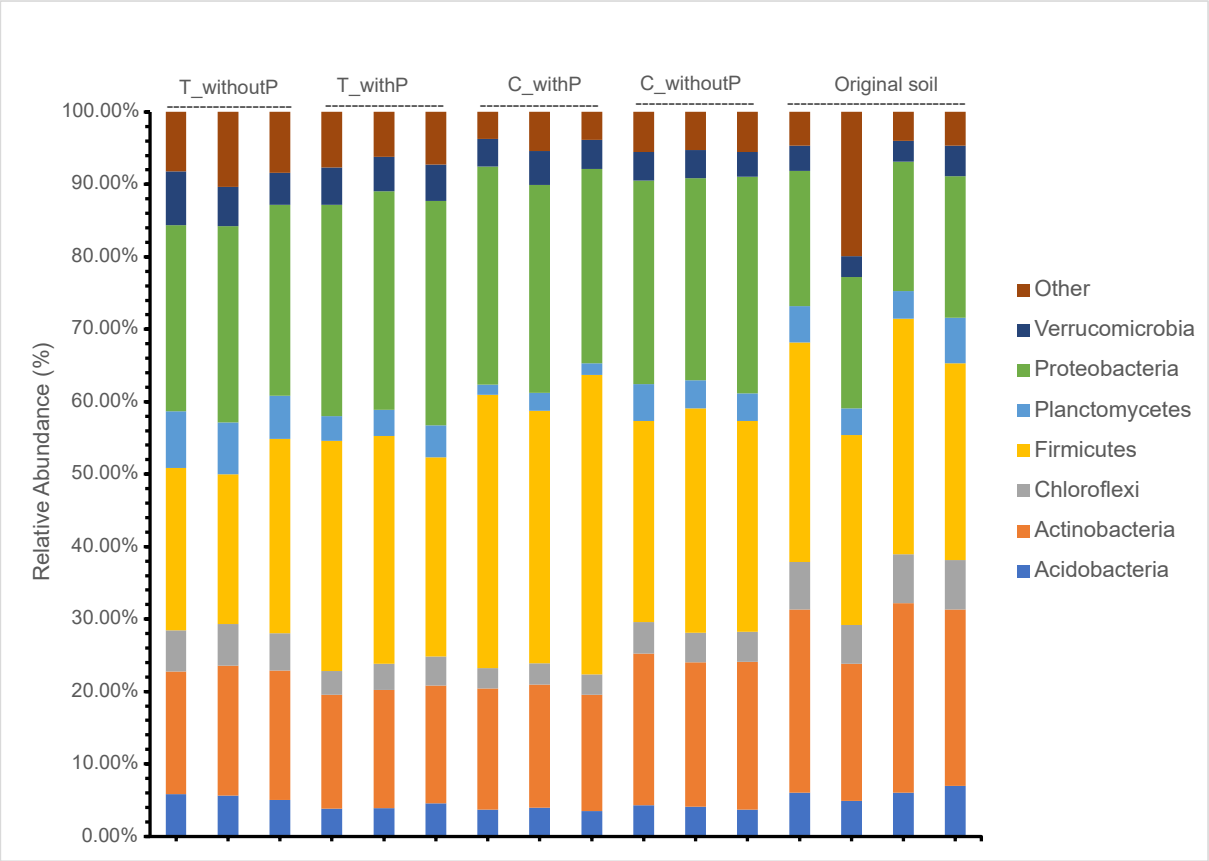

Figure 2.6 Stacked bar chart showing the relative abundance of bacterial phyla across different treatment groups. Only taxa with >1% relative abundance are shown; taxa with <1% relative abundance are grouped into "Other". T = inoculated with *R. irregularis*, C = uninoculated, with P = with phosphorus addition, without P = without phosphorus addition. Original soil = untreated natural soil.

Principal component analysis (PCA) was then carried out to visualise the microbial community data from 16S and 18S rRNA gene sequencing (Keyes et al., 2022), in order to examine whether the inoculation of the *R. irregularis* had effects on the soil community near the hyphae.

We first visualised the overall microbial community structure across all treatments, including inoculation status, phosphorus condition, and time point (Figure 2.7). One inoculated sample under P+ condition was excluded from the 18S PCA analysis due to substantially lower sequencing depth (~32,000 reads) compared to its biological replicates (~101,000 and ~170,000 reads), and because it lacked many ASVs consistently detected in the other two samples, suggesting a sequencing failure. This sample was also excluded from all subsequent analyses involving the 18S sequencing dataset to avoid potential bias.

In the PCA plot for bacteria (Figure 2.7 a), The first two principal components (PC1 and PC2) together explain approximately 34% of the variance (21.07% and 12.88%, respectively). Clear clustering patterns were observed based on both inoculation status and phosphorus treatment. Inoculated and uninoculated samples generally separated along the PC1 axis, particularly under P+ conditions, suggesting a strong influence of inoculation on microbial composition. Additionally, samples with added phosphorus (P+) cluster distinctly from P– samples, especially along the PC2 axis. Original soil samples cluster separately from the experimental treatments, indicating a shift in microbial composition due to controlled growth conditions. No strong clustering by time point (2 vs. 4 weeks) was observed, indicating that sampling time had a limited influence on overall community composition.

For the eukaryotic community (Figure 2.7 b), the first two principal components (PC1 and PC2) explain 16.54% and 12.85% of the variance, respectively. Compared to the 16S dataset, clustering patterns are less distinct. Separation between inoculated and uninoculated samples was still observed along both PC1 and PC2 axis. Phosphorus condition (P+ vs. P–) also appears to influence clustering, with some distinction visible along PC2. While original soil samples partially overlap with uninoculated treatments, they remain distinct from inoculated samples.As with the bacterial community, no strong grouping by time point (2 vs. 4 weeks) was observed, indicating limited temporal effects on overall eukaryotic composition.

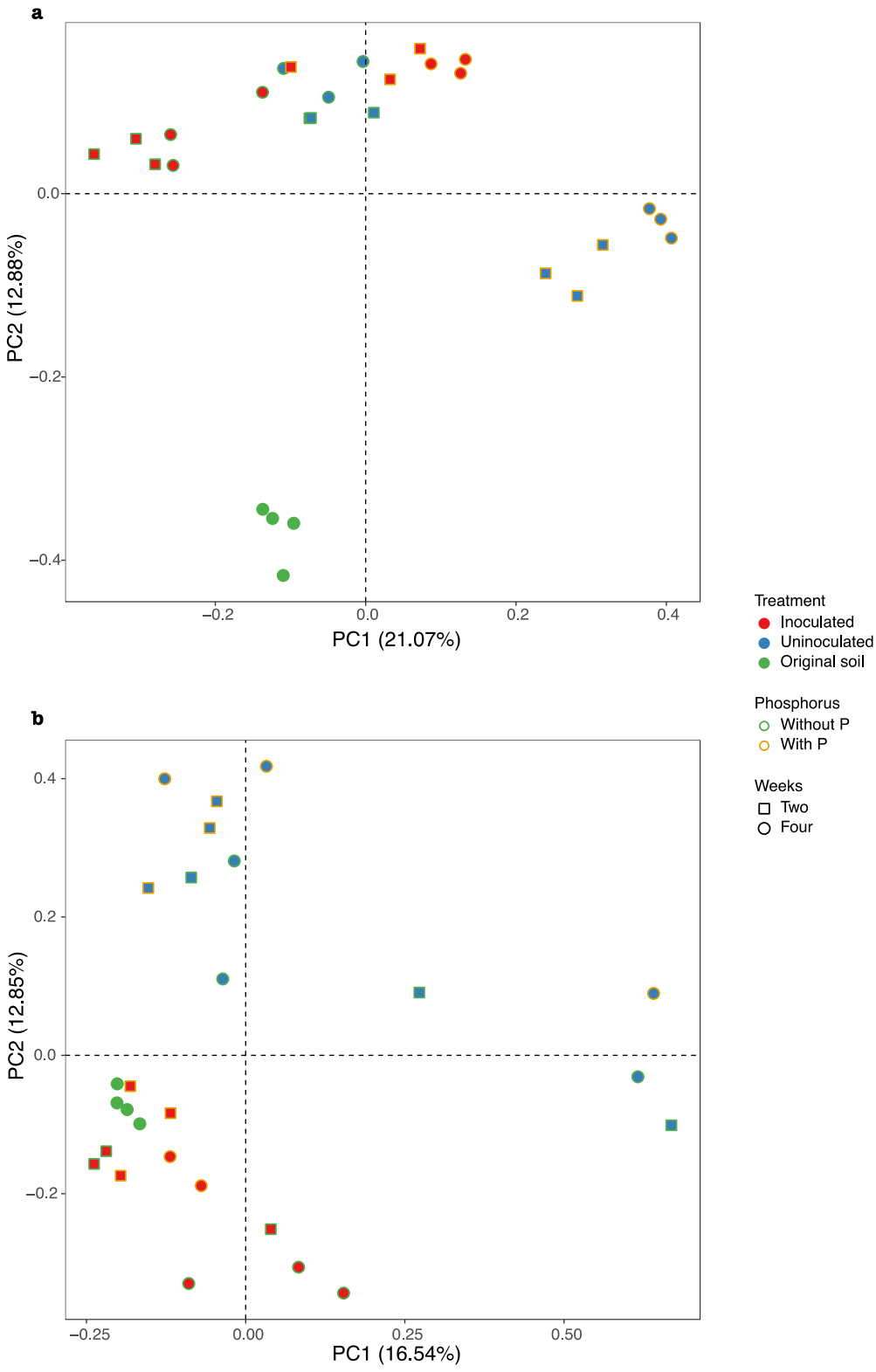

Figure 2.7 Principal component analysis (PCA) plot of samples from 16S (a)/18S (b) rRNA sequencing. Different colours (inner fill) denote whether the samples were inoculated with *R. irregularis* or not. The shapes of the dots (i.e., square, circle) represent the time point: 2 weeks or 4 weeks. The colours of the borders indicate whether phosphorus was added. Note: One inoculated P+ sample was excluded from the 18S analysis due to low read count and missing ASVs, suggesting sequencing failure.

To explore inoculation effects more closely, we next analysed samples within each phosphorus condition (P+ and P−) separately (Figure 2.8).

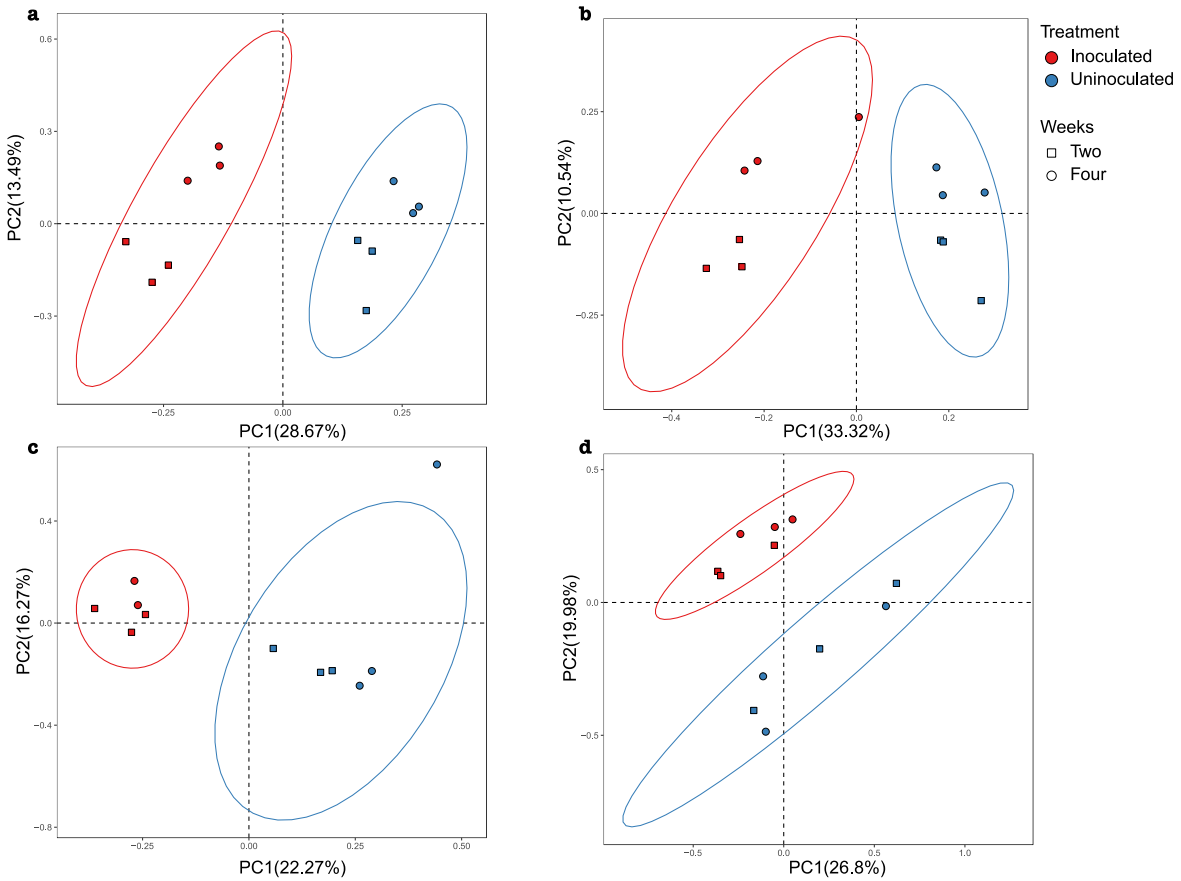

Figure 2.8 Principal component analysis (PCA) plot of samples from 16S (a,b)/18S (c,d) rRNA sequencing. Different colours (inner fill) denote whether the samples were inoculated with *R. irregularis* or not. The shapes of the dots (i.e., square, circle) represent the time point: 2 weeks or 4 weeks. Ellipses were drawn based on 95% confidence interval. (a) & (c): P+. (b) &(d): P−. Note: One inoculated P+ sample was excluded from the 18S analysis due to low read count and missing ASVs, suggesting sequencing failure.

For 16S rRNA sequencing results, samples inoculated with *R. irregularis* are obviously separated from the samples of non-mycorrhizal controls along the PC1 axes, which explained 28.67% and 33.32% of the variance, respectively (Figure 2.8a,b). For sequencing results of 18S rRNA, in those groups with P added (P+), samples are separating alone the PC1 axis, which explained 22.27% of the variance (Figure 2.8c); whilst samples are separating alone both the PC1 and PC2 axis in the groups without P added (P-), which explained 26.8% and 19.98% of the variance, respectively (Figure 2.8d). No distinct clustering by time point (2 vs. 4 weeks) was observed.

2.4.2 Heatmap representation of the relative abundance

According to the method of De Cáceres and Legendre (2009); Deng et al. (2014), by selecting taxa that are most strongly associated with specific treatments based on indicator species analysis, the difference between treatments can be visualised more effectively.

Indicator species analysis identified ASVs significantly associated with either the inoculated or uninoculated groups across both 16S and 18S datasets ($p < 0.05$). In the 16S dataset, 140 ASVs were identified under P+ condition , including 87 ASVs associated with the inoculated group and 53 with the uninoculated group; under P− condition, 197 ASVs were identified, with 97 enriched in the inoculated group and 100 in the uninoculated group. For the 18S dataset, 331 ASVs were identified under P+ condition, with 8 associated with the uninoculated group and 323 with the inoculated group; under P− condition, 251 ASVs were identified, including 7 associated with the uninoculated group and 244 associated with the inoculated group. The selected ASVs were used to construct the heatmaps (Figure 2.9; Figure 2.10; Figure 2.11; Figure 2.12).

For the bacterial community (16S rRNA dataset) under phosphorus addition, the heatmap (Figure 2.9) shows the relative abundance of ASVs identified through indicator species analysis ($p < 0.05$), highlighting differences between inoculated and uninoculated treatments. The overall pattern reflects the separation observed in the PCA (Figure 2.8a), where samples group distinctly by inoculation status along the PC1 axis. ASVs associated with inoculated samples are generally concentrated at the top right corner of the heatmap, while ASVs linked to uninoculated samples form a separate region with higher relative abundance. For the bacterial community under P− conditions, a similar separation between inoculated and uninoculated samples was observed, as shown in both the heatmap (Figure 2.10) and the corresponding PCA (Figure 2.8b). Samples from both 2- and 4-week time points are intermixed in the heatmaps and show no clear separation in the PCA plots, suggesting that sampling time had limited influence on community composition.

For the group of bacteria (16S rRNA) under both P+ and P− conditions, Proteobacteria account for the largest proportion among ASVs identified through indicator species analysis ($p < 0.05$) (Figure 2.9; Figure 2.10). However, despite their prevalence in ASVs

differentiating inoculated and uninoculated samples, the overall relative abundance of Proteobacteria (combined across P+ and P-) does not differ significantly between treatments (28.24% ± 0.42% in inoculated and 28.60% ± 0.26% in uninoculated samples; p= 0.515, t-test).

Chi-square analysis was used to assess whether specific bacterial families were selectively enriched in inoculated samples under P+ conditions. Several families were significantly overrepresented ($p < 0.0001$), particularly within Proteobacteria, including Sphingomonadaceae, Xanthomonadaceae, and Devosiaceae, as well as families from other phyla such as Geodermatophilaceae (Actinobacteria) and Gemmatimonadaceae (Gemmatimonadetes) (Appendix Table S 5). Under P- conditions, six families overlap with those enriched under P+, including Nitrosomonadaceae (Proteobacteria), Chitinophagaceae (Bacteroidetes), Gemmatimonadaceae (Gemmatimonadetes), WD2101 soil group (Planctomycetes), Solibacteraceae (Subgroup 3) (Acidobacteria), and Acidothermaceae (Actinobacteria), suggesting a consistent inoculation effect. However, distinct enrichments were also observed under P-, including Acetobacteraceae, Micropepsaceae, and TRA3-20 (Proteobacteria), Caldilineaceae and JG30-KF-CM45 (Chloroflexi), and Pirellulaceae (Planctomycetes). Full results are presented in Appendix Table S 6, with overlapping families highlighted in yellow.

For the eukaryotic community (18S rRNA), the ASVs detected included not only common soil fungi (e.g., Ascomycota, Basidiomycota, and Mucoromycota phyla), but also other eukaryotic groups, including plant-derived sequences (e.g., Phragmoplastophyta), protists (e.g., Hemimastigophora (Foissner et al., 1988) and Ciliophora), Nematoda, and numerous unclassified or uncultured eukaryotes. For clarity, only fungal ASVs from the three common soil phyla were highlighted in the heatmaps (Figure 2.11; Figure 2.12).

Heatmaps under both P+ and P- conditions (Figure 2.11; Figure 2.12) show clear differences between inoculated and uninoculated samples, consistent with the separation in the corresponding PCA plots (Figure 2.8 c,d). As with the bacterial (16S) data, inoculation was the primary driver of community shifts. However, 18S samples exhibit greater variability overall, with replicates more dispersed in ordination space and one uninoculated sample falling outside the confidence ellipse under P+ conditions. This variation was not strongly reflected in the heatmap (Figure 2.11), where all uninoculated replicates show broadly similar ASV abundance profiles. In P-, additional separation along

PC2 (Figure 2.8d) aligns with greater inter-replicate variability visible in the heatmap (Figure 2.12), particularly among uninoculated samples. While treatment-based clustering remains evident, ASV abundance profiles showed more within-group divergence than under P+. As with 16S, sampling time had minimal influence.

For the group of eukaryotes (18S rRNA), the heatmaps include not only fungi but also other taxa such as protozoa and nematodes, as previously described. Therefore, we focused the comparison on the relative abundance of the common fungal phyla (i.e., Ascomycota, Basidiomycota, and Mucoromycota) between inoculated and uninoculated samples. The results show that the overall relative abundance of these fungi was significantly lower in inoculated samples compared to the uninoculated samples (inoculated=42% ± 1.04%; uninoculated=68% ± 3.76%; $p < 0.001$, t-test).

Besides, we also compared the Shannon diversity indices between inoculated and the uninoculated (non-mycorrhizal control). For the bacterial groups (16S rRNA), the diversity of species did not show significant change between inoculated and uninoculated (inoculated=6.421± 0.10, uninoculated=6.075 ± 0.10; $p = 0.078$, t-test). Whereas for the eukaryote groups (18S rRNA), significant change was found between inoculated and uninoculated (inoculated= 4.915 ± 0.08, uninoculated=3.730 ± 0.26; $p = 0.001$, t-test). In general. The diversity of eukaryotes was higher after inoculation.

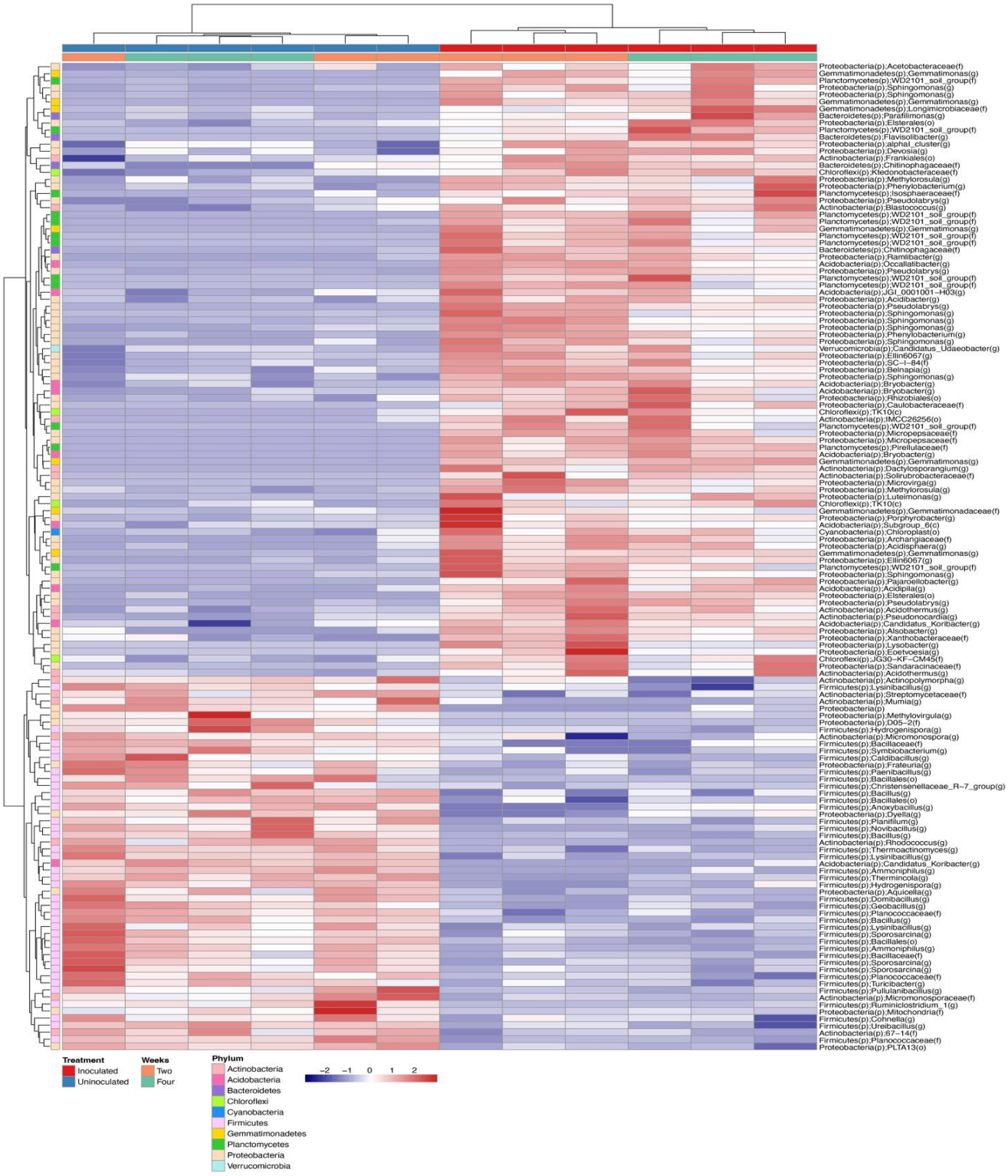

Figure 2.9 Heatmap showing the relative abundance of ASVs (16S rRNA with P addition), selected by indicator species analysis ($p < 0.05$). Samples and ASVs are clustered by Manhattan distance. Cell colours represent row-normalised z-scores (–2 to 2), where 0 is the mean abundance across samples. Positive values indicate higher-than-average abundance; negative values indicate lower. The coloured sidebar on the left indicates the phylum assignment of each ASV. Abbreviations indicate: p=phylum, c=class, o=order, f=family, g=genus.

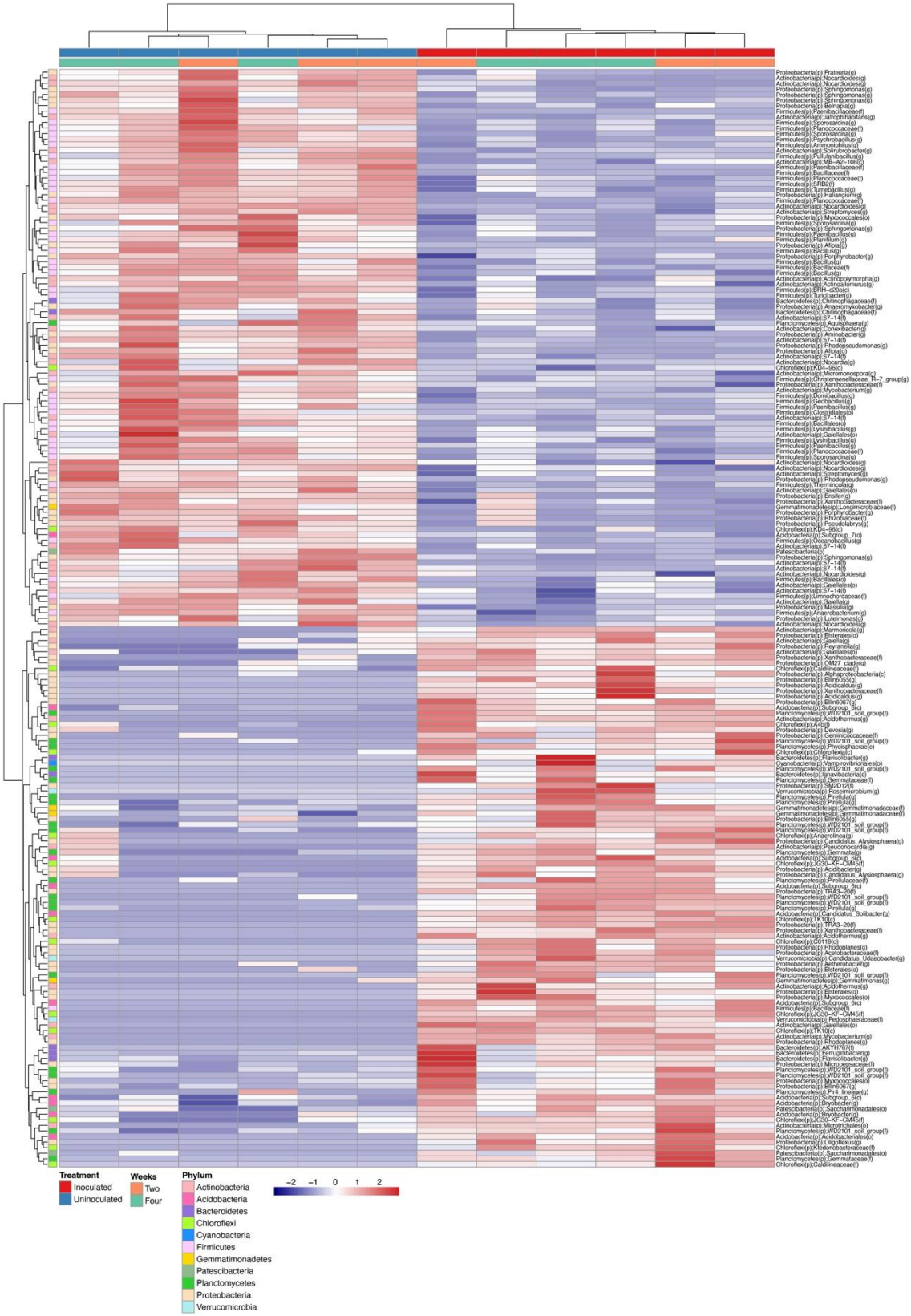

Figure 2.10 Heatmap showing the relative abundance of ASVs (16S rRNA without P addition), selected by indicator species analysis ($p < 0.05$). Samples and ASVs are clustered by Manhattan distance. Cell colours represent row-normalised z-scores (–2 to 2), where 0 is the mean abundance across samples. Positive values indicate higher-than-average abundance;negative values indicate lower. The coloured sidebar on the left indicates the phylum assignment of each ASV. Abbreviations indicate: p=phylum, c=class, o=order, f=family, g=genus.

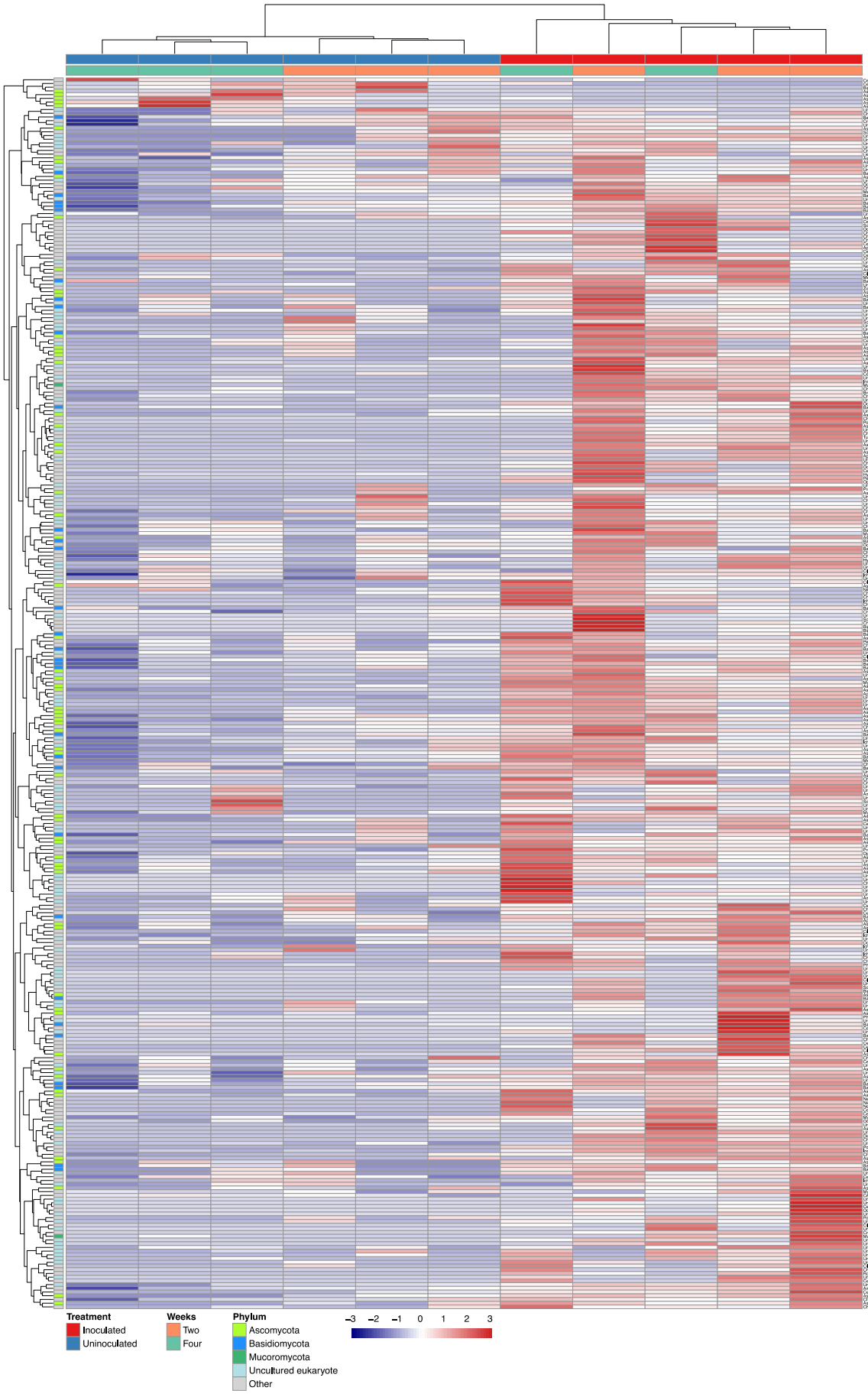
Treatment
Inoculated
Uninoculated
Weeks
Two
Four
Phylum
Ascomycota
Basidiomycota
Mucoromycota
Uncultured eukaryote
Other
−3
−2
−1
0
1
2
3

Figure 2.11 Heatmap showing the relative abundance of ASVs (18S rRNA with P addition), selected by indicator species analysis ($p < 0.05$). Samples and ASVs are clustered by Manhattan distance. Cell colours represent row-normalised z-scores (–3 to 3), where 0 is the mean abundance across samples. Positive values indicate higher-than-average abundance;negative values indicate lower. The coloured sidebar on the left indicates the phylum assignment of each ASV. For simplicity, only ASVs belonging to Ascomycota, Basidiomycota, and Mucoromycota were explicitly labelled. Abbreviations indicate: p=phylum, c=class, o=order, f=family, g=genus. Note: One inoculated P+ sample was excluded from the 18S analysis due to low read count and missing ASVs, suggesting sequencing failure.

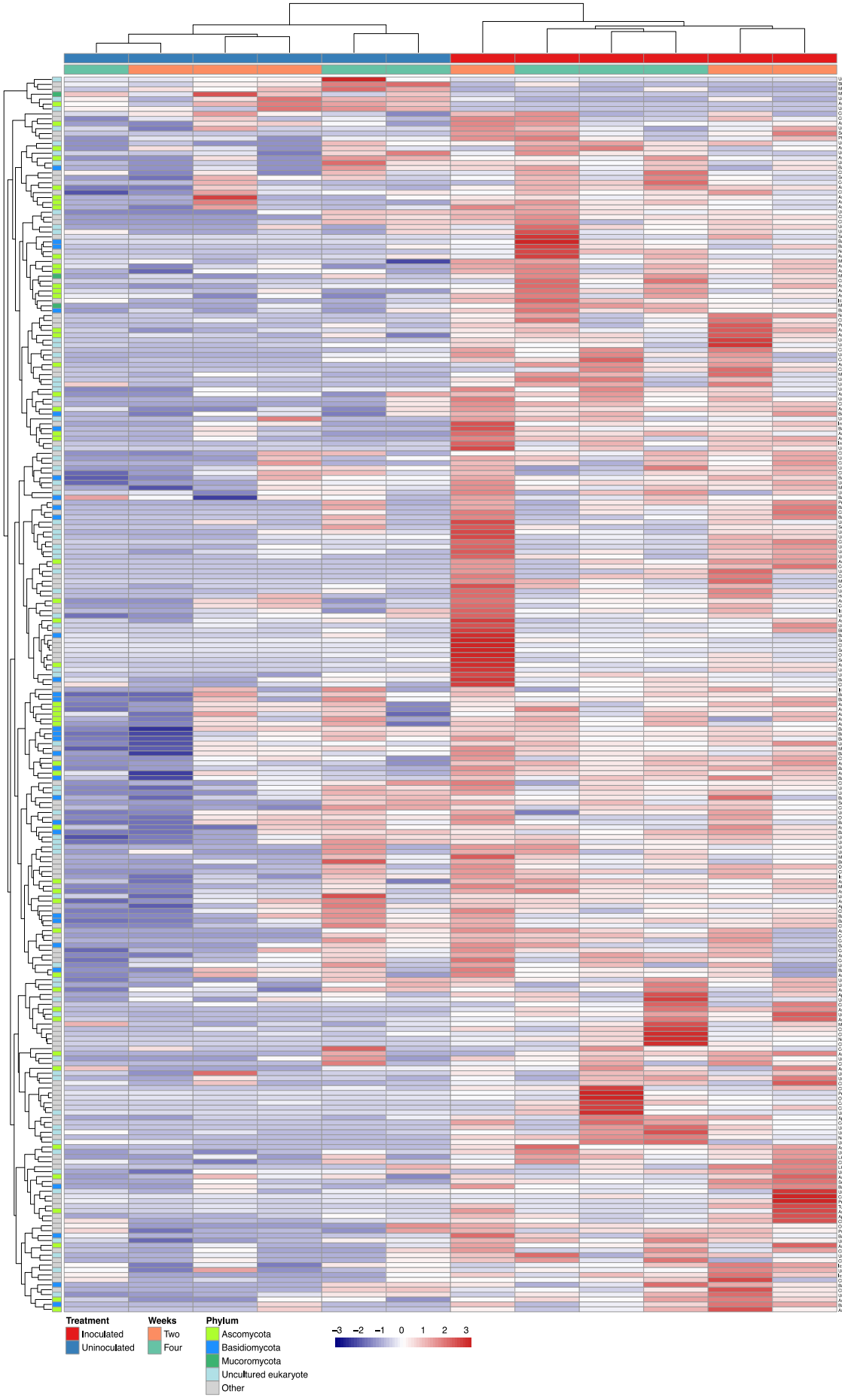
Treatment
Inoculated
Uninoculated
Weeks
Two
Four
Phylum
Ascomycota
Basidiomycota
Mucoromycota
Uncultured eukaryote
Other
−3 −2 −1 0 1 2 3

Figure 2.12 Heatmap showing the relative abundance ASVs (18S rRNA without P addition), selected by indicator species analysis ($p < 0.05$). Samples and ASVs are clustered by Manhattan distance. Cell colours represent row-normalised z-scores (–3 to 3), where 0 is the mean abundance across samples. Positive values indicate higher-than-average abundance;negative values indicate lower. The coloured sidebar on the left indicates the phylum assignment of each ASV. For simplicity, only ASVs belonging to Ascomycota, Basidiomycota, and Mucoromycota were explicitly labelled. Abbreviations indicate: p=phylum, c=class, o=order, f=family, g=genus.

2.4.3 Hyphae counting

The original set up in Table 2.2 from Keyes et al. (2022) was adapted and extra controls were included to further validate the results by counting the hyphae number in the side chambers. The impact of different treatments on the number of hyphae per gram of soil was assessed. Hyphae number per gram of soil in the inoculated samples containing plant ("plant + inoculant") exhibit a significantly lower hyphal count compared to both unplanted and uninoculated controls ("soil alone") (Figure 2.13). These two controls correspond to "inoculated" and "uninoculated" in the above-mentioned study. Furthermore, samples that were not planted consistently showed higher hyphal counts than those that were both planted and inoculated.

Additionally, treatments inoculated with sterilised inoculum do not show significant differences in hyphal numbers compared to other controls (excluding "plant + inoculant").

Success of colonisation was verified by staining the wheat roots in the inoculated samples (Figure 2.5).

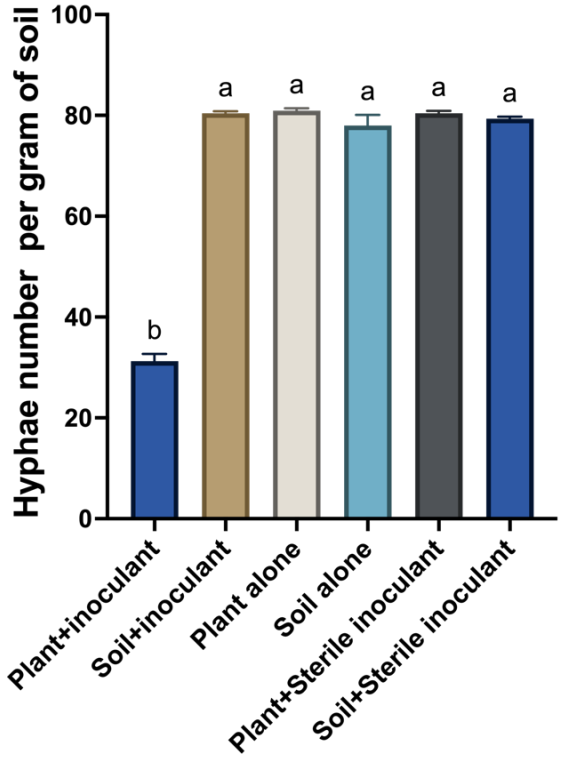

Figure 2.13 Hyphae counting of different samples. Different letters indicate statistically significant differences (Tukey's Multiple Comparisons test, $p \leq 0.05$). Bars represent the mean values (n=3). Error bars represent the standard error of the mean (SEM).

2.4.4 Competition experiment

To further study the impact of *R. irregularis* inoculation on the fungal community, a competition experiment was conducted. This experiment aimed to determine whether competition for nutrients exists within the hyphosphere community. The setup for this experiment was similar to that used in the previous experiment, with some slight variations in the controls. Specifically, a nutritional condition was introduced as an additional control alongside the inoculum.

We first sought to identify the point at which hyphal counts in the soil would reach a relatively stable stage. To do this, we set up samples and monitored hyphal numbers at different time points: 0, 3, 6, and 9 days post wetting (T0, T3, T6, T9). As expected, the hyphal count was close lowest at the start of the experiment (T0) and increased steadily on days 3 (T3) and 6 (T6) post wetting. The growth curve then began to plateau around day 9 (T9) (Figure 2.14). Based on these observations, we decided to use a 14-day growing period for the wheat plants. All measurements were taken in biological triplicate.

As illustrated by Figure 2.14, the addition of nutrient significantly increased the counts in the hyphal chambers, regardless of inoculation. Although the MS medium boosted hyphal numbers in the inoculated samples, the effects of inoculation on hyphal numbers were still evident. With or without the addition of MS medium, hyphal counts in the hyphal chamber soil were consistently lower in the inoculated samples than in the uninoculated samples.

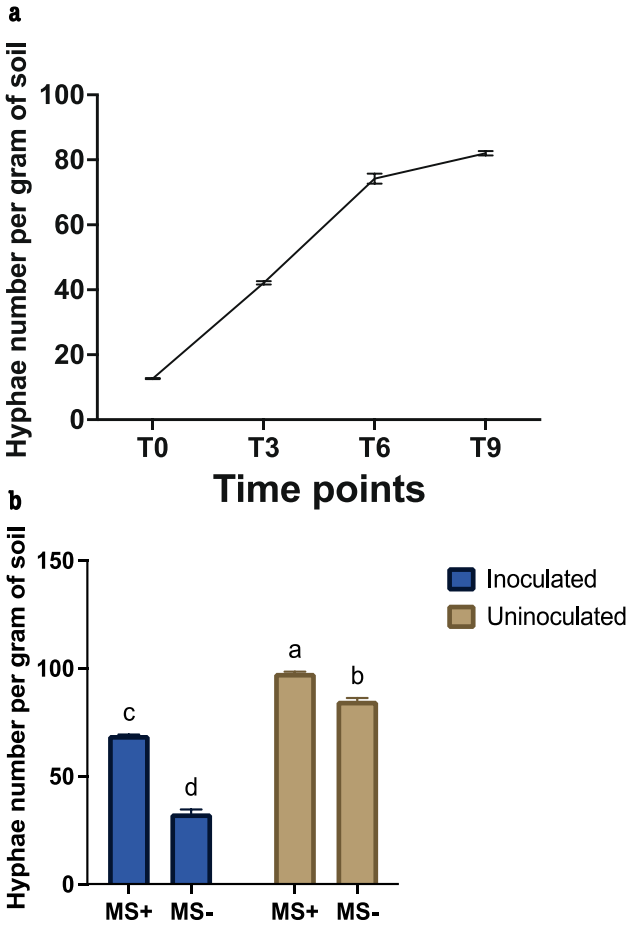

Figure 2.14 Competition experiment. (a) Time series on hyphae counting to decide until when the hyphae numbers will reach a plateau. T0, T3, T6, T9: start day, day 3, day 6, day 9 of counting. Error bars represent the standard error of the mean (SEM; n = 3). (b): Hyphae count in the competition experiment. MS: Murashige & Skoog Modified Basal Medium with Gamborg Vitamins. All counting were done under 40x magnification. The y-axis represents the number of hyphae per gram of soil, and the x-axis categorises different nutrition conditions applied. Different colours indicate different treatment groups. Bars represent the mean values (n=3). Error bars represent the standard error of the mean (SEM). Different letters indicate statistically significant differences based on two-way ANOVA followed by Tukey's Multiple Comparisons test ($p \leq 0.05$).

2.4.5 Effects of inoculation and nutrient on soil communities

To further explore the competition experiment, the same settings were used to study the effect of inoculation and nutrition on the hyphal chamber soil communities. Amplicon sequencing was performed, targeting the V4 region of the 16S rRNA gene for bacterial community analysis and the ITS1 region for fungal community profiling. Principal coordinates analysis (PCoA) was conducted to visualise the impacts of inoculation and MS supplementation on the composition of bacterial and fungal communities in the hyphosphere. The PCoA plot for bacterial communities (Figure 2.15, left panel) reveals distinct clustering patterns based on both inoculation and nutrient conditions. The first axis (PCoA Axis 1) explained 38.71% of the variation, while the second axis (PCoA Axis 2) accounted for 13.58% of the variation. Inoculated samples (both with and without MS medium) tended to cluster separately from uninoculated samples, and the presence of MS medium also appears to influence bacterial communities, as indicated by the distinct clustering of MS+ and MS− treatments. The impact of nutrient supplementation (MS medium) is highly significant ($p=0.001$, PERMANOVA), while the effect of inoculation is marginally significant ($p=0.076$, PERMANOVA).

In the PCoA plot for fungal communities (Figure 2.15, right panel), the first axis (PCoA Axis 1) accounts for 46.40% of the total variation, while the second axis (PCoA Axis 2) explains 9.96% of the total variation. Unlike bacterial communities, no distinct clustering pattern is observed between inoculated and uninoculated samples; however, the MS medium results in some differentiation within fungal communities, as MS+ samples cluster separately from MS− samples along the first axis. Statistical analysis reveals a dominant effect of nutrient supplementation (MS medium) ($p=0.001$, PERMANOVA), while the effect of inoculation is non-significant ($p=0.155$, PERMANOVA).

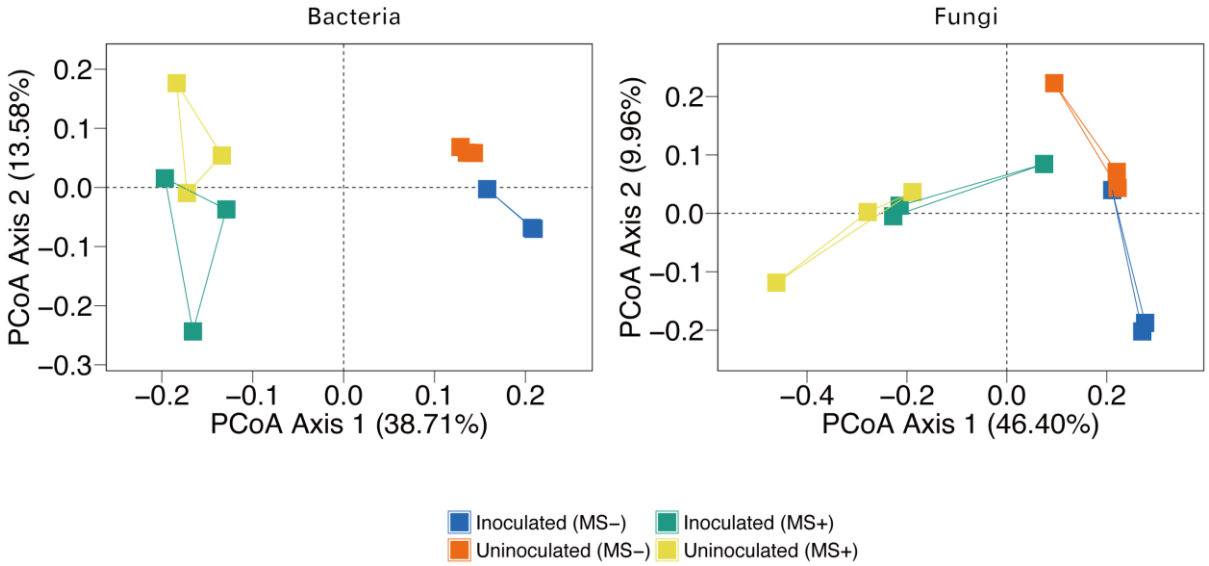

Figure 2.15 Principal Coordinates Analysis (PCoA) plots of microbial community composition based on 16S rRNA gene sequencing (left) and ITS sequencing (right), using Bray-Curtis dissimilarity matrices. Points represent individual samples, with colours indicating different sample groups.

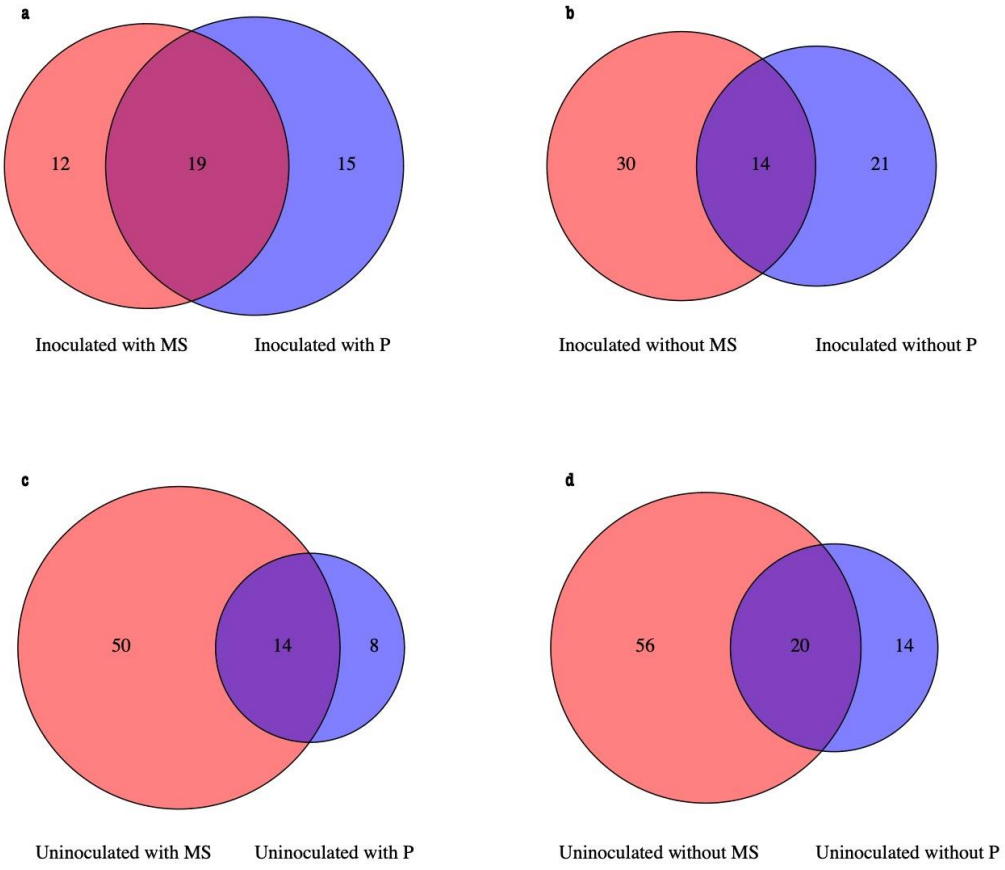

Figure 2.16 Venn diagrams comparing bacterial families associated with inoculated and uninoculated treatments under MS+/MS- and P+/P- conditions. Families were grouped based on indicator ASVs identified using indicator species analysis ($p < 0.05$) in 16S rRNA data. Each panel

shows the number of shared and unique bacterial families between matching conditions: (a) Inoculated with P vs. Inoculated with MS; (b) Inoculated without P vs. Inoculated without MS; (c) Uninoculated with P vs. Uninoculated with MS; (d) Uninoculated without P vs. Uninoculated without MS.

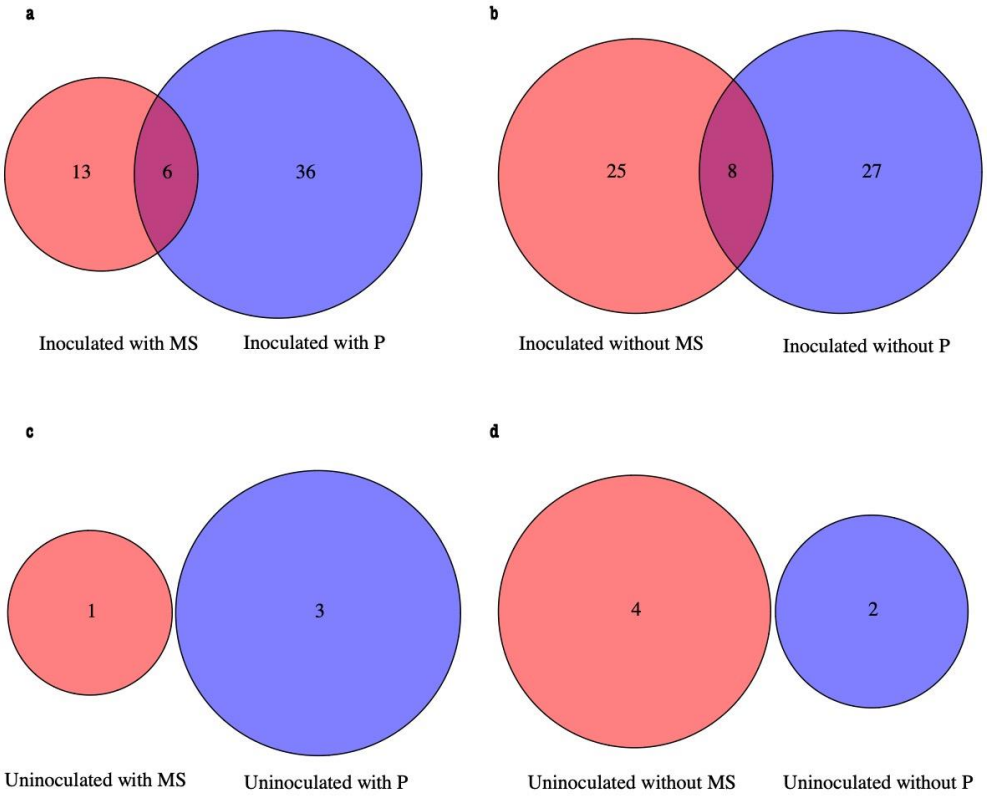

Figure 2.17 Venn diagrams comparing fungal families associated with inoculated and uninoculated treatments under MS+/MS- (ITS data) and P+/P- (18S data) conditions. Families were grouped based on fungal ASVs identified through indicator species analysis ($p < 0.05$), using the ITS dataset for MS+/MS- comparisons and the 18S rRNA dataset (fungal subset only) for P+/P- comparisons. Each panel shows the number of shared and unique fungal families between corresponding conditions: (a) Inoculated with P (18S) vs. Inoculated with MS (ITS); (b) Inoculated without P vs. Inoculated without MS; (c) Uninoculated with P vs. Uninoculated with MS; (d) Uninoculated without P vs. Uninoculated without MS.

Indicator species analysis identified ASVs significantly associated with either the inoculated or uninoculated groups across both 16S and ITS datasets ($p < 0.05$). In the 16S dataset, 235 ASVs were identified under MS+ condition, including 68 ASVs associated with the inoculated group and 167 with the uninoculated group; under MS– condition, 436 ASVs were identified, with 181 enriched in the inoculated group and 255 in the uninocu-

lated group. For the ITS dataset, 67 ASVs were identified under MS+ condition, with 5 associated with the uninoculated group and 62 with the inoculated group; under MS− condition, 114 ASVs were identified, including 24 associated with the uninoculated group and 90 associated with the inoculated group.

To assess whether similar indicator taxa were identified across nutrient conditions, ASVs from both the MS and previous P experiments (Section 2.4.2) were grouped by family and compared using Venn diagrams (Figure 2.16; Figure 2.17). For the 18S dataset (P conditions), only fungal families were included in the comparison to align with the ITS dataset used for the MS conditions. Comparisons were made separately for each treatment condition: (a) Inoculated with P vs. Inoculated with MS; (b) Inoculated without P vs. Inoculated without MS; (c) Uninoculated with P vs. Uninoculated with MS; and (d) Uninoculated without P vs. Uninoculated without MS.

In the 16S dataset, moderate overlap in bacterial families was observed between the P and MS conditions for inoculated samples, with 19 families shared under P+ and MS+ (Figure 2.16 a) and 14 families under P− and MS− (Figure 2.16 b). The remaining families were unique to each condition, suggesting that while some inoculation-responsive taxa were consistent across nutrient regimes, many were condition-specific. For uninoculated samples, 14 families overlapped under P+ and MS+ (Figure 2.16 c) and 20 families under P− and MS− (Figure 2.16 d), though the MS conditions—particularly MS− —included a greater number of unique families.

In the fungal dataset, comparisons were made between ASVs identified under P conditions using the 18S rRNA gene and those under MS conditions using the ITS region. Under inoculated treatments, 6 fungal families were shared between P+ and MS+, and 8 families were shared between P− and MS− (Figure 2.17 a,b). In contrast, no families were shared between P and MS conditions in uninoculated treatments (Figure 2.17 c,d).

To determine if inoculation also affected the number of bacteria in the soil, similar to fungi, qPCR was conducted to assess the impact of inoculation and nutrient supplementation on the bacterial community by quantifying the 16S rRNA gene copy numbers across samples (Figure 2.18), including inoculated (I) vs. uninoculated (U) and with (M+) vs. without (M−) the addition of MS medium. The results indicate that, under both inoculated and uninoculated conditions, differences in 16S rRNA gene copy numbers are non-significant, regardless of the presence or absence of MS medium.

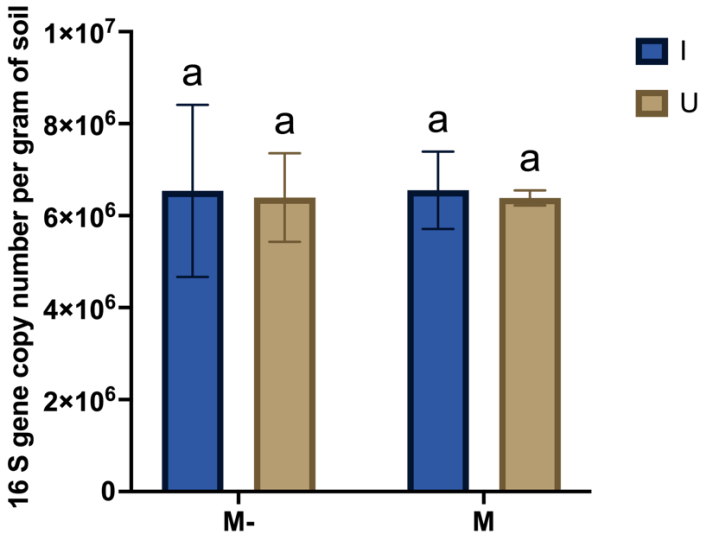

Figure 2.18 Quantitative PCR (qPCR) analysis showing the 16S rRNA gene copy numbers across different sample groups. M: Murashige & Skoog Modified Basal Medium with Gamborg Vitamins. The y-axis represents the 16S rRNA gene copy number per gram of soil, and the x-axis categorises different nutrition conditions applied. I: inoculated, U: uninoculated, M-: without MS medium added, M+: with MS medium added. Different colours indicate different treatment groups. Bars represent the mean values (n=3), Error bars represent the standard error of the mean (SEM). Different letters indicate statistically significant differences (Tukey's Multiple Comparisons test, $p \leq 0.05$).

2.5 Discussion

This study aimed to investigate the effects of AM fungus (*R. irregularis*) inoculation on soil microorganisms, with specific focus on changes within the bacterial and fungal communities in the wheat hyphosphere. To address this, we designed a system to include both root chambers and hyphal chambers that separate the communities associated with each compartment.

The results showed that the inoculation made a difference between the bacterial communities, with distinct clustering patterns found between inoculated and uninoculated samples, suggesting that *R. irregularis* inoculation had a significant impact on community structure in the hyphal chamber. Both nutrient availability (P and MS) and inoculation influenced bacterial community composition, with the dominant factor varying between the experiments. Nonetheless, inoculated samples, regardless of nutrient conditions, clustered separately from uninoculated samples. Specific groups of bacteria were enriched in the hyphosphere, while overall diversity stayed unchanged. Enriched

taxa included members of Alphaproteobacteria (e.g., Sphingomonadaceae, Xanthobacteraceae, Devosiaceae) and Gammaproteobacteria (e.g., Xanthomonadaceae) which were associated with the inoculation of *R. irregularis* (Table S 5). This is consistent with the finding of Emmett et al. (2021). Although many of the enriched families overlapped between P+ and P- conditions, including Gemmatimonadaceae and Nitrosomonadaceae, several taxa were unique to either condition (Table S 5; Table S 6). This suggests that while inoculation had a consistent effect, nutrient availability also shaped which bacterial groups responded. Despite the observed shifts in bacterial community structure, qPCR of 16S rRNA genes showed no difference after *R. irregularis* inoculation and MS addition, suggesting that these treatments did not change the overall bacterial abundance in the hyphosphere.

The overlap of bacterial families in the inoculated treatment suggests a degree of consistency in the taxa responding to *R. irregularis* inoculation, regardless of whether P or MS was added. However, each condition also had unique families, providing further evidence that bacterial responses to inoculation are at least partly shaped by nutrient availability (Figure 2.16 a).

18S rRNA sequencing not only targeted the fungi, but eukaryotes in general. While the 18S rRNA sequencing revealed a range of eukaryotes, we focused on the common soil fungi (i.e., Ascomycota, Basidiomycota, and Mucoromycota) which showed a significant reduction in the abundance of fungi in the inoculated samples. When compared the relative abundance of the common soil fungi (i.e., Ascomycota, Basidiomycota, and Mucoromycota), the abundance in inoculated samples was significantly lower compared to uninoculated samples. This was consistent with the results reported by Keyes et al. (2022), with lower hyphal abundance in the inoculated samples observed by synchrotron X-ray computed tomography (SXRCT). However, there was no clear differentiation for fungal taxa based on inoculation by ITS analysis, while nutrient supplementation clearly had an effect. Unfortunately, neither the 18S rRNA nor ITS primers detected *R. irregularis* in the soil, despite the fungus being clearly visible associated with the roots and in the hyphal chambers. Mismatches between the 18S rRNA primers and the 18S rRNA gene of *R. irregularis* were identified, which may explain its absence from these datasets (Figure S 11 a,b). Although the ITS primers showed better overall alignment to

the *R. irregularis* genome than the 18S primers, the ITS1 forward primer showed a perfect match with its target region, and the reverse primer aligned from the fifth base onward. Both primers also showed multiple off-target matches within the *R. irregularis* genome, which may have reduced amplification specificity and efficiency (Figure S 11 c,d).

The absence of *R. irregularis* in both 18S and ITS datasets, despite clear microscopic evidence of its presence (Figure 2.5), highlights a key limitation of universal primers. This not only affected the detection of *R. irregularis*, but also likely contributed to the broader underrepresentation of Glomeromycota (Lee et al., 2018). This was evident in our study: Glomeromycota was not detected in the 18S dataset, and only one ASV from this phylum was found in the ITS dataset. By contrast, fungal genera commonly expected in soils — such as *Aspergillus*, *Mortierella*, *Fusarium*, and *Penicillium* (Warcup, 1951) — were detected across both datasets, suggesting partial success in capturing expected taxa. To improve detection of *R. irregularis*, primers could be designed to amplify a longer rDNA fragment spanning the partial small subunit (SSU), full ITS rDNA region, and partial large subunit (LSU), as demonstrated by Krüger et al. (2009). This approach offers higher specificity and species-level resolution for Glomeromycota compared to standard 18S or ITS primers.

The overlap of fungal families across all treatments and nutrient conditions (P and MS) (Figure 2.17) was lower compared to the bacterial dataset (Figure 2.16). This may reflect a stronger influence of nutrient availability on fungal responses to inoculation. Although some overlap was observed between inoculated samples under P and MS conditions, the number of shared families was limited (Figure 2.17 a), suggesting only partial consistency in fungal taxa associated with *R. irregularis*. In contrast, no overlap was found among uninoculated samples across all conditions (Figure 2.17 c,d), which likely reflects a difference in nutrient regimes. Additionally, the limited overlap overall may be partly due to primer differences between the ITS and 18S datasets, which could have led to the under-detection of certain fungal taxa — an issue explored in more detail later in this section.

It is also worth noting that different DNA extraction kits were used in the P and MS experiments, which may have introduced subtle biases in ASV recovery and relative abundance. Although the overall patterns of taxonomic overlap are interpretable, some of

the differences in detected bacterial and fungal families could partly reflect methodological variation rather than true biological divergence.

Competition for nutrients was considered as a likely explanation for the lower abundance of hypha in the inoculated chambers. Therefore, the impact of nutrient supplementation (MS medium) alone with inoculation was also studied to test if a competition existed between *R. irregularis* and native fungi in the hyphosphere. Although the MS medium addition increased hyphal counts in all the samples (both inoculated and uninoculated), lower hyphal counts in inoculated samples was always observed (Figure 2.14b). This indicates that *R. irregularis* has an advantage in competing for nutrients with other fungi, even under relatively nutrient-rich conditions, which is possibly due to more efficient nutrient uptake and the advantage of a carbon and energy supply from the plant giving them a strong competitive advantage.

A finding of particular note in this study was that fewer fungi were found when the samples were inoculated. It is intriguing and counter-intuitive that *R. irregularis* inoculation had lower hyphal counts but suggests that even a low number of AM hyphae can dramatically reduce the growth of saprophytic soil fungi in this system. Furthermore, it would be expected that fungi would increase when there is a plant present because many AM fungi can establish symbiosis with the plants (Smith and Read, 2008). However, this analysis focused on the hyphosphere and was at a considerable distance to the root, which likely limited the interaction in the hyphal chamber except for the mycorrhiza.

There are two possible explanations for the lower fungal abundance following inoculation. One possible explanation is that *R. irregularis* dominated the hyphosphere by having a more efficient nutrient uptake system, hence outcompeting native fungi for nutrients, such as P. This has been suggested (e.g., Zhang et al. (2014), but to our knowledge never shown as clearly as in our study. Another possibility is that *R. irregularis* secretes chemicals that can supress the growth of other native fungi directly, similar to its recognised impacts on bacterial activity (Welc et al., 2010; Filion et al., 1999). Rinaudo et al. (2010) also reported that AM fungi suppressed aggressive agricultural weeds. If there was a suppression mechanism against saprophytic fungi, it appeared to act broadly

against all the fungi in the hyphal chamber since there was little difference in the diversity of fungi (as detected by ITS analysis) between the inoculated and uninoculated hyphal chambers.

This study also highlighted the limitations of 18S rRNA gene primers (Hadziavdic et al., 2014), which amplified a broad range of non-fungal eukaryotic taxa. For example, sequences assigned to the phylum Phragmoplastophyta — which includes land plants (e.g., *Arabidopsis*) and their green algal relatives (e.g., *Cylindrocystis*) — were detected. Other non-target groups included Hemimastigophora, a group of single-celled protists (Foissner et al., 1988); protozoa such as Ciliophora; and members of the phylum Nematoda. To overcome this, we employed the fungal-specific internal transcribed spacer (ITS) primers, which can discriminate between fungal and plant sequences (Martin and Rygiewicz, 2005). This adjustment provided better insight into the fungal community in the MS experiment, although *R. irregularis* sequences were still not detected.

As previously noted, using different primers across experiments introduces limitations for cross-comparison, as 18S and ITS target different genomic regions and vary in their taxonomic resolution and group coverage. For example, 18S rRNA primers capture a broader range of eukaryotic taxa and can detect early-diverging fungal lineages such as Cryptomycota and Chytridiomycota (Rojas-Jimenez et al., 2017), both of which were detected in this study (Figure 2.11; Figure 2.12). Nonetheless, they tend to underrepresent Glomeromycota and have limited species-level resolution (Schoch et al., 2012). In contrast, ITS primers are more specific to fungi and provide finer taxonomic resolution, particularly for Ascomycota and Basidiomycota (Schoch et al., 2012). Some differences in fungal composition between experiments may therefore reflect primer-driven detection biases rather than true biological variation.

Future research should focus on exploring the potential suppression of *R. irregularis* on non-mycorrhizal fungi. Given the limitations of amplicon sequencing observed in this study — specifically its failure to detect *R. irregularis* despite visual confirmation — a metagenomic approach could offer more comprehensive detection, as it bypasses the biases introduced by primer selection. Additionally, a qPCR assay targeting *R. irregularis*-specific regions could serve as a sensitive and cost-effective method for confirming its presence. Proteomic and metabolomic approaches could be applied to study if *R. irregularis* secretes inhibitory compounds into the surrounding environment. Due to

time pressure, we did not analyse the impact of nutrient supplementation on fungi at the taxonomic level, which should also be incorporated into the analysis of ITS sequencing results in the future. A better understanding of these concepts would help in the design of more effective field studies.

Chapter 3 Effect of root exudates on microbial growth in soil

Abstract

Root exudates play a vital role in shaping rhizosphere microbial communities, yet the specific microbial responses to exudate composition and concentration remain poorly resolved. This study examined the effects of artificial and natural exudates, as well as volatile organic compounds (VOCs) emitted from artificial exudate-treated soils, on soil bacterial communities. Artificial exudates mimicking plant-derived compounds were applied at five concentrations, with and without the secondary metabolite 6-methoxy-benzoxazolin-2-one (MBOA), while natural exudates were collected from wheat, sorghum, and chicory. VOCs emitted from artificial exudate-treated soils were assessed using an air-ventilated Petri dish system. Bacterial community composition was analysed using 16S rRNA amplicon sequencing.

Artificial exudates induced clear dose-dependent shifts in community structure, with Actinobacteria—particularly Micrococcaceae—responding strongly across concentrations. MBOA introduced additional selective pressure under high-carbon conditions, although its specific role could not be isolated. Natural exudates stimulated more taxonomically diverse communities than artificial formulations, but unquatified composition and biomass variation between plant types limited mechanistic interpretation. VOCs from artificial exudate-treated soils altered recipient soil communities, though not in a dose-dependent manner. Some bacterial families (e.g., Burkholderiaceae, Rhodanobacteraceae, Nocardioidaceae) were selectively enriched, but the absence of direct VOC profiling limits conclusions about underlying mechanisms.

Although this study could not determine whether enriched taxa were actively selected or whether others were suppressed, the wider literature suggests both processes are possible. Overall, the findings underscore the importance of exudate identity and concentration in shaping microbial communities and highlight the need for future studies integrating chemical and functional analyses to better understand belowground plant–microbe interactions.

3.1 Introduction

3.1.1 Root exudates and the rhizosphere

The plant rhizosphere is a zone of high microbial activity stimulated by plant root exudates. This requires a large investment from the plant considering they release up to 20-40% of photosynthetic carbon as root exudates (Badri and Vivanco, 2009). Root exudates are in fact complex mixtures of compounds including simple sugars, organic acids, amino acids, tannins, steroids, terpenoids, alkaloids, polyacetylenes, and vitamins (Inderjit and Weston, 2003). Included in these mixtures are antimicrobial allelopathic compounds, which inhibit the growth of some microbes (Inderjit and Weston, 2000). These compounds, often referred to as phytoalexins, also differ between plant taxa and are produced in wheat, including benzoxazinoids such as DIMBOA with antimicrobial properties. The net effect from the different combinations of nutrients and antimicrobial compounds in root exudates is the formation of a rhizosphere microbial community that is specific to the plant species and changes based on the plant growth stage and stress conditions (Song et al., 2012; Chai and Schachtman, 2021).

In agricultural practice, roots exudates play an important role in improving soil health as well as nutrient availability, which is critical given the urgent global demand for increasing crop yields (Chandra et al., 2024b). The ability of plants to release exudates containing sugars, amino acids, organic acids and allelopathic compounds would help enhance nutrient cycling hence improving productivity of crops.

3.1.2 The soil microbial communities

The rhizosphere microbial community contains a large proportion of plant growth-promoting bacteria (PGPB) that benefit plants by facilitating the uptake of nutrients, producing phytohormones, or modulating plant stress responses (Glick, 2012). The mechanistic basis for selection of PGPB in the rhizosphere and the relative inhibition of phytopathogens is unclear. For example, plants might select for PGPB by providing unique mixtures of microbial growth substrates, or some PGPB might be relatively resistant to the phytoalexins produced by a particular plant species. The composition of the root ex-

udates also has undetermined consequences for the growth rate and turnover of microbial populations within the rhizosphere. Presumably, rapid growth and turnover will stimulate the recycling of nutrients that will benefit the plant.

Besides PGPB, the rhizosphere is home to a diverse array of microorganisms, including mycorrhizal fungi. Mycorrhizal fungi can form symbiosis relationship with the root system, thus extending the capacity of plants to access nutrient further down the soil, particularly P, which is often present in trace amounts in soil (Smith and Read, 2008). Through the development of hyphae, mycorrhizal fungi significantly increase the surface area of the root system, allowing access to nutrients beyond the reach of roots. P-solubilising microbes convert insoluble soil P into soluble forms, making them accessible for plants (Sharma et al., 2013), while N-fixing bacteria convert atmospheric N_2 into ammonia, making N available (Glick, 2012). Together, these diverse functions of microbes contribute to maintaining the nutrient cycling in the rhizosphere, benefiting both soil fertility and plant health. Root exudates play a central role in this process by serving as carbon sources that stimulate microbial activity and turnover (Badri and Vivanco, 2009).

The interaction between soil microbes and plants helps maintain a constant nutrient supply, as increased microbial activity leads to higher supply of vital nutrient elements such as P and N (Eze et al., 2024). In summary, the interaction between soil microbes and root exudates form a strong nutrient circle within the rhizosphere, which is particularly important in nutrient-deficient soils, where functions like P-solubilising, N-fixing can significantly improve plant growth and resilience to the environment (Vives-Peris et al., 2020). A better understanding of these interactions can help us make crucial progress to achieving sustainable agriculture.

3.1.3 Plant root exudates: wheat, sorghum, and chicory

Root exudates vary significantly between plant species and these variations can significantly influence the structure and composition of rhizosphere communities. The unique composition of each exudate is a reflection of its own metabolic pathway and adaptation to the environment (Ma et al., 2022). Understanding the compositions of different plant exudates, such as wheat, sorghum and chicory, is essential to understanding how they affect soil microbial communities.

Wheat, sorghum and chicory are considered important plants in agriculture, each contributing in different ways to farming systems. Wheat is a staple food crop globally, which is widely grown in temperate regions (Shiferaw et al., 2013). Sorghum is also a cereal crop like wheat, but it is more resilient to drought and often cultivated in arid or semi-arid regions (Kubiku et al., 2022). Chicory, although not a cereal crop, is well known for its deep roots, which improve soil structure, reduce soil erosion, and benefit crop rotation (Zhang et al., 2024b). These three plants were selected based on their differing characteristics and practical relevance: wheat and sorghum are both cereal crops but differ in traits such as drought tolerance, while chicory — though unrelated and not a cereal crop — was included because it was used by the supplier as part of the host mixture for culturing the AM fungus *R irregularis* in Chapter 2.

These plants belong to different phylogenetic branches of the plant kingdom - wheat and sorghum belong to the Poaceae family (grasses), while chicory belongs to the Asteraceae family (daisies) – and thus have different root exudate compositions. For example, wheat produces amino acids such as ornithine, isoleucine and citrulline, sugars such as glucose and fructose, and organic acids such as gluconic acid and citric acid (Yahya et al., 2021). These compounds stimulate microbial activity by supplying essential nutrients. Additionally, wheat can also produce secondary metabolites such as cyclohexanol, cyclohexanone and *N*-methyl phenylethylamine (Wang et al., 2006), which may act as antimicrobial agent and shape the microbial community by inhibiting certain pathogens. Sorghum produces the luteolinidin and apigeninidin phytoalexins (Awika et al., 2005), which are known to inhibit growth of pathogens. Chicory, on the other hand, is known for its secretion of sesquiterpene lactones (Graziani et al., 2014), bioactive compounds known for health-related and antimicrobial properties.

Evidence also indicates notable chemical differences at the cultivar level within each species. For wheat, a study comparing three wheat varieties — Faisalabad-08, Fakhr-e-Sarhad, and Benazir-13 — revealed significant differences in the exudation of amino acids (e.g., leucine, ornithine), sugars (e.g., glucose, fructose), and organic acids (e.g., gluconic acid, citric acid) (Yahya et al., 2021). For sorghum, a study examining seven varieties of different origins (BRS330, BRS509, BRS655, BRS802, CMSxS912, SRN-39, and Shanqui-Red) showed that each exhibited a unique strigolactone profile: sorgomol was produced by BRS330, BRS509, BRS655, BRS802 and CMSxS912, and was most abundantly exuded by BRS655. All cultivars were found to produce 5-deoxystrigol, which was

highly exuded by BRS509 and Shanqui-Red but minimally by SRN-39. In contrast, orobanchol was exuded by SRN-39 at levels 300 to 1100 times higher than in the other six varieties (Schlemper et al., 2017). For chicory, the study by Peña-Espinoza et al. (2015) reported that the variety Spadona showed greater anti-parasitic effects than Puna II against nematode *Ostertagia ostertagi*, attributed to its higher concentration of sesquiterpene lactones.

In this experiment, root exudates from wheat, sorghum, and chicory were each applied separately to study their effects.

3.1.4 Natural vs. artificial exudates

Natural exudates are complex mixtures of compounds, including simple sugars, organic acids, amino acids, and secondary metabolites, which vary from plant to plant, depending on the species, stage of growing as well as the surrounding environment (Dakora and Phillips, 2002). Natural exudates play a critical role in shaping soil communities, promoting PGPMs, and inhibiting pathogens by releasing antimicrobial compounds like phytoalexins (Vives-Peris et al., 2020).

Benzoxazinoids, such as DIMBOA (2,4-dihydroxy-7-methoxy-(2H)-1,4-benzoxazin-3(4H)-one), are allelopathic compounds produced by common grass crops such as maize and wheat. Using mutant maize plants unable to produce benzoxazinoids, Hu et al. (2018) showed that these compounds alter root-associated fungal and bacterial communities, decrease plant growth, increase jasmonate signaling and plant defence, and suppress herbivory. These effects appeared to be the consequence of the DIMBOA breakdown product MBOA (6-methoxy-benzoxazolin-2-one), which accumulated in rhizosphere soil. The findings also suggested that the effects on plants were not a direct consequence of MBOA rather due to changes in the rhizosphere microbial community induced by MBOA.

Artificial exudates are simplified versions of natural exudates, designed to mimic at least part of the functions of natural exudates. Artificial exudates contain primary metabolites such as sugars, organic acids, and amino acids, but normally are lack of the secondary metabolites that found in natural exudates , which might reduce the complexity. Nonetheless, artificial exudates still reflect part of the plant-microbe interaction (Vaidya et al., 2022).

Despite the use of artificial exudates in research, questions remain about whether artificial exudates can fully replicate the ecological functions of natural exudates. The secondary metabolites and signalling molecules in natural exudates may play important roles in shaping microbial communities, which might not be mimicked fully by artificial exudates (Strickland et al., 2015). Moreover, another area of uncertainty is the dose-dependent effects of exudates on soil microbial communities. Natural exudates are released in different amounts at different growing stages and under different environmental conditions (Ahlawat et al., 2024). However, most research focused on the composition of exudates instead of the concentrations. Artificial exudates mimic at least part of the functions of natural exudates by providing carbon sources, impact of the concentration gradients of artificial exudates on microbial community still remains under-studied. Although some studies researched the role of artificial exudates, the effects of concentration gradient are still not fully understood (Vaidya et al., 2022).

3.1.5 Volatile Organic Compounds (VOCs) produced by soil microbes

Microbes in the soil produce chemicals called volatile organic compounds (VOCs), which can also shape the soil microbial communities and promote the growth of PGPMs, similar to the plant exudates. As signalling molecules, VOCs also improve nutrient acquisition and enhance plant defence (Srikamwang et al., 2023; Waseem et al., 2021). These compounds, including a range of low molecular weight chemicals such as alcohols, esters, ketones, and terpenes, are able to diffuse through the soil matrix and into the surrounding atmosphere, where they can influence neighbouring microbial communities (Almeida et al., 2023).

The long-distance effects of VOCs on microbial communities have been reported by Schulz-Bohm et al. (2015), claiming that VOCs produced by microbes in soil can affect interactions among bacterial populations in the surrounding, particularly in nutrient-limited soils. Effects of VOCs on the soil microbes and their effects as signalling molecules have been extensively studied (Waseem et al., 2021), the influence of exudate concentration on VOC production and its subsequent effects on neighbouring microbial communities remains largely unexplored. Whether there is a dose-dependent effect of VOCs produced by artificial exudate stimulation on the surrounds remains unclear, and further research is required to understand the relationship. A better understanding of

the links between artificial exudate concentration, VOC production, and their downstream impacts on surrounding microbial communities, alone with the dose-dependent effects of artificial exudates on soil microbial communities, will provide a clearer vision of the plant-microbe dynamics belowground and provide a solid theoretical foundation for sustainable agricultural practices.

The aim of this study is to investigate the influence of artificial and natural exudates on microbial communities in the soil, focusing on concentration effects, exudate type, and the effect of VOCs produced by artificial exudate-treated soils.

3.2 Objectives

The objectives of this chapter are:

1. To compare the impacts of natural exudates from wheat, sorghum and chicory on the composition of soil bacterial communities.
2. To study the effect of artificial exudates on soil bacterial community compositions, with a focus on the concentration effects.
3. To contrast the differences between artificial exudates with a constant MBOA concentration and those with diluted concentrations in shaping the soil bacterial communities.
4. To investigate the impact of volatile organic compounds (VOCs) produced by soil samples treated with artificial exudate on recipient soil bacterial communities.

3.3 Materials and methods

3.3.1 Plant growth

Seeds of wheat (*Triticum aestivum* cv. Apache, WBCDB0003-PG-1), sorghum (a mixture of Sprint 11 and Penn 110), and chicory (*Cichorium intybus* Puna II) were used in this experiment. Wheat seeds were obtained from the Germplasm Resources Unit of the John Innes Centre (Norwich, UK), while sorghum and chicory seeds were provided by Plant-Works Ltd. (UK), with the chicory sourced from Cotswold Seeds Ltd. (UK).

Seeds were first germinated at 23 ±1 °C for 96h under dark conditions on moist Millipore filter paper in Petri dishes. After germination, seeds were planted into pots filled with

Eutric Cambisol soil (as described in Section 2.3.1) and kept in the University of Southampton glasshouse facility (Southampton, UK), with daytime temperatures of 23°C, nighttime temperatures of 18°C, and 16 hours of daylight at 55% humidity. All plants were grown for three months prior to exudate collection.

3.3.2 Extraction of root exudates

The method from Williams et al. (2021) was used for the extraction of root exudates from wheat, sorghum and chicory roots. Briefly, plant roots were washed by shaking and suspending carefully in milli-Q water, in order to remove adhering material. After root washing, plants were subjected to the next stage: hydroponic recovery. At this stage, plants were transferred to an aerated hydroponics solution (500 mL per plant) for recovery. The hydroponic recovery solution was prepared using a ratio of 200g of stored Chilworth soil (collected near Southampton) per 1L of Milli-Q water, followed by filtration through 0.2 mm mesh. Plants underwent recovery in the glasshouse, maintained under the same conditions as during growth.

Root exudate collection was carried out 7 days after the recovery. For each species of plant, four plants were put into a sterile glass bottle and roots were submerged in 100 ml of pure milli-Q water. The bottles were chilled on ice to prevent the exudate from turning over (i.e., to slow microbial and enzymatic activity), and the whole system was placed on an orbital shaker at room temperature in natural ambient light for 2 h at 60 rpm. After shaking, the exudate solution was filtered using 0.22µm syringe filter (Merck Millipore, Germany), the filtered exudate solution was collected using 50ml CellStar Falcon tubes (Item: 227261, Greiner Bio-one, Gloucester, UK) (Figure 3.1). For each beaker, 90 mL of solution was collected and split in to three 50ml CellStar Falcon tubes. All samples were frozen to -80 °C right after collection and stored in the freezer for future use.

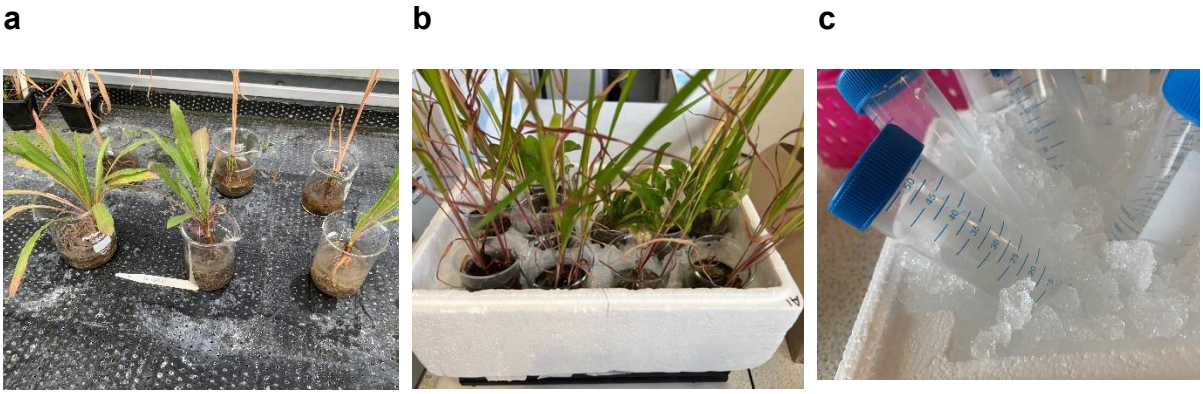

Figure 3.1 Root exudate collection process. a: hydroponic recovery; b: hydroponic collection; c: exudate collected in CellStar Falcon tubes.

After freezing, all samples were freeze-dried in an Edwards (Thermo Scientific) Modulyo freeze dryer (Thermo Scientific, UK) and returned to -80 °C for storage.

3.3.3 Preparation of natural exudates (wheat, sorghum and chicory)

For natural exudates, freeze-dried pellets of wheat in 15 tubes were resuspended in 2 ml of sterile Milli-Q water and combined into one Falcon tube, then filter-sterilised using 0.22 µm syringe filter (Merck Millipore, Germany). Exudates of sorghum and chicory were prepared in the same manner.

3.3.4 Preparation of artificial exudates

Five different concentration gradients were prepared for artificial exudates: 0, 8, 25, 60, 100%, following the method modified from Griffiths et al. (1998). All chemicals including MBOA were obtained from Merck. Three different types of artificial exudates were prepared: artificial exudate without MBOA (AE), artificial exudate with MBOA in constant concentration across concentration gradients (ACM), and artificial exudate with MBOA diluted together with AE (AEM). Each type of artificial exudate was prepared in 5 different concentrations.

The full-strength AE (AE100) solution was prepared by mixing 50 mM fructose, 50 mM glucose, 50 mM sucrose, 25 mM succinic acid, 25 mM malic acid, 12.5 mM arginine, 12.5 mM serine and 12.5 mM cysteine, and then filter-sterilising the mixture by passing

it through 0.22 µm syringe filters (Merck Millipore, Germany) (Griffiths et al., 1998). AE solutions with different concentrations - AE60, AE25, AE8 and AE0 - were prepared by serial dilution using sterile Milli-Q water.

ACM100 and AEM100 solutions were prepared by transferring 2.5 mM MBOA stock into AE100 to create a final MBOA concentration of 50 µM, following the method of Liu et al. (2022a) and Otaka et al. (2023). AEM60, AEM25, AEM8, and AEM0 were prepared by diluting AEM100 in sterile Milli-Q water, thereby diluting the MBOA across the gradients. AEM0 consisted of sterile Milli-Q water only, and was labeled as AEM0 to maintain consistency across treatments, as was done for AE0. For ACM60, ACM25, ACM8 and ACM0, the solutions were first diluted across the gradients using sterile milli-Q water, then 2.5 mM MBOA stock was added into each dilution to create a constant MBOA solution of 50 µM across the gradients.

In total, 18 different exudate solutions were prepared, including natural exudates: AE (100,60,25,8,0), AEM (100,60,25,8,0), ACM (100,60,25,8,0), as well as wheat, sorghum and chicory.

3.3.5 Application of exudates to the soil

The same soil used in Chapter 2 was utilised for this experiment. The soil was pre-wetted using milli-Q water at a ratio of 300 µl per gram of soil, covered with foil, and left on a bench at 22 °C in the dark for 9 days. During the experiment, 1 g of soil was placed into the cap of a 50-ml CellStar Falcon tube (Greiner Bio-one, Gloucester, UK), and 50 µl of exudate was added to the soil daily for 5 days (Zhao et al., 2021a). Each cap was placed inside a Petri dish and incubated at 22 °C in the dark. Samples were stirred after each exudate application to homogenise to soil. Triplicate samples were prepared for each type of exudate.

3.3.6 Volatile organic compound (VOC) production

The effect of VOCs on soil microbial communities following exudate addition was studied by adding different concentrations of AE solutions to soil to produce VOCs and assessing their impact on the surroundings.

As illustrated in Figure 3.2a, in each setup, 4 caps were placed into each Petri dish, 30 grams of soil were put into each of the 3 caps (VOC producing) and 1 g of soil was put in the fourth cap (recipient soil). The Petri dishes were covered with their lids but not sealed airtight, allowing air exchange with the external environment. For each concentration, AE was applied to each VOC producing cap at a dose of 50 µl per gram of soil per day for 5 days. The recipient soil was pre-wetted with 300 µl of milli-Q water at the beginning of the experiment to maintain soil moisture. Plates were incubated at 22 °C in the dark, and triplicate samples were prepared for VOC production for each AE concentration: AE100, AE60, AE25, AE8 and AE0. A control was set up by not adding soil to the VOC producing caps but just milli-Q water the same amount as the exudate each day (Figure 3.2b). Control and treatment setups were incubated separately and not placed in the same box on the bench. Triplicates were also prepared for the control setup.

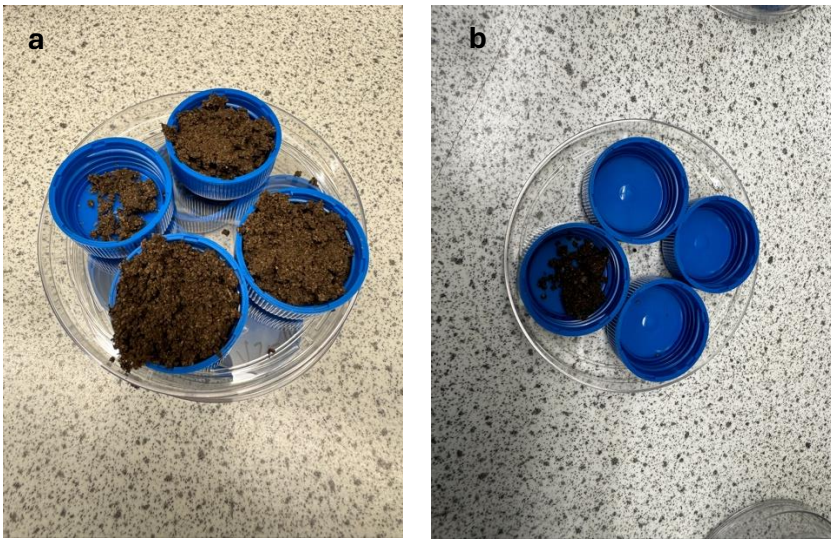

Figure 3.2 Experimental setup for VOC producing. (a): Treatment. Three caps with more soil added were used for producing VOCs, the fourth cap served as recipient (b): Control. Soil was only added to recipient cap, the other 3 were filled with Milli-Q water.

3.3.7 DNA sequencing of 16S rRNA genes

After incubation, DNA extraction was performed using the NucleoSpin® Soil kit (MACHEREY-NAGEL GmbH & Co. KG, Düren, Germany), with 0.3 g of soil taken from each sample for extraction. The DNA concentration (ng/µL) of each sample was measured using the BioDrop Duo+ Spectrophotometer (Biochrom Ltd, Cambridge, UK), and sam-

ples were stored at -20 °C before being sent for sequencing. Amplicon sequencing targeted the V4 region of the 16S rRNA gene of the bacterial community and was conducted at Biomarker Technologies (BMK) GmbH.

3.3.8 Data analysis

R software version 4.3.2 (http://www.r-project.org/) was used to analyse and visualise the data for the experiment.

Sequencing data were processed using DADA2 pipeline (Callahan et al., 2016) as described in Chapter 2. ASVs were classified using the Wang Bayesian classifier in DADA2 (Callahan et al., 2016; Wang et al., 2007) , referencing the Silva taxonomy database (Quast et al., 2013) . The ASV counts were subjected to a Hellinger transformation using the decostand function in the vegan package (version 2.5-6) (Oksanen et al., 2019) in R. Bray-Curtis dissimilarity matrices were calculated, and PCoA was then performed using the R function pcoa. To determine whether exudates and VOCs had a significant impact on soil communities ($P<0.05$), Permutational Multivariate Analysis of Variance (PERMANOVA) was conducted using the adonis2 function in the vegan package.

Indicator species analysis was conducted to identify species significantly associated with each treatment, in comparison to the controls. The analysis was conducted using the indicspecies package (version 1.7.15) in R based on the approach described by De Cáceres and Legendre (2009). The multipatt() function was used to compare the species composition between treatments and controls. The Indicator Value (IndVal) index was calculated which includes both the abundance and occurrence pattern of species across treatments. Permutation tests were carried out to assess the significance of the associations. Species with significant indicator values ($P < 0.05$) were recognised as associated with the treatments compared to the controls.

The relative abundances of selected ASVs were calculated by dividing the read count of each ASV by the total number of reads in the corresponding sample. Heatmaps were constructed using the pheatmap function in the Pheatmap (Kolde, 2019) package.

Enrichment analysis was performed to determine whether specific bacterial families were overrepresented among the indicator ASVs identified for each treatment. The ap-

proach used was the same as described in Chapter 2 (Section 2.3.1.4), where the observed frequency of each family in the indicator subset was compared to its expected frequency based on its proportion in the full ASV dataset using chi-square (χ^2) tests. Analyses were conducted in GraphPad Prism version 10, and families with $p < 0.05$ were considered significantly enriched.

3.4 Results

3.4.1 Effects of artificial exudates (AE, AEM & ACM)

Principal Coordinate Analysis (PCoA) was conducted to visualise the effects of different concentrations of artificial exudate (AE, AEM and ACM) on microbial community composition. Each type of artificial exudate was applied individually to the soil. The effects of artificial exudates on soil bacterial communities across different concentrations are shown in Figure 3.3, where the gradients are labelled in different colours. AEM25 samples were excluded from all AEM-related analyses because they showed complete overlap with AEM100, a pattern not observed in AE or ACM samples. This suggested a likely sequencing error, potentially due to sample mislabeling or duplication by the sequencing provider.

In the PCoA plot of AE, the first axis (PCoA Axis 1) explains 31.42% of the variation, while the second axis (PCoA Axis 2) explains 17.7% of the variation (Figure 3.3d). The microbial community composition shows distinct clustering, with clear separation of communities based on the AE concentration. Samples treated with 100% of AE, 60% of AE, 25% of AE, 8% of AE, and 0% of AE are separated alone the first and second axes (Pseudo-F= 4.077, p=0.001, PERMANOVA). A Similar clustering pattern is also illustrated in the PCoA plots of AEM and ACM, where samples treated with different concentration gradients are clearly separated from each other (Figure 3.3b,c).

The effects of different types of artificial exudates on soil bacterial communities were also compared by plotting together (Figure 3.3a). In the PCoA plots including both AE, AEM and ACM, the first axis (PCoA Axis 1) explains 42.80% of the variation, while the second axis (PCoA Axis 2) explains 9.46 % of the variation. Samples treated with high

concentration gradients (100% and 60%) tend to cluster on the right, while low concentration gradients (8% and 0%) tend to cluster on the left. Forming a clear separation across different concentrations.

When the concentrations are low (8%,0%), sample across all artificial exudate types are tightly clustered together, indicating they have similar impacts on the communities. AE starts to separate from AEM and ACM at the 60% gradients, and by the time the concentration reaches 100%, the separation becomes more obvious.

Indicator species analysis was performed to identify species significantly associated with AE treatments (AE100, AE60, AE25, and AE8) in comparison to the control (AE0). The four AE treatments were grouped together as a single class and compared against AE0. From this analysis, 60 ASVs highly associated with the treatments (AE100, AE60, AE25, and AE8) ($p < 0.01$) were selected and visualised using a heatmap (Figure 3.4).

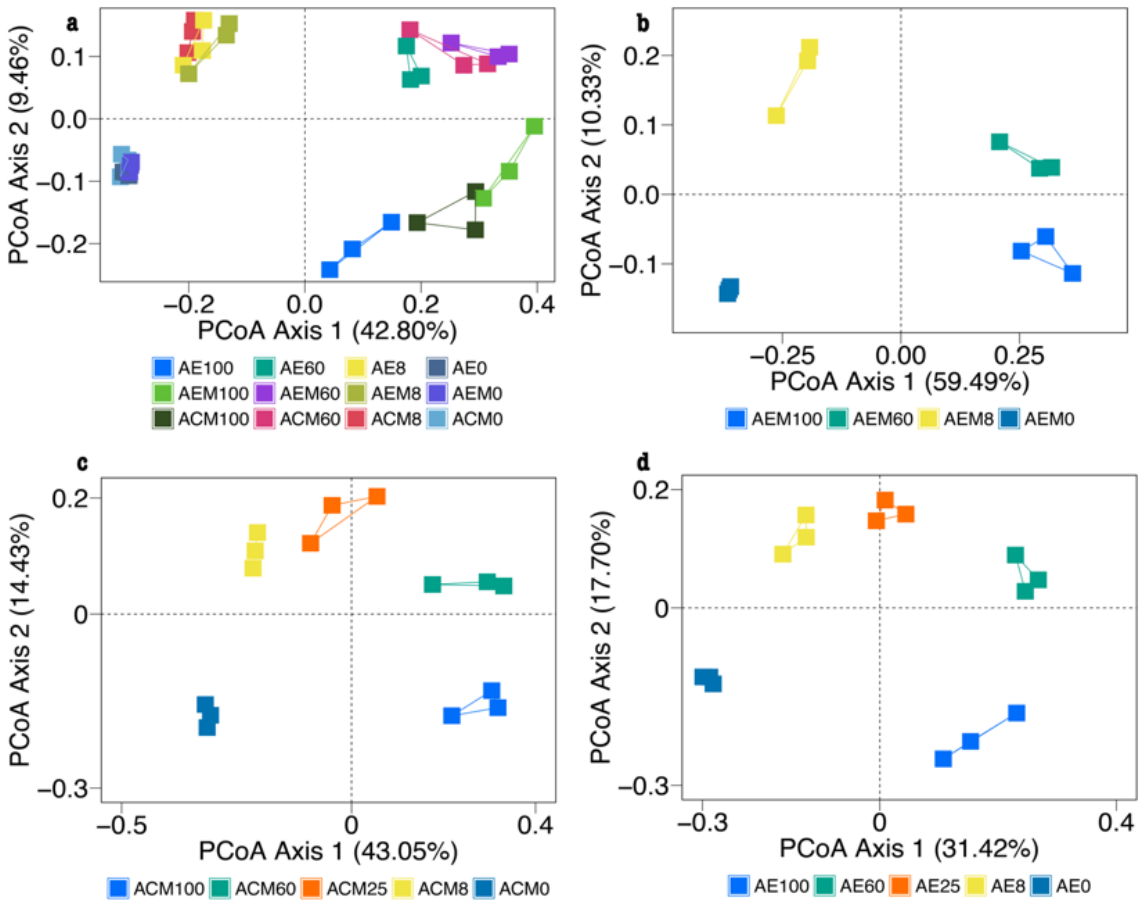

Figure 3.3 Principal Coordinates Analysis (PCoA) plots of microbial community composition based on 16S rRNA gene sequencing, using Bray-Curtis dissimilarity matrices. Points represent individual samples, with colours indicating different artificial exudate treatments. AE: artificial

exudate only. AEM: AE+MBOA (MBOA diluted together with AE through the concentration gradients). ACM: AE+MBOA (MBOA in constant concentration; only AE diluted through the concentration gradients). 100, 60, 25, 8, 0: concentration gradients of AE (100%, 60%, 25%, 8%, and 0%). (a): PCoA of all artificial exudate treatments combined. (b): PCoA for AEM treatments only. (c): PCoA for ACM treatments only. (d): PCoA for AE treatments only.

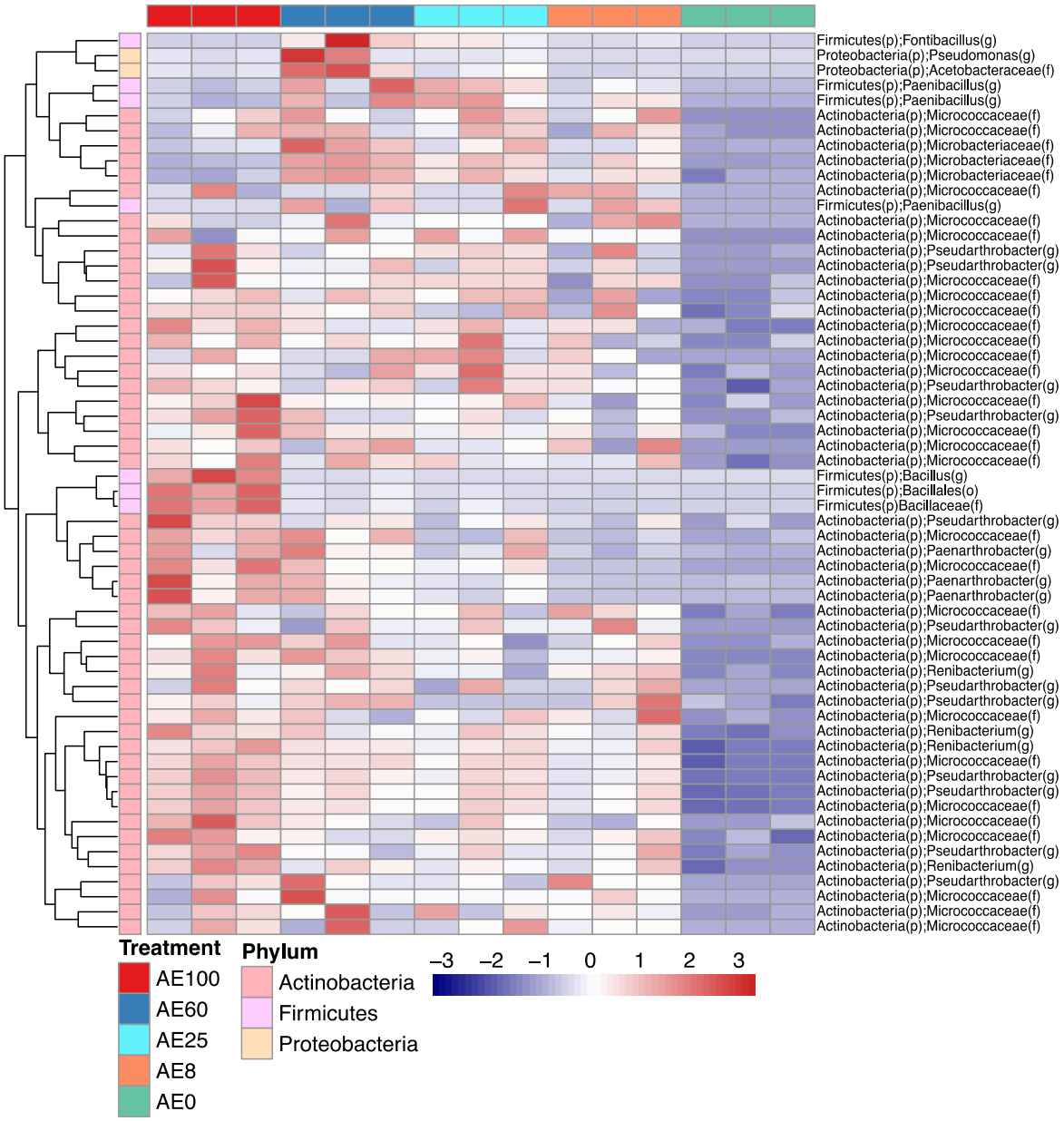

Figure 3.4 Heatmap showing the relative abundance of ASVs across samples treated with artificial exudates (AE), selected by indicator species analysis ($p < 0.01$), comparing all AE treatments combined against the AE0 control. The ASVs shown were identified as indicators in the combined comparison and are present across all AE samples (excluding AE0), though their relative abundances vary between treatments. Rows (ASVs) are clustered by Manhattan distance. Cell colours represent row-normalised z-scores (–3 to 3), where 0 is the mean abundance across samples. Positive values indicate higher-than-average abundance; negative values indicate lower. The coloured sidebar on the left indicates the phylum assignment of each ASV; the top sidebar indicates different treatment concentrations. Abbreviations indicate: p=phylum, c=class, o=order, f=family, g=genus.

These ASVs were present across all four AE treatments, though their relative abundances varied among them. The heatmap reveals three distinct clusters of ASVs based on their relative abundance patterns across artificial exudate (AE) treatments. The top cluster includes ASVs most abundant at AE60, with reduced signals at other concentrations, and consists mainly of Actinobacteria and Firmicutes. The middle cluster comprises ASVs with relatively uniform abundance across AE100 to AE8, indicating a stable presence regardless of exudate concentration. The bottom cluster includes ASVs that peak in abundance under AE100, with a sharp decline through AE60 to AE8; this cluster, along with the middle one, is dominated by Actinobacteria.

The ASVs identified belong to the phyla Actinobacteria, Firmicutes and Proteobacteria, with Actinobacteria being the dominant group. A majority of ASVs from phylum Actinobacteria belong to the Micrococcaceae family (Figure S5). Enrichment analysis (Table S 7) further shows that within Actinobacteria both Micrococcaceae and Microbacteriaceae are significantly over–represented at all non–zero AE concentrations (AE100, AE60, AE25, AE8). Among the Firmicutes, Bacillaceae was specifically enriched at AE25, while the sole Proteobacteria family enriched is Acetobacteraceae at AE60.

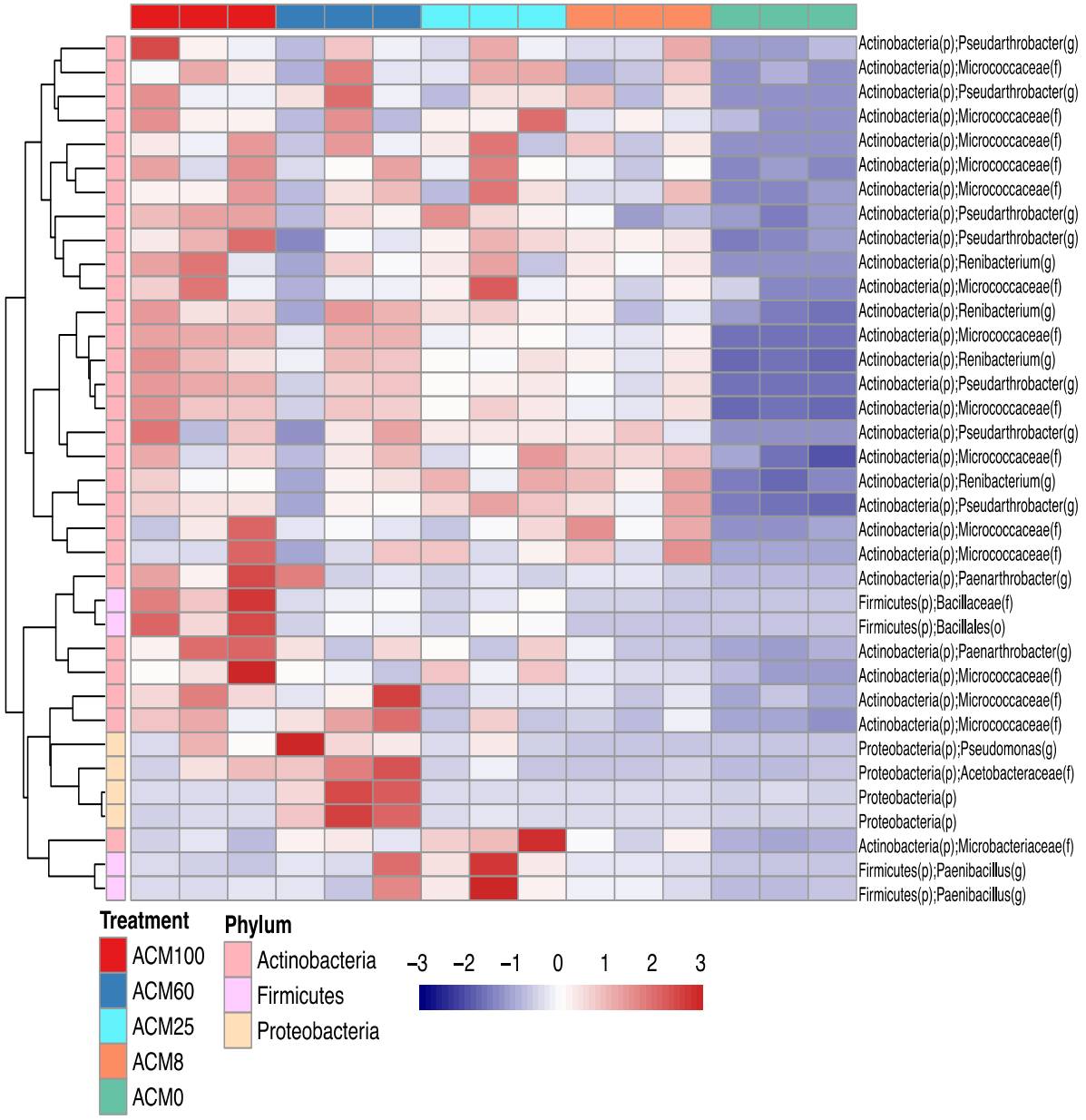

Figure 3.5 Heatmap showing the relative abundance of ASVs across samples treated with artificial exudates (ACM), selected by indicator species analysis ($p < 0.01$), comparing all ACM treatments combined against the ACM0 control. The ASVs shown were identified as indicators in the combined comparison and are present across all ACM samples (excluding ACM0), though their relative abundances vary between treatments. Rows (ASVs) are clustered by Manhattan distance. Cell colours represent row-normalised z-scores (–3 to 3), where 0 is the mean abundance across samples. Positive values indicate higher-than-average abundance; negative values indicate lower. The coloured sidebar on the left indicates the phylum assignment of each ASV; the top sidebar indicates different treatment concentrations. Abbreviations indicate: p=phylum, c=class, o=order, f=family, g=genus.

Indicator species analysis identified 36 ASVs significantly associated with ACM treatments (ACM100, ACM60, ACM25, and ACM8) compared to the control (ACM0) ($p < 0.01$). The four ACM treatments were grouped as a single class and compared against ACM0. These ASVs were present across all four ACM treatments, though their relative abundances varied among them. The selected ASVs were visualised using a heatmap (Figure 3.5).

The heatmap reveals four distinct clusters of ASVs based on their relative abundance patterns across ACM treatments. The top cluster includes ASVs most abundant at ACM100, with moderate signals at ACM60 and ACM25, predominantly from Actinobacteria. The middle cluster shows relatively uniform abundance across ACM100 to ACM8, suggesting a consistent presence regardless of exudate concentration, and is also dominated by Actinobacteria. The mid-bottom cluster features ASVs that peak sharply at ACM100 but are much lower at other concentrations, comprising mainly Actinobacteria, with a small presence of Firmicutes. The bottom cluster consists of ASVs that peak under ACM25 or ACM60, with reduced abundance at both the highest and lowest concentrations, including representatives from Firmicutes and Proteobacteria.

As with AE treatments, the ASVs belong to Actinobacteria, Firmicutes, and Proteobacteria, with Actinobacteria remaining dominant. The Micrococcaceae family still dominates the Actinobacteria phylum (Figure S6).Enrichment analysis (Table S 8) shows that Micrococcaceae was significantly enriched across all non-zero ACM concentrations. Among Firmicutes, Bacillaceae was specifically enriched at ACM25. Within Proteobacteria, Acetobacteraceae was enriched at both ACM100 and ACM60, while Pseudomonadaceae was enriched only at ACM25.

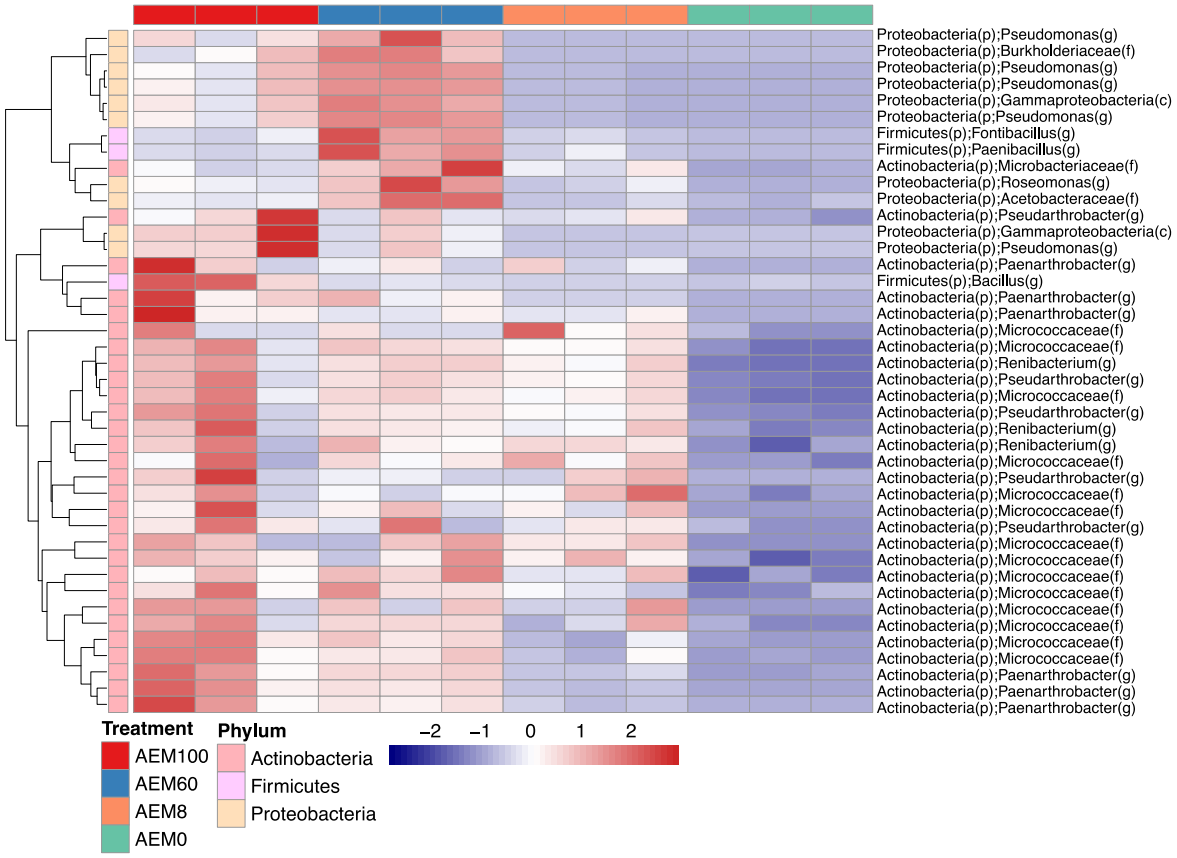

Figure 3.6 Heatmap showing the relative abundance of ASVs across samples treated with artificial exudates (AEM), selected by indicator species analysis ($p < 0.01$), comparing all AEM treatments combined against the AEM0 control. The ASVs shown were identified as indicators in the combined comparison and are present across all AEM samples (excluding AEM0), though their relative abundances vary between treatments. Rows (ASVs) are clustered by Manhattan distance. Cell colours represent row-normalised z-scores (–2 to 2), where 0 is the mean abundance across samples. Positive values indicate higher-than-average abundance; negative values indicate lower. The coloured sidebar on the left indicates the phylum assignment of each ASV; the top sidebar indicates different treatment concentrations. Abbreviations indicate: p=phylum, c=class, o=order, f=family, g=genus.

Indicator species analysis identified 42 ASVs that were strongly associated with treatments of AEM (AEM100, AEM60, and AEM8) compared to the control (AEM0) ($p < 0.01$). The three AEM treatments were grouped as a single class and compared against AEM0. These ASVs were present across all three AEM treatments, though their relative abundances varied among them. The selected ASVs were visualised in a heatmap (Figure 3.6), which show two distinct clusters are based on ASV abundance.

The heatmap reveals two main clusters of ASVs based on their relative abundance patterns across AEM treatments. The top cluster consists of ASVs most abundant at

AEM60, with moderate presence at AEM100 and much lower abundance at AEM8. These primarily include members of Proteobacteria and Firmicutes, along with a few Actinobacteria. The bottom cluster is dominated by Actinobacteria, particularly from the Micrococcaceae family, and shows a strong peak at AEM100, followed by a sharp decline at AEM60 and AEM8.

As in previous analyses, the ASVs identified belong to the phyla Actinobacteria, Firmicutes, and Proteobacteria, with the Actinobacteria remaining dominant. The Micrococcaceae family continues to dominate the Actinobacteria phylum (Figure S7). Enrichment analysis (Table S 9) indicates that Micrococcaceae was enriched across all non-zero AEM concentrations, alongside Acetobacteraceae and Pseudomonadaceae from Proteobacteria.

Heatmap analyses of artificial exudates (AE, AEM, and ACM) reveal selective enrichment of bacteria from three main phyla: Actinobacteria, Firmicutes, and Proteobacteria, with Actinobacteria being dominant. The phylum is largely composed of ASVs from the Micrococcaceae family, which was consistently enriched across all non-zero concentrations in AE, AEM, and ACM treatments, along with Acetobacteraceae (Proteobacteria). Other families show more treatment-specific enrichment patterns: for example, Pseudomonadaceae (Proteobacteria) was enriched only in ACM and AEM, while Bacillaceae (Firmicutes) was enriched in AE and ACM but absent in AEM (Table S 7; Table S 8; Table S 9).

This pattern is further illustrated by comparing the ASVs identified in indicator species analysis across the three artificial exudate treatments (Figure 3.7). A core set of 16 ASVs was shared among AE, AEM, and ACM, highlighting a consistent microbial response to artificial exudates regardless of treatment. This overlap corresponds to the observed enrichment of families such as Micrococcaceae and Acetobacteraceae across all treatments. Meanwhile, partial overlaps — such as 23 ASVs shared between AE and AEM, and 29 between AE and ACM — suggest partial similarity in microbial responses between treatments. In contrast, the presence of treatment-unique ASVs (24 in AE, 19 in AEM, and 7 in ACM) underscores the distinct selectivity of each treatment.

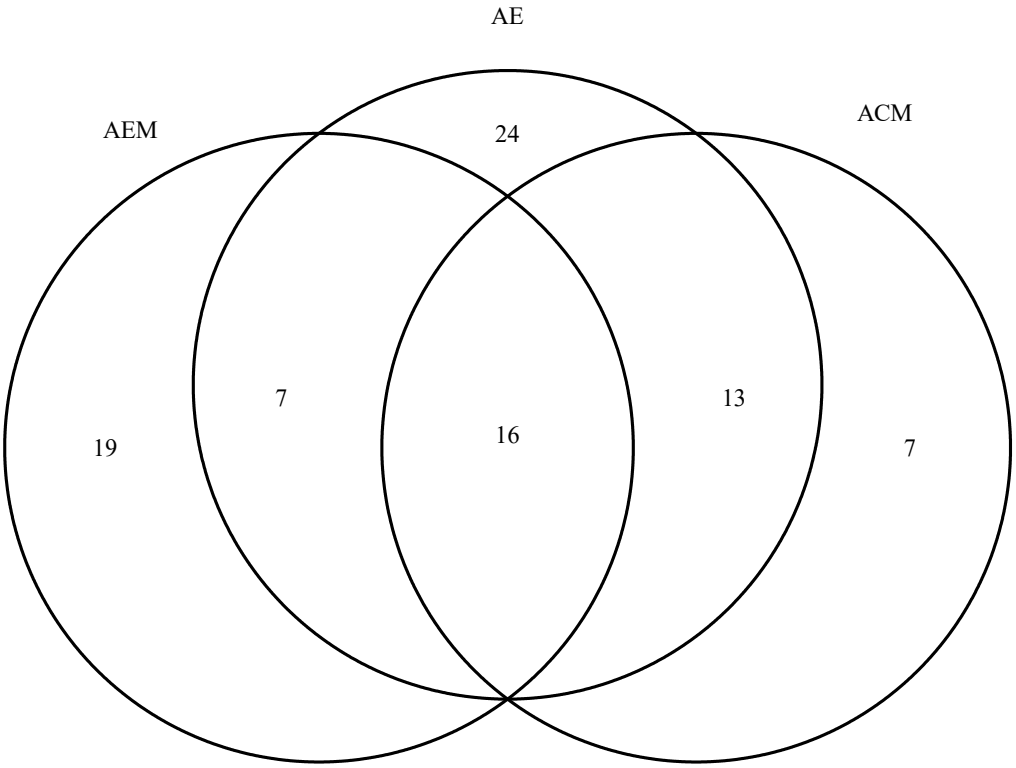

Figure 3.7 Venn diagram showing the overlap of bacterial ASVs identified in the indicator species analysis in response to three artificial exudate treatments: AE, ACM, and AEM. The diagram illustrates the number of ASVs uniquely associated with each treatment, as well as those shared between two or all three treatments.

3.4.2 Effects of natural exudates

PCoA was conducted to visualise the effects of different natural exudates (wheat, sorghum, and chicory) on microbial community composition. Each type of natural exudate was applied individually to the soil in the cap, and its effects on soil bacterial communities was assessed across treatments (Figure 3.8).

In the PCoA plot, the first axis (PCoA Axis 1) explained 16.88% of the variation, while the second axis (PCoA Axis 2) explains 14.75% of the variation (Figure 3.8). The microbial community composition shows distinct clustering, with clear separation of communities based on the exudate types. Specifically, samples treated with wheat, sorghum and

chicory exudates are clearly separated along the first and second axes (Pseudo-F= 1.259, p=0.003, PERMANOVA), indicating differences in the microbial communities associated with each type of exudate.

To further explore the differences between natural and artificial exudates, a comparison of their effects on soil bacterial communities was conducted by plotting both together, as illustrated in Figure 3.9. In the PCoA plots including both artificial exudates (AE) and the natural exudates (wheat, sorghum and chicory), the first axis (PCoA Axis 1) explains 32.23 % of the variation, while the second axis (PCoA Axis 2) explains 13.98% of the variation.

The samples treated with artificial exudates (AE100, AE60, AE25 and AE8) tend to cluster on the right of the plot, while control samples treated with only pure water (AE0) cluster on the left (Figure 3.9), similar to the natural exudate treated samples (wheat, sorghum, and chicory). Distinct clusters are formed between the samples treated with AE and those treated with natural exudates, suggesting that these two types of exudates lead to different community compositions.

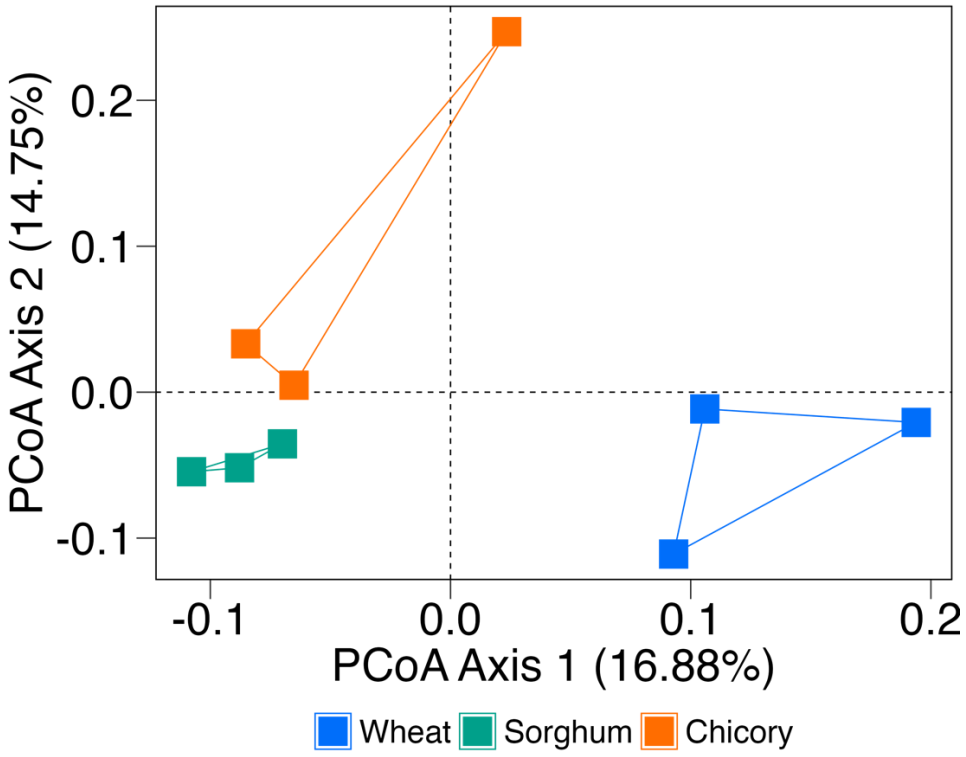

Figure 3.8 Principal Coordinates Analysis (PCoA) plots of microbial community composition based on 16S rRNA gene sequencing, using Bray-Curtis dissimilarity matrices. Points represent individual samples, with colours indicating different treatment groups of natural exudates.

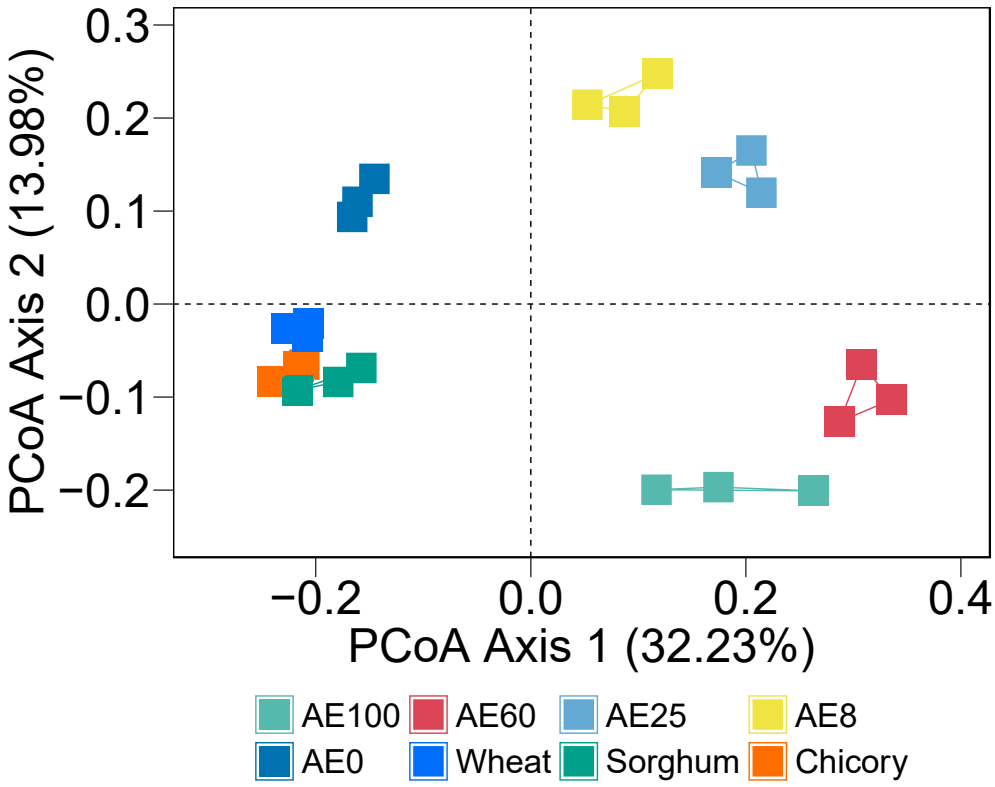

Figure 3.9 Principal Coordinates Analysis (PCoA) plots comparing natural and artificial exudate microbial communities' composition based on 16S rRNA gene sequencing, using Bray-Curtis dissimilarity matrices. Points represent individual samples, with colours indicating different treatment groups of exudates. AE: artificial exudate only. 100,60,25,8,0: concentration gradients of AE: 100%, 60%, 25%, 8%, 0%.

Indicator species analysis was performed using the three natural exudate treatments (wheat, sorghum, and chicory) as distinct groups to identify ASVs significantly associated with each plant type. From this analysis, a total of 75 ASVs were identified ($p < 0.05$), including 30 associated with chicory, 19 with sorghum, and 26 with wheat. These ASVs were visualised using a heatmap (Figure 3.10), which also includes their relative abundance in AE0 and AE8 for reference. The heatmap reveals distinct clustering patterns based on the exudate types.

One prominent cluster toward the upper section of the heatmap shows high abundance in wheat-treated samples, while a separate cluster toward the bottom is dominated by ASVs enriched in sorghum-treated samples. A third cluster, located mid-heatmap, shows ASVs most abundant in chicory-treated samples. These clusters are taxonomically diverse, comprising ASVs from several phyla including Proteobacteria, Actinobacteria, Chloroflexi, and Bacteroidetes. Some ASVs associated with sorghum and chicory

belong to Cyanobacteria and Firmicutes, while wheat-enriched ASVs also include members from Acidobacteria and Planctomycetes. AE0 and AE8 samples were not part of the indicator species analysis but are included for reference; across these two controls, most indicator ASVs show lower relative abundance.

Each natural exudate stimulated distinct microbial communities, with enrichment patterns varying across phyla (Table S 11). In wheat-treated samples, enriched families includ Solirubrobacteraceae and Gemmataceae (Actinobacteria and Planctomycetes, respectively), while sorghum enriched for families such as Mycobacteriaceae (Actinobacteria) and Acetobacteraceae (Proteobacteria). Chicory-treated soils uniquely enriched families including Sporichthyaceae (Actinobacteria), JG30-KF-CM45 (Chloroflexi), and Desulfovibrionaceae (Proteobacteria).

Indicator species analysis was also performed by grouping natural exudate treatments (wheat, sorghum, and chicory) as a single class and compared against AE0 to identify exudate-specific taxa that were not only found in one exudate. The analysis identified 136 ASVs that were strongly associated with treatments of natural exudates compared to the control (AE0) ($p < 0.01$). These ASVs were present across all three natural exudates treatments, though their relative abundances varied among them. The selected ASVs were visualised in a heatmap (Figure 3.11).

The heatmap reveals four main clusters of ASVs based on their relative abundance patterns across natural exudate treatments. The top cluster includes ASVs most abundant in sorghum- and chicory-treated samples, with lower abundance in wheat, comprising mainly Actinobacteria and Firmicutes. The second (upper-middle) cluster shows a relatively uniform abundance across all three exudate types and inlcudes ASVs from Actinobacteria, Bacteroidetes, Chloroflexi, and Firmicutes. The third (lower-middle) cluster contains ASVs that are more abundant in chicory-treated samples, with moderate abundandce in sorghum and low in wheat, mainly from Actinobacteria, Firmicutes, and Proteobacteria. The bottom cluster includes ASVs with mixed abundance patterns across treatments, but many show moderate levels in sorghum and wheat, dominated by Firmicutes.

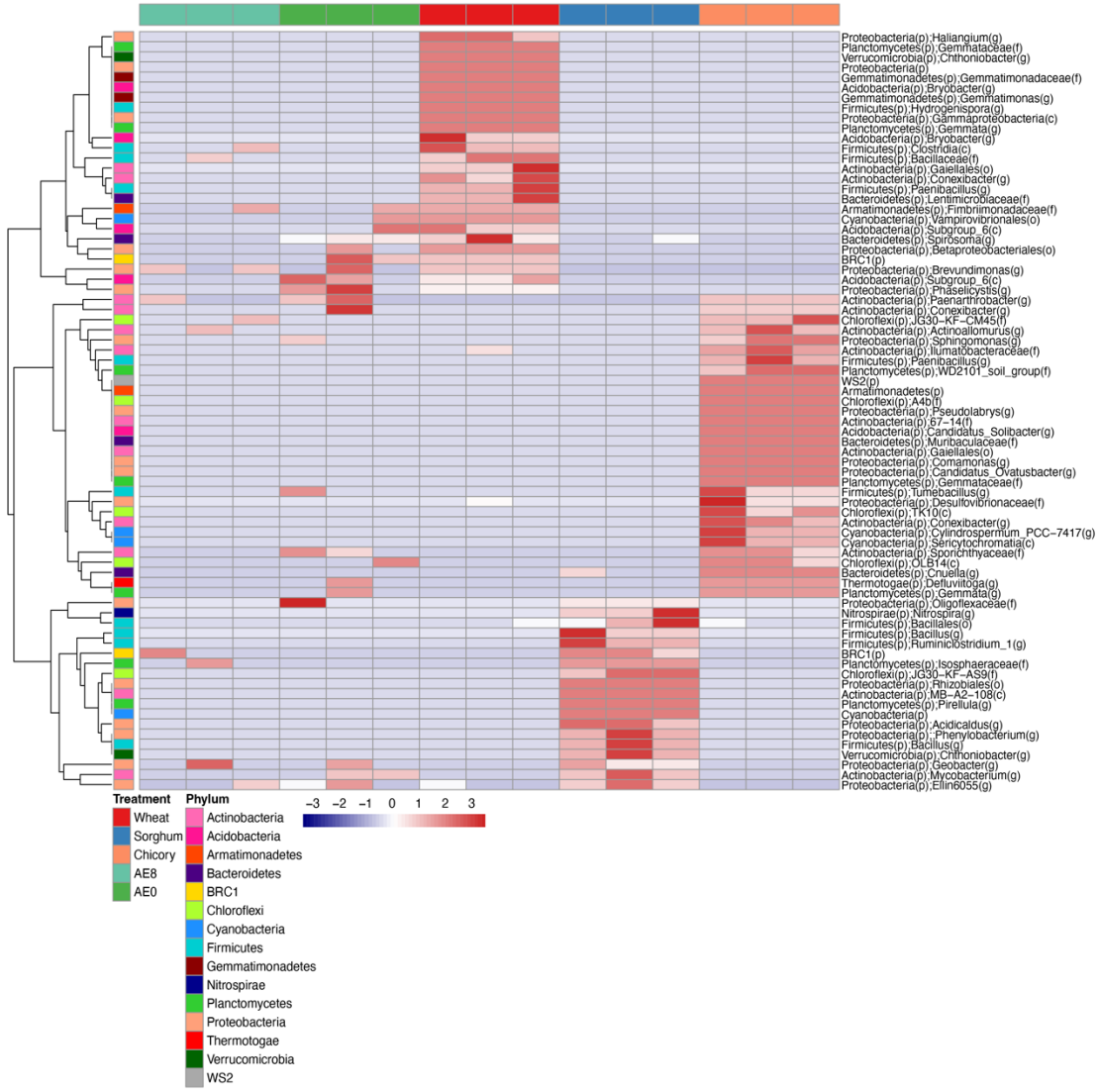

Figure 3.10. Heatmap showing the relative abundance of ASVs across samples treated with natural root exudates from wheat, sorghum, and chicory. ASVs were selected by indicator species analysis ($p < 0.05$), using the three natural exudate treatments as distinct groups to identify ASVs significantly associated with each plant type. The heatmap also includes their relative abundance in AE0 and AE8 for reference. Rows (ASVs) are clustered by Manhattan distance. Cell colours represent row-normalised z-scores (–3 to 3), where 0 is the mean abundance across samples. Positive values indicate higher-than-average abundance; negative values indicate lower. The coloured sidebar on the left indicates the phylum assignment of each ASV; the top sidebar indicates different treatment concentrations and natural exudate types. Abbreviations indicate: p=phylum, c=class, o=order, f=family, g=genus.

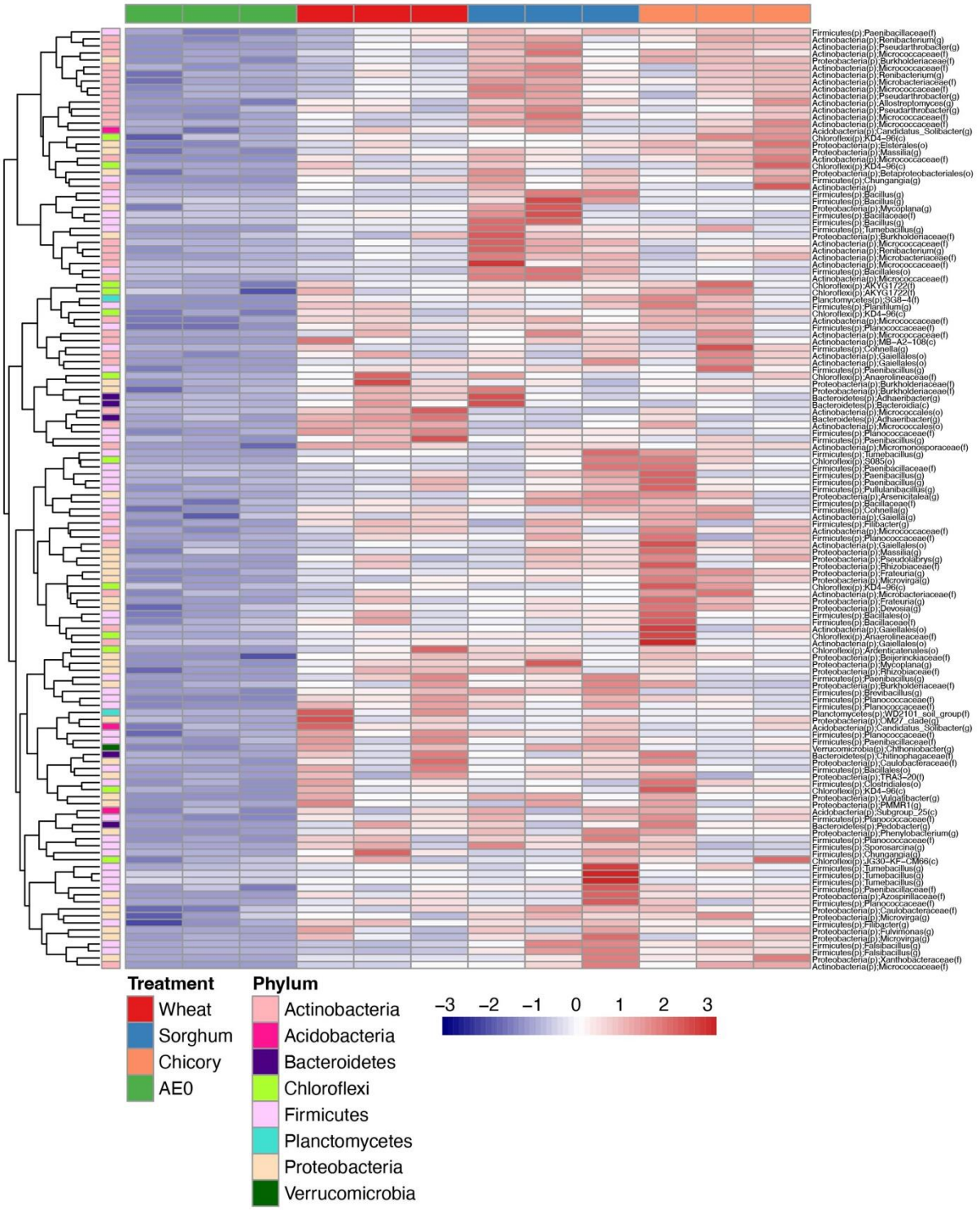

Figure 3.11 Heatmap showing the relative abundance of ASVs across samples treated with natural exudates, selected by indicator species analysis ($p < 0.01$), comparing all natural exudate treatments combined against the AE0 control. The ASVs shown were identified as indicators in the combined comparison and are present across all wheat, sorghum, and chicory samples, though their relative abundances vary between treatments. Rows (ASVs) are clustered by Manhattan distance. Cell colours represent row-normalised z-scores (–3 to 3), where 0 is the mean abundance across samples. Positive values indicate higher-than-average abundance; negative values indicate lower. The coloured sidebar on the left indicates the phylum assignment of each ASV. Abbreviations indicate: p=phylum, c=class, o=order, f=family, g=genus.

To complement the previous enrichment analysis, a second analysis was conducted using ASVs identified as indicators of natural exudate treatments (wheat, sorghum, and chicory combined) relative to the AE0 control (Table S 10). Several bacterial families were significantly enriched across all three plant types, including Micrococcaceae and Microbacteriaceae (Actinobacteria), and Alicyclobacillaceae, Bacillaceae, and Planococcaceae (Firmicutes). Among Proteobacteria, Devosiaceae and Rhodanobacteraceae were enriched in all treatments, while Rhizobiaceae was enriched only in wheat and chicory.

Compared to artificial exudates, natural exudates enriched a broader range of bacterial families across multiple phyla. Within Actinobacteria, families such as Micrococcaceae and Microbacteriaceae were enriched in both natural and artificial treatments, while others like Solirubrobacteraceae, Ilumatobacteraceae, Mycobacteriaceae, and Sporichthyaceae are specific to natural exudates. Among Firmicutes, Bacillaceae is shared between both exudate types, whereas Alicyclobacillaceae is unique to natural exudates. Within Proteobacteria, Acetobacteraceae appear in both natural and artificial treatments, while families such as Devosiaceae and Rhodanobacteraceae are exclusive to natural exudates. Additional enriched families from other phyla, such as Gemmataceae (Planctomycetes) and JG30-KF-CM45 (Chloroflexi), also appear uniquely in natural exudate treatments (Table S 7 - Table S 11).

Together, these findings demonstrate that although artificial exudates share some enriched bacterial families with natural exudates, the latter support a greater variety of bacterial families from different phyla.

One important point to note is that no separate Milli-Q water control was included in the natural exudate PCoA analysis (Figure 3.9), and Milli-Q water is known to contain trace organic material. However, all AE0, AEM0, and ACM0 controls in the artificial exudate experiments — prepared using the same batch of Milli-Q water as the natural exudates — cluster tightly in their own PCoA plot (Figure 3.3a), supporting their use as effective Milli-Q controls for the natural exudates. Moreover, Milli-Q water contains only trace levels of organic material (~ 5ng/mL) (Wang and Wang, 2019), whereas visible powdered exudates were weighed out in our study, with approximately 75 mg of dry material resuspended in 2 mL Milli-Q water, equivalent to 37.5 mg/mL. The organic content in the natural exudate solutions therefore far exceeds that of Milli-Q water. Any microbial shifts

observed in response to natural exudate treatments likely reflect the presence of chemical compounds released from the plant roots during the collection process.

3.4.3 Effects of volatiles

PCoA was conducted to visualise the effects of volatile organic compounds (VOCs) produced by soil treated with different concentrations of AE on the recipient soil microbial community composition. The effects of VOCs on the recipient soil bacterial communities across different treatment concentrations are shown in Figure 3.12, where the concentrations of AE used to treat the soil are labelled in different colours.

Samples of recipient soil were labelled as “AV”. For instance, AV100 refers to recipient soil exposed to VOCs produced from soil treated with AE100, while AV60 refers to recipient soil exposed to VOCs produced from soil treated with AE60, and so on. VC refers to the samples without any VOCs produced in it, only recipient soil alone.

In the PCoA plot, the first axis (PCoA Axis 1) explains 34.0% of the variation, while the second axis (PCoA Axis 2) explains 23.3% of the variation (Figure 3.12). The microbial community composition shows distinct clustering, with clear separation between recipient soils exposed to VOCs produced from soil treated with high AE concentrations (100, 60) and those exposed to low AE concentrations (25, 8, 0). Samples exposed to VOCs from different AE concentrations are separated alone the first and second axes, while the control samples (VC) are clearly separated from the others (Pseudo-F= 1.445, p= 0.001, PERMANOVA).

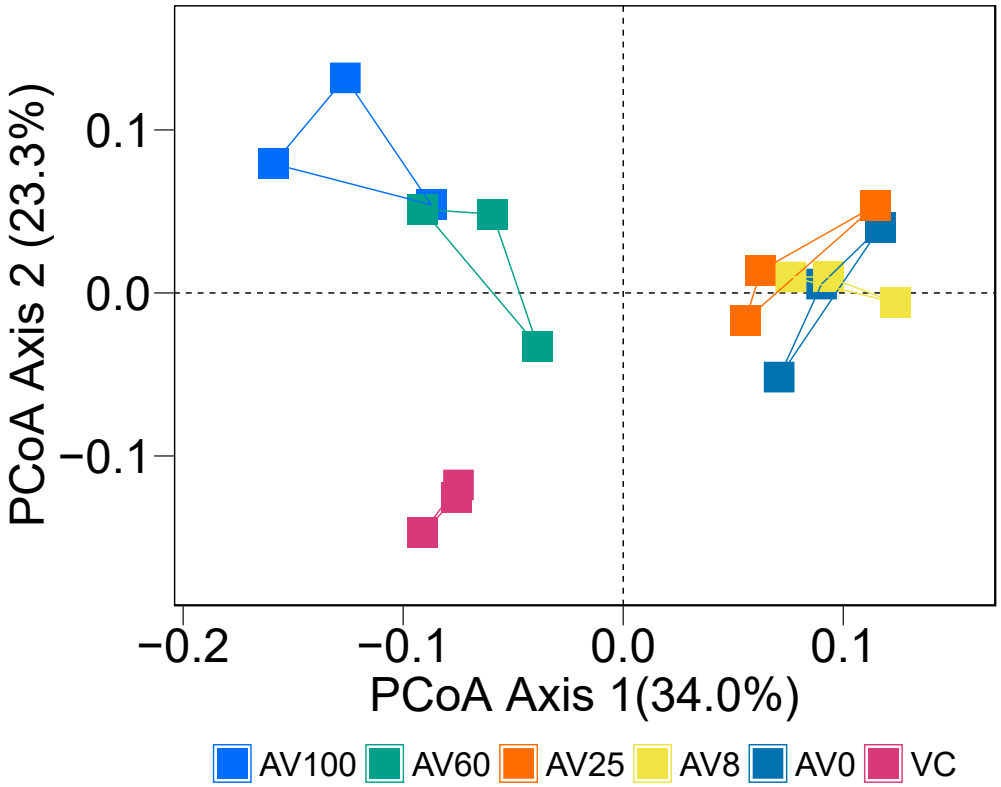

Figure 3.12 Principal Coordinates Analysis (PCoA) plots of microbial community composition based on 16S rRNA gene sequencing, using Bray-Curtis dissimilarity matrices. Points represent individual samples, with colours indicating different treatments of soil to produce volatiles. 100,60,25,8,0: concentration gradients of AE: 100%, 60%, 25%, 8%, 0% added to soil to produce volatiles. VC refers to the control setup, in which only recipient soil was included. No VOC-producing soil was added; instead, Milli-Q water was applied to the empty caps to match the volume used in treatment conditions. VC samples were incubated under the same conditions as the treatments but kept in a separate box.

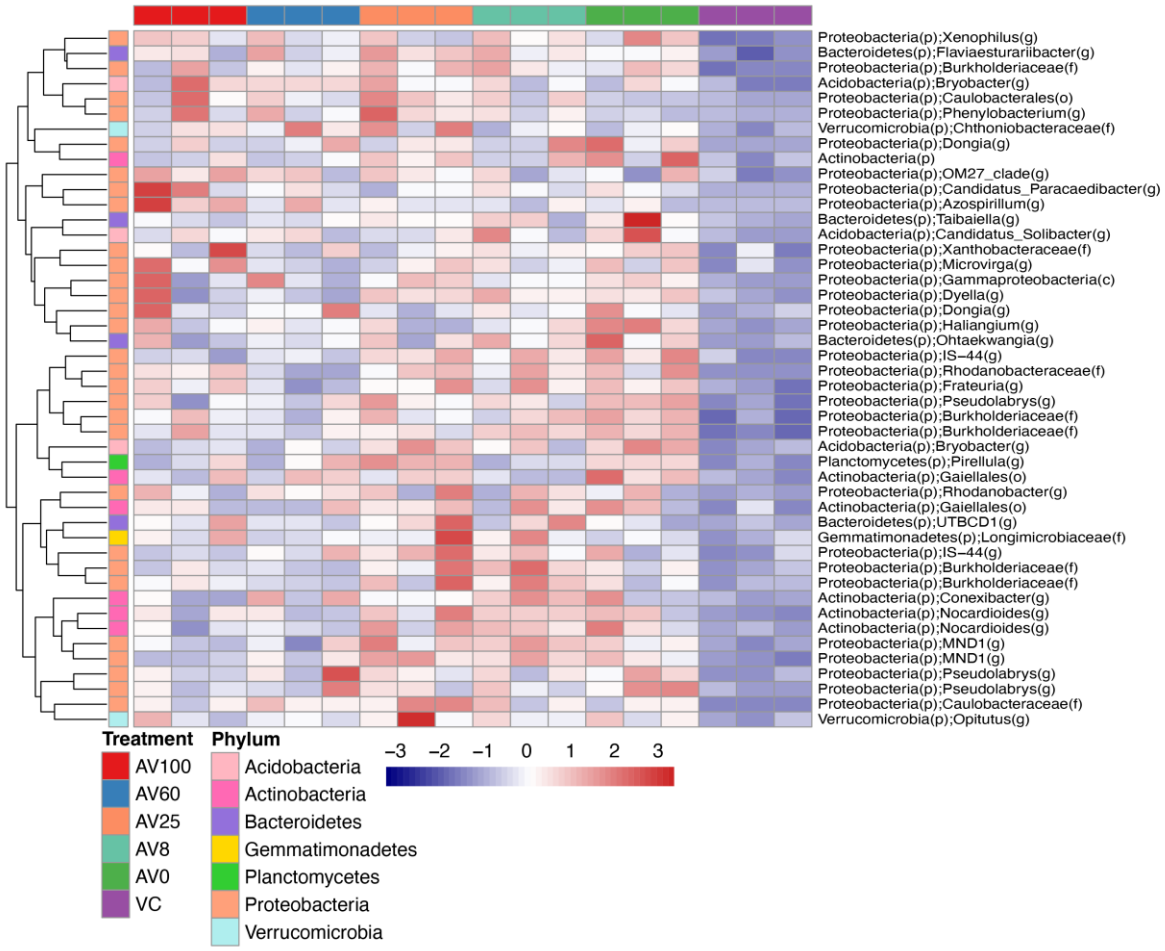

Figure 3.13 Heatmap showing the relative abundance of ASVs across recipient soil samples exposed to volatiles produced by soils treated with different concentrations of AE. ASVs were selected by indicator species analysis ($p < 0.01$), comparing all AV treatments combined against the VC control. The ASVs shown were identified as indicators in the combined comparison and are present across all AV samples (excluding VC), though their relative abundances vary between treatments. VC is the control with no volatiles produced. Rows (ASVs) are clustered by Manhattan distance. Cell colours represent row-normalised z-scores (–3 to 3), where 0 is the mean abundance across samples. Positive values indicate higher-than-average abundance; negative values indicate lower. The coloured sidebar on the left indicates the phylum assignment of each ASV; the top sidebar indicates the concentration used to treat the volatile-producing soil. Abbreviations indicate: p=phylum, c=class, o=order, f=family, g=genus.

Indicator species analysis was performed to identify ASVs significantly associated with AV treatments (AV100, AV60, AV25, AV8, and AV0) compared to the control (VC). The five AV treatments were grouped as a single class and compared against VC. From this analysis, 46 ASVs significantly associated with AVs ($p < 0.01$) were selected and visualised using a heatmap (Figure 3.13). These ASVs were present across all five AV treatments, though their relative abundances varied.

The heatmap reveals two main clusters of ASVs based on their relative abundance patterns across volatile exposure treatments. The top half displays scattered abundance patterns with no clear trend linked to AE concentration. In contrast, the lower half shows a slightly more structured pattern: ASVs tend to be more abundant when soils were exposed to volatiles produced from AE-treated soils at lower concentrations (AV25, AV8, and AV0), and less abundant under AV100 and AV60. This suggests that volatiles generated from lower AE concentrations may exert a more consistent influence on this subset of ASVs. ASVs in both clusters span several phyla, including Actinobacteria, Proteobacteria, and Bacteroidetes, with proteobacteria being dominant throughout.

Enrichment analysis shows that bacterial families enriched are primarily from the phyla Actinobacteria, Bacteroidetes, and Proteobacteria. Among Proteobacteria, Burkholderiaceae, Dongiaceae, Nitrosomonadaceae, Rhodanobacteraceae, and Xanthobacteraceae were consistently enriched across all VOC concentrations, while Beijerinckiaceae was enriched only at AV100. The Microscillaceae family (Bacteroidetes) was also enriched at all concentrations. For Actinobacteria, Nocardioidaceae was uniquely enriched at AV100, whereas Solirubrobacteraceae was enriched at both AV60 and AV8 (Table S 12).

In summary, although all selected ASVs were identified based on their association with the combined AV treatments (i.e., all AV concentrations grouped and compared against VC) and appear across all concentrations, their abundance patterns vary across VOCs generated from soils treated with different AE concentrations. Some ASVs showed consistent abundance across all treatments, while others respond more strongly under VOCs produced at lower AE concentrations (AV25, AV8, and AV0). In line with these observations, enrichment analysis reveals both bacterial families shared across all treatments and others that were selectively enriched under specific VOC exposures.

3.5 Discussion

This study aimed to investigate the influence of artificial and natural exudates on soil microbial communities, focusing on the effects of concentration, the comparison between exudate types, and the effects of VOCs produced by soils treated with artificial exudates. We found that artificial exudates caused dose-dependent effects on soil microbial communities, with distinct impacts from treatments with constant MBOA and

diluted MBOA, particularly at higher concentrations. Meanwhile, natural exudates had different impacts on bacterial communities based on plant type (wheat, sorghum, and chicory), resulting in more diverse microbial communities than those shaped by artificial exudates. However, since the composition and concentration of the natural exudates were not measured in this study, interpretations of their effects on microbial diversity should be made with caution. Additionally, VOCs produced by AE-treated soils influenced recipient soil communities, though the dose-dependent pattern was less pronounced than that observed with direct AE treatments. Some ASVs responded more strongly to VOCs derived from lower AE concentrations, while others showed less structured abundance patterns.

3.5.1 Dose-dependent effects of artificial exudates

The concentration gradients of artificial exudates had a great impact on bacterial communities in AE, AEM, and ACM treatments, with samples from each concentration clustering separately in the PCoA plots (Figure 3.3). Visualisation of the indicator species on heatmaps for artificial exudates (AE, AEM, and ACM) reveals that artificial exudates were selective for bacteria from three phyla: Actinobacteria, Firmicutes, and Proteobacteria, with Actinobacteria being dominant. The Actinobacteria phylum was predominantly composed of ASVs from the Micrococcaceae family, which was also enriched in AE, AEM, and ACM (Table S 7 - Table S 9).

Although the ASVs in the artificial exudates treatments were selected based on indicator species analysis (all treatment concentrations combined against the “0” controls) and were present across all concentrations, a clear response based on the concentration gradients was observed, suggesting their abundance varied among different concentrations. Enrichment analyses also suggest that there are differences between concentrations at the family level. While some families overlapped across different cocnentratios within each treatment (e.g., Micrococcaceae in AE and Acetobacteraceae in AEM), others were only enriched at specific concentrations (e.g., Bacillaceae at AE25 and Pseudomonadaceae at ACM25).

Actinobacteria is a phylum well known for its crucial role in organic matter decomposition (Ventura et al., 2007). These findings align with previous studies, which showed that Actinobacteria can be stimulated by high carbon inputs and grow well in nutrient-rich

environments (Bao et al., 2021). A previous study by Griffiths et al. (1998) also revealed that microbial community composition is sensitive to the concentration gradients of artificial exudates, largely due to the availability of carbon sources — consistent with the dose-dependent effects observed in our study. The enrichment of Micrococcaceae across all concentrations of all artificial exudate treatments potentially indicates that members of this family possess ecological traits consistent with r-strategists, including rapid growth in response to elevated carbon availability. Although rRNA operon copy number could not be determined directly from our 16S rRNA amplicon data, previous genomic studies have shown that members of the Micrococcaceae family possess two rRNA operons (Young et al., 2010), a feature associated with faster reproductive rates and higher protein synthesis potential (Klappenbach et al., 2000). This growth strategy likely contributes to their consistent enrichment across a range of carbon concentrations introduced by artificial exudate additions, indicating a broad capacity to respond to elevated carbon availability.

In contrast, families from the Proteobacteria phylum showed a less pronounced response, suggesting that their preference may not depend on total carbon amount but rather on specific compositions of the exudates. At specific concentrations, the exudate components like sugars, organic acids, or amino acids may be present in optimal ratios to allow them to thrive (Zhang et al., 2022). Alternatively, their competitive advantage at specific concentrations may be driven by resource uptake kinetics (Roller et al., 2016).

.

3.5.2 Effects of MBOA

In this experiment, we employed two different settings for adding MBOA to artificial exudates: a constant MBOA concentration across the concentration gradients (ACM) and MBOA diluted with other compounds together alone the concentration gradients (AEM). We aimed to compare the effects of artificial exudates with constant MBOA concentration (ACM) and diluted MBOA concentration (AEM) in shaping soil communities. Since MBOA is a breakdown product of secondary metabolite DIMBOA, it adds an extra layer complexity to the artificial exudates.

At low concentrations (0% and 25%), we observed no significant differences between AE, ACM, and AEM, as shown in Figure 3.3a. This suggests that MBOA, even at a constant concentration, may have limited impact on bacterial communities when little or no carbon source is available. Under these conditions, MBOA likely exerts minimal selective pressure, highlighting the importance of carbon in shifting the microbial community. However, at higher concentrations (60% and 100%), the effects of MBOA became apparent. At high carbon concentrations, ACM and AEM treatments began to separate from AE in the PCoA plot, suggesting that MBOA exerted selective pressure and shifted the microbial communities under conditions where more carbon became available (Hu et al., 2018). While this shift may reflect positive selection for taxa adapted to MBOA, it is also possible that MBOA inhibited the growth of sensitive bacterial groups, contributing to the observed community changes. This aligns with previous findings that MBOA and its derivatives can have antimicrobial properties (Dai et al., 2022), suggesting both promotion and inhibition may shape the resulting microbial profiles.

Although MBOA was present at different concentrations in AEM (diluted) and ACM (constant), both treatments diverged from AE at higher concentrations (Figure 3.3a), indicating that MBOA contributed to community-level shifts, particularly when more carbon was available. Venn diagram analysis revealed that AEM and ACM shared only 16 indicator ASVs and each contained unique ASVs (26 in AEM, 20 in ACM) (Figure 3.7), suggesting that the concentration or formulation of MBOA further modulated specific microbial responses. While MBOA clearly influenced overall community composition, its concentration appears to shape finer taxonomic outcomes, with both shared and distinct ASVs emerging between AEM and ACM.

While MBOA clearly influenced microbial composition in combination with other exudate components, its individual contribution remains uncertain, as it was not tested in isolation in this study. When MBOA is not the sole carbon source, microbes are likely to prioritise more readily available compounds, potentially reducing its detectable impact on community structure. Recent findings show that microbial utilisation of MBOA relies on specialised metabolic pathways and becomes more prominent when it serves as the primary carbon source (Thoenen et al., 2024). These observations highlight the need for future studies testing MBOA alone to better clarify its ecological role.

3.5.3 Effects of natural exudates

Each natural exudate — wheat, sorghum, and chicory — had different effects on bacterial communities (Figure 3.8), and collectively, they shaped distinct microbial profiles compared to artificial exudates (Figure 3.9), as evidenced by the separation in the PCoA plot.

Through indicator species analysis, we identified species significantly associated with each type of natural exudates (wheat, sorghum, and chicory), and visualised their relative abundance in both natural exudates and low concentration artificial exudates (AE8, AE0) on the heatmap (Figure 3.10). We chose AE8 and AE0 to compare with natural exudates because these concentrations are closest to the natural exudates in the PCoA plot (Figure 3.9). ASVs form three distinct clusters across natural exudates which was expected as species were selected based on their association with each exudate type.

Actinobacteria, Firmicutes, and Proteobacteria were present among the ASVs associated with natural exudates, and enrichment analysis shows overlaps between families enriched in natural and artificial exudates. However, natural exudates enriched a more diverse range of bacterial families compared to the artificial exudates (Table S 10; Table S 11), suggesting that some bacteria are more adapted to compounds found in natural exudates. Although the chemical composition of the natural exudates was not measured in this study, it is possible that they contained secondary metabolites such as cyclohexanol, cyclohexanone, and *N*-methyl phenylethylamine from wheat (Wang et al., 2006), luteolinidin and apigeninidin phytoalexins from sorghum (Awika et al., 2005), and sesquiterpene lactones from chicory (Graziani et al., 2014), which may have contributed to the observed microbial patterns.

These findings indicate that although artificial exudates can be used as a simplified versions of natural exudates in research, they cannot fully replicate the diverse functions of natural exudates, especially in terms of microbial diversity and secondary metabolite secretion (Tong et al., 2020; Strickland et al., 2015).

It is important to note that exudate composition can vary substantially not only between plant species but also among cultivars within the same species. Previous studies have shown cultivar-specific exudation patterns in wheat (e.g., differences in amino acids, sugars, and organic acids), sorghum (e.g., distinct strigolactone profiles), and chicory (e.g., variable sesquiterpene lactone levels) (Yahya et al., 2021; Schlemper et al., 2017;

Peña-Espinoza et al., 2015). These differences suggest that the microbial responses observed in this study could be influenced by the particular cultivars used. Although only one cultivar per species was tested here, it is possible that different cultivars would elicit distinct microbial shifts. Furthermore, environmental and growth conditions may also alter exudate profiles, potentially affecting microbial community outcomes.

Finally, as the chemical profiles of natural exudates were not characterised in this study, it is possible that their relatively low compound concentrations led to weaker microbial growth stimulation. This may have limited the enrichment of dominant taxa and allowed a broader range of bacterial families to persist, contributing to the higher microbial diversity observed. Moreover, since the exudates were applied undiluted and not standardised based on root biomass, differences in microbial responses between wheat, sorghum, and chicory may reflect not only variations in chemical composition but also differences in the total quantity of exudates released by each plant species. For example, species with greater root biomass may have contributed a higher absolute load of compounds into the same collection volume, leading to stronger microbial shifts.

These limitations highlight the complexity of natural exudate effects and underscore the need for future studies to quantify both their chemical composition and concentration in parallel with microbial analyses.

3.5.4 Effects of VOCs

VOCs emitted from AE-treated soils at different concentrations influenced bacterial communities in the recipient soils. PCoA analysis showed distinct clustering between communities exposed to VOCs from high AE concentrations (AV100 and AV60) and those from moderate to low AE concentrations (AV25, AV8, and AV0), but did not indicate a gradual dose-dependent pattern (Figure 3.12). Heatmap analysis further illustrated this, showing that some ASVs responded more clearly to VOCs from lower concentrations (AV25, AV8), while others showed less structured abundance patterns across the treatments (Figure 3.13).

Although no dose-dependent effects like those observed in the artificial exudate treatems were observed in the experiment, enrichment analysis at the family level still showed notable differences. Some families were enriched across all AV treatments,

such as Burkholderiaceae, Rhodanobacteraceae, and Nitrosomonadaceae (Proteobacteria), as well as Microscillaceae (Bacteroidetes). Others were only enriched in AV samples treated with specific AE concentrations; for example, Nocardioidaceae (Actinobacteria) and Beijerinckiaceae (Proteobacteria) were only enriched at AV100, while Solirubrobacteraceae (Actinobacteria) was enriched at both AV60 and AV8.

VOCs are well-known as signalling molecules that influence neighbouring bacterial communities (Schulz-Bohm et al., 2015). In this experiment, VOCs emitted from AE-treated soils exerted selective effects on recipient bacterial communities across all concentrations, particularly on families within Proteobacteria. Only bacteria that were either able to metabolise VOCs or resistant to VOCs would thrive (Schulz-Bohm et al., 2017; Weisskopf et al., 2021). VOCs and root exudates play complementary roles in shaping microbial communities. While root exudates typically act as local nutrient sources and chemical signals in the rhizosphere, VOCs function through the soil air phase, often influencing microbes at a distance as signalling compounds or antimicrobials (Zhou et al., 2024).

Proteobacteria are known for their ability to thrive in a range of environments, including contaminated soils that are often rich in VOCs and other pollutants. Labbé et al. (2007) reported a shift in the structure of Proteobacteria following soil contamination, highlighted they are highly adaptive to dynamic environment. Many species within this phylum harbour specialised enzyme systems that allow them to utilise VOCs as substrates, giving them a distinct advantage over other bacterial groups. Families such as Burkholderiaceae, Beijerinckiaceae and Nocardioidaceae have been reported to metabolise a range of VOCs, including aromatic hydrocarbons (e.g., naphthalene, phenanthrene, and toluene) and halogenated volatiles (Yang et al., 2019; Chaignaud et al., 2018). Quorum sensing may also be a mechanism proteobacteria used to regulate their response to VOCs, which enable them to utilise these compounds and thrive under high concentrations (Abisado et al., 2018). Although Actinobacteria also possess VOC-degrading capabilities (Barka et al., 2015), Proteobacteria are often more dominant in VOC-rich environments due to their faster growth rates, metabolic plasticity, and quorum-sensing-mediated regulation (Abis et al., 2020; Lu et al., 2018).

While this experiment revealed distinct VOC-driven shifts in microbial communities, several limitations should be noted. First, the chemical composition of the emitted

VOCs was not directly measured, making it difficult to link specific compounds to the observed microbial responses. Additionally, VOC effects were interpreted based on community shifts in recipient soils, but we were not able to test whether the effects were caused by the metabolism of, or the resistance to VOCs. Future work integrating VOC profiling (e.g., gas chromatography-mass spectrometry [GC-MS]) and functional assays (e.g., metabolic enzyme assays) could provide deeper insights into the interactions between specific volatiles and microbial taxa.

3.5.5 Conclusions

This study investigated the influence of artificial and natural exudates, as well as VOCs emitted from artificial exudate (AE)-treated soils, on soil microbial communities. Artificial exudates produced clear dose-dependent shifts in community composition, with Actinobacteria, particularly Micrococcaceae, responding strongly across all concentrations. However, the study could not directly link microbial growth responses to r-strategist traits such as rRNA operon copy number due to the limitations of amplicon sequencing.

The inclusion of MBOA, either diluted or at constant concentration, added further complexity to artificial exudate treatments. MBOA appeared to exert selective pressure particularly under high-carbon conditions, but its role remains difficult to isolate, as it was not tested independently. Additionally, it is unclear whether microbial responses to MBOA reflected positive selection for tolerant taxa or suppression of sensitive groups.

Natural exudates stimulated more taxonomically diverse bacterial communities than artificial exudates. However, their composition and concentration were not quantified, limiting mechanistic interpretation. Variations in root biomass and secondary metabolite content across plant species and cultivars may also have contributed to the observed differences, but these factors were not accounted for in this study.

Finally, VOCs emitted from AE-treated soils influenced recipient soil communities, although a dose-dependent pattern was not observed. While certain families, such as Burkholderiaceae and Rhodanobacteraceae, were consistently enriched, and others (e.g., Nocardioidaceae) were only enriched at specific treatments, the lack of direct

VOC profiling and functional validation limits conclusions about the underlying mechanisms — whether these taxa were selected for due to metabolic traits or simply survived because others were inhibited remains unknown.

3.5.6 Future directions

Future research should focus on fine-tuning artificial exudates by adding secondary metabolites to better replicate the ecological functions of natural exudates. For instance, different concentrations of MBOA could be tested in high-carbon artificial exudate formulations to evaluate its specific role in shaping microbial communities. As MBOA was not tested independently in this study, its effects remain difficult to isolate. Additional experiments using MBOA as a sole carbon source or in minimal media would help clarify its selective or inhibitory impact.

The chemical compositions of VOCs emitted under different artificial exudate concentrations should also be characterised (e.g., via GC-MS), as their presence influenced recipient microbial communities despite no clear dose-dependent pattern. Linking specific volatile compounds to microbial responses could improve our understanding of the role of VOCs as selective agents or signalling molecules. Moreover, functional assays assessing microbial resistance to or metabolic utilisation of VOCs, alongside identification of VOC-producing taxa through metagenomics or VOC profiling, would help determine whether enriched taxa are selected for, or whether other groups are simply inhibited.

Natural exudates should be chemically profiled and quantified to allow more direct comparisons with artificial exudates. In this study, exudate composition and concentration were not measured, limiting interpretation. Future studies should also consider normalising exudate inputs based on root biomass to account for variation between plant species and cultivars. In addition, cultivar-level differences in root exudation patterns and associated microbial responses should be investigated to better understand plant–microbe specificity.

Furthermore, while this study could not determine whether enriched taxa were positively selected or whether others were competitively excluded, the wider literature suggests both mechanisms can occur in parallel. For instance, fast-growing r-strategists,

such as some Actinobacteria, are known to rapidly respond to increased carbon availability, and reproduce quickly in favourable environments; additionally, some bacteria are better adapted to specific conditions such as pH, temperature, or oxygen levels, while others are less so (Klappenbach et al., 2000; Young et al., 2010; Hibbing et al., 2010), suggesting active selection. At the same time, allelopathic or antimicrobial compounds in root exudates and VOCs can inhibit susceptible taxa, resulting in the apparent dominance of resistant groups (Hu et al., 2018; Sun et al., 2022). Deciphering these selective pressures remains a challenge, but future studies using community-level functional trait profiling and transcriptomics could help clarify whether enriched taxa are actively selected for their metabolic traits or persist due to the suppression of competitors (Salazar et al., 2019).

Chapter 4 Isolation, identification, characterisation of plant growth-promoting bacteria and their impacts on *Arabidopsis thaliana* growth

Abstract

Soil microbes play a central role in nutrient cycling and plant health, yet culturable plant growth-promoting bacteria (PGPB) remain underexplored. This chapter describes the isolation and characterisation of bacteria from three UK agricultural sites—Boxworth, Chilworth, and Rosemaund—using three media types: the nutrient-rich Vegitone and two minimal media, VL55 and VL70.

A total of 70 bacterial isolates were obtained and screened for two plant growth-promoting traits: phosphate solubilisation (via Pikovskaya medium) and production of indole-related compounds (via the Salkowski assay). The VL media yielded a greater number of isolates and, overall, isolates from VL media showed stronger IAA-related signals and a higher frequency of phosphate solubilisation, although the latter was not statistically significant. From these, 20 phosphate-solubilising isolates were selected for further testing on *Arabidopsis thaliana* under controlled conditions. These isolates had varying effects on total fresh weight, primary root length, and lateral root number, with several strains promoting growth while others showed neutral or inhibitory effects. Whole genome sequencing and phylogenetic analysis revealed that some isolates—particularly within *Streptomyces* and *Mesorhizobium*—were phylogenetically distinct from known reference genomes, suggesting potential novelty. Notably, while most isolates were pure cultures, some were later identified as co-cultures through genome sequencing and bioinformatic analysis, suggesting potential metabolic dependency or synergy.

Although the study was limited by the use of non-selective media and the nonspecific nature of the Salkowski assay, it demonstrates the value of minimal media in isolating diverse bacteria with plant-beneficial traits and provides a foundation for future studies on their ecological roles and functional capabilities.

4.1 Introduction

4.1.1 Background

Soil is home to a diverse array of microorganisms, including bacteria, fungi, protozoa, and nematodes, which coexist within the soil matrix (Ekelund et al., 2009). Among these, certain microbes play a crucial role in enhancing plant growth and are collectively known as plant growth-promoting microbes (PGPMs). One of the primary categories of these beneficial microbes are plant growth-promoting bacteria (PGPB) (Richardson et al., 2009a; Ku et al., 2024).

PGPB are known to enhance plant growth through various mechanisms, such as nitrogen (N) fixation, nutrient solubilisation, pathogen suppression and hormone production (Dobereiner, 1992; Patten and Glick, 2002; Glick, 2012; Sharma et al., 2013; Gupta et al., 2015; El Attar et al., 2022). With the increasing demand for increasing crop yield and protecting the environment, there is a growing interest in utilising PGPB to reduce the reliance on chemical fertilisers, therefore making agricultural practices sustainable (Yang et al., 2024).

Two key mechanisms by which PGPB promote plant developments are phosphorus (P)-solubilisation and indole-3-acetic acid (IAA) production. P is crucial for plant development, involved in key physiological processes: P plays a key part in the synthesis of phospholipids and nucleic acids. Also, P forms part of ATP (adenosine triphosphate), which helps the transfer of energy from sunlight to plants through oxidative phosphorylation (light energy to chemical energy) (Kayoumu et al., 2023).

P is abundant in soils, but this element mainly exists in the form of insoluble or poorly soluble inorganic (Munshi and Dave, 2005), whereas plants can only directly absorb P as orthophosphate anions (mainly HPO_4^{2-} and $H_2PO_4^-$) from the soil solution (Richardson et al., 2009a). In most soils, the concentration of these anions is typically low, ranging from 1 to 5 μM (Bieleski, 1973). The deficiency of P leads to limitation on growth and productivity.

Among PGPB, phosphate-solubilising bacteria (PSB) are able to convert these insoluble P into soluble forms for the plants, hence enhancing plant growth. PSB make insoluble

P accessible to plants through mechanisms such as releasing organic acids, phosphonatases and phytases (Rodríguez et al., 2006; Emami-Karvani and Chitsaz-Esfahani, 2021). PSB present a great potential to improve soil fertility and make crop-growing more eco-friendly if they can be integrated into the agriculture system.

Besides P solubilisation, phytohormone production by bacteria also plays a key part in plant growth promotion. IAA is the most well-studied phytohormone produced by many PGPB. IAA plays a key role in various aspects of plant physiology, including cell division, extension, and differentiation. Additionally, IAA can stimulate the germination of seeds and tubers, enhances the development rate of xylem and root, and regulates vegetative growth process. It also initiates the formation of lateral and adventitious roots, mediates plant responses to light, gravity and florescence, and influences pigment formation, photosynthesis , the biosynthesis of various metabolites, and resistance to stressful conditions (Spaepen and Vanderleyden, 2011).

By enhancing root architecture, plants are able to better explore nutrients in the soil, which improves plant health. Bacteria that are able to produce IAA are as important as PSB, as both of them can lead to higher crop productivity. However, the production of IAA is not limited to PGPB as it is also produced by some plant pathogens, which could increase plant vulnerability by increasing growth during infection (Kunkel and Harper, 2017).

4.1.2 Selection of culture medium

PGPB can play diverse roles in promoting plant development, making the identification and characterisation of bacterial strains harbour plant growth-promoting traits highly important. Soil harbours a vast array of bacteria, yet only a small fraction of these microorganisms has been studied. One of the biggest challenges in this field is the ability to isolate and cultivate these bacteria on media (Steen et al., 2019). The composition of the culture media significantly affects the types of bacteria that can be cultured from soil samples.

Enriched media, such as Luria Bertani (LB), tryptic soy and Vegitone, are able to enrich a wide variety of bacteria. However, these media may benefit fast-growing species as they contain relatively high concentrations of nutrients, while slow-growing bacteria might be

outcompeted. This may result in the loss of valuable isolates as these underrepresented species may possess functions related to plant growth promotion (Stewart, 2012). On the contrary, minimal media such as VL55 and VL70 (Schoenborn et al., 2004; Sait et al., 2002), contain minimal nutrients, which can enrich bacteria that are able to survive under nutrient-limited conditions. This approach helps prevent the dominance of fast-growing species.

By using minimal media, slow-growing bacteria that may harbour specialised metabolic pathways, such as the production of phytohormones or the ability to solubilise P, can be selected. Hence, employing a combination of enriched media and minimal media can help obtain a broader range of bacterial isolates, increasing the likelihood of discovering bacteria with valuable plant growth-promoting traits.

4.1.3 Selection of soil samples

The selection of soil also plays an important role for isolating PGPB. As a heterogeneous environment, soil harbours various types of microorganisms, with microbial communities varying significantly between different locations. This diversity in soil is largely shaped by various soil properties, such as local climate conditions (e.g., temperature, moisture), soil type (e.g., clay, sandy), land use (e.g., forestry, agriculture), and organic matter content (Fierer, 2017). Soils from three sites were chosen that have an agricultural research history and offer various soil types and environmental conditions (Ridgman, 1993; Guardo et al., 1994; Hernández et al., 2023). By including soil samples from different sites, we can capture a more diverse soil microbial community, potentially a larger biobank of PGPB.

4.1.4 Aims & objectives

Although the potential benefits of PGPB are well-established, a gap remains in the understanding of how the properties and diversity of isolated bacteria are influenced by different enrichment media. Many studies of PGPB solely focused on a limited range of bacterial taxa or utilised a single type of culture medium for bacteria enrichment. This approach might omit many bacteria that have great potentials to carry out plant growth-

promoting functions, especially those that are slow-growing or thrive under specific nutrient conditions. This is in line with the study by Wang et al. (2023), which highlighted the importance of better understanding the ecological adaptation of different PGPB through comparative functional genome analysis.

Moreover, most of the studies on PGPB heavily focused on in vitro traits, such as P solubilisation, siderophore production, and phytohormone production in laboratory conditions. However, while many studies have investigated these bacteria in agricultural contexts, there have been limited studies on their effects on model plants, such as *Arabidopsis thaliana*, particularly under controlled and more realistic conditions, such as growth on a solid medium. Assessing PGPB on solid media such as Murashige & Skoog (MS) medium offers a better representation of natural plant-microbe interactions, which can provide insights into how PGPB can contribute to plant growth promotion in soil (Schwachtje et al., 2012).

To address these gaps, the aim of this study is to isolate and characterise soil bacteria with potential plant growth-promoting properties using different enrichment media. The objectives of this study are: (1) to construct a biobank of soil bacteria isolated from different media (Vegitone, VL55, and VL70); (2) to assess the phosphate solubilisation and indole-3-acetic acid (IAA) production abilities of these bacterial isolates; (3) to evaluate the impact of selected isolates on *Arabidopsis thaliana* growth using MS medium; and (4) to perform whole-genome sequencing (WGS) to classify the selected isolates and analyse their phylogenetic relationships.

4.2 Materials and methods

4.2.1 Construction of biobank

In this experiment, three different types of media were used for enrichment: Plate Count Agar, Vegitone (19718-500G-F, Sigma-Aldrich, Merck, Germany), VL55 medium, and VL70 medium (Schoenborn et al., 2004; Sait et al., 2002). Plate Count Agar, Vegitone, is a medium used for general bacteria culture and is nutrient-rich, similar to Luria Bertani (LB) medium. Unlike the Vegitone medium, VL55 and VL70 medium are both minimal media, which have been proven efficient for obtaining a high yield of bacteria and are

commonly used in research to isolate bacteria from soil samples (Campanharo et al., 2016; Joseph et al., 2003; Schoenborn et al., 2004).

Plate Count Agar, Vegitone (19718-500G-F, Sigma-Aldrich, Merck, Germany), contained 15.0 g agar, 1.0 g dextrose, 5.0 g tryptone (vegetable) and 2.5 g yeast extract per litre. To prepare the Vegitone medium, 23.5g of Vegitone agar was suspended in milli-Q water, then dissolved and sterilised by autoclaving at 121℃ for 15 minutes. The completed medium was then dispensed into sterile Petri dishes using a consistent volume (~ 30 mL per plate) to ensure uniform depth across all samples.

The double-strength medium VL55 base contained 3.9 g 2-[N-morpholino]ethanesulfonic acid, 0.4 mmol $MgSO_4 \cdot 7H_2O$, 0.6 mmol $CaCl_2$, 0.4 mmol $(NH_4)_2HPO_4$, 2ml of selenite-tungstate solution (Tschech and Pfennig, 1984) and 2ml of trace element solution SL-10 (Widdel and Pfennig, 1981) per litre, the final pH was adjusted to 5.5 using a mixture of 200mM NaOH and 100mM KOH. Double-strength medium VL70 base has similar ingredients with VL 55, but 3.9 g 2-[N-morpholino]ethanesulfonic acid was replaced with 4.18g 3-[*N* morpholino]propanesulfonic acid, the final pH was adjusted to 7.0 instead of 5.5.

The double-strength media were autoclaved at 121℃ for 15 minutes and cooled down to 50℃. Then, 2 ml of vitamin solution 1 and 6 ml of vitamin solution 2 were added per litre of the double-strength medium base (Janssen et al., 1997). An equal volume of 3% agar, pre-washed with Milli-Q water to minimise nutrient contamination and sterilised by autoclaving at 121℃ for 15 minutes, was cooled down to 50℃, added to the double-strength media base, and mixed well. Ten millilitres of growth substrate were added per litre of the completed medium from a concentrated stock, and the media were dispensed into sterile Petri dishes for enumeration. The growth substrate stock contained 50 mM fructose, 50 mM glucose, 50 mM sucrose, 25 mM succinic acid, 25 mM malic acid, 12.5 mM arginine, 12.5 mM serine and 12.5 mM cysteine (Griffiths et al., 1998). The stock was sterilised by passing it through a 0.22µm syringe filter (Merck Millipore, Germany).

Soil samples were collected from three different sites across the UK: Boxworth (B), Chilworth (C), and Rosemaund (R). Boxworth is located in Cambridgeshire in the East of England (52°15'04.7"N 0°01'58.4"W), Chilworth is located in Hampshire in the South of England (50°57'50.2"N 1°25'22.9"W), while Rosemaund (52°07'48.6"N 2°38'08.5"W) is

located in Herefordshire in the West Midlands region of England. These three sites were chosen because they exhibit different characteristics: R soil is more clay-like, C soil is more sand-like, while B soil is in between the two in terms of texture.

One gram of each soil sample was weighed and suspended in 100 ml of sterile milli-Q water. Each mixture was shaken in a horizontal shaker (New Brunswick Innova 4300 Incubator Shaker, New Brunswick Scientific, U.S.) at 200 r.p.m. for 15 minutes. A ten-fold serial dilution was then performed on the resultant suspensions by adding 2 ml of previous dilution to 18 ml of diluent. Sterile Phosphate Buffer Saline (PBS) was used as the diluent for the suspensions plated on Vegitone medium, while the diluent for plates containing VL55 and VL70 media was the sterile single-strength medium base of VL55 or VL70. Two hundred microlitres of suspensions from 10^{-4} to 10^{-7} dilutions were spread onto solid media (see above) using a sterile glass spreader. The agar plates were incubated at 30℃ for one week, a condition commonly used for the cultivation of diverse environmental bacteria, including both fast- and slow-growing species.

Single colonies were obtained from each medium by streaking on agar plates four times.

4.2.2 Phosphorus solubilisation assay of the isolates

A phosphate solubilisation assay was carried out to test the phosphate solubility of the isolates. The medium used for the study was called the Pikovskaya (PVK) medium, which was developed by Nautiyal (1999) as an efficient medium for screening phosphate-solubilising microorganisms. The PVK medium contained 10 g glucose, 5 g hydroxyapatite (as $Ca_3(PO_4)_2$, KT), 0.5 g $(NH_4)_2SO_4$, 0.2g NaCl, 0.1 g $MgSO_4 \cdot 7H_2O$, 0.2 g KCl, 0.5g yeast extract, 0.002 g $MnSO_4 \cdot H_2O$ and 0.002 g $FeSO_4 \cdot 7H_2O$ per litre, with the final pH adjusted to 6.7. Isolates were inoculated into the agar plates containing PVK medium using sterile inoculation loops. The agar plates were incubated at 30℃ for 7 days.

4.2.3 Screening and quantification of Indole-3-acetic Acid (IAA) from isolates using Salkowski reagent

The method used in this study was called the Salkowski reagent method (Gang et al., 2019; Glickmann and Dessaux, 1995). For the bacteria grown in Vegitone medium, a single colony of each selected isolate was inoculated into liquid Luria Bertani (LB) medium

and incubated at 30°C. After 2 days, 100µl of each bacterial suspension was transferred to liquid LB medium with 0.15 % of L-tryptophan (w/v) added. The isolates were then incubated at 30°C in dark conditions for 24h.

A 750 µl sample of culture was taken from each isolate and transferred to Eppendorf tubes, which were then centrifuged at 15,000 rpm for 5 minutes using a Sigma 4-16KS centrifuge (Sigma, UK). After centrifugation, for each isolate, 650 µl of the supernatant was carefully withdrawn and transferred to a new Eppendorf tube, then mixed with an equal volume of Salkowski reagent and vortexed gently to mix well. Then, 150 µl of each mixture was transferred to a Costar 96-well plate (Thermo Fisher Scientific, United States) and incubated at 30 °C for 30 min in the dark by covering the plate with aluminium foil. Triplicates were prepared for each selected isolate, and blanks were prepared by replacing the supernatant with 650 µl of uninoculated LB liquid medium and mixing with equal volume of Salkowski reagent. The Salkowski reagent contained 12g of $FeCl_3$ per litre in 9M H_2SO_4 (Glickmann and Dessaux, 1995).

The IAA was detected by measuring the development of pink colour. The optical density (OD) of each sample was measured at 536 nm and compared with the OD of a standard IAA curve prepared (5-50 µg/ml). The concentration of IAA produced by each sample was then calculated based on this standard curve. The OD values were measured by CLARIOstar Plus multimode microplate reader (BMG LABTECH, UK).

For the bacteria grown in VL55/70 media, the bacteria were incubated in the liquid VL55/70 media for 2 weeks before inoculating into the media with tryptophan added. The IAA test was conducted 3 weeks after the samples were inoculated into the media with tryptophan. A longer incubation period was applied to the bacteria from VL55/70 because, according to previous observations, bacteria grew slower in these two media compared to Vegitone medium.

4.2.4 Bacterial plant growth promotion assay

Arabidopsis thaliana wild type Columbia-8 (Col-8) was used as a model plant for the growth promotion assay. The seeds were first sterilised by shaking them in a 10% (v/v) solution of Domestos thick bleach (Unilever, United Kingdom) on a roller for 15 minutes. They were then rinsed with sterile milli-Q water three times. Half - strength Murashige

and Skoog (½MS) medium was used for plant cultivation. The ½MS medium was prepared by mixing 2.22 g of Murashige & Skoog Modified Basal Medium with Gamborg Vitamins (Product ID: M404; PhytoTech Labs, U.S) with 1% of sucrose and 0.8% of agar per litre of milli-Q water. The pH of the medium was adjusted to 5.8 using 0.5M KOH before autoclaving.

The plant growth promotion assay was conducted using methods modified from Ramandi et al. (2023). Four seedlings were placed onto the surface of half-strength MS medium in each Petri dish. The plates were sealed with 3M micropore surgical tape (3M, Minnesota, United States), wrapped in foil, and kept at 4 °C in the dark for 2 days. They were then transferred to a Percival plant growth chamber (Percival, Perry, Iowa, United States) and incubated vertically with a photoperiod of 16 hours of light and 8 hours of darkness at 22 °C. The seedlings were grown for 5 days before bacterial inoculation.

Lawns of bacterial cultures were prepared by spreading liquid cultures of bacteria (OD_{600} = 0.5) from 20 isolates that demonstrated the ability to utilise phosphate on agar plates (Vegitone, VL55, or VL70) 24 hours before inoculation, and incubating them at 30 °C. Round-shaped plugs were carefully cut out from the lawn cultures using sterile 200 µL pipette tubes and placed next to the roots of each seedling. Mocks were prepared in the same way using empty plugs from Vegitone, VL55 and VL70 media. Triplicates were prepared for each isolate.

After inoculation, the plants were grown together with the bacteria for another 14 days. At harvest, total fresh weight, primary root length, and number of lateral roots were measured. The primary root length and lateral root number were measured using ImageJ software (https://imagej.net/).

4.2.5 Whole genome sequencing (WGS) of isolates

DNA from the 20 isolates, selected based on their ability to utilise phosphate, was extracted using PureLink™ Genomic DNA Mini Kit (Thermo Fisher Scientific, Massachusetts, United States) according to the manufacturer's instructions. The DNA concentration (ng/µL) of each sample was measured using the BioDrop Duo+ Spectrophotometer (Biochrom Ltd, Cambridge, UK), and samples were stored at -20 °C before being sent for

sequencing. Illumina 2 × 250 bp paired-end whole genome sequencing (WGS) was performed, with genome sequencing services provided by MicrobesNG (https://microbesng.com, Birmingham, United Kingdom).

4.2.6 Data analysis

IAA measurement data were visualised using GraphPad Prism version 10 (GraphPad Software, California USA). Data from root measurements were analysed using analysis of variance (ANOVA) followed by Tukey's Multiple Comparisons test, which was implemented in GraphPad Prism version 10. The results were then visualised using the same software.

Genome sequencing data were analysed using tools within the KBase platform (https://www.kbase.us/) (Arkin et al., 2018). The CheckM - v1.0.18 lineage workflow in KBase was first used to assess the completeness and contamination of the genomes (Parks et al., 2015). An initial screen of the data was performed with Kaiju (Menzel et al., 2016), which performs a taxonomic classification of the sequence reads. Genomes with more than one taxon were assumed to be mixed cultures and analysed as metagenomes as described below using the pipeline described by Chivian et al. (2023). Those genome assemblies with only one taxon were annotated with RASTtk (Brettin et al., 2015) and the taxonomy determined by GTDB-Tk - v1.7.0 (Parks et al., 2020).

Genomic datasets identified as mixed cultures were assembled with metaSPAdes - v3.15.3 (Nurk et al., 2017) . Other assemblers were also tested, including MEGAHIT and IDBA-UD, but the best assemblies were always obtained with metaSPAdes. Assembly quality was assessed based on standard metrics, including total number of contigs, N50, L50, longest contig length, and the number of contigs exceeding 1 Mb. metaSPAdes consistently produced higher N50 values, lower L50, longer contigs, and more large contigs (>1 Mb), indicating greater contiguity and completeness. As a result, metaSPAdes assemblies were used for subsequent steps. Assembled contigs were binned with MetaBAT2 -v1.7 (Kang et al., 2019), MaxBin2 - v2.2.4 (Wu et al., 2015), and CONCOCT - v1.1 (Alneberg et al., 2014). The bins were optimised using DAS Tool - v1.1.2 (Sieber et al., 2018), with each bin representing a metagenome-assembled genome (MAG). The MAGs were re-analysed using CheckM to reassess their completeness and contamination, and were annotated with RASTtk and GTDB-Tk, as described above.

A phylogenetic tree of the genomes and MAGs was constructed using SpeciesTree - v2.2.0 within the KBase platform, based on 49 core, universal genes. Reference sequences of closely related organisms were selected from the public KBase genomes from RefSeq. Average Nucleotide Identity (ANI) values between different cultures were calculated using Compute ANI with FastANI - v0.1.3 to assess the genomic similarity between isolates. An ANI value >=95% is commonly used to define species-level similarity, while values ⩾99% suggest that isolates are likely the same strain (Goris et al., 2007).

4.3 Results

4.3.1 Isolation of bacteria

A total of 70 different isolates were obtained from three different media: Vegitone, VL55, and VL70. Among these, 56 isolates were obtained from the VL media, with 27 isolates from VL 55 and 29 from VL70.

A selection of the isolates is shown in Figure 4.1, while a summary of all the isolates can be found in Table S1, Table S2, and Table S3. The isolates were named based on their appearance on the media.

The VL media, particularly VL70, yielded a wider range of morphologically distinct colonies than Vegitone. These isolates were then subjected to further assays.

R3a

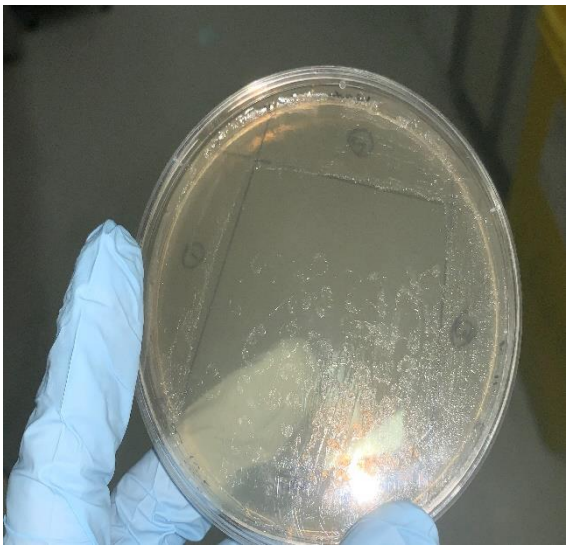

R3b

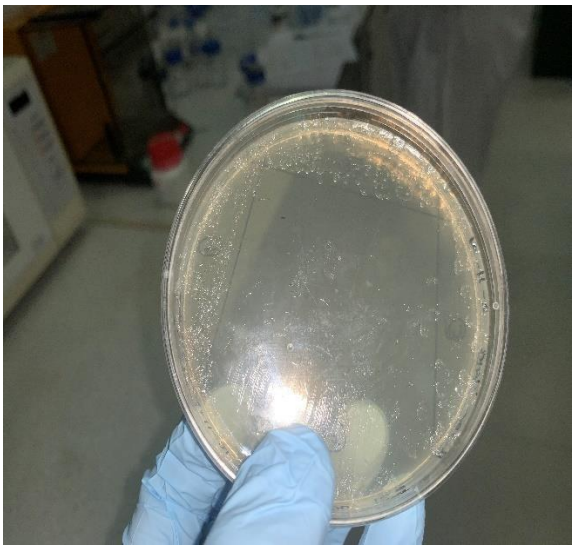

1C-55

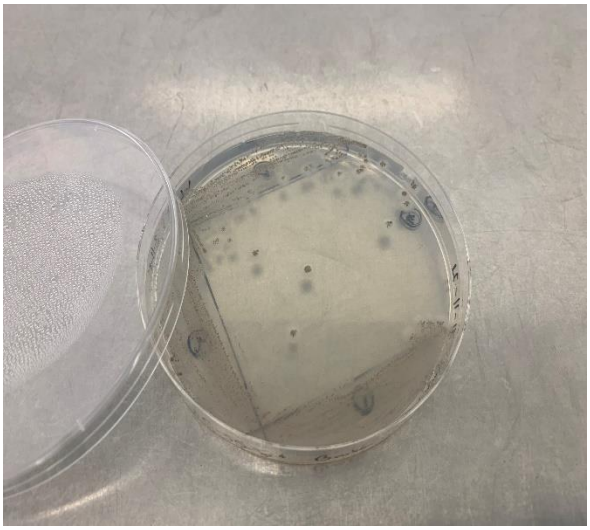

3R-55

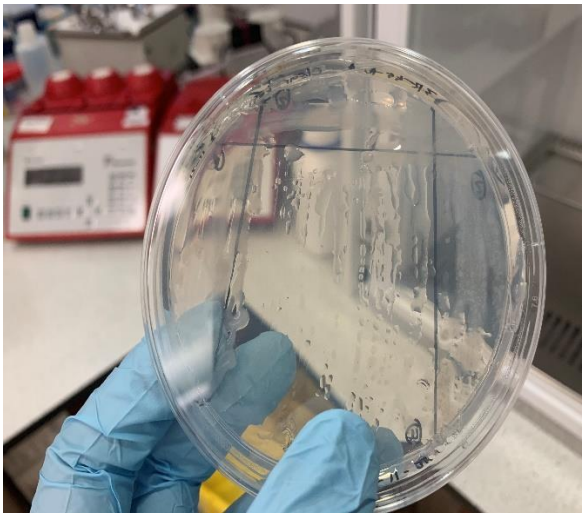

9R-70

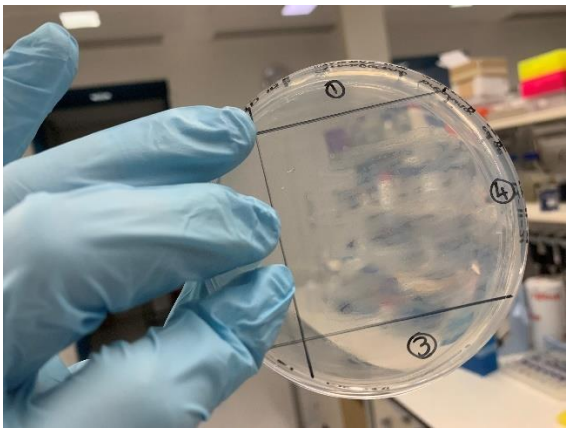

4B-70

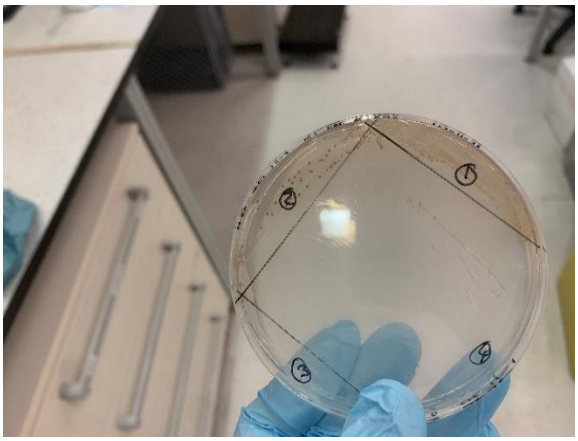

Figure 4.1 Selection of isolates from different media. B, C and R stand for the locations from where the bacteria were isolated, Boxworth, Chilworth and Rosemaund, respectively. “-55”,”-70”: the isolates were obtained from VL55 or VL70 medium.

4.3.2 Phosphate solubilisation assay

All 70 isolates obtained from the soil were first tested for their ability to solubilise water-insoluble phosphate, which in this study was hydroxyapatite. This compound served as the sole source of phosphorus available to the bacteria in the medium although there would have been some carryover of phosphate from the original culture. Halos formed around the isolates that were capable of solubilising the hydroxyapatite (Figure 4.2a,b). The cultures with no halos were classified as unable to solubilise hydroxyapatite (Figure 4.2c) and these strains tended to grow less well on these plates.

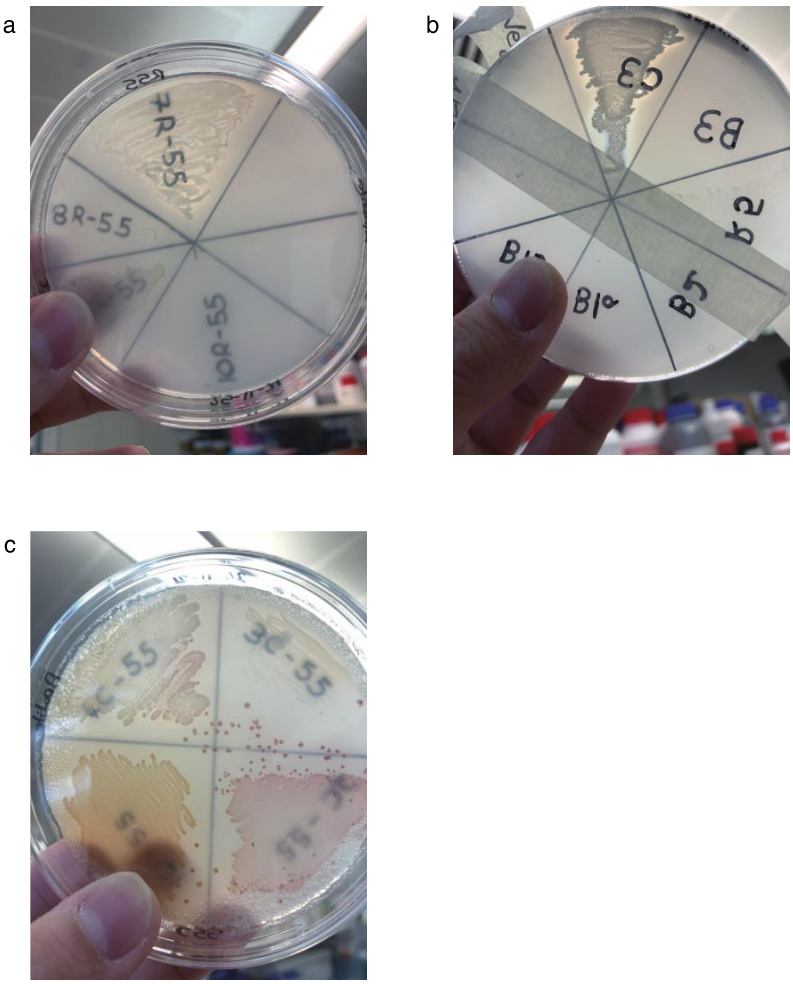

Figure 4.2 Results of P solubilisation assay. Halos were observed around bacteria that grew and solubilised the calcium phosphate in the medium (a, b). For bacteria that could not solubilise the calcium phosphate, no halos were found (c).

The results indicate that not all the isolates were able to utilise water-insoluble phosphate in the medium. According to our observation, 20 out of the 70 isolates were capable of solubilising the phosphate. Among these, 5 isolates were obtained from the Vegitone medium, 10 strains were isolated from the VL55 medium, and 5 strains were isolated from the VL70 medium. Among these, the majority of phosphate-solubilising isolates originated from the Boxworth and Rosemaund soils (8 and 11 isolates, respectively), while only one was obtained from the Chilworth soil.

4.3.3 Colorimetric assay to detect the IAA using Salkowski reagent

Bacteria from each medium in the gene bank were randomly selected for colorimetric assay to test their ability to produce IAA. Blank-corrected values of IAA concentration (in µg/mL) are shown in Figure 4.3. The bacteria isolates demonstrated varying abilities to produce IAA.

As shown in Figure 4.3a, the bacteria isolated from the Vegitone medium showed relatively low IAA signals, with concentration ranges from 4 to approximately 6 µg/mL. The bacterial isolates from the VL55 medium demonstrated higher production of IAA, with concentrations ranging from 4 to around 35 µg/mL (Figure 4.3b). The bacterial isolates from the VL70 medium showed the widest range of IAA production among the three media, with several strains producing concentrations higher than 50 µg/mL (Figure 4.3c). In the following experiments, we proceeded with the 20 isolates that demonstrated the ability to utilise phosphate.

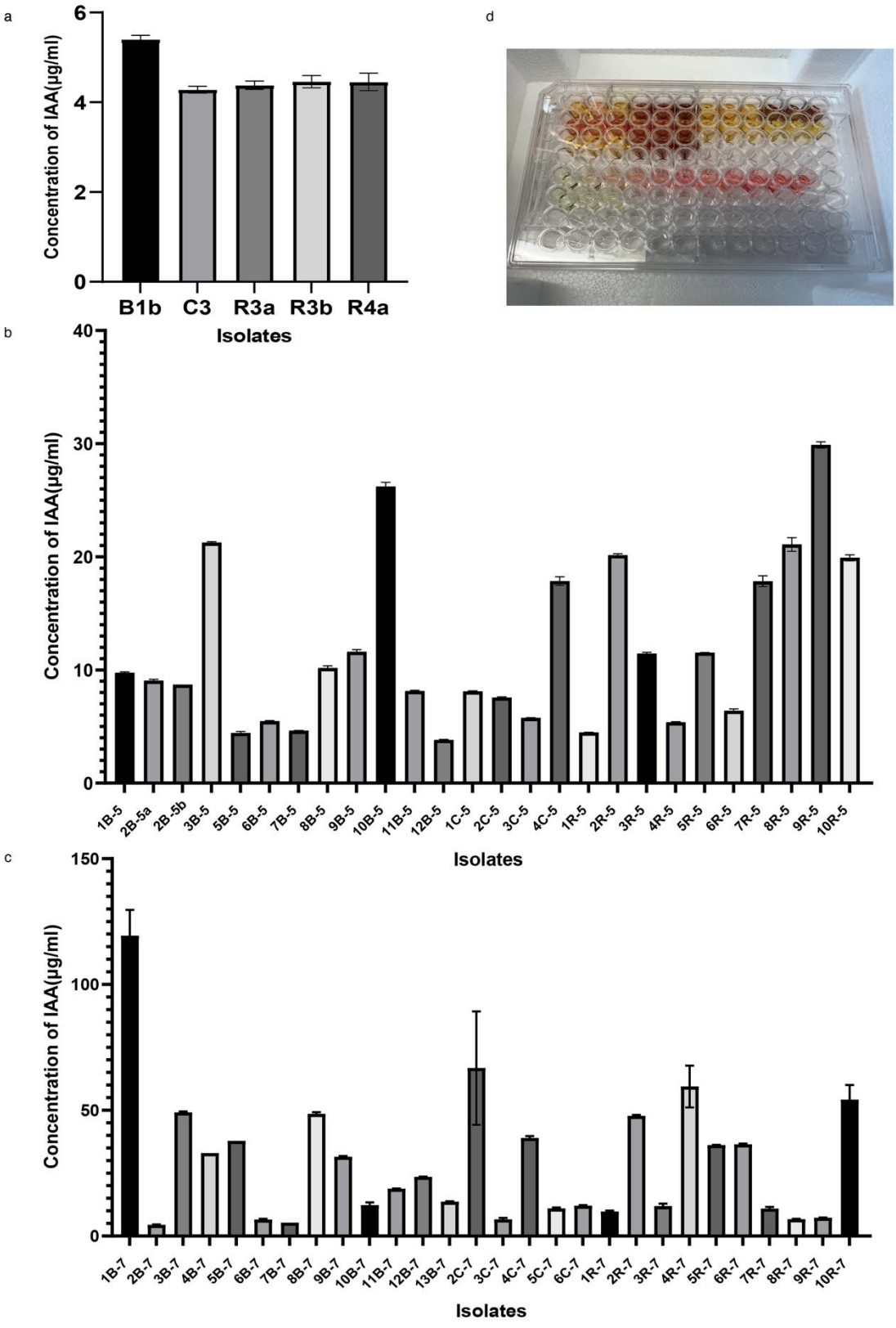

Figure 4.3 Results of colorimetric assay using Salkowski reagent. Error bars indicate standard error of the mean (SEM) calculated based on technical replicates (n=3). (a): IAA concentration of selected isolates from Vegitone medium. (b): IAA concentration of selected isolates from VL55 medium. (c): IAA concentration of selected isolates from VL70 medium. (d): An example of pink colour development in the colorimetric reaction.

4.3.4 Plant growth promotion assay

The isolates from the Vegitone medium had varying effects on the growth of *Arabidopsis*. All of the isolates from Vegitone medium showed negative impacts on the total fresh weight of *Arabidopsis*, particularly R1, R3a, and R3b ($P < 0.05$) (Figure 4.4a). Isolate R1 also significantly reduced primary root length and lateral root number (Figure 4.4b,c) ($p < 0.05$), while R3b negatively affected lateral root number but not root length. The remaining isolates—C3, R2, and R3a—did not significantly affect root length or lateral root number ($p > 0.05$).

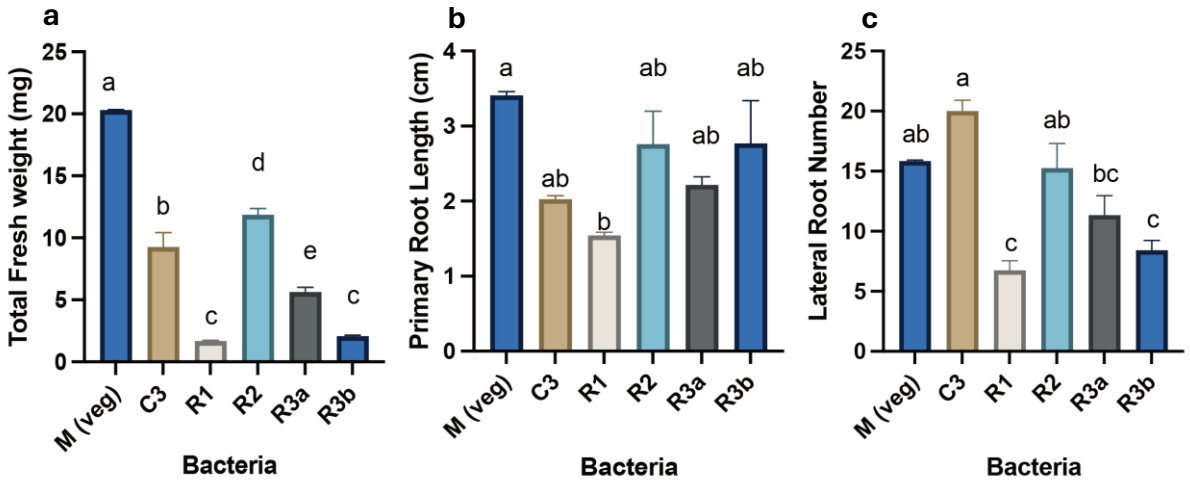

Figure 4.4 The effects of the Vegitone bacteria inoculation on the root traits of the *Arabidopsis* seedlings in the plant growth promotion assay. (a) Total fresh weight, (b) primary root length, and (c) lateral root number were measured 14 days after inoculation. Bars represent the mean values (n=3), Error bars represent the standard error of the mean (SEM). Different letters indicate statistically significant differences (Tukey's Multiple Comparisons test, $p \leq 0.05$).

Bacteria isolated from the VL55 medium demonstrated varying impacts on *Arabidopsis* growth (Figure 4.5). Isolates 2B-5b, 3B-5, 8R-5, and 9R-5 significantly reduced the fresh weight of *Arabidopsis* compared to the mock (Figure 4.5a) ($p < 0.05$). In contrast, 5R-5 had a positive effect on fresh weight ($p < 0.05$). The other isolates, including 1B-5, 6B-5, 9B-5, 2R-5, and 7R-5 did not influence the fresh weight ($p > 0.05$).

In terms of primary root length, isolates 3B-5, 8R-5, and 9R-5 showed a negative impact, while 1B-5 and 9B-5 exhibited positive effects on root length ($p < 0.05$). Conversely, isolates 2B-5b, 6B-5, 2R-5, 5R-5 and 7R-5 showed no significant changes compared to the mock ($p > 0.05$) (Figure 4.5b).

For lateral root number, isolates 8R-5 and 9R-5 caused a significant reduction ($p < 0.05$). In contrast, isolates 1B-5, 2B-5b, 6B-5, 9B-5, 2R-5, 5R-5, and 7R-5 had positive impacts on lateral root number ($p < 0.05$). Isolate 3B-5 had neither a positive nor negative impact ($p > 0.05$) (Figure 4.5c).

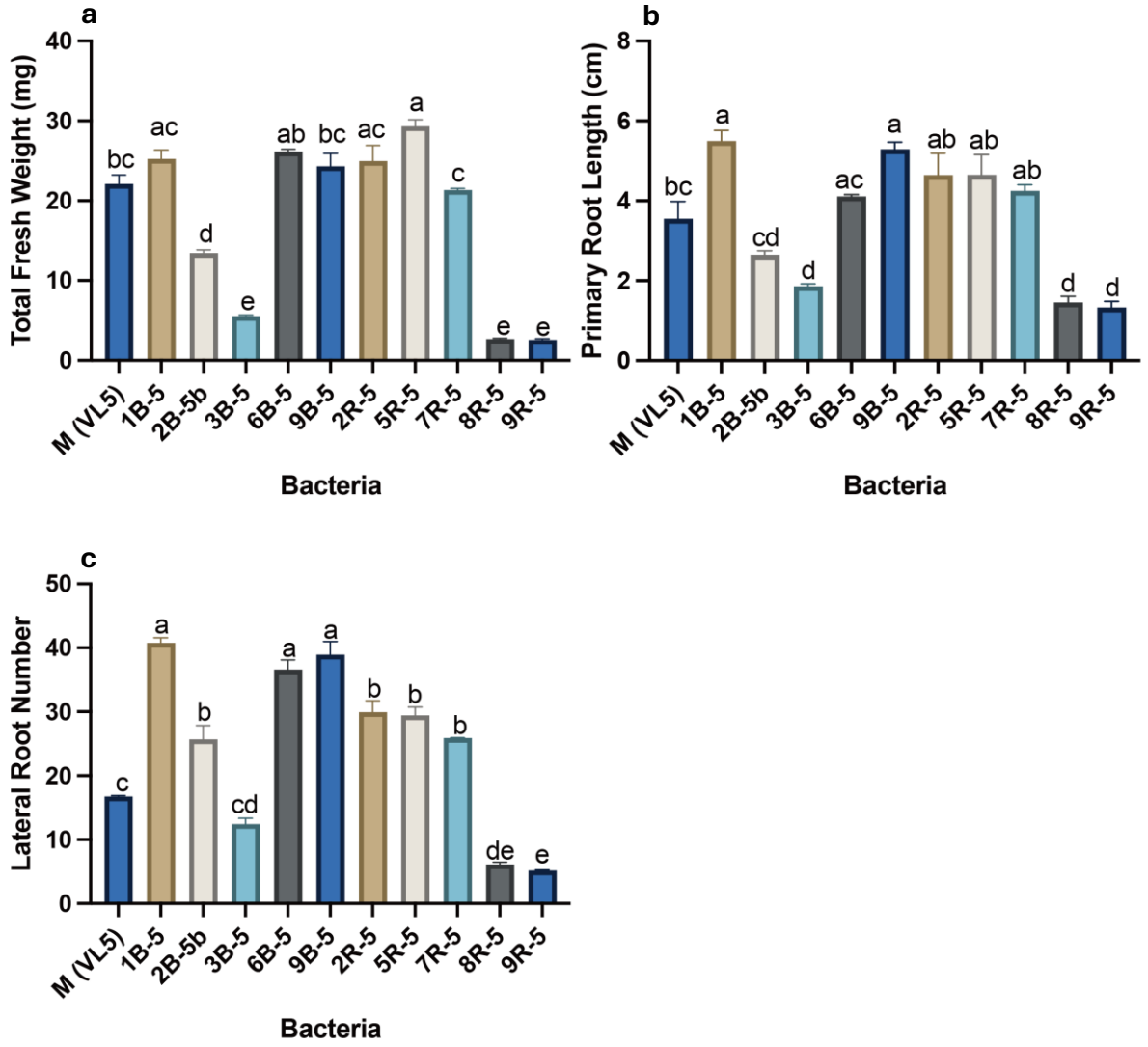

Figure 4.5 The effects of the VL55 bacteria inoculation on the root traits of the *Arabidopsis* seedlings in the plant growth promotion assay. (a) Total fresh weight, (b) primary root length, and (c) lateral root number were measured 14 days after inoculation. Bars represent the mean values (n=3), Error bars represent the standard error of the mean (SEM). Different letters indicate statistically significant differences (Tukey's Multiple Comparisons test, $p \leq 0.05$).

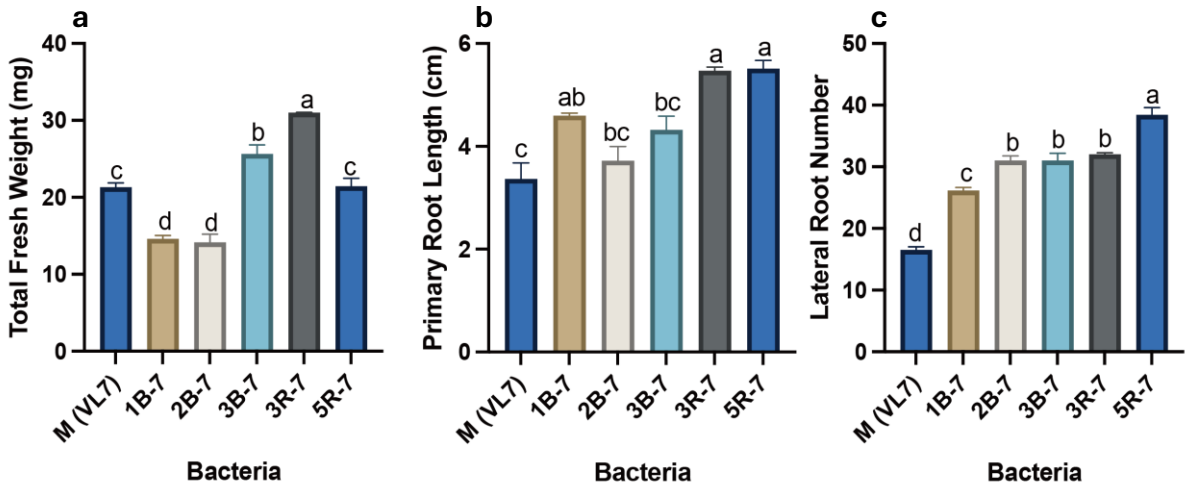

Figure 4.6 The effects of the VL70 bacteria inoculation on the root traits of the *Arabidopsis* seedlings in the plant growth promotion assay. (a) Total fresh weight, (b) primary root length, and (c) lateral root number were measured 14 days after inoculation. Bars represent the mean values (n=3), Error bars represent the standard error of the mean (SEM). Different letters indicate statistically significant differences (Tukey's Multiple Comparisons test, $p \leq 0.05$).

Table 4.1 IAA production and corresponding effect on *Arabidopsis* lateral root number for bacterial isolates. IAA concentrations were measured using the Salkowski reagent method. Concentrations (µg/mL) are reported as means ± SEM (n=3). Isolates were categorised based on their observed effect on lateral root number in *Arabidopsis*, relative to controls, as Positive (significantly increased), Neutral (no significant change), or Negative (significantly reduced).

Isolate	IAA (µg/mL)	Effect on lateral root number
1B-5	9.76 ± 0.07	Positive
2B-5b	8.71	Positive
6B-5	5.47 ± 0.06	Positive
9B-5	11.61 ± 0.19	Positive
2R-5	20.15 ± 0.13	Positive
5R-5	11.53 ± 0.02	Positive
7R-5	17.84 ± 0.48	Positive
1B-7	119.40 ± 10.22	Positive
2B-7	4.48 ± 0.12	Positive
3B-7	49.14 ± 0.38	Positive
3R-7	11.96 ± 0.95	Positive
5R-7	36.17 ± 0.12	Positive
C3	4.28 ± 0.04	Neutral
R3a	4.38 ± 0.05	Neutral
3B-5	21.25 ± 0.09	Neutral
8R-5	21.09 ± 0.61	Negative
9R-5	29.88 ± 0.28	Negative
R3b	4.46 ± 0.08	Negative

Isolates from the VL70 medium also had varying impacts on the growth of *Arabidopsis* (Figure 4.6). Isolates 1B-7 and 2B-7 demonstrated negative impacts on total fresh

weight, while 3B-7 and 3R-7 significantly increased total fresh weight ($p < 0.05$). Isolate 5R-7 showed no impact on total fresh weight compared to the mock ($p > 0.05$) (Figure 4.6a). Regarding primary root length, none of the isolates showed negative impacts. Isolates 1B-7, 3R-7, and 5R-7 showed positive effects on root length ($p < 0.05$), while 2B-7 and 3B-7 showed no significant differences compared to the mock ($p > 0.05$) (Figure 4.6b). In terms of lateral root number, all isolates demonstrated positive impacts ($p < 0.05$) (Figure 4.6**Error! Reference source not found.**).

In summary, bacteria isolated from Vegitone primarily had negative impacts on the growth of *Arabidopsis*. Bacteria isolated from the VL55 medium displayed mixed effects, with some isolates promoting plant growth, particularly in lateral root number, while others reduced total fresh weight and primary root length. In contrast, VL70 isolates exhibited growth-promoting effects, especially for lateral number and primary root length, with only two of them reducing the total fresh weight of the plants.

We compared the IAA levels across the isolates selected for growth promoting assays (Table 4.1) and found that IAA levels varied widely among those that positively influenced lateral root number (range: 4.48–119.40 µg/mL). High IAA levels were also observed in isolates with neutral or negative effects. Notably, 8R-5 and 9R-5 produced IAA levels above 20 µg/mL but reduced lateral root number. No clear pattern was observed between IAA production levels and the direction of plant growth response.

4.3.5 Classification of isolates

After sequencing, an initial quality check using CheckM revealed that 14 of the 20 identified isolates were pure cultures with high completeness (>90%) and low contamination (<5%). The remaining 6 isolates were considered mixed cultures, as they exhibited high contamination. The genomes of mixed cultures were binned into a total of 14 MAGS. CheckM was then redone on the MAGs to reassess the completeness and contamination, with the majority of the bins showing high completeness and low contamination. Taxonomy assignments for all isolates and enrichments were made using CheckM (Table S4). Except for *Rhodococcus*, *Staphylococcus*, and *Acinetobacter*, all other genera identified are common PGPB.

The phylogenetic tree built from 49 core genes showed distinct evolutionary relationships among the isolates and enrichments (Figure 4.7). Several isolates or genome bins

appeared closely related based on the phylogenetic tree, such as 6B-5_bin1 and 1B-5, and R2_bin4 and 3R-7_bin2. To determine whether these represented truly identical strains or distinct but related isolates, pairwise ANI values were calculated using FastANI. All comparisons yielded ANI values above 99%, indicating that these isolate pairs are likely to be identical or highly similar at the strain level (Table S 13). Some isolates also appeared phylogenetically distinct from available reference genomes, suggesting possible novelty. For instance, isolates 5R-5, 3B-7, and 9B-5 form a separate, well-supported clade related to *Streptomyces griseus* and *S. atroolivaceus*, but are clearly distant, indicating they may represent a novel lineage within *Streptomyces* or a related genus. Similarly, 7R-5 clusters near *Mesorhizobium*, but sits on its own branch, while 1B-7_bin2 also clusters near *Mesorhizobium* yet occupies an even more distinct branch, suggesting potential taxonomic novelty. A summary of genome size, GC content, and ANI values with the closest cultivated relatives for all isolates and MAGs is provided in Table 4.2.

Isolates 1B-5 and enrichment 6B-5_bin1 form a distinct cluster at the top of the tree within the genus *Rhodococcus*. Organisms in this clade generally showed positive effects on *Arabidopsis* growth, particularly in lateral root number. The *Cellulosimicrobium* clade demonstrated a mixed impact on *Arabidopsis* growth, with R2_bin4 being associated with a negative effect on fresh weight, while 3R-7_bin2 associated with a significant enhancement of all the growth parameters. The *Pseudarthrobacter* clade (R2_bin1, 3B-5_bin1, 9R-5_bin1) generally showed negative effects, particularly on fresh weight and primary root length.

The *Curtobacterium* and *Microbacterium* clades displayed varying effects on growth parameters. The *Curtobacterium* clade (R2_bin3, 3B-5_bin3) generally demonstrated negative impacts on plant growth, while the *Microbacterium* clades, which only includes 3R-7_bin1, showed significant improvement in all the parameters. *Streptomyces* formed the largest clade in the phylogenetic tree. Isolates in the *Streptomyces* group, including 2B-7, 2R-5, 5R-5, 3B-7, and 9B-5, generally showed positive effects on plant growth, especially in lateral root number.

Staphylococcus (R1) and *Bacillus* (8R-5, R2_bin2, C3, R3a, R3b) clades are clustered next to each other, and none of them had positive effects on plant growth. In contrast, all of them had negative effects on total fresh weight as well as lateral root length. The

Acinetobacter clade (6B-5_bin2, 2B-5b) significantly increased lateral root number. The *Azospirillum* clade (1B-7_bin1, 3B-5_bin2) and *Paracoccus* (1B-7_bin2) exhibited mixed impacts on plant growth. *Paracoccus* demonstrated a positive impact, while *Azospirillum* had both positive and negative effects. Finally, the *Mesorhizobium* isolates (7R-5, 5R-7) demonstrated overall positive effects on plant growth, especially in lateral root number.

Table 4.2 Summary of isolates/enrichments, including closest cultivated relative, ANI value, assembly size (bp), and GC content. The names of enrichments are indicated as “bin”, whereas those names without “bin” are presumed to be pure cultures.

Genome	Closest cultivated relative	ANI value with the closest relative	Genome (bp)	G+C%
1B-5	*Rhodococcus erythropolis*	96.11%	7032660	62%
1B-7_bin1	*Azospirillum lipoferum 4B*	90.73%	7302453	67%
1B-7_bin2	*Mesorhizobium plurifarium*	76.29%	3956367	68%
2B-5b	*Acinetobacter pittii PHEA-2*	96.85%	4132565	39%
2B-7	*Streptomyces phaeochromogenes*	97.71%	11696974	70%
2R-5	*Streptomyces aureus*	90.88%	9882550	71%
3B-5_bin1	*Pseudarthrobacter phenanthrenivorans*	86.27%	4240142	66%
3B-5_bin2	*Azospirillum lipoferum 4B*	90.70%	7202344	67%
3B-5_bin3	*Curtobacterium flaccumfaciens UCD-AKU*	86.27%	3756313	71%
3B-7	*Streptomyces griseus subsp. griseus*	84.42%	10466205	69%
3R-7_bin1	*Microbacterium paraoxydans DH1b*	93.17%	3076506	71%
3R-7_bin2	*Cellulosimicrobium cellulans J36*	89.31%	4345164	75%
5R-5	*Streptomyces griseus subsp. griseus*	84.36%	9718816	69%
5R-7	*Mesorhizobium ciceri biovar biserrulae WSM1271*	91.62%	7212304	62%
6B-5_bin2	*Acinetobacter pittii PHEA-2*	96.81%	3831264	39%
6B-5_bin1	*Rhodococcus erythropolis*	96.29%	6413756	62%
7R-5	*Mesorhizobium amorphae CCNWGS0123*	87.29%	5968260	63%
8R-5	*Bacillus megaterium NBRC 15308*	96.97%	5613152	38%
9B-5	*Streptomyces griseus subsp. griseus*	84.43%	10557037	69%
9R-5_bin1	*Pseudarthrobacter sulfonivorans*	85.24%	4773603	66%
C3	*Bacillus licheniformis DSM 13 = ATCC 14580*	99.59%	4309614	46%
R1	*Staphylococcus hominis*	97.37%	2219541	32%
R2_bin1	*Pseudarthrobacter phenanthrenivorans*	86.27%	4246888	66%
R2_bin2	*Bacillus licheniformis DSM 13 = ATCC 14580*	99.58%	4291428	46%
R2_bin3	*Curtobacterium flaccumfaciens UCD-AKU*	86.25%	3672007	71%
R2_bin4	*Cellulosimicrobium cellulans J36*	88.26%	602865	73%
R3a	*Bacillus licheniformis DSM 13 = ATCC 14580*	99.64%	4311893	46%
R3b	*Bacillus licheniformis DSM 13 = ATCC 14580*	99.64%	4311073	46%

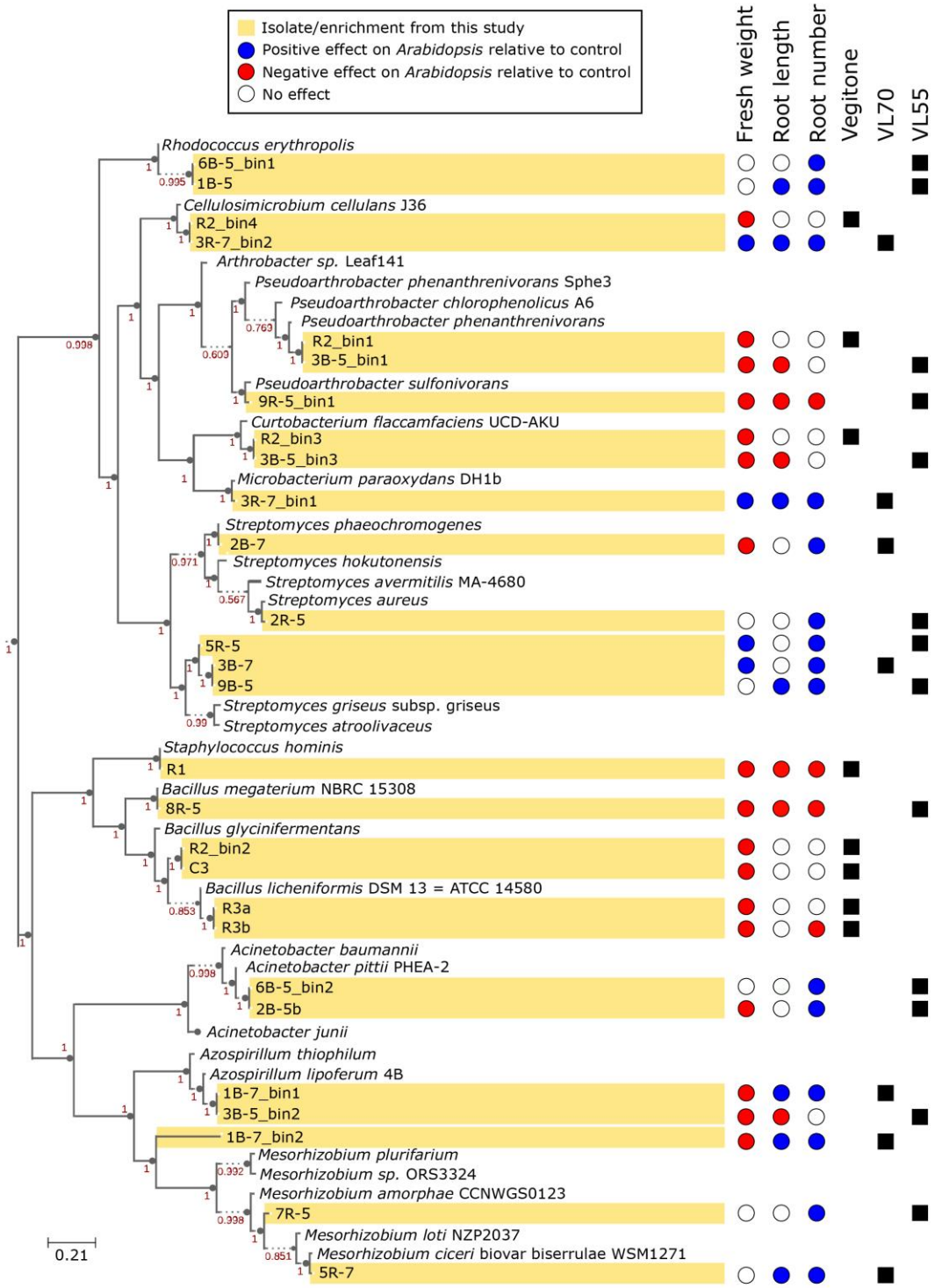

Figure 4.7 Phylogenetic tree of isolates and enrichments. The tree was built from 49 core, universal genes, using SpeciesTree - v2.2.0 within KBase. Organisms from this study are highlighted in yellow. Reference sequences of closely related organisms were selected from the public KBase genomes from RefSeq. The names of enrichments are indicated as "bins", whereas those names without "bin" are presumed to be pure cultures. The effect of the enrichments/isolates on Arabidopsis growth are indicated with circles (blue circle: positive effect relative to control ($p<0.05$); red circle: negative effect relative to the control ($p<0.05$); open circle: no effect). The medium used for cultivation is indicated with squares.

4.4 Discussion

4.4.1 Summary of findings

In this study, we isolated bacteria from three different sampling sites across the UK: Boxworth (B), Chilworth (C), and Rosemaund (R), enriching these bacteria using three different media: Vegitone (19718-500G-F, Sigma-Aldrich, Merck, Germany), VL55 medium, and VL70 medium (Schoenborn et al., 2004; Sait et al., 2002). Overall, the VL media yielded a higher number of isolates compared to the Vegitone medium, with VL55 resulting in 27 isolates, VL70 in 29 isolates, and Vegitone in 14 isolates. Although not all isolates were subjected to taxonomic identification, this suggests that minimal media may favour the growth of a broader range of culturable bacterial types than nutrient-rich Vegitone.

We assayed these isolates for their ability to produce IAA and solubilise phosphate. All 70 isolates produced a positive IAA signal and isolates from the VL media generally produced higher signals compared to those from the Vegitone medium (Figure 4.3) ($U = 136$, $p < 0.0001$, Mann-Whitney test). The results of the IAA assay need to be treated with caution since the Salkowski reagent can detect other compounds, including indolepyruvic acid and indoleacetamide (Glickmann and Dessaux, 1995). A closer analysis of the genomes might indicate if genes encoding enzymes for IAA production, as there are six potential metabolic pathways for IAA production in bacteria: the indole-3-acetamide (IAM) pathway, indole-3-pyruvate (IPA) pathway, tryptamine pathway, tryptophan side-chain oxidase (TSO) pathway, indole-3-acetonitrile (IAN) pathway, and the potential existence of a tryptophan-independent pathway (Spaepen et al., 2007). Genome annotation using RASTtk provided some insight into potential IAA pathways present in the 15 isolates/enrichments that promoted plant growth in this study. Genes encoding indole-3-pyruvate decarboxylase (*ipdC*) and indole-3-acetaldehyde dehydrogenase (*dhaS*), both part of the IPA pathway, were detected in some *Acinetobacter* and *Mensorhizobium* strains. Gene encoding nitrilase (*nit*), which is involved in the IAN pathway, was detected in several *Streptomyces* stains and in *Cellulosimicrobium* (Table S 14). However, no single isolate contained the complete set of genes for any one IAA bio-

synthesis pathway, suggesting that IAA production in these strains may proceed via alternative mechanisms. Moreover, the IAA signals detected using the Salkowski reagent may represent intermediate compounds rather than IAA itself.

Only 20 of the 70 were able to solubilise phosphate, with just 5 of these obtained from the Vegitone medium (Figure 4.2). These 20 isolates were selected for further plant growth promotion assays. In these assays, isolates from the Vegitone medium generally showed negative impacts on *Arabidopsis* growth (Figure 4.4) , while isolates from the VL55 medium had mixed effects (Figure 4.5), and isolates from the VL70 medium demonstrated generally positive impacts (Figure 4.6).

The whole genome sequencing (WGS) revealed that the isolates belong to three phyla: Actinobacteria, Firmicutes, and Proteobacteria (Table 4.2). A total of 28 microorganisms were identified, including both pure culture and enrichments. Several isolates also appeared phylogenetically distinct from available reference genomes, suggesting potential taxonomic novelty.

4.4.2 Effects of different media in isolating PGPB

The Vegitone medium selected for a narrower range of bacteria compared to VL55 and VL70. This may be explained by its nutrient-rich nature, which favors fast-growing bacteria (Stewart, 2012).

Additionally, isolates from the VL media generally produced stronger signals in the IAA assay compared to those from the Vegitone medium (Figure 4.3). A higher number of bacteria in the VL media also displayed the ability to solubilise phosphate compared to the Vegitone medium, but this difference was not statistically significant ($\chi^2 = 0.44$, df = 1, $p > 0.5$). Nevertheless, these findings suggest that minimal media may be more suitable for isolating bacteria that carry out plant growth promoting functions compared to standard nutrient media (Sarhan et al., 2018).

4.4.3 Impacts on *Arabidopsis thaliana* growth

The 20 isolates selected for the plant growth promotion assay all solubilised phosphate and produced a detectable signal for indole-related compounds in the Salkowski assay. However, the signal intensity varied among isolates, and due to the nonspecific nature

of the assay, the actual levels of biologically active IAA and their contribution to *Arabidopsis* growth promotion remain unclear (Table 4.1). In line with this, not all of them had positive effects on the growth parameters of *Arabidopsis* (total fresh weight, primary root length, and lateral root number). Isolates from the Vegitone medium generally had negative impacts across all the growth parameters (Figure 4.4). This might be attributed to the nature of the bacteria cultivated on Vegitone medium. Being a nutrient-rich medium, Vegitone may prefer fast-growing bacterial species, which might not necessarily be the best plant growth promoters. These bacteria, while thriving quickly, may become competitive or even antagonistic toward plants, either by outcompeting them for nutrients or by producing harmful metabolites that inhibit plant growth (Kuzyakov and Xu, 2013).

In contrast, isolates from the VL55 medium showed mixed effects on *Arabidopsis* growth. Some isolates promoted plant growth by increasing total fresh weight and lateral root number, such as 5R-5, while others, like 8R-5 and 9R-5, had the opposite effect. This variation suggests that even within the same group of bacteria isolated using minimal media, their overall impact on plant growth is determined by other factors. These may include the production of additional metabolites, such as siderophores and antibiotics, as well as their ability to efficiently colonise the plants (Compant et al., 2005) (Figure 4.5).

Most isolates from the VL70 medium generally demonstrated positive impacts on *Arabidopsis* growth, particularly in increasing primary root length and lateral root number (Figure 4.6). The fresh weight measurement of *Arabidopsis* in this study should be treated with caution due to potential artifacts with this measurement (Bashan and de-Bashan, 2005) . Although VL70 differs from VL55 only in terms of one chemical compound and pH, this slight variation in culture environment can selectively enrich different bacterial species (Schoenborn et al., 2004; Sait et al., 2002). The pH can play a crucial part in bacterial growth, and the specific composition of pH and chemical might have enriched the bacteria that were not only able to produce IAA and solubilise phosphate but were also better suited for interacting with plant roots. This finding is consistent with research indicating that even slight alterations in the culture environment can substantially influence the composition and functional potential of bacterial communities (Steinrücken et al., 2023).

The varied effects observed among the isolates highlight the complex nature of plant-microbe interactions. Functions like IAA production and phosphate solubilization are important for promoting plant growth; however, they do not work in isolation. The overall impact of bacteria on plants is influenced by numerous factors, including how well bacteria can colonise the roots and modulate the plant's growth processes through signaling pathways (Compant et al., 2005; Patten and Glick, 2002; Gupta et al., 2015). The complexity implies that a bacterial isolate's ability to carry out single function of plant growth promotion does not necessarily result in a direct positive effect on plant, even in a controlled environment.

4.4.4 Co-existing effects of bacteria

WGS revealed that 14 out of the 20 isolates were pure cultures, while the remaining 6 were mixed cultures, comprising multiple bacterial taxa that could not be separated through repeated streaking on agar (Table 4.2). This persistence of co-cultures suggests potential co-existence among bacteria, where they may depend on each other for essential nutrients, signaling molecules, or environmental conditions not present when separated (Louis, 2017; Deines et al., 2020; de Vos et al., 2017).

The collective functions of co-existing bacteria may influence *Arabidopsis* growth in varying ways. Certain bacteria in co-cultures might enhance each other's beneficial traits, potentially leading to synergistic effects on plant growth (Li et al., 2022). For example, the enrichment 6B-5_bin1 (*Rhodococcus erythropolis*) and 6B-5_bin2 (*Acinetobacter pittii*) both showed positive effects on lateral root number in this study (Figure 4.7). While their individual contributions cannot be fully separated, their co-occurrence may contribute to an amplified plant growth effect.

In contrast, antagonistic interactions within mixed cultures may lead to competition for nutrients or the production of inhibitory compounds, thereby diminishing potential benefits to the plant (Frey-Klett et al., 2007). For example, the coexisting *Curtobacterium* and *Pseudoarthrobacter* (e.g.,3B-5_bin1, 3B-5_bin3) were associated with negative outcomes for plant growth (Figure 4.7). It is possible that these genera, both of which were individually linked to negative effects, may compete for limited resources when coexisting, reducing overall nutrient availability to the plant. Furthermore, the production of

secondary metabolites by one bacterium could inhibit the growth of other beneficial microbes or directly affect the plant, further intensifying the negative effects on plant growth (Koksharova and Safronov, 2022; Shapiro et al., 2011).

Among the coexisting *taxa were genera such as Rhodococcus, Cellulosimicrobium, Pseudarthrobacter, Paracoccus, Acinetobacter, and Azospirillum* (Table S4). *Rhodococcus* is known to engage in mutualistic biofilm formation with *Acinetobacter* in hydrocarbon degradation systems (Trond et al., 2015; Das et al., 2023), and *Azospirillum* has been reported to form synergistic plant-beneficial consortia with *Paracoccus* (Faridy et al., 2024). While these studies do not demonstrate strict co-dependence, they support the possibility that such bacterial interactions may underlie the persistence of co-cultures observed here.

Regarding the annotation of *Arabidopsis* growth effects on the phylogenetic tree (Figure 4.7), the mixed cultures could only be resolved bioinformatically after sequencing. The plant growth promotion experiment was conducted prior to genome classification, when each isolate was treated as a single genome, without distinguishing between pure cultures and enrichments. Therefore, the growth effects shown on the phylogenetic tree reflect the observed phenotype of the whole culture—whether pure or mixed—as originally tested. These genome names (e.g., 1B-7, R2, 3R-7) were annotated on the tree based on their original labels from the growth assay. After sequencing, we identified which genomes were pure and which were enrichments, but we retained the same names for consistency with the experimental results.

4.4.5 Limitations and future directions

This study has several limitations. Firstly, the bacteria were directly enriched from soil samples using non-selective media, which may cause a significant portion of bacteria with certain plant growth-promoting traits to be masked by others, as space on the agar was limited. This could potentially bias the experiment. Secondly, the *Arabidopsis* growth promotion assay was conducted under controlled conditions using MS medium, which will not reflect the complexity of natural soil conditions. Elements such as soil structure, nutrient availability, and environmental fluctuations in natural environments can profoundly affect the behaviour of bacterial isolates (Bevivino et al., 2014; Qiu et al.,

2020; Yu et al., 2021). Consequently, the outcomes observed in this study may vary when these bacteria are introduced under field conditions.

Thirdly, due to time constraints, this study primarily investigated two plant growth-promoting traits: the solubilisation of phosphate and the production of IAA. However, PGPB can promote plant growth through various other mechanisms, including siderophore production, nitrogen fixation, and the secretion of phytohormones other than IAA (Dobereiner, 1992; Patten and Glick, 2002; Glick, 2012; Gupta et al., 2015). The addition of these traits might give us a more comprehensive assessment of the plant growth-promoting potential of the isolated bacteria. Moreover, IAA was only tentatively identified using the Salkowski assay, which reacts with various indole-containing compounds. As such, the actual presence and concentration of bioactive IAA remain uncertain. Future studies should apply more accurate detection methods, such as liquid chromatography–mass spectrometry (LC–MS), to confirm IAA production.

Furthermore, while this study recognized the coexistence of various bacterial species within certain isolates, it did not thoroughly explore the specific interactions among these coexisting species. The precise nature of these interactions—whether they are synergistic, or reflect a form of obligate co-dependence—was suggested rather than directly observed. To gain a deeper understanding of the mechanisms driving these interactions, advanced techniques such as transcriptomic or metabolomic analyses could be employed.

In the future, instead of using non-selective media such as Vegitone, bacteria should first be isolated using selective media—such as Pikovskaya (PVK) medium (Nautiyal, 1999) to select strains that can solubilise phosphate, chrome azurol sulphonate (CAS) agar to detect siderophore-producing bacteria (Schwyn and Neilands, 1987; Arora and Verma, 2017), or Jensen's medium to select bacteria capable of N fixation (Jensen, 1942). This approach would allow for a higher yield of PGPB. To explore their potential in agricultural settings, future studies could examine the performance of these bacterial isolates under natural soil conditions. Future research should include field trials to evaluate the effectiveness of these bacteria in enhancing plant growth across different soil types, environmental conditions, and crop species. This approach will provide insights into the practical applicability of the isolated strains in real-world agricultural settings (Jiménez-Gómez et al., 2020).

A thorough evaluation of plate growth promoting traits should also be considered. This includes siderophore production, N_2 fixation, phytohormone production (other than IAA), and biocontrol (Dobereiner, 1992; Patten and Glick, 2002; Glick, 2012; Gupta et al., 2015; Abo-Elyousr et al., 2019). A more detailed evaluation of plant growth-promoting traits can offer a holistic understanding of how these bacteria interact with plants and contribute to growth promotion.

As a complementary direction, future research could explore the interactions between co-existing bacterial species in greater detail. Techniques such as co-culturing experiments, transcriptomics, and metabolomics can be conducted to uncover the specific metabolic and signalling interactions that occur among these bacteria. The knowledge gained can then be employed to develop synthetic bacterial consortia specifically designed for particular soil conditions and crop types. By selecting bacteria that demonstrate complementary plant growth-promoting traits and synergistic interactions, these consortia may provide more reliable and effective plant growth promotion compared to single-strain inoculants (Weidner et al., 2015; Blake et al., 2021; Priyanka et al., 2022). Indeed, the original aim of this work was to perform follow-up experiments, but these were not possible due to time constraints.

Chapter 5 General Discussion

This thesis investigatted plant-soil microbe interactions through three complementary aspects: (1) the impact of arbuscular mycorrhizal (AM) fungi inoculation on hyphosphere soil microbial communities, (2) the influence of root exudates—both natural and artificial—on shaping rhizpsphere soil microbiomes, and (3) the the role of culturable bacteria in promoting plant growth. These themes are interconnected and reflect key research directions in microbial ecology and sustainable agriculture. A growing body of literature highlights the importance of belowground interactions in enhancing nutrient use efficiency, promoting plant health, and reducing reliance on chemical inputs (Smith et al., 2011; Kavamura et al., 2021; Gross, 2017; Khan et al., 2023). By integrating ecological, functional, and genomic approaches, this work advances our understanding of how plants recruit and interact with microbial communities under different nutrient and inoculation regimes, offering insights that may inform a broader understanding of how microbial communities support plant performance.

Building on these three themes, the findings of this thesis provide practical insights into how specific microbial interactions influence plant–soil systems. AM fungal inoculation was shown to selectively shape hyphosphere communities, potentially enhancing nutrient uptake and altering fungal-bacterial communities. Root exudate experiments demonstrated that both compound identity and concentration play critical roles in structuring microbial communities, with artificial and natural exudates driving distinct compositional shifts. However, results from the natural exudates should be interpreted with caution, as their composition and conecnetration were not characterised. Finally, screening of culturable bacteria revealed diverse plant growth-promoting traits, including phosphate solubilisation and IAA-related activity, with several isolates positively influencing *Arabidopsis* growth under controlled conditions. Together, these results highlight context-specific microbial responses that may help guide more tailored microbial management strategies in agricultural settings.

5.1 Microbial interactions in the rhizosphere: bacteria, fungi, and root exudates

Microbial interactions in the rhizosphere—particularly among bacteria, fungi, and the chemical signals released by plant roots—are central to the functioning of soil ecosystems and crop productivity (Solomon et al., 2024). This thesis examined three complementary dimensions of these interactions in Chapter 2, Chapter 3, and Chapter 4, respectively. Together, these studies provide a broader perspective on how microbial processes operate under different ecological and experimental contexts.

The hyphosphere study (Chapter 2) revealed that inoculation with *R. irregularis* reshaped microbial communities, especially by reducing native fungal abundance and selectively enriching bacterial families such as Sphingomonadaceae, Xanthobacteraceae, Devosiaceae, and Xanthomonadaceae. These shifts were observed under both nutrient-replete and nutrient-deficient conditions, suggesting potential nutrient competition and microbial selection along hyphal network (Zhang et al., 2014; Rinaudo et al., 2010).

Root exudates further shaped the microbial communities in both a dose-dependent and composition-dependend manner (Chapter 3). Artificial exudate blends (AE, AEM, ACM) produced overlapping but distinct shifts in bacterial community structure, with MBOA addition further altering communities at a finer scale. VOCs emitted from AE-treated soils elicited distant effects, though these were not clearly dose-dependent. Natural exudates induced plant-specific community differentiation and showed greater microbial diversity than artificial blends, although limitations in compositional characterisation warrant cautious interpretation. These results support the view that root-derived compounds not only act as nutrient sources but potentially as selective agents in microbial recruitment (Dai et al., 2022).

Finally, screening culturable bacteria (Chapter 4) revealed that slow-growing microbes isolated from minimal media potentially exhibited stronger plant growth-promoting traits, such as IAA production, compared to isolates from nutrient-rich media. Functional assays in *Arabidopsis* demonstrated a wide spectrum of growth responses, from promotion to inhibition. The promotion of plant growth is not just simply through mechanisms such as phosphate solubilisation and the production of indole-3-acetic acid (IAA); instead, is a complex system that includes the production of additional metabolites, as well as their ability to efficiently colonise the plants (Compant et al., 2005). Notably, genome sequencing revealed that several isolates were in fact co-cultures or enrichments, suggesting metabolic interdependence or synergistic interactions that are

difficult to separate using conventional culturing, which remains an area worth studying (Louis, 2017; Li et al., 2022).

These findings reveals that microbial dynamics in the rhizosphere are shaped by both biotic factors (e.g., AM fungi, bacterial inocula) and plant-derived compounds. AM fungi and bacteria do not act in isolation; rather, their effects are mediated through root inputs and microbial competition (Hodge and Fitter, 2013). Taken together, Chapter 2, Chapter 3, and Chapter 4 integrate different aspects of beneficial microbial interations, providing a better understanding of how different aspects of interactions can influence the belowground dynamics.

5.2 Microbial Consortia

The findings from this thesis collectively highlight the potential of building microbial consortia—combinations of two or more microbial species, such as bacteria, fungi, or other microorganisms, that live and function together in a shared environment (Duncker et al., 2021). While this thesis did not construct consortia directly, the distinct roles of AM fungi, root exudates, and culturable bacteria explored across Chapters 2 to 4 provide foundational insights into how such consortia might be assembled and optimised in future applications.

Studies on AM fungus *R. irregularis*, root exudates, and PGPB presents future opportunities to integrate the bacteria and AM fungi into effective consortia. For instance, AM fungi can serve as a central component by facilitating nutrient uptake, while root exudates shape the surrounding soil community to benefit the PGPB. PGPB such as *Streptomyces* and *Mesorhizobium* can be added to create a synergistic system that promotes plant growth and health.

Microbial consortia offer a feasible solution for reducing chemical fertiliser use while sustainably boosting crop productivity. Future studies could focus on designing and adapting these consortia for different crops, such as rice, sorghum and potato, which represent distinct plant functional types (monocots and dicots), diverse root architectures, and varying agricultural systems across both temperate and tropical regions. Additionally, future studies could evaluate microbial consortia under more realistic conditions, including soil microcosms or greenhouse trials, to begin bridging the gap between

controlled experiments and field applications. This intermediate step is essential for assessing the consistency and robustness of microbial interactions across different soils and plant hosts before moving toward full-scale implementation.

5.3 Microbial community network modelling: towards precision agriculture

Building on the work presented here, there is potential to use insights from rhizosphere microbial interactions—including those involving AM fungi, root exudates, and PGPB—to inform future computational models of microbial community dynamics. Although such modelling was beyond the scope of this thesis, the observed interactions highlight the complexity and interconnectedness of the rhizosphere system, where microbial taxa influence one another and collectively contribute to plant growth (Srinivasan et al., 2024).

Simulating these microbial networks can provide valuable insights into plant-microbe interactions under different environment conditions. By integrating experiment data into computational models, it becomes possible to predict the precise effects of microbes on plant growth promotion, nutrient cycling, and pathogen control.

Moreover, such models could be used to quickly tailor microbial consortia to specific soil types, crops, and weather conditions, optimizing microbial communities for precision agriculture. This approach holds the potential to enhance crop productivity and sustainability by fine-tuning microbial interactions for different agricultural contexts.

Future studies should focus on refining the data of microbial community networks by conducting field experiments in various environmental conditions. Additionally, the integration of multi-omics data, such as metagenomics, transcriptomics, and metabolomics into these computational models could potentially enhance their predictive power(Aguiar-Pulido et al., 2016). This would enable a more comprehensive understanding of microbial interactions and their effects on plant performance, further ensuring the reliability and adaptability of the models for real-world agricultural systems. By continuously refining computational models, agricultural practices can move toward a more sustainable, precision-based approach.

5.4 Concluding remarks

This thesis highlights the vital role of microbial communities in enhancing plant growth and contributing to indicators of soil health, particularly through their influence on microbial diversity, community structure, and functional potential. Although direct measures of soil health (e.g., enzymatic activity, respiration) were not assessed, the observed shifts in microbial composition—such as reduced native fungi following AM fungal inoculation (Chapter 2) and increased diversity in response to plant-specific root exudates (Chapter 3)—suggest ecological outcomes that can influence nutrient dynamics and plant resilience.

By studying the dynamic interactions among bacteria, fungi, and plants under controlled experimental conditions, this work provides insight into how targeted microbial recruitment (e.g., through AM fungi, exudate application, or bacterial inoculation) may shift microbial assemblies toward communities associated with beneficial traits.

The findings also support the development of bio-fertilisers composed of AM fungi and PGPB. For example, the culturable bacteria screened in Chapter 4 exhibited traits such as phosphate solubilisation and potential IAA production and influenced *Arabidopsis* growth in ways that may support higher yields. While field-scale effects and long-term environmental impacts were beyond the scope of this thesis, these results establish a foundational understanding of the microbial processes that underpin such applications. Together, they suggest that tailored microbial inputs could reduce reliance on chemical fertilisers and support more sustainable agricultural practices.

Appendix

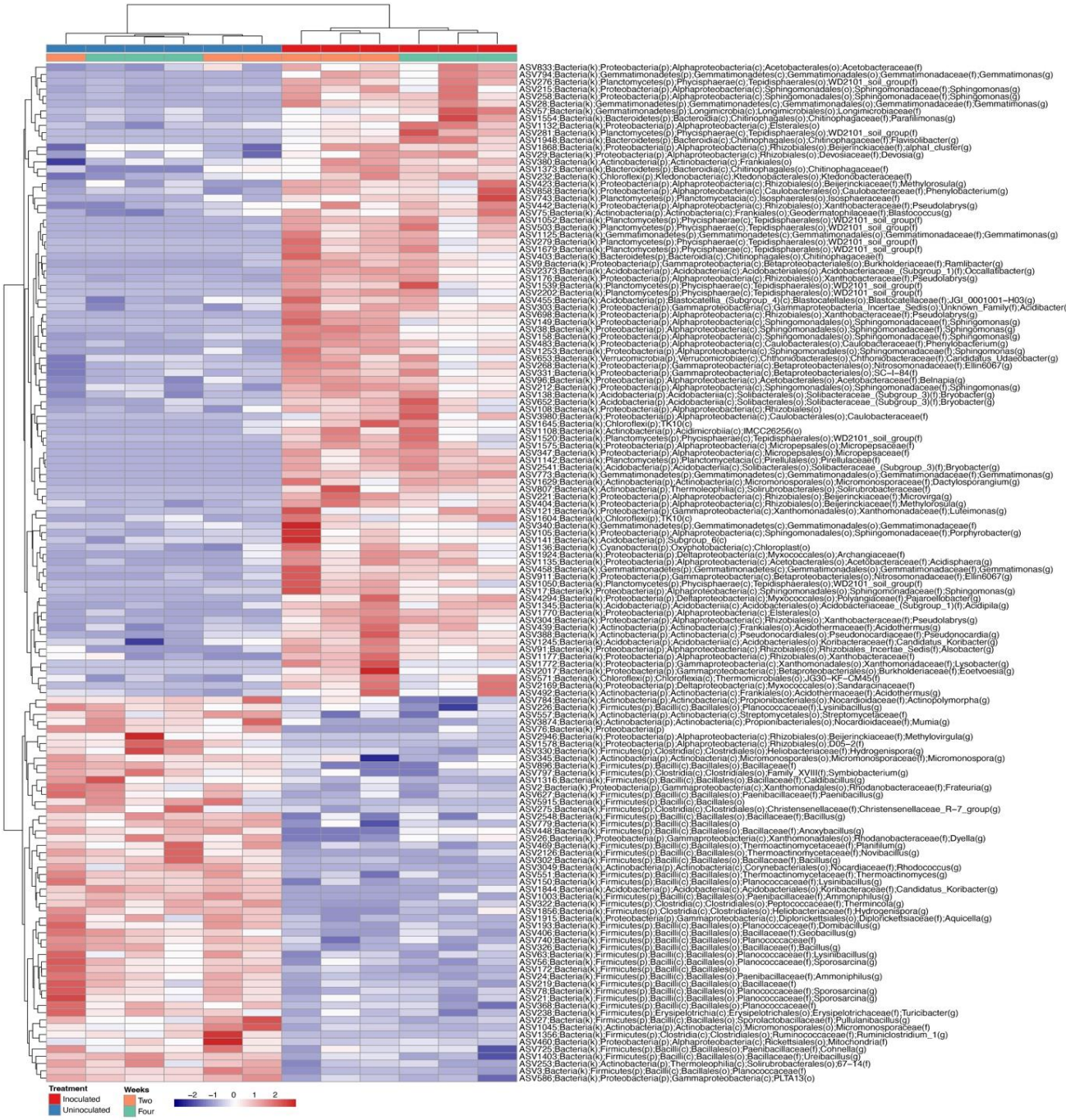

Figure S 1 Complete heatmap showing the relative abundance of ASVs (16S with P addition), selected by indicator species analysis ($p < 0.05$). Samples and ASVs are clustered by Manhattan distance. Cell colours represent row-normalised z-scores (–2 to 2), where 0 is the mean abundance across samples. Positive values indicate higher-than-average abundance; negative values indicate lower.The taxonomy of each ASV is labelled to the lowest level that could be obtained during the classification. Abbreviations indicate: k=kingdom, p=phylum, c=class, o=order, f=family, g=genus.

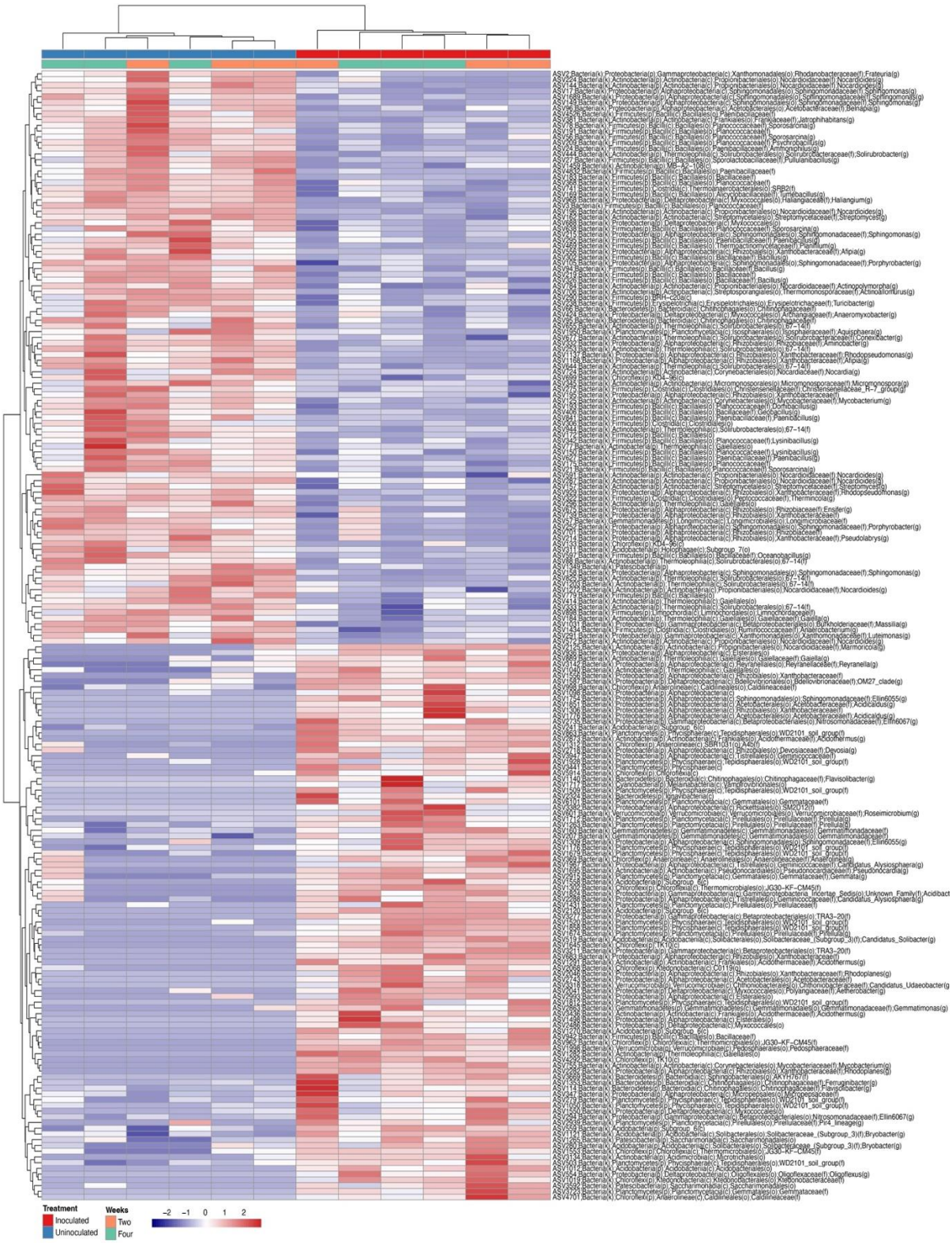

Figure S 2 Complete heatmap showing the relative abundance of ASVs (16S without P addition), selected by indicator species analysis ($p < 0.05$). Samples and ASVs are clustered by Manhattan distance. Cell colours represent row-normalised z-scores (–2 to 2), where 0 is the mean abundance across samples. Positive values indicate higher-than-average abundance; negative values indicate lower.The taxonomy of each ASV is labelled to the lowest level that could be obtained during the classification. Abbreviations indicate: k=kingdom, p=phylum, c=class, o=order, f=family, g=genus.

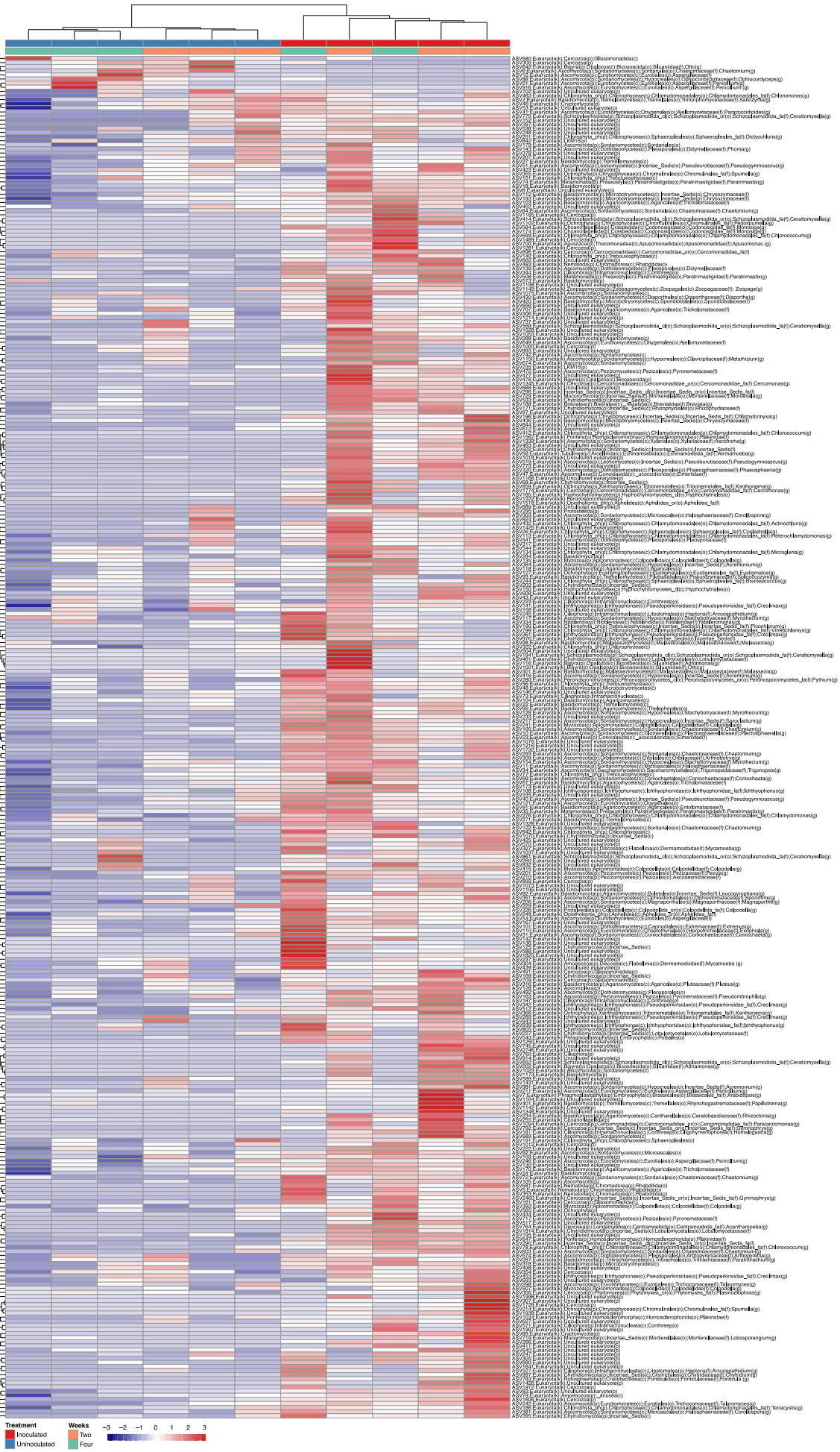
Treatment
Inoculated
Uninoculated
Weeks
Two
Four
−3 −2 −1 0 1 2 3

Figure S 3 Complete heatmap showing the relative abundance of ASVs (18S with P addition), selected by indicator species analysis ($p < 0.05$). Samples and ASVs are clustered by Manhattan distance. Cell colours represent row-normalised z-scores (–3 to 3), where 0 is the mean abundance across samples. Positive values indicate higher-than-average abundance;negative values indicate lower.The taxonomy of each ASV is labelled to the lowest level that could be obtained during the classification. Abbreviations indicate: k=kingdom, p=phylum, c=class, o=order, f=family, g=genus. Note: One inoculated P+ sample was excluded from the 18S analysis due to low read count and missing ASVs, suggesting sequencing failure.

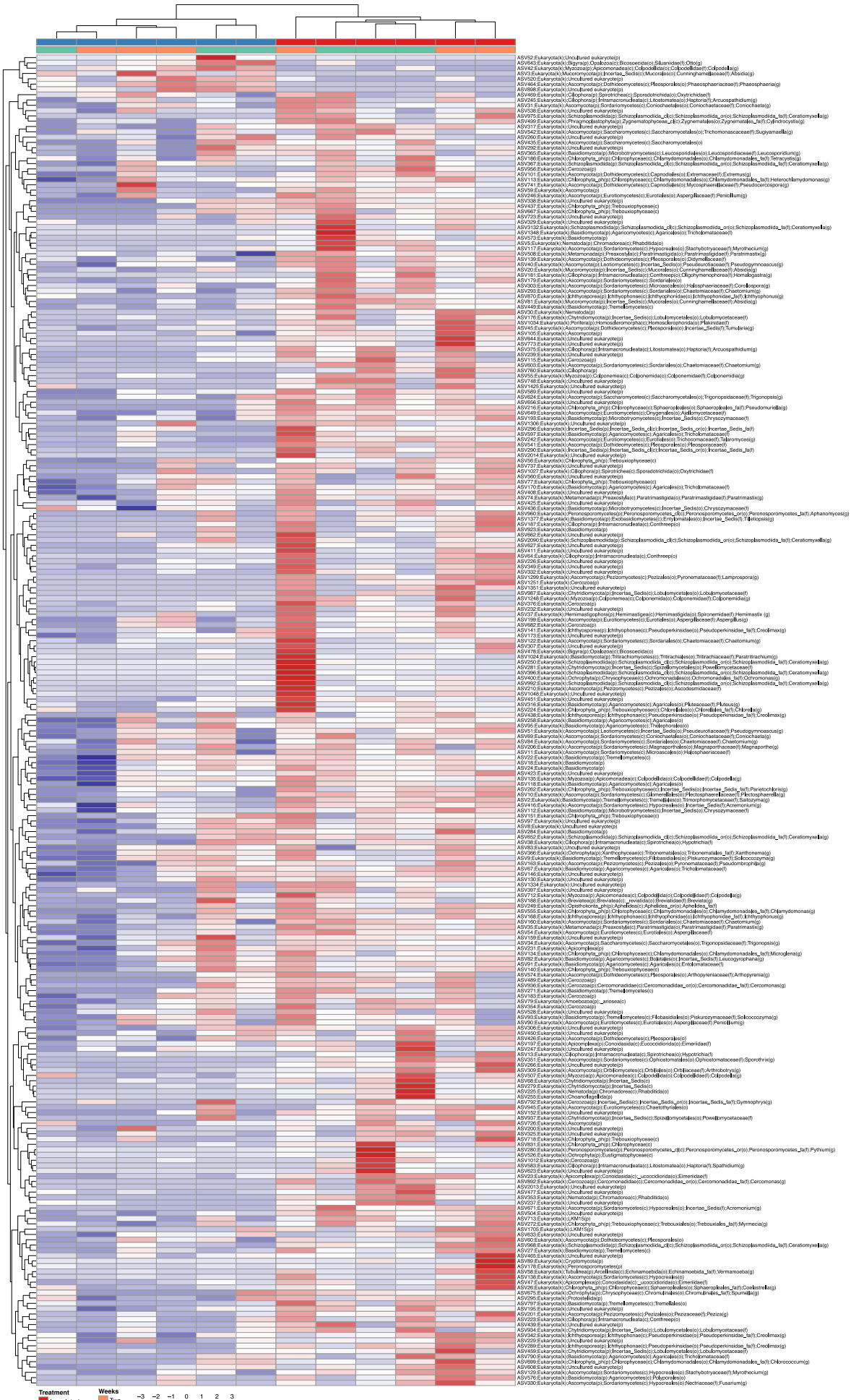
Treatment
Inoculated
Uninoculated
Weeks
Two
Four
−3 −2 −1 0 1 2 3

Figure S 4 Complete heatmap showing the relative abundance of ASVs (18S without P addition), selected by indicator species analysis ($p < 0.05$). Samples and ASVs are clustered by Manhattan distance. Cell colours represent row-normalised z-scores (–3 to 3), where 0 is the mean abundance across samples. Positive values indicate higher-than-average abundance; negative values indicate lower.The taxonomy of each ASV is labelled to the lowest level that could be obtained during the classification. Abbreviations indicate: k=kingdom, p=phylum, c=class, o=order, f=family, g=genus.

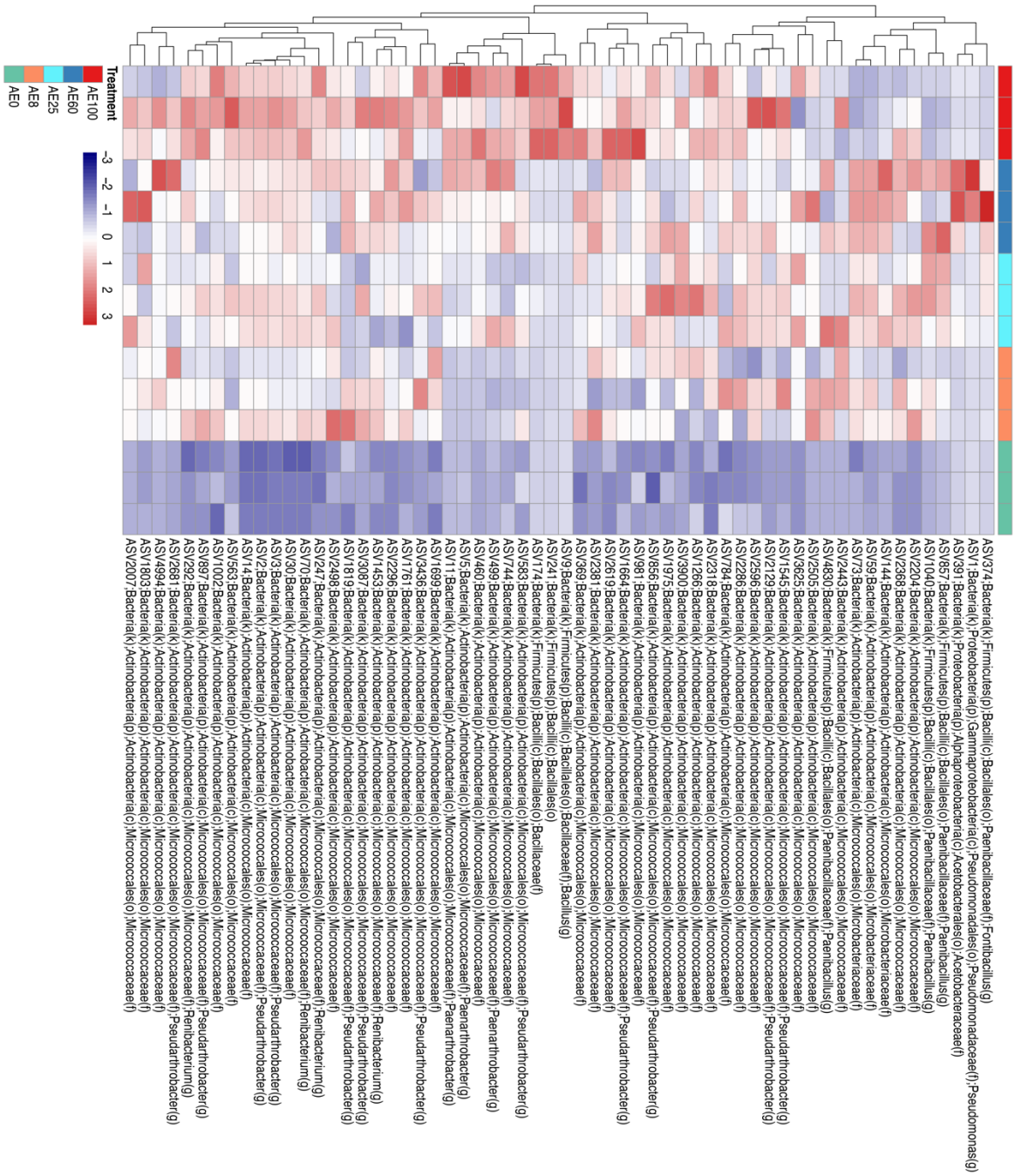

Figure S5 Complete heatmap showing the relative abundance of ASVs across samples treated with artificial exudtes (AE), selected by indicator species analysis ($p < 0.01$), comparing all AE treatments combined against the AE0 control. The ASVs shown were identified as indicators in the combined comparison and are present across all AE samples (excluding AE0), though their relative abundances vary between treatments. Rows (ASVs) are clustered by Manhattan distance. Cell colours represent row-normalised z-scores (–3 to 3), where 0 is the mean abundance across samples. Positive values indicate higher-than-average abundance; negative values indicate lower. The top sidebar indicates different treatment concentrations. Abbreviations indicate: k=kingdom,p=phylum, c=class, o=order, f=family, g=genus.

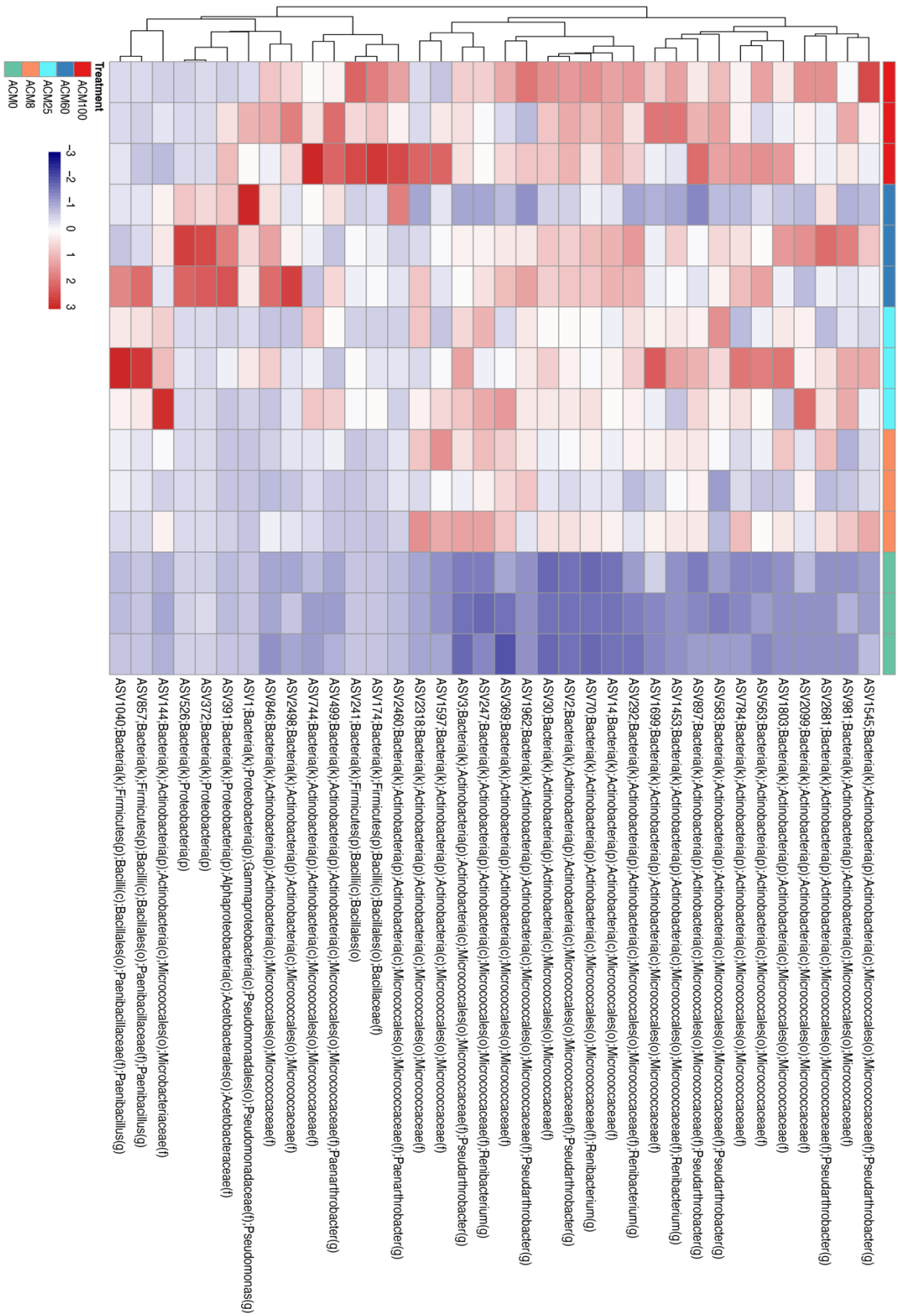

Figure S6 Complete heatmap showing the relative abundance of ASVs across samples treated with artificial exudates (ACM), selected by indicator species analysis ($p < 0.01$), comparing all

ACM treatments combined against the ACM0 control. The ASVs shown were identified as indicators in the combined comparison and are present across all ACM samples (excluding ACM0), though their relative abundances vary between treatments. Rows (ASVs) are clustered by Manhattan distance. Cell colours represent row-normalised z-scores (–3 to 3), where 0 is the mean abundance across samples. Positive values indicate higher-than-average abundance; negative values indicate lower. The top sidebar indicates different treatment concentrations. Abbreviations indicate: k=kingdom,p=phylum, c=class, o=order, f=family, g=genus.

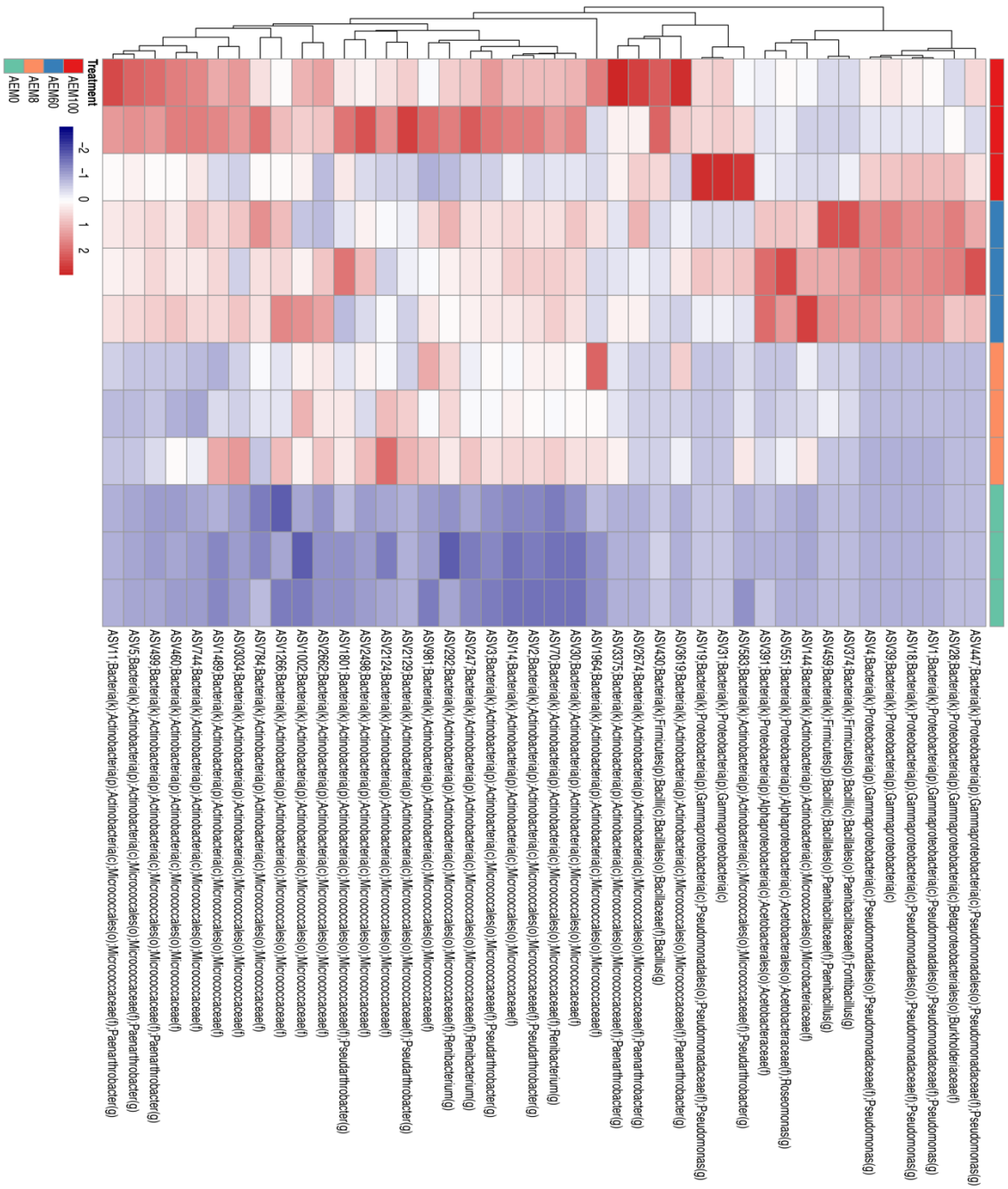

Figure S7 Complete heatmap showing the relative abundance of ASVs across samples treated with artificial exudates (AEM), selected by indicator species analysis ($p < 0.01$), comparing all AEM treatments combined against the AEM0 control. The ASVs shown were identified as indicators in the combined comparison and are present across all AEM samples (excluding AEM0), though their relative abundances vary between treatments. Rows (ASVs) are clustered by Manhattan distance. Cell colours represent row-normalised z-scores (–2 to 2), where 0 is the mean abundance across samples. Positive values indicate higher-than-average abundance; negative values indicate lower. The top sidebar indicates different treatment concentrations. Abbreviations indicate: k=kingdom, p=phylum, c=class, o=order, f=family, g=genus.

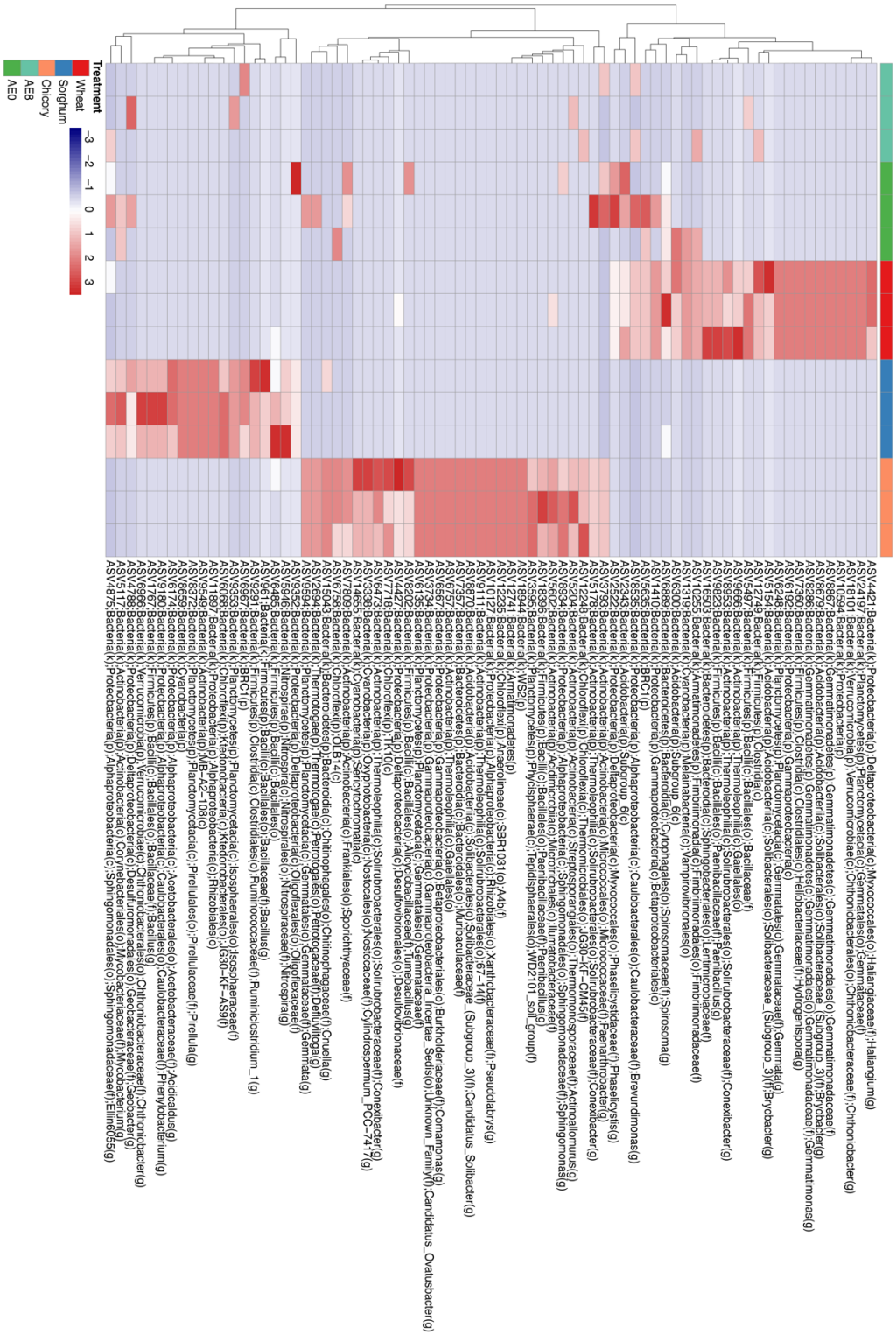

Figure S8 Complete heatmap showing the relative abundance of ASVs across samples treated with natural root exudates from wheat, sorghum, and chicory. ASVs were selected by indicator species analysis ($p < 0.05$), using the three natural exudate treatments as distinct groups to identify ASVs significantly associated with each plant type. The heatmap also includes their relative abundance in AE0 and AE8 for reference. Rows (ASVs) are clustered by Manhattan distance. Cell colours represent row-normalised z-scores (–3 to 3), where 0 is the mean abun-

dance across samples. Positive values indicate higher-than-average abundance; negative values indicate lower. The top sidebar indicates different treatment concentrations and natural exudate types. Abbreviations indicate: k=kingdom, p=phylum, c=class, o=order, f=family, g=genus.

Figure S 9 Complete heatmap showing the relative abundance of ASVs across samples treated with natural exudates, selected by indicator species analysis ($p < 0.01$), comparing all natural exudate treatments combined against the AE0 control. The ASVs shown were identified as indicators in the combined comparison and are present across all wheat, sorghum, and chicory samples, though their relative abundances vary between treatments. Rows (ASVs) are clustered by Manhattan distance. Cell colours represent row-normalised z-scores (–3 to 3), where 0 is the mean abundance across samples. Positive values indicate higher-than-average abundance; negative values indicate lower. Abbreviations indicate: k=kingdom, p=phylum, c=class, o=order, f=family, g=genus.

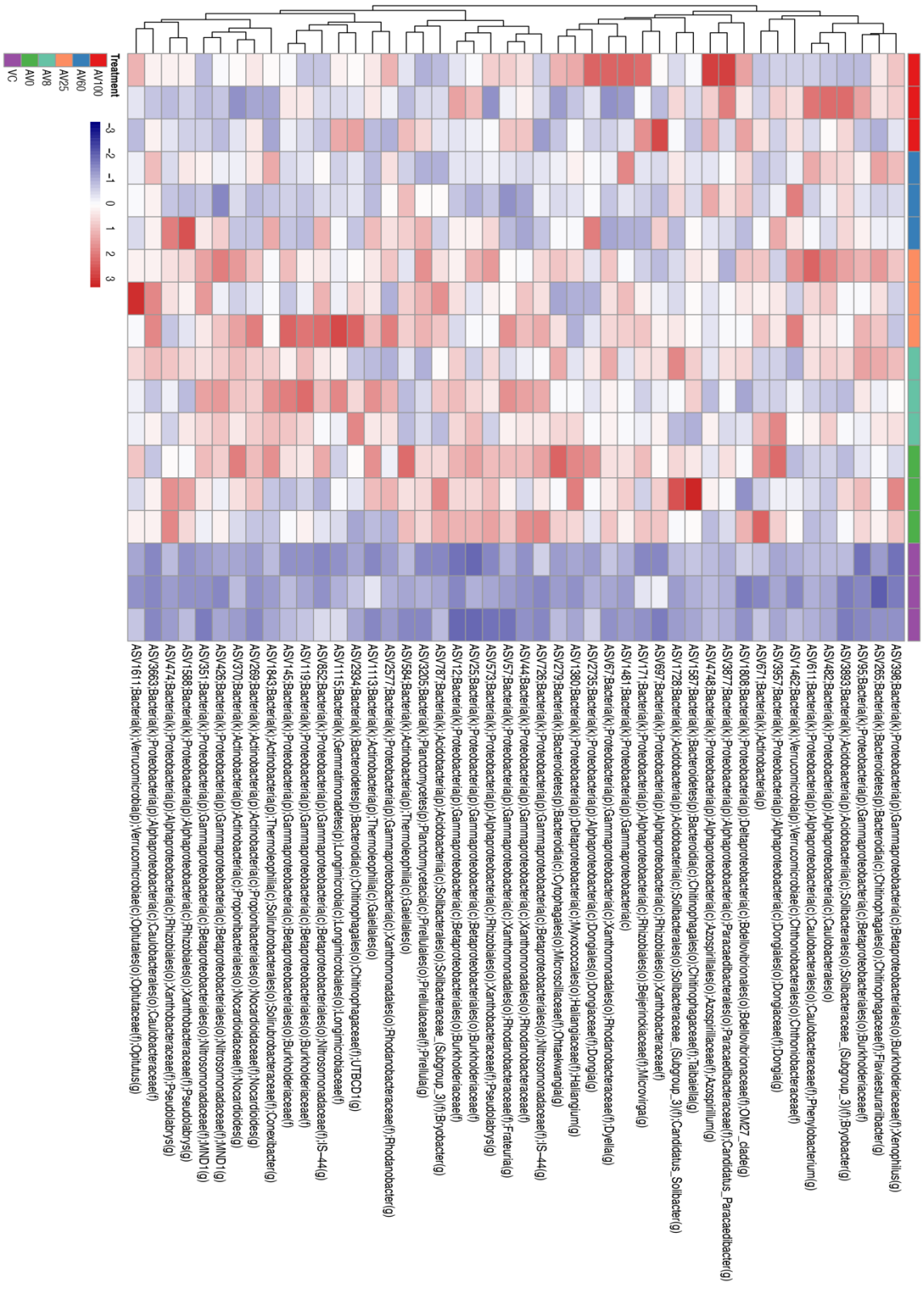

Figure S10. Complete heatmap showing the relative abundance of ASVs across recipient soil samples exposed to volatiles produced by soils treated with different concentrations of AE. ASVs were selected by indicator species analysis ($p < 0.01$), comparing all AV treatments combined against the VC control. The ASVs shown were identified as indicators in the combined

comparison and are present across all AV samples (excluding VC), though their relative abundances vary between treatments. VC is the control with no volatiles produced. Rows (ASVs) are clustered by Manhattan distance. Cell colours represent row-normalised z-scores (–3 to 3), where 0 is the mean abundance across samples. Positive values indicate higher-than-average abundance; negative values indicate lower. The top sidebar indicates the concentration used to treat the volatile-producing soil. Abbreviations indicate: k=kingdom, p=phylum, c=class, o=order, f=family, g=genus.

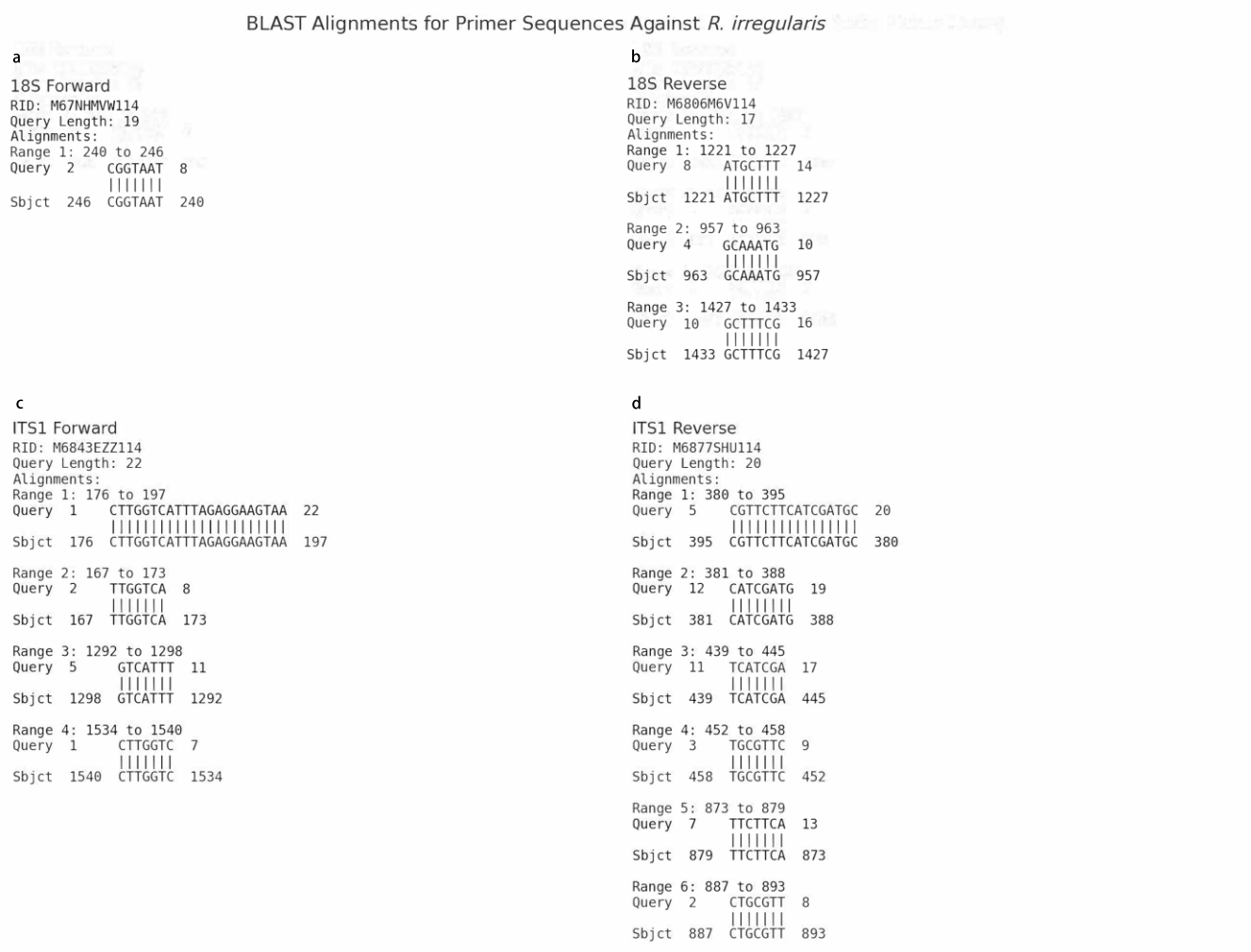

Figure S 11 BLAST alignments of primer sequences against *Rhizophagus irregularis* (isolate Att690-23 (DAOM197198); GenBank: FM992377.1). Primer sequences (queries) were aligned against the *R. irregularis* 18S/ITS reference sequence (subject) to assess alignment specificity. Panels show matches for each primer used in 18S and ITS amplicon sequencing: (a) 18S forward primer; (b) 18S reverse primer; (c) ITS1 forward primer; (d) ITS1 reverse primer. Bars indicate alignment positions along the *R. irregularis* reference sequence.

Table S1 Summary of isolates from Vegitone agar. B, C, R: locations of the soil from where the bacteria were isolated.

Bacteria code	Dilution factor	Name (by bacterial appearance)
B1a	10^-4	White colony
B1b	10^-4	Yellow colony
B2	10^-4	White colony-brownish inside
B3	10^-5	Breaking edge colonies
C1	10^-5	Small white colony
C2	10^-6	Small red colony
C3	10^-7	Edge bacteria
R1	10^-5	Small yellow colony
R2	10^-6	Light brown colony
R3a	10^-6	River bacteria
R3b	10^-6	River stones
R4a	10^-7	Dark yellow colony
R4b	10^-7	Cloudy white colony
R5	10^-7	Large white net

Table S2 Summary of isolates from VL55 agar. B, C, R: Locations of the soil from where the bacteria were isolated.

Bacteria code	Dilution factor	Name (by bacterial appearance)
1B-5	10^-4	Yellow colony
2B-5a	10^-4	Transparent white colony
2B-5b	10^-4	Solid white colony
3B-5	10^-4	Grey colony
4B-5	10^-4	Large branch (redone)
5B-5	10^-4	Oreo colony
6B-5	10^-4	Small brown-red colony
7B-5	10^-5	Solid brown colony
8B-5	10^-5	Liquid yellow colony
9B-5	10^-5	Oreo net
10B-5	10^-5	Fuzzy white colony
11B-5	10^-5	Oreo spiral
12B-5	10^-6	Solid yellow colony
1C-5	10^-4	Broken oreo colony
2C-5	10^-5	Covid oreo colony
3C-5	10^-5	Pale orange colony
4C-5	10^-5	Crater colony

Bacteria code	Dilution factor	Name (by bacterial appearance)
1R-5	10^-4	White colony
2R-5	10^-4	Brown colony
3R-5	10^-4	Clear liquid colony
4R-5	10^-4	Dark brown colony
5R-5	10^-4	Breaking brown colony
6R-5	10^-5	Mould oreo colony
7R-5	10^-5	Light orange colony
8R-5	10^-5	Light yellow colony
9R-5	10^-5	Cloudy colony
10R-5	10^-7	White colony

Table S3 Summary of isolates from VL70 agar. B, C, R: Locations of the soil from where the bacteria were isolated.

Bacteria code	Dilution Factor	Name (by bacterial appearance)
1B-7	10^-4	Liquid colony
2B-7	10^-4	White center colony
3B-7	10^-4	Dark white colony
4B-7	10^-5	Small brown colony
5B-7	10^-5	Liquid yellow dots
6B-7	10^-5	Orange colony
7B-7	10^-5	Yellow-brown colony
8B-7	10^-5	White breaking edge colony
9B-7	10^-6	Brown colony
10B-7	10^-6	Dark bloody colony
11B-7	10^-7	White star colony
12B-7	10^-7	Liquid white colony
13B-7	10^-7	Pink colony
1C-7	10^-4	Feather colony
2C-7	10^-5	Jellyfish colony
3C-7	10^-5	Pink jellyfish colony
4C-7	10^-5	Very light brown colony

Bacteria code	Dilution Factor	Name (by bacterial appearance)
5C-7	10^-6	Light brown breaking edge
6C-7	10^-7	Small white colony
1R-7	10^-4	White colony
2R-7	10^-4	Yellow middle colony
3R-7	10^-4	Light pink colony
4R-7	10^-4	Breaking edge colony
5R-7	10^-4	Yellow colony
6R-7	10^-5	Cloudy yellow colony
7R-7	10^-5	Red colony
8R-7	10^-5	Yellow with dark middle
9R-7	10^-5	Transparent breaking edge
10R-7	10^-7	White colony

Table S4 Summary of genome sequencing results.

Genome	Taxonomy	Complete%	Contamin%	Contig no.	Genome (bp)	N50	G+C%	CDS
1B-5	*Rhodococcus erythropolis*	99.9%	2.17%	100	7032660	619317	62%	7068
1B-7_bin1	*Azospirillum* sp. 003116065	100.0%	4.17%	80	7302453	200147	67%	6814
1B-7_bin2	*Paracoccus yeei*	88.7%	0.98%	305	3956367	16483	68%	4291
2B-5b	*Acinetobacter pittii*	100.0%	0.19%	62	4132565	208149	39%	4000
2B-7	*Streptomyces*	99.9%	0.48%	279	11696974	128441	70%	10796
2R-5	*Streptomyces*	100.0%	1.63%	212	9882550	199061	71%	9251
3B-5_bin1	*Pseudarthrobacter*	99.7%	0.00%	19	4240142	391695	66%	3960
3B-5_bin2	*Azospirillum* sp. 003116065	99.0%	3.87%	210	7202344	62671	67%	6832
3B-5_bin3	*Curtobacterium*	99.0%	1.11%	44	3756313	162415	71%	3670
3B-7	*Streptomyces*	100.0%	2.31%	234	10466205	215414	69%	10510
3R-7_bin1	*Microbacterium* sp. 002456035	96.6%	1.01%	204	3076506	21929	71%	3160
3R-7_bin2	*Cellulosimicrobium funkei*	99.4%	0.96%	25	4345164	209534	75%	3925
5R-5	*Streptomyces*	100.0%	0.89%	157	9718816	229282	69%	9496
5R-7	*Mesorhizobium*	99.5%	1.06%	40	7212304	424320	62%	7264
6B-5_bin2	*Acinetobacter pittii*	100.0%	0.00%	28	3831264	208001	39%	3642
6B-5_bin1	*Rhodococcus erythropolis*	99.7%	0.93%	72	6413756	145745	62%	6225
7R-5	*Mesorhizobium*	99.5%	0.82%	26	5968260	462888	63%	5988
8R-5	*Priestia megaterium*	99.4%	0.67%	36	5613152	973334	38%	6037
9B-5	*Streptomyces*	100.0%	3.63%	381	10557037	240317	69%	10469
9R-5_bin1	*Pseudarthrobacter*	99.7%	0.10%	23	4773603	403751	66%	4406
C3	*Bacillus licheniformis*	98.9%	0.00%	24	4309614	314340	46%	4760
R1	*Staphylococcus hominis*	99.5%	1.29%	45	2219541	584991	32%	2211
R2_bin1	*Pseudarthrobacter*	99.7%	0.00%	12	4246888	938208	66%	3962
R2_bin2	*Bacillus licheniformis*	98.9%	0.00%	22	4291428	289881	46%	4754
R2_bin3	*Curtobacterium*	97.5%	1.78%	67	3672007	91994	71%	3587
R2_bin4	*Cellulosimicrobium*	14.0%	0.00%	45	602865	13458	73%	538
R3a	*Bacillus licheniformis*	98.9%	0.00%	20	4311893	661041	46%	4783
R3b	*Bacillus licheniformis*	98.9%	0.00%	18	4311073	661041	46%	4773

Table S 5 Bacterial families significantly enriched in inoculated samples under P+ conditions based on Chi-square tests (*df* = 1 for all). Families are grouped by phylum. Overlapping families between P+ and P- conditions are highlighted in yellow.

Phylum	Family	χ^2	p-value
Acidobacteria	Solibacteraceae_(Subgroup_3)	58.98	<0.0001
Actinobacteria	Acidothermaceae	102.4	<0.0001
	Geodermatophilaceae	110.3	<0.0001
	Pseudonocardiaceae	110.0	<0.0001
Bacteroidetes	Chitinophagaceae	25.48	<0.0001
Gemmatimonadetes	Gemmatimonadaceae	670.9	<0.0001
Planctomycetes	WD2101_soil_group	532.3	<0.0001
Proteobacteria	Beijerinckiaceae	174.8	<0.0001
	Caulobacteraceae	254.3	<0.0001
	Devosiaceae	268.4	<0.0001
	Nitrosomonadaceae	203.0	<0.0001
	Sphingomonadaceae	5606.0	<0.0001
	Xanthobacteraceae	220.0	<0.0001
	Xanthomonadaceae	491.2	<0.0001

Table S 6 Bacterial families significantly enriched in inoculated samples under P- conditions based on Chi-square tests (df = 1 for all). Families are grouped by phylum. Overlapping families between P+ and P- conditions are highlighted in yellow.

Phylum	Family	χ^2	p-value
Acidobacteria	Solibacteraceae_(Subgroup_3)	62.15	<0.0001
Actinobacteria	Acidothermaceae	33.08	<0.0001
Bacteroidetes	Chitinophagaceae	253.9	<0.0001
Chloroflexi	Caldilineaceae	67.53	<0.0001
	JG30-KF-CM45	60.40	<0.0001
Gemmatimonadetes	Gemmatimonadaceae	105.7	<0.0001
Planctomycetes	Pirellulaceae	118.8	<0.0001
	WD2101_soil_group	413.7	<0.0001
Proteobacteria	Acetobacteraceae	49.17	<0.0001
	Geminicoccaceae	42.43	<0.0001
	Micropepsaceae	128.6	<0.0001
	Nitrosomonadaceae	134.7	<0.0001
	TRA3-20	49.23	<0.0001
Verrucomicrobia	Pedosphaeraceae	7.921	0.0049
	Verrucomicrobiaceae	359.7	<0.0001

Table S 7 Bacterial families significantly enriched in AE-treated samples at different concentrations (AE100, AE60, AE25, and AE8), based on Chi-square tests (df = 1 for all). Families are grouped by phylum. All enrichments shown are significant at $p < 0.0001$. Numbers in each cell represent Chi-square (χ^2) values.

Phylum	Family	AE100	AE60	AE25	AE8
Actinobacteria	Microbacteriaceae	151.3	716.3	1068	880.9
Actinobacteria	Micrococcaceae	20533	13683	26040	24584
Firmicutes	Bacillaceae	–	–	26.9	–
Proteobacteria	Acetobacteraceae	–	55.6	–	–

Table S 8 Bacterial families significantly enriched in ACM-treated samples at different concentrations (ACM100, ACM60, ACM25, and ACM8), based on Chi-square tests (df = 1 for all). Families are grouped by phylum. All enrichments shown are significant at $p < 0.0001$. Numbers in each cell represent Chi-square (χ^2) values.

Phylum	Family	ACM100	ACM60	ACM25	ACM8
Actinobacteria	Micrococcaceae	9820	5517	15029	21546
Firmicutes	Bacillaceae	–	–	24.25	–
Proteobacteria	Acetobacteraceae	40.14	106	–	–
Proteobacteria	Pseudomonadaceae	–	–	418.8	–

Table S 9 Bacterial families significantly enriched in AEM -treated samples at different concentrations (AEM100, AEM60, and AEM8), based on Chi-square tests (df = 1 for all). Families are grouped by phylum. All enrichments shown are significant at $p < 0.0001$ unless otherwise specified. Numbers in each cell represent Chi-square (χ^2) values.

Phylum	Family	AEM100	AEM60	AEM8
Actinobacteria	Micrococcaceae	7007	1359	24391
Proteobacteria	Acetobacteraceae	5.899 (p=0.0151)	3.869 (p=0.0492)	4.979 (p=0.0257)
Proteobacteria	Pseudomonadaceae	1385	2211	776.1

Table S 10 Bacterial families significantly enriched in samples treated with natural exudates (wheat, sorghum, and chicory), grouped together during indicator species analysis and compared against the AE0 control. Families are grouped by phylum. All enrichments shown are significant at $p < 0.0001$ based on Chi-square tests (df = 1). Numbers in each cell represent Chi-square (χ^2) values.

Phylum	Family	Wheat	Sorghum	Chicory
Actinobacteria	Microbacteriaceae	376.7	518.9	505.8
Actinobacteria	Micrococcaceae	2681	3939	3708
Firmicutes	Alicyclobacillaceae	327.5	758.6	456.1
Firmicutes	Bacillaceae	242.5	183.4	272.2
Firmicutes	Planococcaceae	5982	3828	3759
Proteobacteria	Devosiaceae	64.63	16.37	82.22
Proteobacteria	Rhizobiaceae	37.95	–	28.91
Proteobacteria	Rhodanobacteraceae	67.23	19.62	94.78

Table S 11 Bacterial families significantly enriched in samples treated with natural exudates (wheat, sorghum, or chicory), identified by indicator species analysis, where the three exudate treatments were analysed as distinct groups. Families are grouped by phylum. Numbers in each cell represent Chi-square (χ^2) values; corresponding p values are shown in parentheses. All Chi-square tests had df = 1.

Phylum	Family	Wheat	Sorghum	Chicory
Acidobacteria	Solibacteraceae_(Subgroup_3)	5.691 (p=0.0171)	–	–
Actinobacteria	Solirubrobacteraceae	6.178 (p=0.0129)	–	–
Actinobacteria	Mycobacteriaceae	–	4.092 (p=0.0431)	–
Actinobacteria	Sporichthyaceae	–	–	5.097 (p=0.024)
Actinobacteria	Ilumatobacteraceae	–	–	7.192 (p=0.0073)
Bacteroidetes	Spirosomaceae	13.87 (p=0.0002)	–	–
Chloroflexi	JG30-KF-CM45	–	–	4.062 (p=0.0439)
Cyanobacteria	Nostocaceae	–	–	4.062 (p=0.0439)
Planctomycetes	Gemmataceae	6.178 (p=0.0129)	–	–
Proteobacteria	Haliangiaceae	5.123 (p=0.0236)	–	–
Proteobacteria	Acetobacteraceae	–	5.145 (p=0.0233)	–
Proteobacteria	Geobacteraceae	–	4.092 (p=0.0431)	–
Proteobacteria	Desulfovibrionaceae	–	–	13.68 (p=0.0002)

Table S 12 Bacterial families significantly enriched in samples exposed to volatile organic compounds (VOCs) from AE-treated soils at five concentrations (AV100, AV60, AV25, AV8, and AV0), based on Chi-square tests (df = 1 for all). Families are grouped by phylum. All enrichments shown are significant at $p < 0.0001$ unless otherwise specified. Numbers in each cell represent Chi-square (χ^2) values.

Phylum	Family	AV100	AV60	AV25	AV8	AV0
Actinobacteria	Nocardioidaceae	30.87	–	–	–	–
Actinobacteria	Solirubrobacteraceae	–	5.245 (p=0.022)	–	6.580 (p=0.0103)	–
Bacteroidetes	Microscillaceae	62.49	52.81	29.48	45.02	57.22
Proteobacteria	Beijerinckiaceae	6.859 (p=0.0088)	–	–	–	–
Proteobacteria	Burkholderiaceae	4952	4548	6271	7442	7336
Proteobacteria	Dongiaceae	12.48 (p=0.0004)	16.16	7.123 (p=0.0076)	9.010 (p=0.0027)	18.97
Proteobacteria	Nitrosomonadaceae	147.1	215.4	292.1	265.9	212.9
Proteobacteria	Rhodanobacteraceae	529.1	280.3	547.0	522.0	562.4
Proteobacteria	Xanthobacteraceae	87.52	104.4	92.28	84.42	127.2

Table S 13 Pairwise comparison of Average Nucleotide Identity (ANI) values between closely related bacterial isolates. ANI values $\geq$99.99% suggest that the isolates are likely the same strain.

Bacteria pair	ANI estimate
6B-5_bin1 and 1B-5	99.99%
R2_bin4 and 3R-7_bin2	99.91%
R2_bin1 and 3B-5_bin1	99.99%
R2_bin3 and 3B-5_bin3	99.97%
3B-7 and 9B-5	99.42%
R2_bin2 and C3	99.99%
R3a and R3b	99.99%
6B-5_bin2 and 2B-5b	99.99%
1B-7_bin1 and 3B-5_bin2	99.98%

Table S 14 Presence of IAA biosynthesis-related genes across selected bacterial genomes. Presence of the gene is indicated by "Y".

Genome	Taxonomy	Indole-3-pyruvate decarboxylase (*ipdC*)	Indole-3-acetaldehyde dehydrogenase (*dhaS*)	Nitrilase (*nit*)
1B-5	*Rhodococcus erythropolis*			
2B-5b	*Acinetobacter pittii*	Y		Y
6B-5_bin2	*Acinetobacter pittii*	Y		Y
6B-5_bin1	*Rhodococcus erythropolis*			
9B-5	*Streptomyces*			Y
2R-5	*Streptomyces*			
5R-5	*Streptomyces*			Y
7R-5	*Mesorhizobium*			Y
1B-7_bin2	*Paracoccus yeei*			
1B-7_bin1	*Azospirillum sp. 003116065*			
2B-7	*Streptomyces*			
3B-7	*Streptomyces*			Y
3R-7_bin2	*Cellulosimicrobium funkei*			Y
3R-7_bin1	*Microbacterium sp. 002456035*			
5R-7	*Mesorhizobium*		Y	

References

Abarenkov, K., Zirk, A., Piirmann, T., Pöhönen, R., Ivanov, F., Nilsson, R. H. & Kõljalg, U. (2024). UNITE general FASTA release for Fungi. *In:* Community, U. (ed.) 10.0 ed.

Abdenaceur, R. (2023). Phytohormones and biomolecules produced by *Trichoderma* strains as eco-friendly alternative for stimulation of plant growth. *In:* Basharat, A. & Javed, I. (eds.) *New Insights into Phytohormones.* Rijeka: IntechOpen.

Abis, L., Loubet, B., Ciuraru, R., Lafouge, F., Houot, S., Nowak, V., Tripied, J., Dequiedt, S., Maron, P. A. & Sadet-Bourgeteau, S. (2020). Reduced microbial diversity induces larger volatile organic compound emissions from soils. *Scientific Reports,* 10**,** pp. 6104.

Abisado, R. G., Benomar, S., Klaus, J. R., Dandekar, A. A. & Chandler, J. R. (2018). Bacterial quorum sensing and microbial community interactions. *Microbial Community Interactions,* 9(3)**,** pp. e02331-02317.

Abo-Elyousr, K. A. M., Khalil Bagy, H. M. M., Hashem, M., Alamri, S. A. M. & Mostafa, Y. S. (2019). Biological control of the tomato wilt caused by *Clavibacter michiganensis subsp. michiganensis* using formulated plant growth-promoting bacteria. *Egyptian Journal of Biological Pest Control,* 29(1)**,** pp. 54.

Adesemoye, A. O. & Kloepper, J. W. (2009). Plant–microbes interactions in enhanced fertilizer-use efficiency. *Applied Microbiology and Biotechnology,* 85(1)**,** pp. 1-12.

Aguiar-Pulido, V., Huang, W., Suarez-Ulloa, V., Cickovski, T., Mathee, K. & Narasimhan, G. (2016). Metagenomics, metatranscriptomics, and metabolomics approaches for microbiome analysis. *Evol Bioinform Online,* 12(1)**,** pp. 5-16.

Ahemad, M. & Kibret, M. (2014). Mechanisms and applications of plant growth promoting rhizobacteria: current perspective. *Journal of King Saud University - Science,* 26(1)**,** pp. 1-20.

Ahlawat, O. P., Yadav, D., Walia, N., Kashyap, P. L., Sharma, P. & Tiwari, R. (2024). Root exudates and their significance in abiotic stress amelioration in plants: a review. *Journal of Plant Growth Regulation,* 43(6)**,** pp. 1736-1761.

Aioub, A. A. A., Elesawy, A. E. & Ammar, E. E. (2022). Plant growth promoting rhizobacteria (PGPR) and their role in plant-parasitic nematodes control: a fresh look at an old issue. *Journal of Plant Diseases and Protection,* 129(6)**,** pp. 1305-1321.

Ajijah, N., Fiodor, A., Pandey, A. K., Rana, A. & Pranaw, K. (2023). Plant growth-promoting bacteria (PGPB) with biofilm-forming ability: a multifaceted agent for sustainable agriculture. *Diversity,* 15(1)**,** pp. 112.

Akiyama, K., Matsuzaki, K. & Hayashi, H. (2005). Plant sesquiterpenes induce hyphal branching in arbuscular mycorrhizal fungi. *Nature,* 435(7043)**,** pp. 824-827.

Al-Karaki, G. N. & Al-Raddad, A. (1997). Effects of arbuscular mycorrhizal fungi and drought stress on growth and nutrient uptake of two wheat genotypes differing in drought resistance. *Mycorrhiza,* 7(2)**,** pp. 83-88.

Alejandro, S., Höller, S., Meier, B. & Peiter, E. (2020). Manganese in plants: from acquisition to subcellular allocation. *Frontiers in Plant Science,* 11(Article 300)**,** pp. 1-23.

Almeida, O. A. C., de Araujo, N. O., Dias, B. H. S., de Sant'Anna Freitas, C., Coerini, L. F., Ryu, C.-M. & de Castro Oliveira, J. V. (2023). The power of the smallest: the inhibitory activity of microbial volatile organic compounds against phytopathogens. *Frontiers in Microbiology,* 13**,** pp. 1-31.

Alneberg, J., Bjarnason, B. S., de Bruijn, I., Schirmer, M., Quick, J., Ijaz, U. Z., Lahti, L., Loman, N. J., Andersson, A. F. & Quince, C. (2014). Binning metagenomic contigs by coverage and composition. *Nature Methods,* 11(11)**,** pp. 1144-1146.

Altomare, C., Norvell, W. A., Björkman, T. & Harman, G. E. (1999). Solubilization of phosphates and micronutrients by the plant-growth-promoting and biocontrol fungus *Trichoderma harzianum* Rifai 1295-22. *Applied and Environmental Microbiology,* 65(7)**,** pp. 2926-2933.

Antoun, H. & Kloepper, J. (2001). Plant growth promoting rhizobacteria (PGPR). *In:* Brenner, S. & Miller, J. H. (eds.) *Encyclopedia of Genetics*. USA: Academic Press.

Apprill, A., McNally, S., Parsons, R. & Weber, L. (2015). Minor revision to V4 region SSU rRNA 806R gene primer greatly increases detection of SAR11 bacterioplankton. *Aquatic Microbial Ecology,* 75(2)**,** pp. 129-137.

Arkin, A. P., Cottingham, R. W., Henry, C. S., Harris, N. L., Stevens, R. L., Maslov, S., Dehal, P., Ware, D., Perez, F., Canon, S., Sneddon, M. W., Henderson, M. L., Riehl, W. J., Murphy-Olson, D., Chan, S. Y., Kamimura, R. T., Kumari, S., Drake, M. M., Brettin, T. S., Glass, E. M., Chivian, D., Gunter, D., Weston, D. J., Allen, B. H., Baumohl, J., Best, A. A., Bowen, B., Brenner, S. E., Bun, C. C., Chandonia, J.-M., Chia, J.-M., Colasanti, R., Conrad, N., Davis, J. J., Davison, B. H., DeJongh, M., Devoid, S., Dietrich, E., Dubchak, I., Edirisinghe, J. N., Fang, G., Faria, J. P., Frybarger, P. M., Gerlach, W., Gerstein, M., Greiner, A., Gurtowski, J., Haun, H. L., He, F., Jain, R., Joachimiak, M. P., Keegan, K. P., Kondo, S., Kumar, V., Land, M. L., Meyer, F., Mills, M., Novichkov, P. S., Oh, T., Olsen, G. J., Olson, R., Parrello, B., Pasternak, S., Pearson, E., Poon, S. S., Price, G. A., Ramakrishnan, S., Ranjan, P., Ronald, P. C., Schatz, M. C., Seaver, S. M. D., Shukla, M., Sutormin, R. A., Syed, M. H., Thomason, J., Tintle, N. L., Wang, D., Xia, F., Yoo, H., Yoo, S. & Yu, D. (2018). KBase: the united states department of energy systems biology knowledgebase. *Nature Biotechnology,* 36(7)**,** pp. 566-569.

Arora, N. K. & Verma, M. (2017). Modified microplate method for rapid and efficient estimation of siderophore produced by bacteria. *3 Biotech,* 7(6)**,** pp. 381.

Artursson, V., Finlay, R. D. & Jansson, J. K. (2006). Interactions between arbuscular mycorrhizal fungi and bacteria and their potential for stimulating plant growth. *Environmental Microbiology,* 8(1)**,** pp. 1-10.

Asea, P. E. A., Kucey, R. M. N. & Stewart, J. W. B. (1988). Inorganic phosphate solubilization by two Penicillium species in solution culture and soil. *Soil Biology and Biochemistry,* 20(4)**,** pp. 459-464.

Augé, R. M. (2001). Water relations, drought and vesicular-arbuscular mycorrhizal symbiosis. *Mycorrhiza,* 11(1)**,** pp. 3-42.

Averill, C., Turner, B. L. & Finzi, A. C. (2014). Mycorrhiza-mediated competition between plants and decomposers drives soil carbon storage. *Nature,* 505**,** pp. 543-545.

Awika, J., Rooney, L. & Waniska, R. (2005). Anthocyanins from black sorghum and their antioxidant properties. *Food Chemistry,* 90**,** pp. 293-301.

Ayiti, O. E. & Babalola, O. O. (2022). Factors influencing soil nitrification process and the effect on environment and health. *Frontiers in Sustainable Food Systems,* 6(Article 821994)**,** pp. 1-12.

Azam, F. & Memon, G. (1996). Soil organisms. *Soil science. National Book Foundation, Islamabad***,** pp. 200-232.

Badri, D. V. & Vivanco, J. M. (2009). Regulation and function of root exudates. *Plant, Cell & Environment,* 32(6)**,** pp. 666-681.

Bagyaraj, D. (2014). Mycorrhizal fungi. *Indian National Science Academy,* 80 (2)**,** pp. 415-428

Bakki, M., Banane, B., Marhane, O., Esmaeel, Q., Hatimi, A., Ait Barka, E., Azim, K. & Bouizgarne, B. (2024). Phosphate solubilizing *Pseudomonas* and *Bacillus* combined with rock phosphates promoting tomato growth and reducing bacterial canker disease. *Frontiers in Microbiology,* 15**,** pp.

Bao, Y., Dolfing, J., Guo, Z., Chen, R., Wu, M., Li, Z., Lin, X. & Feng, Y. (2021). Important ecophysiological roles of non-dominant Actinobacteria in plant residue decomposition, especially in less fertile soils. *Microbiome,* 9(1)**,** pp. 84.

Barka, E. A., Vatsa, P., Sanchez, L., Gaveau-Vaillant, N., Jacquard, C., Meier-Kolthoff, J. P., Klenk, H. P., Clément, C., Ouhdouch, Y. & van Wezel, G. P. (2015). Taxonomy, physiology, and natural products of Actinobacteria. *Microbiology and Molecular Biology Reviews,* 80(1)**,** pp. 1-43.

Bashan, Y. & de-Bashan, L. E. (2005). Fresh-weight measurements of roots provide inaccurate estimates of the effects of plant growth-promoting bacteria on root growth: a critical examination. *Soil Biology and Biochemistry,* 37(10)**,** pp. 1795-1804.

Bashan, Y. & de-Bashan, L. E. (2010). Chapter Two - How the plant growth-promoting bacterium *Azospirillum* promotes plant growth—a critical assessment. *In:* Sparks, D. L. (ed.) *Advances in Agronomy.* Academic Press.

Basiru, S., Ait Si Mhand, K. & Hijri, M. (2023). Disentangling arbuscular mycorrhizal fungi and bacteria at the soil-root interface. *Mycorrhiza,* 33(3)**,** pp. 119-137.

Begum, N., Qin, C., Ahanger, M. A., Raza, S., Khan, M. I., Ashraf, M., Ahmed, N. & Zhang, L. (2019). Role of arbuscular mycorrhizal fungi in plant growth regulation: implications in abiotic stress tolerance. *Frontiers in Plant Science,* 10(1068)**,** pp. 1-15.

Bell, G. D. H. (1987). The history of wheat cultivation. *In:* Lupton, F. G. H. (ed.) *Wheat Breeding.* Dordrecht: Springer.

Beneduzi, A., Ambrosini, A. & Passaglia, L. M. P. (2012). Plant growth-promoting rhizobacteria (PGPR): Their potential as antagonists and biocontrol agents. *Genetics and Molecular Biology,* 35(4 (suppl))**,** pp. 1044-1051.

Berg, G. & Smalla, K. (2009). Plant species and soil type cooperatively shape the structure and function of microbial communities in the rhizosphere. *FEMS Microbiology Ecology,* 68(1)**,** pp. 1-13.

Besserer, A., Puech-Pagès, V., Kiefer, P., Gomez-Roldan, V., Jauneau, A., Roy, S., Portais, J. C., Roux, C., Bécard, G. & Séjalon-Delmas, N. (2006). Strigolactones stimulate arbuscular mycorrhizal fungi by activating mitochondria. *PLoS Biol,* 4(7)**,** pp. e226.

Bevivino, A., Paganin, P., Bacci, G., Florio, A., Pellicer, M. S., Papaleo, M. C., Mengoni, A., Ledda, L., Fani, R., Benedetti, A. & Dalmastri, C. (2014). Soil bacterial community response to differences in agricultural management along with seasonal changes in a mediterranean region. *PLOS ONE,* 9(8)**,** pp. e105515.

Bhattacharyya, P. N. & Jha, D. K. (2012). Plant growth-promoting rhizobacteria (PGPR): emergence in agriculture. *World Journal of Microbiology and Biotechnology,* 28(4)**,** pp. 1327-1350.

Bieleski, R. (1973). Phosphate pools, phosphate transport, and phosphate availability. *Annual Review of Plant Physiology,* 24(1)**,** pp. 225-252.

Bishop, P. E. & Joerger, R. D. (1990). Genetics and molecular biology of alternative nitrogen fixation systems. *Annual Review of Plant Biology,* 41(1)**,** pp. 109-125.

Blake, C., Christensen, M. N. & Kovács, Á. T. (2021). Molecular aspects of plant growth promotion and protection by *Bacillus subtilis*. *Molecular Plant-Microbe Interactions,* 34(1), pp. 15-25.

Bogino, P. C., Oliva, M. D. l. M., Sorroche, F. G. & Giordano, W. (2013). The role of bacterial biofilms and surface components in plant-bacterial associations. *International Journal of Molecular Sciences,* 14(8), pp. 15838-15859.

Bojović, B. & Marković, A. (2009). Correlation between nitrogen and chlorophyll content in wheat (*Triticum aestivum* L.). *Kragujevac Journal of Science,* 31, pp. 69-74.

Borah, P., Gogoi, N., Asad, S. A., Rabha, A. J. & Farooq, M. (2023). An insight into plant growth-promoting rhizobacteria-mediated mitigation of stresses in plant. *Journal of Plant Growth Regulation,* 42(5), pp. 3229-3256.

Brettin, T., Davis, J. J., Disz, T., Edwards, R. A., Gerdes, S., Olsen, G. J., Olson, R., Overbeek, R., Parrello, B., Pusch, G. D., Shukla, M., Thomason, J. A., Stevens, R., Vonstein, V., Wattam, A. R. & Xia, F. (2015). RASTtk: A modular and extensible implementation of the RAST algorithm for building custom annotation pipelines and annotating batches of genomes. *Scientific Reports,* 5(1), pp. 8365.

Briat, J.-F., Dubos, C. & Gaymard, F. (2015). Iron nutrition, biomass production, and plant product quality. *Trends in Plant Science,* 20(1), pp. 33-40.

Butterly, C. R., Bünemann, E. K., McNeill, A. M., Baldock, J. A. & Marschner, P. (2009). Carbon pulses but not phosphorus pulses are related to decreases in microbial biomass during repeated drying and rewetting of soils. *Soil Biology and Biochemistry,* 41(7), pp. 1406-1416.

Cai, C., Lv, L., Wei, S., Zhang, L. & Cao, W. (2024). How does climate change affect potential yields of four staple grain crops worldwide by 2030? *PLoS One,* 19(5), pp. e0303857.

Callahan, B. J., McMurdie, P. J. & Holmes, S. P. (2017). Exact sequence variants should replace operational taxonomic units in marker-gene data analysis. *The ISME Journal,* 11(12), pp. 2639-2643.

Callahan, B. J., McMurdie, P. J., Rosen, M. J., Han, A. W., Johnson, A. J. A. & Holmes, S. P. (2016). DADA2: High-resolution sample inference from Illumina amplicon data. *Nature Methods,* 13(7), pp. 581-583.

Campanharo, J. C., Kielak, A. M., Castellane, T. C. L., Kuramae, E. E. & Lemos, E. G. d. M. (2016). Optimized medium culture for Acidobacteria subdivision 1 strains. *FEMS Microbiology Letters,* 363(21), pp.

Caris, C., Hördt, W., Hawkins, H.-J., Römheld, V. & George, E. (1998). Studies of iron transport by arbuscular mycorrhizal hyphae from soil to peanut and sorghum plants. *Mycorrhiza,* 8**,** pp. 35-39.

Castaldi, S., Petrillo, C., Donadio, G., Piaz, F. D., Cimmino, A., Masi, M., Evidente, A. & Isticato, R. (2021). Plant growth promotion function of *Bacillus sp.* strains isolated from salt-pan rhizosphere and their biocontrol potential against *Macrophomina phaseolina*. *International Journal of Molecular Sciences,* 22(7)**,** pp. 3324.

Chai, Y. N. & Schachtman, D. P. (2021). Root exudates impact plant performance under abiotic stress. *Trends in Plant Science***,** pp.

Chaignaud, P., Morawe, M., Besaury, L., Kröber, E., Vuilleumier, S., Bringel, F. & Kolb, S. (2018). Methanol consumption drives the bacterial chloromethane sink in a forest soil. *The ISME Journal,* 12(11)**,** pp. 2681-2693.

Chandra, P., Rai, A., Basak, N., Sundha, P., Prajapat, K., Singh, A. & Yadav, R. (2024a). In vitro P–solubilization activity of halophilic fungi in salt–affected soils and their potential as bio–inoculants. *Environmental Engineering Research,* 29(6)**,** pp. 230760

Chandra, T., Sahu, J., Jaiswal, S., Iquebal, M. A. & Kumar, D. (2024b). Current research status and emerging trends in wheat: An integrated scientometric analysis based on ploidy uncovers hidden footprints in the scientific landscape. *Heliyon,* 10(16)**,** pp. e36375.

Chen, H. & Boutros, P. C. (2011). VennDiagram: a package for the generation of highly-customizable Venn and Euler diagrams in R. *BMC Bioinformatics,* 12**,** pp. 35.

Chen, Z., Wang, L., Cardoso, J. A., Zhu, S., Liu, G., Rao, I. M. & Lin, Y. (2023). Improving phosphorus acquisition efficiency through modification of root growth responses to phosphate starvation in legumes. *Frontiers in Plant Science,* 14 pp. 1-15.

Chieb, M. & Gachomo, E. W. (2023). The role of plant growth promoting rhizobacteria in plant drought stress responses. *BMC Plant Biology,* 23(1)**,** pp. 407.

Chilvers, G. A., Lapeyrie, F. F. & Horan, D. P. (1987). Ectomycorrhizal vs endomycorrhizal fungi within the same root system. *New Phytologist,* 107(2)**,** pp. 441-448.

Chivian, D., Jungbluth, S. P., Dehal, P. S., Wood-Charlson, E. M., Canon, R. S., Allen, B. H., Clark, M. M., Gu, T., Land, M. L., Price, G. A., Riehl, W. J., Sneddon, M. W., Sutormin, R., Zhang, Q., Cottingham, R. W., Henry, C. S. & Arkin, A. P. (2023). Metagenome-assembled genome extraction and analysis from microbiomes using KBase. *Nature Protocols,* 18(1)**,** pp. 208-238.

Compant, S., Duffy, B., Nowak, J., Clément, C. & Barka, E. A. (2005). Use of plant growth-promoting bacteria for biocontrol of plant diseases: principles, mechanisms of

action, and future prospects. *Applied and Environmental Microbiology,* 71(9)**,** pp. 4951-4959.

Cotton, T. E. A., Pétriacq, P., Cameron, D. D., Meselmani, M. A., Schwarzenbacher, R., Rolfe, S. A. & Ton, J. (2019). Metabolic regulation of the maize rhizobiome by benzoxazinoids. *The ISME Journal,* 13(7)**,** pp. 1647-1658.

Criquet, S., Ferre, E., Farnet, A. M. & Le petit, J. (2004). Annual dynamics of phosphatase activities in an evergreen oak litter: influence of biotic and abiotic factors. *Soil Biology and Biochemistry,* 36(7)**,** pp. 1111-1118.

Dai, X., Chen, L., Liu, M., Liu, Y., Jiang, S., Xu, T., Wang, A., Yang, S. & Wei, W. (2022). Effect of 6-methoxybenzoxazolinone on the cecal microbiota of adult male Brandt's vole. *Frontiers in Microbiology,* 13**,** pp. 847073.

Dakora, F. D. & Phillips, D. A. (2002). Root exudates as mediators of mineral acquisition in low-nutrient environments. *Plant and Soil,* 245(1)**,** pp. 35-47.

Das, N., Das, A., Das, S., Bhatawadekar, V., Pandey, P., Choure, K., Damare, S. & Pandey, P. (2023). Petroleum hydrocarbon catabolic pathways as targets for metabolic engineering strategies for enhanced bioremediation of crude-oil-contaminated environments. *Fermentation,* 9(2)**,** pp. 196.

De Cáceres, M. & Legendre, P. (2009). Associations between species and groups of sites: indices and statistical inference. *Ecology,* 90(12)**,** pp. 3566-3574.

de Vos, M. G. J., Zagorski, M., McNally, A. & Bollenbach, T. (2017). Interaction networks, ecological stability, and collective antibiotic tolerance in polymicrobial infections. *Proceedings of the National Academy of Sciences,* 114(40)**,** pp. 10666-10671.

Deines, P., Hammerschmidt, K. & Bosch , T. C. G. (2020). Microbial species coexistence depends on the host environment. *mBio,* 11(4)**,** pp. 10.1128.

Deng, Y., Cui, X., Hernández, M. & Dumont, M. G. (2014). Microbial diversity in hummock and hollow soils of three wetlands on the Qinghai-Tibetan Plateau revealed by 16s rRNA pyrosequencing. *PLOS ONE,* 9(7)**,** pp. e103115.

Dinkelaker, B., RÖmheld, V. & Marschner, H. (1989). Citric acid excretion and precipitation of calcium citrate in the rhizosphere of white lupin (*Lupinus albus* L.). *Plant, Cell & Environment,* 12(3)**,** pp. 285-292.

Dobereiner, J. (1992). History and new perspectives of diazotrophs in association with non-leguminous plants. *Symbiosis,* 13**,** pp. 1–13.

Dodd, J. C., Clapp, J. P. & Zhao, B. (2001). *Arbuscular mycorrhizal fungi in plant production systems: detection, taxonomy, conservation and ecophysiology* [Online]. Wuhan, P.R. China: Huazhong Agricultural University. Available:

https://www2.dijon.inrae.fr/mychintec/Protocole/protoframe.html [Accessed 02/09 2024].

Doran, J. W. & Zeiss, M. R. (2000). Soil health and sustainability: managing the biotic component of soil quality. *Applied Soil Ecology,* 15(1), pp. 3-11.

Duncker, K. E., Holmes, Z. A. & You, L. (2021). Engineered microbial consortia: strategies and applications. *Microbial Cell Factories,* 20(1), pp. 211.

Eivazi, F. & Tabatabai, M. A. (1977). Phosphatases in soils. *Soil Biology and Biochemistry,* 9(3), pp. 167-172.

Ekelund, F., Saj, S., Vestergård, M., Bertaux, J. & Mikola, J. (2009). The “soil microbial loop” is not always needed to explain protozoan stimulation of plants. *Soil Biology and Biochemistry,* 41(11), pp. 2336-2342.

El Attar, I., Hnini, M., Taha, K. & Aurag, J. (2022). Phosphorus availability and its sustainable use. *Journal of Soil Science and Plant Nutrition,* 22(4), pp. 5036-5048.

Elshafie, H. S. & Camele, I. (2021). An overview of metabolic activity, beneficial and pathogenic aspects of *Burkholderia* spp. *Metabolites,* 11(5), pp. 321.

Emami-Karvani, Z. & Chitsaz-Esfahani, Z. (2021). Phosphorus solubilization: mechanisms, recent advancement and future challenge. *In:* Yadav, A. N. (ed.) *Soil Microbiomes for Sustainable Agriculture: Functional Annotation.* Cham: Springer International Publishing.

Emmett, B. D., Lévesque-Tremblay, V. & Harrison, M. J. (2021). Conserved and reproducible bacterial communities associate with extraradical hyphae of arbuscular mycorrhizal fungi. *The ISME Journal,* 15(8), pp. 2276-2288.

Evelin, H., Kapoor, R. & Giri, B. (2009). Arbuscular mycorrhizal fungi in alleviation of salt stress: a review. *Ann Bot,* 104(7), pp. 1263-1280.

Eze, Chijioke, K., Obasi, Patrick, N., Ewa, Chikaodis, S., Eyibio & Usenekong, N. (2024). Soil microbiome in nutrient conservation for plant growth. *In:* Aransiola, S. A., Babaniyi, B. R., Aransiola, A. B. & Maddela, N. R. (eds.) *Prospects for Soil Regeneration and Its Impact on Environmental Protection.* Cham: Springer Nature Switzerland.

Fan, J., Shi, Y. & Li, Y. (2024). Editorial: Microorganisms in sustainable and green agriculture: synergistic effect on carbon sequestration and crop productivity. *Frontiers in Microbiology,* 15(1470240.), pp.

Faridy, N., Torabi, E., Pourbabaee, A. A., Osdaghi, E. & Talebi, K. (2024). Efficacy of novel bacterial consortia in degrading fipronil and thiobencarb in paddy soil: a survey for community structure and metabolic pathways. *Frontiers in Microbiology,* 15, pp. 1366951.

Feng, G., Zhang, F. S., Li, X. L., Tian, C. Y., Tang, C. & Rengel, Z. (2002). Improved tolerance of maize plants to salt stress by arbuscular mycorrhiza is related to higher accumulation of soluble sugars in roots. *Mycorrhiza,* 12(4)**,** pp. 185-190.

Fierer, N. (2017). Embracing the unknown: disentangling the complexities of the soil microbiome. *Nature Reviews Microbiology,* 15(10)**,** pp. 579-590.

Filion, M., St-arnaud, M. & Fortin, J. A. (1999). Direct interaction between the arbuscular mycorrhizal fungus *Glomus intraradices* and different rhizosphere microorganisms. *New Phytologist,* 141**,** pp. 525-533.

Fiorilli, V., Lanfranco, L. & Bonfante, P. (2013). The expression of *GintPT*, the phosphate transporter of *Rhizophagus irregularis*, depends on the symbiotic status and phosphate availability. *Planta,* 237**,** pp. 1267-1277.

Fogel, R. (1988). Interactions among soil biota in coniferous ecosystems. *Agriculture, Ecosystems & Environment,* 24(1)**,** pp. 69-85.

Foissner, W., Blatterer, H. & Foissner, I. (1988). The hemimastigophora (*Hemimastix amphikineta* nov. gen., nov. spec.), a new protistan phylum from gondwanian soils. *European Journal of Protistology,* 23(4)**,** pp. 361-383.

Fontaine, S., Abbadie, L., Aubert, M., Barot, S., Bloor, J. M. G., Derrien, D., Duchene, O., Gross, N., Henneron, L., Le Roux, X., Loeuille, N., Michel, J., Recous, S., Wipf, D. & Alvarez, G. (2023). Plant–soil synchrony in nutrient cycles: Learning from ecosystems to design sustainable agrosystems. *Global Change Biology,* 30(1)**,** pp. e17034.

Franche, C., Lindström, K. & Elmerich, C. (2009). Nitrogen-fixing bacteria associated with leguminous and non-leguminous plants. *Plant and Soil,* 321(1)**,** pp. 35-59.

Frey-Klett, P., Garbaye, J. & Tarkka, M. (2007). The mycorrhiza helper bacteria revisited. *New Phytologist,* 176(1)**,** pp. 22-36.

Gaby, J. C. & Buckley, D. H. (2012). A comprehensive evaluation of PCR primers to amplify the *nifH* gene of nitrogenase. *PLOS ONE,* 7(7)**,** pp. e42149.

Galloway, J. N., Dentener, F. J., Capone, D. G., Boyer, E. W., Howarth, R. W., Seitzinger, S. P., Asner, G. P., Cleveland, C. C., Green, P. A., Holland, E. A., Karl, D. M., Michaels, A. F., Porter, J. H., Townsend, A. R. & Vöosmarty, C. J. (2004). Nitrogen cycles: past, present, and future. *Biogeochemistry,* 70(2)**,** pp. 153-226.

Gang, S., Sharma, S., Saraf, M., Buck, M. & Schumacher, J. (2019). Analysis of Indole-3-acetic acid (IAA) production in *Klebsiellaby* LC-MS/MS and the Salkowski method. *Bio-protocol,* 9(9)**,** pp. e3230-e3230.

Genre, A., Chabaud, M., Balzergue, C., Puech-Pagès, V., Novero, M., Rey, T., Fournier, J., Rochange, S., Bécard, G., Bonfante, P. & Barker, D. G. (2013). Short-chain chitin

oligomers from arbuscular mycorrhizal fungi trigger nuclear Ca2+ spiking in Medicago truncatula roots and their production is enhanced by strigolactone. *New Phytol,* 198(1), pp. 190-202.

Genre, A., Chabaud, M., Timmers, T., Bonfante, P. & Barker, D. G. (2005). Arbuscular mycorrhizal fungi elicit a novel intracellular apparatus in Medicago truncatula root epidermal cells before infection. *Plant Cell,* 17(12), pp. 3489-3499.

Gerke, J. (2015). Phytate (inositol hexakisphosphate) in soil and phosphate acquisition from inositol phosphates by higher plants. A review. *Plants (Basel, Switzerland),* 4(2), pp. 253-266.

Gianinazzi, S., Gollotte, A., Binet, M.-N., van Tuinen, D., Redecker, D. & Wipf, D. (2010). Agroecology: the key role of arbuscular mycorrhizas in ecosystem services. *Mycorrhiza,* 20(8), pp. 519-530.

Gilbert, N. (2009). Environment: the disappearing nutrient. *Nature,* 461(7265), pp. 716-718.

Giri, B., Kapoor, R. & Mukerji, K. G. (2007). Improved tolerance of Acacia nilotica to salt stress by Arbuscular mycorrhiza, Glomus fasciculatum may be partly related to elevated K/Na ratios in root and shoot tissues. *Microb Ecol,* 54(4), pp. 753-760.

Glick, B. R. (1995). The enhancement of plant growth by free-living bacteria. *Canadian journal of microbiology,* 41(2), pp. 109-117.

Glick, B. R. (2012). Plant growth-promoting bacteria: mechanisms and applications. *Scientifica,* 2012, pp. 963401.

Glick, B. R. (2014). Bacteria with ACC deaminase can promote plant growth and help to feed the world. *Microbiological Research,* 169(1), pp. 30-39.

Glick, B. R., Patten, C. L., Holguin, G. & Penrose, D. M. (1999). *Biochemical and Genetic Mechanisms Used by Plant Growth Promoting Bacteria. ,* London, Imperial College Press.

Glick, B. R., Todorovic, B., Czarny, J., Cheng, Z., Duan, J. & McConkey, B. (2007). Promotion of plant growth by bacterial acc deaminase. *Critical Reviews in Plant Sciences,* 26(5-6), pp. 227-242.

Glickmann, E. & Dessaux, Y. (1995). A critical examination of the specificity of the salkowski reagent for indolic compounds produced by phytopathogenic bacteria. *Applied and Environmental Microbiology,* 61(2), pp. 793-796.

Goldstein, A. (1994). *Phosphate in Microorganisms: Cellular and Molecular Biology*. Washington (DC): ASM Press, Washington.

Goldstein, A. H. (1995). Recent progress in understanding the molecular genetics and biochemistry of calcium phosphate solubilization by gram negative bacteria. *Biological Agriculture & Horticulture,* 12(2), pp. 185-193.

Goris, J., Konstantinidis, K. T., Klappenbach, J. A., Coenye, T., Vandamme, P. & Tiedje, J. M. (2007). DNA–DNA hybridization values and their relationship to whole-genome sequence similarities. *International Journal of Systematic and Evolutionary Microbiology,* 57(1), pp. 81-91.

Grayston, S. J., Griffith, G. S., Mawdsley, J. L., Campbell, C. D. & Bardgett, R. D. (2001). Accounting for variability in soil microbial communities of temperate upland grassland ecosystems. *Soil Biology and Biochemistry,* 33(4), pp. 533-551.

Grayston, S. J., Wang, S., Campbell, C. D. & Edwards, A. C. (1998). Selective influence of plant species on microbial diversity in the rhizosphere. *Soil Biology and Biochemistry,* 30(3), pp. 369-378.

Graziani, G., Ferracane, R., Sambo, P., Santagata, S., Nicoletto, C. & Fogliano, V. (2014). Profiling Chicory Sesquiterpene Lactones by High Resolution Mass Spectrometry. *Food Research International,* 67, pp.

Gregory, P. J., Hutchison, D. J., Read, D. B., Jenneson, P. M., Gilboy, W. B. & Morton, E. J. (2003). Non-invasive imaging of roots with high resolution X-ray micro-tomography. *Plant and Soil,* 255(1), pp. 351-359.

Griffiths, B. S., Ritz, K., Ebblewhite, N. & Dobson, G. (1998). Soil microbial community structure: Effects of substrate loading rates. *Soil Biology and Biochemistry,* 31(1), pp. 145-153.

Gross, M. (2017). Where is all the phosphorus? *Current Biology,* 27(21), pp. R1141-R1144.

Guardo, A. D., Williams, R. J., Matthiessen, P., Brooke, D. N. & Calamari, D. (1994). Simulation of pesticide runoff at Rosemaund Farm (UK) using the SoilFug model. *Environmental Science and Pollution Research,* 1(3), pp. 151-160.

Gupta, G., Parihar, S. S., Ahirwar, N. K., Snehi, S. K. & Singh, V. (2015). Plant growth promoting rhizobacteria (PGPR): current and future prospects for development of sustainable agriculture. *J Microb Biochem Technol,* 7(2), pp. 096-102.

Guyonnet, J. P., Guillemet, M., Dubost, A., Simon, L., Ortet, P., Barakat, M., Heulin, T., Achouak, W. & Haichar, F. e. Z. (2018). Plant nutrient resource use strategies shape active rhizosphere microbiota through root exudation. *Frontiers in Plant Science,* 9, pp. 1-13.

Gyaneshwar, P., Naresh Kumar, G., Parekh, L. J. & Poole, P. S. (2002). Role of soil microorganisms in improving P nutrition of plants. *Plant and Soil,* 245(1), pp. 83-93.

Hadziavdic, K., Lekang, K., Lanzen, A., Jonassen, I., Thompson, E. M. & Troedsson, C. (2014). Characterization of the 18S rRNA gene for designing universal eukaryote specific primers. *PLoS One,* 9(2), pp. e87624.

Hamdali, H., Bouizgarne, B., Hafidi, M., Lebrihi, A., Virolle, M. J. & Ouhdouch, Y. (2008). Screening for rock phosphate solubilizing *Actinomycetes* from Moroccan phosphate mines. *Applied Soil Ecology,* 38(1), pp. 12-19.

Han, H.-S. & Lee, K. (2006). Effect of co-inoculation with phosphate and potassium solubilizing bacteria on mineral uptake and growth of pepper and cucumber. *Plant Soil and Environment,* 52(3), pp. 130-136.

Hariprasad, P. & Niranjana, S. R. (2009). Isolation and characterization of phosphate solubilizing rhizobacteria to improve plant health of tomato. *Plant and Soil,* 316(1), pp. 13-24.

Hasan, A., Tabassum, B., Hashim, M. & Khan, N. (2024). Role of plant growth promoting rhizobacteria (PGPR) as a plant growth enhancer for sustainable agriculture: a review. *Bacteria,* 3(2), pp. 59-75.

Hawkins, H.-J., Cargill, R. I. M., Van Nuland, M. E., Hagen, S. C., Field, K. J., Sheldrake, M., Soudzilovskaia, N. A. & Kiers, E. T. (2023). Mycorrhizal mycelium as a global carbon pool. *Current Biology,* 33(11), pp. R560-R573.

Hawkins, H.-J., Johansen, A. & George, E. (2000). Uptake and transport of organic and inorganic nitrogen by arbuscular mycorrhizal fungi. *Plant and Soil,* 226, pp. 275-285.

Hayat, R., Ali, S., Amara, U., Khalid, R. & Ahmed, I. (2010). Soil beneficial bacteria and their role in plant growth promotion: a review. *Annals of Microbiology,* 60(4), pp. 579-598.

Hernández, M., Roy, S., Keevil, C. W. & Dumont, M. G. (2023). Identification of diverse antibiotic resistant bacteria in agricultural soil with H218O stable isotope probing combined with high-throughput sequencing. *Environmental microbiome,* 18(1), pp. 34.

Hetherington, A. M. & Woodward, F. I. (2003). The role of stomata in sensing and driving environmental change. *Nature,* 424(6951), pp. 901-908.

Hibbing, M. E., Fuqua, C., Parsek, M. R. & Peterson, S. B. (2010). Bacterial competition: surviving and thriving in the microbial jungle. *Nature Reviews Microbiology,* 8, pp. 15-25.

Hinsinger, P. (2001). Bioavailability of soil inorganic P in the rhizosphere as affected by root-induced chemical changes: a review. *Plant and Soil,* 237(2), pp. 173-195.

Hodge, A. & Fitter, A. H. (2013). Microbial mediation of plant competition and community structure. *Functional Ecology,* 27(4), pp. 865-875.

Hodge, A. & Storer, K. (2015). Arbuscular mycorrhiza and nitrogen: implications for individual plants through to ecosystems. *Plant and Soil,* 386**,** pp. 1-19.

Hoffman, B. M., Lukoyanov, D., Yang, Z.-Y., Dean, D. R. & Seefeldt, L. C. (2014). Mechanism of nitrogen fixation by nitrogenase: the next stage. *Chemical Reviews,* 114(8)**,** pp. 4041-4062.

Hu, L., Robert, C. A. M., Cadot, S., Zhang, X., Ye, M., Li, B., Manzo, D., Chervet, N., Steinger, T., van der Heijden, M. G. A., Schlaeppi, K. & Erb, M. (2018). Root exudate metabolites drive plant-soil feedbacks on growth and defense by shaping the rhizosphere microbiota. *Nature Communications,* 9(1)**,** pp. 2738.

Hunter, P., Teakle, G. & Bending, G. (2014). Root traits and microbial community interactions in relation to phosphorus availability and acquisition, with particular reference to *Brassica*. *Frontiers in Plant Science,* 5(27)**,** pp.

Hütsch, B. W., Augustin, J. & Merbach, W. (2002). Plant rhizodeposition-an important source for carbon turnover in soils. *Journal of Plant Nutrition and Soil Science,* 165(4)**,** pp. 397-407.

Hyakumachi, M. (1994). Plant-growth-promoting fungi from turfgrass rhizosphere with potential for disease suppression. *Soil Microorganisms,* 44**,** pp. 53-68.

Idriss, E. E., Makarewicz, O., Farouk, A., Rosner, K., Greiner, R., Bochow, H., Richter, T. & Borriss, R. (2002). Extracellular phytase activity of *Bacillus amyloliquefaciens* FZB45 contributes to its plant-growth-promoting effecta. *Microbiology,* 148(7)**,** pp. 2097-2109.

Illmer, P., Barbato, A. & Schinner, F. (1995). Solubilization of hardly-soluble $AlPO_4$ with P-solubilizing microorganisms. *Soil Biology and Biochemistry,* 27(3)**,** pp. 265-270.

Illmer, P. & Schinner, F. (1995). Solubilization of inorganic calcium phosphates—Solubilization mechanisms. *Soil Biology and Biochemistry,* 27(3)**,** pp. 257-263.

Inderjit, S. & Weston, L. (2000). Are Laboratory Bioassays for Allelopathy Suitable for Prediction of Field Responses? *Journal of Chemical Ecology,* 26**,** pp. 2111-2118.

Inderjit, S. & Weston, L. (2003). Root Exudates: An overview. *In:* Kroon, H. d. & Visser, E. J. W. (eds.) *Root Ecology*. 10 ed. Berlin,Germany: Springer-Verlag London Ltd.

Islam, M. M., Rengel, Z., Storer, P., Siddique, K. H. M. & Solaiman, Z. M. (2023). Phosphorus fertilisation differentially influences growth, morpho-physiological adaptations and nutrient uptake of industrial hemp (*Cannabis sativa L.*). *Plant and Soil,* 492(1)**,** pp. 301-314.

Jacott, C. N., Murray, J. D. & Ridout, C. J. (2017). Trade-Offs in Arbuscular Mycorrhizal Symbiosis: Disease Resistance, Growth Responses and Perspectives for Crop Breeding. *Agronomy,* 7(4)**,** pp. 75.

Jakobsen, I. & Rosendahl, L. (1990). Carbon flow into soil and external hyphae from roots of mycorrhizal cucumber plants. *New Phytologist,* 115**,** pp. 77-83.

Janssen, P. H., Schuhmann, A., Mörschel, E. & Rainey, F. A. (1997). Novel anaerobic ultramicrobacteria belonging to the *Verrucomicrobiales* lineage of bacterial descent isolated by dilution culture from anoxic rice paddy soil. *Applied and Environmental Microbiology,* 63(4)**,** pp. 1382-1388.

Jensen, H. L. (1942). Nitrogen fixation in leguminous plants. II. Is symbiotic nitrogen fixation influenced by Azotobacter? . *Proceedings of The Linnean Society of New South Wales,* 67**,** pp. 205–212.

Jha, C. K., Aeron, A., Patel, B. V., Maheshwari, D. K. & Saraf, M. (2011). *Enterobacter*: Role in plant growth promotion. *In:* Maheshwari, D. K. (ed.) *Bacteria in Agrobiology: Plant Growth Responses.* Berlin, Heidelberg: Springer Berlin Heidelberg.

Jiao, C., Zhang, J., Wang, X. & He, N. (2024). Optimal allocation strategies of plant calcium on qinghai–tibetan plateau. *Journal of Geophysical Research: Biogeosciences,* 129(4)**,** pp. e2023JG007884.

Jiménez-Gómez, A., Saati-Santamaría, Z., Kostovcik, M., Rivas, R., Velázquez, E., Mateos, P. F., Menéndez, E. & García-Fraile, P. (2020). Selection of the root endophyte *Pseudomonas brassicacearum* CDVBN10 as plant growth promoter for *Brassica napus* L. crops. *Agronomy,* 10(11)**,** pp. 1788.

Jin, H., Liu, J., Liu, J. & Huang, X. (2012). Forms of nitrogen uptake, translocation, and transfer via arbuscular mycorrhizal fungi: a review. *Sci China Life Sci,* 55(6)**,** pp. 474-482.

Johansen, A., Jakobsen, I. & Jensen, E. S. (1994). Hyphal N transport by a vesicular-arbuscular mycorrhizal fungus associated with cucumber grown at three nitrogen levels. *Plant and Soil,* 160**,** pp. 1-9.

Johansson, J. F., Paul, L. R. & Finlay, R. D. (2004). Microbial interactions in the mycorrhizosphere and their significance for sustainable agriculture. *FEMS Microbiology Ecology,* 48(1)**,** pp. 1-13.

Jones, D. L. & Kielland, K. (2012). Amino acid, peptide and protein mineralization dynamics in a taiga forest soil. *Soil Biology and Biochemistry,* 55**,** pp. 60-69.

Joseph, S. J., Hugenholtz, P., Sangwan, P., Osborne, C. A. & Janssen, P. H. (2003). Laboratory cultivation of widespread and previously uncultured soil bacteria. *Applied and Environmental Microbiology,* 69(12)**,** pp. 7210-7215.

Jungk, A. (2001). Root hairs and the acquisition of plant nutrients from soil. *Journal of Plant Nutrition and Soil Science,* 164(2)**,** pp. 121-129.

Jurinak, J. J., Dudley, L. M., Allen, M. F. & Knight, W. G. (1986). The role of calcium oxalate in the availability of phosphorus in soils of semiarid regions: A thermodynamic study. *Soil Science,* 142(5), pp. 255-261.

Kalbe, C., Marten, P. & Berg, G. (1996). Strains of the genus *Serratia* as beneficial rhizobacteria of oilseed rape with antifungal properties. *Microbiological Research,* 151(4), pp. 433-439.

Kang, B. G., Kim, W. T., Yun, H. S. & Chang, S. C. (2010). Use of plant growth-promoting rhizobacteria to control stress responses of plant roots. *Plant Biotechnology Reports,* 4(3), pp. 179-183.

Kang, D. D., Li, F., Kirton, E., Thomas, A., Egan, R., An, H. & Wang, Z. (2019). MetaBAT 2: an adaptive binning algorithm for robust and efficient genome reconstruction from metagenome assemblies. *PeerJ,* 7, pp. e7359.

Katyal, J. C. & Sharma, B. D. (1980). A new technique of plant analysis to resolve iron chlorosis. *Plant and Soil,* 55(1), pp. 105-119.

Kavamura, V. N., Mendes, R., Bargaz, A. & Mauchline, T. H. (2021). Defining the wheat microbiome: Towards microbiome-facilitated crop production. *Computational and Structural Biotechnology Journal,* 19, pp. 1200-1213.

Kayoumu, M., Iqbal, A., Muhammad, N., Li, X., Li, L., Wang, X., Gui, H., Qi, Q., Ruan, S., Guo, R., Zhang, X., Song, M. & Dong, Q. (2023). Phosphorus availability affects the photosynthesis and antioxidant system of contrasting low-P-tolerant cotton genotypes. *Antioxidants (Basel, Switzerland),* 12(2), pp. 466.

Keyes, S., van Veelen, A., McKay Fletcher, D., Scotson, C., Koebernick, N., Petroselli, C., Williams, K., Ruiz, S., Cooper, L., Mayon, R., Duncan, S., Dumont, M., Jakobsen, I., Oldroyd, G., Tkacz, A., Poole, P., Mosselmans, F., Borca, C., Huthwelker, T., Jones, D. L. & Roose, T. (2022). Multimodal correlative imaging and modelling of phosphorus uptake from soil by hyphae of mycorrhizal fungi. *New Phytologist,* 234(2), pp. 688-703.

Khaliq, A., Perveen, S., Alamer, K. H., Zia Ul Haq, M., Rafique, Z., Alsudays, I. M., Althobaiti, A. T., Saleh, M. A., Hussain, S. & Attia, H. (2022). Arbuscular mycorrhizal fungi symbiosis to enhance plant–soil interaction. *Sustainability,* 14(13), pp. 7840.

Khan, K. S., Naveed, M., Qadir, M. F., Yaseen, M. & Siddiqui, M. H. (2023). Bio-organically acidified product-mediated improvements in phosphorus fertilizer utilization, uptake and yielding of *zea mays* in calcareous soil. *Plants,* 12(17), pp. 3072.

Khan, M., Khan, S. & Mohidin, F. (2007). Effect of certain fungal and bacterial phosphate solubilizing microorganisms on the fusarial wilt of tomato. *In:* Velázquez, E. & Rodríguez-Barrueco, C. (eds.) *First International Meeting on Microbial Phosphate Solubilization*. The Netherlands: Springer, Dordrecht.

Khan, M. S., Gao, J., Chen, X., Zhang, M., Yang, F., Du, Y., Moe, T. S., Munir, I., Xue, J. & Zhang, X. (2020). Isolation and characterization of plant growth-promoting endophytic bacteria *Paenibacillus polymyxa* sk1 from *Lilium lancifolium*. *BioMed Research International,* 2020**,** pp. 8650957.

Khan, M. S., Zaidi, A., Ahemad, M., Oves, M. & Wani, P. A. (2010). Plant growth promotion by phosphate solubilizing fungi – current perspective. *Archives of Agronomy and Soil Science,* 56(1)**,** pp. 73-98.

Khan, M. S., Zaidi, A. & Wani, P. A. (2009). Role of phosphate solubilizing microorganisms in sustainable agriculture - a review. *In:* Lichtfouse, E., Navarrete, M., Debaeke, P., Véronique, S. & Alberola, C. (eds.) *Sustainable Agriculture*. The Netherlands: Springer, Dordrecht.

Khan, S., Nadir, S., Iqbal, S., Xu, J., Gui, H., Khan, A. & Ye, L. (2021). Towards a comprehensive understanding of free-living nitrogen fixation. *Circular Agricultural Systems,* 1(1)**,** pp. 1-11.

Kiba, T. & Krapp, A. (2016). Plant nitrogen acquisition under low availability: regulation of uptake and root architecture. *Plant and Cell Physiology,* 57(4)**,** pp. 707-714.

Kim, J. & Rees, D. C. (1994). Nitrogenase and biological nitrogen fixation. *Biochemistry,* 33(2)**,** pp. 389-397.

Kim, K., McDonald, G. & Jordan, D. (1997). Solubilization of hydroxyapatite by Enterobacter agglomerans and cloned Escherichia coli in culture medium. *Biology and Fertility of Soils,* 24(4)**,** pp. 347-352.

Kim, K. Y., Jordan, D. & McDonald, G. A. (1998). Enterobacter agglomerans, phosphate solubilizing bacteria, and microbial activity in soil: Effect of carbon sources. *Soil Biology and Biochemistry,* 30(8)**,** pp. 995-1003.

Klappenbach, J. A., Dunbar, J. M. & Schmidt, T. M. (2000). rRNA operon copy number reflects ecological strategies of bacteria. *Applied and Environmental Microbiology,* 66(4)**,** pp. 1328-1333.

Kloepper, J. W., Lifshitz, R. & Zablotowicz, R. M. (1989). Free-living bacterial inocula for enhancing crop productivity. *Trends in Biotechnology,* 7(2)**,** pp. 39-44.

Koike, N., Hyakumachi, M., Kageyama, K., Tsuyumu, S. & Doke, N. (2001). Induction of systemic resistance in cucumber against several diseases by plant growth-promoting fungi: Lignification and superoxide generation. *European Journal of Plant Pathology,* 107(5)**,** pp. 523-533.

Koksharova, O. A. & Safronov, N. A. (2022). The effects of secondary bacterial metabolites on photosynthesis in microalgae cells. *Biophysical Reviews,* 14(4)**,** pp. 843-856.

Kolde, R. (2019). *Package 'pheatmap'* [Online]. Available: https://cran.r-project.org/web/packages/pheatmap/index.html [Accessed 2 February 2021].

Kosuta, S., Chabaud, M., Lougnon, G., Gough, C., Dénarié, J., Barker, D. G. & Bécard, G. (2003). A diffusible factor from arbuscular mycorrhizal fungi induces symbiosis-specific MtENOD11 expression in roots of Medicago truncatula. *Plant Physiol,* 131(3), pp. 952-962.

Kothari, S., Marschner, H. & Romheld, V. (1991). Contribution of the VA mycorrhizal hyphae in acquisition of phosphorus and zinc by maize grown in a calcareous soil *Plant Soil,* 131, pp. 177–185.

Krüger, M., Stockinger, H., Krüger, C. & Schüßler, A. (2009). DNA-based species level detection of *Glomeromycota*: one PCR primer set for all arbuscular mycorrhizal fungi. *New Phytologist,* 183, pp. 212-223.

Ku, Y.-S., Liao, Y.-J., Chiou, S.-P., Lam, H.-M. & Chan, C. (2024). From trade-off to synergy: microbial insights into enhancing plant growth and immunity. *Plant Biotechnology Journal,* 22(9), pp. 2461-2471.

Kubiku, F. N. M., Mandumbu, R., Nyamangara, J. & Nyamadzawo, G. (2022). Sorghum (*Sorghum bicolor L.*) yield response to rainwater harvesting practices in the semi-arid farming environments of Zimbabwe: a meta-analysis. *Heliyon,* 8(3), pp. e09164.

Kucey, R. (1983). Phosphate-solubilizing bacteria and fungi in various cultivated and virgin Alberta soils. *Canadian Journal of Soil Science,* 63(4), pp. 671-678.

Kumari, A., Sharma, H., Kumari, A., Sharma, P., Pathak, N., Singh, R., Al-Tawaha, A. R., Pandey, D. K., Shekhawat, M. S. & Mandal, S. (2024). Chapter 1 - Movement and signaling of macronutrients in plant system. *In:* Husen, A. (ed.) *Essential Minerals in Plant-Soil Systems*. Elsevier.

Kunkel, B. N. & Harper, C. P. (2017). The roles of auxin during interactions between bacterial plant pathogens and their hosts. *Journal of Experimental Botany,* 69(2), pp. 245-254.

Kuzyakov, Y. & Xu, X. (2013). Competition between roots and microorganisms for nitrogen: mechanisms and ecological relevance. *New Phytologist,* 198(3), pp. 656-669.

Labbé, D., Margesin, R., Schinner, F., Whyte, L. G. & Greer, C. W. (2007). Comparative phylogenetic analysis of microbial communities in pristine and hydrocarbon-contaminated Alpine soils. *FEMS Microbiology Ecology,* 59(2), pp. 466-475.

Ladha, J. K., de Bruijn, F. J. & Malik, K. A. (1997). Introduction: assessing opportunities for nitrogen fixation in rice - a frontier project. *Plant and Soil,* 194(1), pp. 1-10.

Lee, S. J., Kong, M., Harrison, P. & Hijri, M. (2018). Conserved proteins of the RNA interference system in the arbuscular mycorrhizal fungus *Rhizoglomus irregulare* provide new insight into the evolutionary history of *Glomeromycota*. *Genome Biology and Evolution,* 10(1), pp. 328-343.

li, B., Boiarkina, I., Young, B., Yu, W. & Singhal, N. (2017). Prediction of future phosphate rock: A demand based model. *Journal of Environmental Informatics,* 31(1), pp. 1-13.

Li, J., Zhang, L., Yao, G., Zhu, L., Lin, J., Wang, C., Du, B., Ding, Y. & Mei, X. (2022). Synergistic effect of co-culture rhizosphere *Streptomyces*: a promising strategy to enhance antimicrobial activity and plant growth-promoting function. *Frontiers in Microbiology,* 13, pp. 976484.

Li, X.-L., Marschner, H. & George, E. (1991). Acquisition of phosphorus and copper by VA-mycorrhizal hyphae and root-to-shoot transport in white clover. *Plant and Soil,* 136(1), pp. 49-57.

Linderman, R. G. (1988). Mycorrhizal interactions with the rhizosphere microflora: the mycorrhizosphere effect. *Phytopathology,* 78, pp. 366–371.

Liu, H., An, T., Zhao, Y., Du, X., Bi, X., Zhang, Z., Chen, Y. & Wen, J. (2022a). Benzoxazines in the root exudates responsible for nonhost disease resistance of maize to *Phytophthora sojae*. *Phytopathology,* 112(7), pp. 1537-1544.

Liu, L., An, M.-m., Li, X.-j., Han, Z., Li, S.-x. & Li, B. (2022b). Molybdenum-induced effects on nitrogen absorption and utilization under different nitrogen sources in *Vitis vinifera*. *Journal of Plant Interactions,* 17(1), pp. 756-765.

Liu, S., Gao, J., Wang, S., Li, W. & Wang, A. (2023). Community differentiation of rhizosphere microorganisms and their responses to environmental factors at different development stages of medicinal plant *Glehnia littoralis*. *PeerJ,* 11, pp. e14988.

Louis, P. (2017). Different substrate preferences help closely related bacteria to coexist in the gut. *mBio,* 8(6), pp. 10.1128.

Lu, L., Wang, G., Yeung, M., Xi, J. & Hu, H.-Y. (2018). Response of microbial community structure and metabolic profile to shifts of inlet VOCs in a gas-phase biofilter. *AMB Express,* 8, pp. 160.

Lucía, S. & Baca, B. (2001). Mechanisms for protecting nitrogenase from inactivation by oxygen. *Revista latinoamericana de microbiología,* 43(1), pp. 37-49.

Lynch, J. M. & Whipps, J. M. (1990). Substrate flow in the rhizosphere. *Plant and Soil,* 129(1), pp. 1-10.

Ma, W., Tang, S., Dengzeng, Z., Zhang, D., Zhang, T. & Ma, X. (2022). Root exudates contribute to belowground ecosystem hotspots: a review. *Frontiers in Microbiology,* 13**,** pp. 1-19.

Maathuis, F. J. M. (2009). Physiological functions of mineral macronutrients. *Current Opinion in Plant Biology,* 12(3)**,** pp. 250-258.

MacNeil, T., MacNeil, D., Roberts, G. P., Supiano, M. A. & Brill, W. J. (1978). Fine-structure mapping and complementation analysis of *nif* (nitrogen fixation) genes in *Klebsiella pneumoniae*. *Journal of Bacteriology,* 136(1)**,** pp. 253-266.

Madigan, M. T., Martinko, J., Dunlap, P. V. & Clark, D. P. (2008). *Brock Biology of Microorganisms,* U.S., Pearson.

Mahdi, I., Fahsi, N., Hijri, M. & Sobeh, M. (2022). Antibiotic resistance in plant growth promoting bacteria: A comprehensive review and future perspectives to mitigate potential gene invasion risks. *Frontiers in Microbiology,* 13**,** pp. 999988.

Maitra, P., Al-Rashid, J., Barman, N. C., Khan, M. N. M., Mandal, D., Rasul, N. M., Chowdhury, A., El-Sappah, A. H. & Li, J. (2021). Sand particle size and phosphorus amount affect *Rhizophagus irregularis* spore production using in vitro propagated spore as a starter inoculum in rhizosphere of maize (*zea mays*) plantlets. *Journal of Fungi,* 7(10)**,** pp. 846.

Marroquí, S., Zorreguieta, A., Santamaría, C., Temprano, F., Soberón, M., Megías, M. & Downie, J. A. (2001). Enhanced symbiotic performance by *rhizobium tropici* glycogen synthase mutants. *Journal of Bacteriology,* 183(3)**,** pp. 854-864.

Marschner, P. (2023). *Marschner's Mineral Nutrition of Plants In:* Rengel, Z., Cakmak, I. & White, P. J. (eds.) 4th ed. United States: Academic Press.

Marschner, P., Solaiman, Z. & Rengel, Z. (2005). Growth, phosphorus uptake, and rhizosphere microbial-community composition of a phosphorus-efficient wheat cultivar in soils differing in pH. *Journal of Plant Nutrition and Soil Science,* 168(3)**,** pp. 343-351.

Martin, K. J. & Rygiewicz, P. T. (2005). Fungal-specific PCR primers developed for analysis of the ITS region of environmental DNA extracts. *BMC Microbiology,* 5**,** pp. 28.

Martinez-Argudo, I., Little, R., Shearer, N., Johnson, P. & Dixon, R. (2004). The *NifL-NifA* system: a multidomain transcriptional regulatory complex that integrates environmental signals. *Journal of Bacteriology,* 186(3)**,** pp. 601-610.

McCauley, A., Jones, C. & Jacobsen, J. (2009). Plant nutrient functions and deficiency and toxicity symptoms. *Nutrient Management Module,* 9**,** pp. 1-16.

McGill, W. & Cole, C. (1981). Comparative aspects of cycling of organic C, N, S and P through soil organic matter. *Geoderma,* 26(4)**,** pp. 267-286.

McNear, D. (2013). The rhizosphere-roots, soil and everything in between. *Nature Education Knowledge,* 4(3)**,** pp. 1.

Menzel, P., Ng, K. L. & Krogh, A. (2016). Fast and sensitive taxonomic classification for metagenomics with Kaiju. *Nature Communications,* 7(1)**,** pp. 11257.

Merryweather, J. & Fitter, A. (1995). Phosphorus and carbon budgets: mycorrhizal contribution in *Hyacinthoides non -scripta (L.)* Chouard ex Rothm. under natural conditions. *New Phytologist,* 129(4)**,** pp. 619-627.

Misra, M., Sachan, A. & Sachan, S. G. (2020). Current Aspects and Applications of Biofertilizers for Sustainable Agriculture. *In:* Yadav, A. N., Singh, J., Rastegari, A. A. & Yadav, N. (eds.) *Plant Microbiomes for Sustainable Agriculture.* Cham: Springer International Publishing.

Mousavi, S. R., Shahsavari, M. & Rezaei, M. (2011). A general overview on manganese (Mn) importance for crops production. *Australian Journal of Basic and Applied Sciences,* 5(9)**,** pp. 1799-1803.

Munshi, N. & Dave, S. (2005). Ecology of phosphate solubilizers in semi-arid agricultural soils. *Italian Journal of Microbiology,* 45(1)**,** pp. 27-32.

Mushtaq, W. & Fauconnier, M.-L. (2024). Phenolic profiling unravelling allelopathic encounters in agroecology. *Plant Stress,* 13**,** pp. 100523.

Muthulakshmi, L., Mohan, S. & Srinivasan, S. (2024). Chapter 18 - Synthesis of trace elements loaded nanofertilizers and their benefits in agriculture. *In:* Abd-Elsalam, K. A. (ed.) *Nanofertilizer Synthesis.* Elsevier.

Nadeem, S. M., Naveed, M., Zahir, Z. A. & Asghar, H. N. (2013). Plant–microbe interactions for sustainable agriculture: Fundamentals and recent advances. *In:* Arora, N. K. (ed.) *Plant Microbe Symbiosis: Fundamentals and Advances.* New Delhi: Springer India.

Nannipieri, P., Giagnoni, L., Landi, L. & Renella, G. (2011). Role of phosphate enzymes in soil. *In:* Bünemann, E. K., Oberson, A. & Frossard, E. (eds.) *Phosphorus in Action: Biological Processes in Soil Phosphorus Cycling.* Germany: Springer-Verlag Berlin Heidelberg.

Nautiyal, C. S. (1999). An efficient microbiological growth medium for screening phosphate solubilizing microorganisms. *FEMS Microbiology Letters* 170(1)**,** pp. 265-270.

Nelsen, C. E. & Safir, G. R. (1982). Increased drought tolerance of mycorrhizal onion plants caused by improved phosphorus nutrition. *Planta,* 154(5)**,** pp. 407-413.

Nguyen, C. (2003). Rhizodeposition of organic c by plants: mechanisms and controls. *Agronomie, EDP Sciences,* 23(5-6)**,** pp. 375-396.

Niu, Y. F., Chai, R. S., Jin, G. L., Wang, H., Tang, C. X. & Zhang, Y. S. (2013). Responses of root architecture development to low phosphorus availability: a review. *Annals of Botany,* 112(2), pp. 391-408.

Nurk, S., Meleshko, D., Korobeynikov, A. & Pevzner, P. A. (2017). metaSPAdes: a new versatile metagenomic assembler. *Genome Research,* 27(5), pp. 824-834.

Oburger, E., Jones, D. L. & Wenzel, W. W. (2011). Phosphorus saturation and pH differentially regulate the efficiency of organic acid anion-mediated P solubilization mechanisms in soil. *Plant and Soil,* 341(1), pp. 363-382.

OECD/FAO. (2017). *OECD-FAO Agricultural Outlook 2017-2026* [Online]. OECD Publishing. Available: https://www.oecd-ilibrary.org/content/publication/agr_outlook-2017-en [Accessed 9 September 2021].

Ohkuma, M. (2003). Termite symbiotic systems: efficient bio-recycling of lignocellulose. *Applied Microbiology and Biotechnology,* 61(1), pp. 1-9.

Oksanen, J., Simpson, G., Blanchet, F., Kindt, R., Legendre, P., Minchin, P., O'Hara, R., Solymos, P., Stevens, M., Szoecs, E., Wagner, H., Barbour, M., Bedward, M., Bolker, B., Borcard, D., Carvalho, G., Chirico, M., De Caceres, M., Durand, S., Evangelista, H., FitzJohn, R., Friendly, M., Furneaux, B., Hannigan, G., Hill, M., Lahti, L., McGlinn, D., Ouellette, M., Ribeiro Cunha, E., Smith, T., Stier, A., Ter Braak, C. & Weedon, J. (2019). *vegan: Community Ecology Package* [Online]. Available: https://CRAN.R-project.org/package=vegan [Accessed 02/01 2020].

Oldroyd, G. E., Murray, J. D., Poole, P. S. & Downie, J. A. (2011). The rules of engagement in the legume-rhizobial symbiosis. *Annual Review of Genetics,* 45, pp. 119-144.

Otaka, J., Subbarao, G. V., MingLi, J., Ono, H. & Yoshihashi, T. (2023). Isolation and characterization of the hydrophilic BNI compound, 6-methoxy-2(3H)-benzoxazolone (MBOA), from maize roots. *Plant and Soil,* 489(1), pp. 341-359.

Palanisamy, S., Singh, A., Hema, P., Lakshmi, P. & Glory, K. (2024). Association of microbial community for soil health through commercialization of PGPR/PGPRF development. *East African Scholars Journal of Agriculture and Life Sciences* 7 (3), pp.

Pan, L. & Cai, B. (2023). Phosphate-solubilizing bacteria: advances in their physiology, molecular mechanisms and microbial community effects. *Microorganisms,* 11(12), pp. 2904.

Pantigoso, H. A., Yuan, J., He, Y., Guo, Q., Vollmer, C. & Vivanco, J. M. (2020). Role of root exudates on assimilation of phosphorus in young and old *Arabidopsis thaliana* plants. *PLoS One,* 15(6), pp. e0234216.

Parada, A. E., Needham, D. M. & Fuhrman, J. A. (2016). Every base matters: assessing small subunit rRNA primers for marine microbiomes with mock communities, time series and global field samples. *Environ Microbiol,* 18(5)**,** pp. 1403-1414.

Parada, M., Vinardell, J. M., Ollero, F. J., Hidalgo, Á., Gutiérrez, R., Buendía-Clavería, A. M., Lei, W., Margaret, I., López-Baena, F. J., Gil-Serrano, A. M., Rodríguez-Carvajal, M. A., Moreno, J. & Ruiz-Sainz, J. E. (2006). *Sinorhizobium fredii* HH103 mutants affected in capsular polysaccharide (KPS) are impaired for nodulation with soybean and *Cajanus cajan*. *Molecular Plant-Microbe Interactions,* 19(1)**,** pp. 43-52.

Park, K. H., Lee, C. Y. & Son, H. J. (2009). Mechanism of insoluble phosphate solubilization by *Pseudomonas fluorescens* RAF15 isolated from ginseng rhizosphere and its plant growth-promoting activities. *Letters in Applied Microbiology,* 49(2)**,** pp. 222-228.

Parks, D. H., Chuvochina, M., Chaumeil, P.-A., Rinke, C., Mussig, A. J. & Hugenholtz, P. (2020). A complete domain-to-species taxonomy for Bacteria and Archaea. *Nature Biotechnology,* 38(9)**,** pp. 1079-1086.

Parks, D. H., Imelfort, M., Skennerton, C. T., Hugenholtz, P. & Tyson, G. W. (2015). CheckM: assessing the quality of microbial genomes recovered from isolates, single cells, and metagenomes. *Genome Research,* 25(7)**,** pp. 1043-1055.

Parks, E. J., Olson, G. J., Brinckman, F. E. & Baldi, F. (1990). Characterization by high performance liquid chromatography (HPLC) of the solubilization of phosphorus in iron ore by a fungus. *Journal of Industrial Microbiology,* 5(2)**,** pp. 183-189.

Parniske, M. (2008). Arbuscular mycorrhiza: the mother of plant root endosymbioses. *Nat Rev Microbiol,* 6(10)**,** pp. 763-775.

Patra, A., Sharma, V. K., Chattopadhyay, A., Mohapatra, K. K. & Rakshit, A. (2021). Rhizodeposition: an unseen teaser of nature and its prospects in nutrients dynamics. *In:* Rakshit, A., Singh, S. K., Abhilash, P. C. & Biswas, A. (eds.) *Soil Science: Fundamentals to Recent Advances*. Singapore: Springer Singapore.

Patten, C. L. & Glick, B. R. (2002). Role of *pseudomonas putida* indoleacetic acid in development of the host plant root system. *Applied and Environmental Microbiology,* 68(8)**,** pp. 3795-3801.

Pedras, M. S. C. & Yaya, E. E. (2015). Plant chemical defenses: are all constitutive antimicrobial metabolites phytoanticipins? *Natural Product Communications,* 10(1)**,** pp. 209-218.

Peña-Espinoza, M., Boas, U., Williams, A. R., Thamsborg, S. M., Simonsen, H. T. & Enemark, H. L. (2015). Sesquiterpene lactone containing extracts from two cultivars of forage chicory (*Cichorium intybus*) show distinctive chemical profiles and *in vitro*

activity against *Ostertagia ostertagi*. *International Journal for Parasitology: Drugs and Drug Resistance,* 5(3)**,** pp. 191-200.

Peters, J. W. & Szilagyi, R. K. (2006). Exploring new frontiers of nitrogenase structure and mechanism. *Current Opinion in Chemical Biology,* 10(2)**,** pp. 101-108.

Phillips, J. M. & Hayman, D. S. (1970). Improved procedures for clearing roots and staining parasitic and vesicular-arbuscular mycorrhizal fungi for rapid assessment of infection. *Transactions of the British Mycological Society,* 55(1)**,** pp. 158-161.

Pineda, A., Zheng, S.-J., Van Loon, J. J. A., Pieterse, C. M. J. & Dicke, M. (2010). Helping plants to deal with insects: the role of beneficial soil-borne microbes. *Trends in Plant Science,* 15(9)**,** pp. 507-514.

Podile, A. & Kishore, G. (2006). Plant growth-promoting rhizobacteria. *In:* Gnanamanickam, S. S. (ed.) *Plant-Associated Bacteria*. Netherland: Springer.

Pozo, M. J. & Azcón-Aguilar, C. (2007). Unraveling mycorrhiza-induced resistance. *Curr Opin Plant Biol,* 10(4)**,** pp. 393-398.

Priyanka, Srivastava, S. & Sharma, S. (2022). Metabolomic insight into the synergistic mechanism of action of a bacterial consortium in plant growth promotion. *Journal of Bioscience and Bioengineering,* 134(5)**,** pp. 399-406.

Qiu, J., Cao, J., Lan, G., Liang, Y., Wang, H. & Li, Q. (2020). The influence of land use patterns on soil bacterial community structure in the Karst Graben Basin of Yunnan Province, China. *Forests,* 11(1)**,** pp. 51.

Quast, C., Pruesse, E., Yilmaz, P., Gerken, J., Schweer, T., Yarza, P., Peplies, J. & Glöckner, F. O. (2013). The SILVA ribosomal RNA gene database project: improved data processing and web-based tools. *Nucleic Acids Research,* 41(D1)**,** pp. D590-D596.

Ramandi, A., Nourashrafeddin, S. M., Marashi, S. H. & Seifi, A. (2023). Microbiome contributes to phenotypic plasticity in saffron crocus. *World Journal of Microbiology and Biotechnology,* 39(1)**,** pp. 9.

Ramírez, M., Valderrama, B., Arredondo-Peter, R., Soberón, M., Mora, J. & Hernández, G. (1999). *Rhizobium etli* genetically engineered for the heterologous expression of *vitreoscilla sp*. hemoglobin: effects on free-living and symbiosis. *Molecular Plant-Microbe Interactions,* 12(11)**,** pp. 1008-1015.

Raouani, N. E. H., Claverie, E., Randoux, B., Chaveriat, L., Yaseen, Y., Yada, B., Martin, P., Cabrera, J. C., Jacques, P., Reignault, P., Magnin-Robert, M. & Lounès-Hadj Sahraoui, A. (2022). Bio-inspired rhamnolipids, cyclic lipopeptides and a chito-oligosaccharide confer protection against wheat powdery mildew and inhibit conidia germination. *Molecules,* 27(19)**,** pp. 6672.

Raymond, J., Siefert, J. L., Staples, C. R. & Blankenship, R. E. (2004). The natural history of nitrogen fixation. *Molecular Biology and Evolution,* 21(3)**,** pp. 541-554.

Reed, S. C., Cleveland, C. C. & Townsend, A. R. (2011). Functional ecology of free-living nitrogen fixation: a contemporary perspective. *Annual Review of Ecology, Evolution, and Systematics,* 42(1)**,** pp. 489-512.

Riaz, U., Murtaza, G., Anum, W., Samreen, T., Sarfraz, M. & Nazir, M. Z. (2021). Plant growth-promoting rhizobacteria (PGPR) as biofertilizers and biopesticides. *In:* Hakeem, K. R., Dar, G. H., Mehmood, M. A. & Bhat, R. A. (eds.) *Microbiota and Biofertilizers: A Sustainable Continuum for Plant and Soil Health.* Cham: Springer International Publishing.

Richards, B. N. & Voigt, G. K. (1964). Role of mycorrhiza in nitrogen fixation. *Nature,* 201(4916)**,** pp. 310-311.

Richardson, A. (1994). Soil microorganisms and phosphorus availability. *In:* Pankhurst, C., Doubeand, B. & Gupta, V. (eds.) *Soil Biota: Management in Sustainable Farming Systems.* Victoria, Australia: CSIRO.

Richardson, A., P. Lynch, J., Ryan, P., Delhaize, E., Smith, F., E. Smith, S., Harvey, P., Ryan, M., Veneklaas, E., Lambers, H., Oberson, A., Culvenor, R. & Simpson, R. (2011). Plant and microbial strategies to improve phosphorus efficiency of agriculture. *Plant Soil,* 349**,** pp. 121-156.

Richardson, A. E., Barea, J.-M., McNeill, A. M. & Prigent-Combaret, C. (2009a). Acquisition of phosphorus and nitrogen in the rhizosphere and plant growth promotion by microorganisms. *Plant and Soil,* 321(1)**,** pp. 305-339.

Richardson, A. E., Hadobas, P. A., Hayes, J. E., O'Hara, C. P. & Simpson, R. J. (2001). Utilization of phosphorus by pasture plants supplied with myo-inositol hexaphosphate is enhanced by the presence of soil micro-organisms. *Plant and Soil,* 229(1)**,** pp. 47-56.

Richardson, A. E., Hocking, P. J., Simpson, R. J. & George, T. S. (2009b). Plant mechanisms to optimise access to soil phosphorus. *Crop and Pasture Science,* 60(2)**,** pp. 124-143.

Richardson, A. E. & Simpson, R. J. (2011). Soil microorganisms mediating phosphorus availability update on microbial phosphorus. *Plant Physiology,* 156(3)**,** pp. 989-996.

Ridgman, W. J. (1993). Pesticides, cereal farming and the environment: the Boxworth project. *The Journal of Agricultural Science,* 121(2)**,** pp. 295-296.

Rillig, M. C. & Mummey, D. L. (2006). Mycorrhizas and soil structure. *New Phytologist,* 171(1)**,** pp. 41-53.

Rinaudo, V., Bàrberi, P., Giovannetti, M. & Van der Heijden, M. (2010). Mycorrhizal fungi suppress aggressive agricultural weeds. *Plant and Soil,* 333(1), pp. 7-20.

Roberts, G. P., MacNeil, T., MacNeil, D. & Brill, W. J. (1978). Regulation and characterization of protein products coded by the *nif* (nitrogen fixation) genes of *Klebsiella pneumoniae*. *Journal of Bacteriology,* 136(1), pp. 267-279.

Rodríguez, H. & Fraga, R. (1999). Phosphate solubilizing bacteria and their role in plant growth promotion. *Biotechnology Advances,* 17(4–5), pp. 319-339.

Rodríguez, H., Fraga, R., Gonzalez, T. & Bashan, Y. (2006). Genetics of phosphate solubilization and its potential applications for improving plant growth-promoting bacteria. *Plant and Soil,* 287(1), pp. 15-21.

Rojas-Jimenez, K., Wurzbacher, C., Bourne, E. C., Chiuchiolo, A., Priscu, J. C. & Grossart, H.-P. (2017). Early diverging lineages within Cryptomycota and Chytridiomycota dominate the fungal communities in ice-covered lakes of the McMurdo Dry Valleys, Antarctica. *Scientific Reports,* 7, pp. 15348.

Roller, B. R. K., Stoddard, S. F. & Schmidt, T. M. (2016). Exploiting rRNA operon copy number to investigate bacterial reproductive strategies. *Nature Microbiology,* 1, pp. 16160.

Rubio, L. M. & Ludden, P. W. (2005). Maturation of nitrogenase: a biochemical puzzle. *Journal of Bacteriology,* 187(2), pp. 405-414.

Rubio, L. M. & Ludden, P. W. (2008). Biosynthesis of the iron-molybdenum cofactor of nitrogenase. *Annual Review of Microbiology,* 62(1), pp. 93-111.

Ruiz-Lozano, J. M., Azcon, R. & Gomez, M. (1995). Effects of arbuscular-mycorrhizal glomus species on drought tolerance: physiological and nutritional plant responses. *Appl Environ Microbiol,* 61(2), pp. 456-460.

Sagwal, A., Wadhwa, P., Shubham & Kaushal, S. (2023). Essentiality of micronutrients in soil: a review. *International Journal of Plant & Soil Science,* 35(24), pp. 56-65.

Sah, S., Krishnani, S. & Singh, R. (2021). *Pseudomonas* mediated nutritional and growth promotional activities for sustainable food security. *Current Research in Microbial Sciences,* 2, pp. 100084.

Sait, M., Hugenholtz, P. & Janssen, P. H. (2002). Cultivation of globally distributed soil bacteria from phylogenetic lineages previously only detected in cultivation-independent surveys. *Environmental Microbiology,* 4(11), pp. 654-666.

Salazar, G., Paoli, L., Alberti, A., Huerta-Cepas, J., Ruscheweyh, H. J., Cuenca, M., Field, C. M., Coelho, L. P., Cruaud, C., Engelen, S., Gregory, A. C., Labadie, K., Marec, C., Pelletier, E., Royo-Llonch, M., Roux, S., Sánchez, P., Uehara, H., Zayed, A. A., Zeller, G.,

Carmichael, M., Dimier, C., Ferland, J., Kandels, S., Picheral, M., Pisarev, S., Poulain, J., Acinas, S. G., Babin, M., Bork, P., Bowler, C., de Vargas, C., Guidi, L., Hingamp, P., Iudicone, D., Karp-Boss, L., Karsenti, E., Ogata, H., Pesant, S., Speich, S., Sullivan, M. B., Wincker, P. & Sunagawa, S. (2019). Gene expression changes and community turnover differentially shape the global ocean metatranscriptome. *Cell,* 179(5)**,** pp. 1068-1083.e1021.

Sarhan, M. S., Patz, S., Hamza, M. A., Youssef, H. H., Mourad, E. F., Fayez, M., Murphy, B., Ruppel, S. & Hegazi, N. A. (2018). G3 phylochip analysis confirms the promise of plant-based culture media for unlocking the composition and diversity of the maize root microbiome and for recovering unculturable candidate divisions/phyla. *Microbes and Environments,* 33(3)**,** pp. 317-325.

Savci, S. (2012). An agricultural pollutant: chemical fertilizer. *International Journal of Environmental Science and Development,* 3(1)**,** pp. 73.

Scheublin, T. R., Sanders, I. R., Keel, C. & van der Meer, J. R. (2010a). Characterisation of microbial communities colonising the hyphal surfaces of arbuscular mycorrhizal fungi. *The ISME Journal,* 4(6)**,** pp. 752-763.

Scheublin, T. R., Sanders, I. R., Keel, C. & van der Meer, J. R. (2010b). Characterisation of microbial communities colonising the hyphal surfaces of arbuscular mycorrhizal fungi. *The ISME Journal,* 4**,** pp. 752-763.

Schlemper, T. R., Leite, M. F. A., Lucheta, A. R., Shimels, M., Bouwmeester, H. J., van Veen, J. A. & Kuramae, E. E. (2017). Rhizobacterial community structure differences among sorghum cultivars in different growth stages and soils. *FEMS Microbiology Ecology,* 93(8)**,** pp. 1-11.

Schoch, C. L., Seifert, K. A., Huhndorf, S., Robert, V., Spouge, J. L., Levesque, C. A., Chen, W., Consortium, F. B., List, F. B. C. A., Bolchacova, E., Voigt, K., Crous, P. W., Miller, A. N., Wingfield, M. J., Aime, M. C., An, K.-D., Bai, F.-Y., Barreto, R. W., Begerow, D., Bergeron, M.-J., Blackwell, M., Boekhout, T., Bogale, M., Boonyuen, N., Burgaz, A. R., Buyck, B., Cai, L., Cai, Q., Cardinali, G., Chaverri, P., Coppins, B. J., Crespo, A., Cubas, P., Cummings, C., Damm, U., de Beer, Z. W., de Hoog, G. S., Del-Prado, R., Dentinger, B., Diéguez-Uribeondo, J., Divakar, P. K., Douglas, B., Dueñas, M., Duong, T. A., Eberhardt, U., Edwards, J. E., Elshahed, M. S., Fliegerova, K., Furtado, M., García, M. A., Ge, Z.-W., Griffith, G. W., Griffiths, K., Groenewald, J. Z., Groenewald, M., Grube, M., Gryzenhout, M., Guo, L.-D., Hagen, F., Hambleton, S., Hamelin, R. C., Hansen, K., Harrold, P., Heller, G., Herrera, C., Hirayama, K., Hirooka, Y., Ho, H.-M., Hoffmann, K., Hofstetter, V., Högnabba, F., Hollingsworth, P. M., Hong, S.-B., Hosaka, K., Houbraken, J., Hughes, K., Huhtinen, S., Hyde, K. D., James, T., Johnson, E. M., Johnson, J. E., Johnston, P. R., Jones, E. B. G., Kelly, L. J., Kirk, P. M., Knapp, D. G., Kõljalg, U., Kovács, G. M., Kurtzman, C. P., Landvik, S., Leavitt, S. D., Liggenstoffer, A. S., Liimatainen, K., Lombard, L., Luangsa-ard, J. J., Lumbsch, H. T., Maganti, H., Maharachchikumbura, S. S. N., Martin, M. P., May, T. W., et al. (2012). Nuclear ribosomal internal transcribed spacer (ITS) region as a universal DNA barcode marker for *Fungi*. *Proceedings of the National Academy of Sciences,* 109(16)**,** pp. 6241-6246.

Schoenborn, L., Yates, P. S., Grinton, B. E., Hugenholtz, P. & Janssen, P. H. (2004). Liquid serial dilution is inferior to solid media for isolation of cultures representative of the phylum-level diversity of soil bacteria. *Applied and Environmental Microbiology,* 70(7), pp. 4363-4366.

Schulz-Bohm, K., Martín-Sánchez, L. & Garbeva, P. (2017). Microbial volatiles: small molecules with an important role in intra- and inter-kingdom interactions. *Frontiers in Microbiology,* 8, pp. 1-10.

Schulz-Bohm, K., Zweers, H., de Boer, W. & Garbeva, P. (2015). A fragrant neighborhood: volatile mediated bacterial interactions in soil. *Frontiers in Microbiology,* 6, pp. 1-11.

Schwachtje, J., Karojet, S., Kunz, S., Brouwer, S. & van Dongen, J. T. (2012). Plant-growth promoting effect of newly isolated rhizobacteria varies between two Arabidopsis ecotypes. *Plant Signaling & Behavior,* 7(6), pp. 623-627.

Schwyn, B. & Neilands, J. B. (1987). Universal chemical assay for the detection and determination of siderophores. *Analytical Biochemistry,* 160(1), pp. 47-56.

Shah, V. K., Stacey, G. & Brill, W. J. (1983). Electron transport to nitrogenase. Purification and characterization of pyruvate: flavodoxin oxidoreductase. The *nifJ* gene product. *Journal of Biological Chemistry,* 258(19), pp. 12064-12068.

Shapiro, R. S., Robbins, N. & Cowen, L. E. (2011). Regulatory circuitry governing fungal development, drug resistance, and disease. *Microbiology and Molecular Biology Reviews,* 75(2), pp. 213-267.

Sharma, A., Johri, B. N., Sharma, A. K. & Glick, B. R. (2003). Plant growth-promoting bacterium *Pseudomonas sp.* strain GRP3 influences iron acquisition in mung bean (*Vigna radiata* L. Wilzeck). *Soil Biology and Biochemistry,* 35(7), pp. 887-894.

Sharma, S. B., Sayyed, R. Z., Trivedi, M. H. & Gobi, T. A. (2013). Phosphate solubilizing microbes: sustainable approach for managing phosphorus deficiency in agricultural soils. *SpringerPlus,* 2(1), pp. 587.

Shehzadi, N., Mahmood, A., Kaleem, M., Chishti, M. S., Bashir, H., Hashem, A., Abd-Allah, E. F., Shahid, H. & Ishtiaq, A. (2024). Zinc and nitrogen mediate the regulation of growth, leading to the upregulation of antioxidant aptitude, physio-biochemical traits, and yield in wheat plants. *Scientific Reports,* 14(1), pp. 12897.

Shen, J., Yuan, L., Zhang, J., Li, H., Bai, Z., Chen, X., Zhang, W. & Zhang, F. (2011). Phosphorus dynamics: from soil to plant. *Plant Physiology,* 156(3), pp. 997.

Shiferaw, B., Smale, M., Braun, H.-J., Duveiller, E., Reynolds, M. & Muricho, G. (2013). Crops that feed the world 10. Past successes and future challenges to the role played by wheat in global food security. *Food Security,* 5(3), pp. 291-317.

Sieber, C. M. K., Probst, A. J., Sharrar, A., Thomas, B. C., Hess, M., Tringe, S. G. & Banfield, J. F. (2018). Recovery of genomes from metagenomes via a dereplication, aggregation and scoring strategy. *Nature Microbiology,* 3(7), pp. 836-843.

Sikes, B. A. (2010). When do arbuscular mycorrhizal fungi protect plant roots from pathogens? *Plant Signal Behav,* 5(6), pp. 763-765.

Singh, A., Yadav, V. K., Chundawat, R. S., Soltane, R., Awwad, N. S., Ibrahium, H. A., Yadav, K. K. & Vicas, S. I. (2023). Enhancing plant growth promoting rhizobacterial activities through consortium exposure: A review. *Frontiers in Bioengineering and Biotechnology,* 11, pp. 1099999.

Sippel, D. & Einsle, O. (2017). The structure of vanadium nitrogenase reveals an unusual bridging ligand. *Nature Chemical Biology,* 13(9), pp. 956-960.

Skoglund, E., Carlsson, N.-G. & Sandberg, A.-S. (2009). Chapter 11-Phytate. *In:* Shewry, P. R. & Ward, J. L. (eds.) *Healthgrain Methods: Analysis of Bioactive Components in Small Grain Cereals*. Saint Paul, Minnesota, US: American Association of Cereal Chemists (AACC) International Press.

Smalla, K., Wieland, G., Buchner, A., Zock, A., Parzy, J., Kaiser, S., Roskot, N., Heuer, H. & Berg, G. (2001). Bulk and rhizosphere soil bacterial communities studied by denaturing gradient gel electrophoresis: plant-dependent enrichment and seasonal shifts revealed. *Applied and Environmental Microbiology,* 67(10), pp. 4742-4751.

Smith, S. E., Jakobsen, I., Grønlund, M. & Smith, F. A. (2011). Roles of arbuscular mycorrhizas in plant phosphorus nutrition: interactions between pathways of phosphorus uptake in arbuscular mycorrhizal roots have important implications for understanding and manipulating plant phosphorus acquisition. *Plant physiology,* 156(3), pp. 1050–1057.

Smith, S. E. & Read, D. (2008). *Mycorrhizal Symbiosis,* London, Academic Press.

Solomon, W., Janda, T. & Molnár, Z. (2024). Unveiling the significance of rhizosphere: implications for plant growth, stress response, and sustainable agriculture. *Plant Physiology and Biochemistry,* 206, pp. 108290.

Song, F., Han, X., Zhu, X. & Herbert, S. J. (2012). Response to water stress of soil enzymes and root exudates from drought and non-drought tolerant corn hybrids at different growth stages. *Canadian Journal of Soil Science,* 92(3), pp. 501-507.

Souchie, E. L., Azcón, R., Barea, J. M., Saggin-Júnior, O. J. & Silva, E. M. R. d. (2006). Phosphate solubilization and synergism between P-solubilizing and arbuscular mycorrhizal fungi. *Pesquisa Agropecuária Brasileira,* 41(9), pp. 1405-1411.

Spaepen, S. & Vanderleyden, J. (2011). Auxin and plant-microbe interactions. *Cold Spring Harbor Perspectives in Biology,* 3(4), pp. a001438.

Spaepen, S., Vanderleyden, J. & Remans, R. (2007). Indole-3-acetic acid in microbial and microorganism-plant signaling. *FEMS Microbiology Reviews,* 31(4), pp. 425-448.

Srikamwang, C., Onsa, N. E., Sunanta, P., Sangta, J., Chanway, C. P., Thanakkasaranee, S. & Sommano, S. R. (2023). Role of microbial volatile organic compounds in promoting plant growth and disease resistance in horticultural production. *Plant Signaling & Behavior,* 18(1), pp. 2227440.

Srinivasan, S., Jnana, A. & Murali, T. S. (2024). Modeling microbial community networks: methods and tools for studying microbial interactions. *Microbial Ecology,* 87(1), pp. 56.

Srivastava, S. & Sharma, S. (2023). Insight into exopolysaccharide-mediated stress tolerance in plants: a feasible approach towards the development of next-generation bioformulations. *Journal of Soil Science and Plant Nutrition,* 23(1), pp. 22-33.

Steen, A. D., Crits-Christoph, A., Carini, P., DeAngelis, K. M., Fierer, N., Lloyd, K. G. & Cameron Thrash, J. (2019). High proportions of bacteria and archaea across most biomes remain uncultured. *The ISME Journal,* 13(12), pp. 3126-3130.

Steinrücken, P., Jackson, S., Müller, O., Puntervoll, P. & Kleinegris, D. M. M. (2023). A closer look into the microbiome of microalgal cultures. *Frontiers in Microbiology,* 14, pp. 1108018.

Stewart, E. J. (2012). Growing unculturable bacteria. *Journal of Bacteriology,* 194(16), pp. 4151-4160.

Stracke, S., Kistner, C., Yoshida, S., Mulder, L., Sato, S., Kaneko, T., Tabata, S., Sandal, N., Stougaard, J., Szczyglowski, K. & Parniske, M. (2002). A plant receptor-like kinase required for both bacterial and fungal symbiosis. *Nature,* 417(6892), pp. 959-962.

Strickland, M. S., McCulley, R. L., Nelson, J. A. & Bradford, M. A. (2015). Compositional differences in simulated root exudates elicit a limited functional and compositional response in soil microbial communities. *Frontiers in Microbiology,* 6, pp. 1-9.

Sun, C., Li, Q., Han, L., Chen, X. & Zhang, F. (2022). The effects of allelochemicals from root exudates of *Flaveria bidentis* on two *Bacillus* species. *Frontiers in Plant Science,* 13, pp. 1001208.

Sutherland, I. W. (2001). Biofilm exopolysaccharides: a strong and sticky framework. *Microbiology,* 147(1), pp. 3-9.

Swaby, R. & Sperber, J. (1958). Phosphate dissolving microorganisms in the rhizosphere of legumes, nutrition of the legumes. *Soils & Fert.,* 22(286), pp. 289-294.

Taiz, L. (2013). Agriculture, plant physiology, and human population growth: past, present, and future. *Theoretical and Experimental Plant Physiology,* 25(3), pp. 167-181.

Tao, L. & Zhao, Z. (2005). Arbuscular mycorrhizas in a hot and arid ecosystem in southwest China. *Applied Soil Ecology,* 29(2), pp. 135-141.

Tarafdar, J. C., Yadav, R. S. & Meena, S. C. (2001). Comparative efficiency of acid phosphatase originated from plant and fungal sources. *Journal of Plant Nutrition and Soil Science,* 164(3), pp. 279-282.

Tariq, M. R., Shaheen, F., Mustafa, S., Ali, S., Fatima, A., Shafiq, M., Safdar, W., Sheas, M. N., Hameed, A. & Nasir, M. A. (2022). Phosphate solubilizing microorganisms isolated from medicinal plants improve growth of mint. *PeerJ,* 10, pp. e13782.

Terry, N. (1976). Effects of sulfur on the photosynthesis of intact leaves and isolated chloroplasts of sugar beets. *Plant physiology,* 57(4), pp. 477-479.

Thepbandit, W. & Athinuwat, D. (2024). Rhizosphere microorganisms supply availability of soil nutrients and induce plant defense. *Microorganisms,* 12(3), pp. 558.

Thoenen, L., Kreuzer, M., Pestalozzi, C., Florean, M., Mateo, P., Züst, T., Wei, A., Giroud, C., Rouyer, L., Gfeller, V., Notter, M. D., Knoch, E., Hapfelmeier, S., Becker, C., Schandry, N., Robert, C. A. M., Köllner, T. G., Bruggmann, R., Erb, M. & Schlaeppi, K. (2024). The lactonase BxdA mediates metabolic specialisation of maize root bacteria to benzoxazinoids. *Nature Communications,* 15, pp. 6535.

Tiecher, T., Fontoura, S. M. V., Ambrosini, V. G., Araújo, E. A., Alves, L. A., Bayer, C. & Gatiboni, L. C. (2023). Soil phosphorus forms and fertilizer use efficiency are affected by tillage and soil acidity management. *Geoderma,* 435, pp. 116495.

Tisserant, E., Malbreil, M., Kuo, A., Kohler, A., Symeonidi, A., Balestrini, R., Charron, P., Duensing, N., Frei dit Frey, N., Gianinazzi-Pearson, V., Gilbert, L. B., Handa, Y., Herr, J. R., Hijri, M., Koul, R., Kawaguchi, M., Krajinski, F., Lammers, P. J., Masclaux, F. G., Murat, C., Morin, E., Ndikumana, S., Pagni, M., Petitpierre, D., Requena, N., Rosikiewicz, P., Riley, R., Saito, K., San Clemente, H., Shapiro, H., van Tuinen, D., Bécard, G., Bonfante, P., Paszkowski, U., Shachar-Hill, Y. Y., Tuskan, G. A., Young, J. P. W., Sanders, I. R., Henrissat, B., Rensing, S. A., Grigoriev, I. V., Corradi, N., Roux, C. & Martin, F. (2013). Genome of an arbuscular mycorrhizal fungus provides insight into the oldest plant symbiosis. *Proceedings of the National Academy of Sciences,* 110(50), pp. 20117-20122.

Tkacz, A., Pini, F., Turner, T. R., Bestion, E., Simmonds, J., Howell, P., Greenland, A., Cheema, J., Emms, D. M., Uauy, C. & Poole, P. S. (2020). Agricultural selection of wheat has been shaped by plant-microbe interactions. *Frontiers in Microbiology,* 11(132), pp.

Tobar, R., Azcón, R. & Barea, J. (1994). Improved nitrogen uptake and transport from 15N labelled nitrate by external hyphae of arbuscular mycorrhiza under wate' stressed conditions. *New Phytologist,* 126, pp. 119-122.

Toljander, J. F., Lindahl, B. D., Paul, L. R., Elfstrand, M. & Finlay, R. D. (2007). Influence of arbuscular mycorrhizal mycelial exudates on soil bacterial growth and community structure. *FEMS Microbiology Ecology,* 61(2), pp. 295-304.

Tong, X.-n., Wang, X.-z., He, X.-j., Wang, Z. & Li, W.-x. (2020). Effects of antibiotics on microbial community structure and microbial functions in constructed wetlands treated with artificial root exudates. *Environmental Science: Processes & Impacts,* 22(1), pp. 217-226.

Toussaint, J. P., St-Arnaud, M. & Charest, C. (2004). Nitrogen transfer and assimilation between the arbuscular mycorrhizal fungus Glomus intraradices Schenck & Smith and Ri T-DNA roots of Daucus carota L. in an in vitro compartmented system. *Can J Microbiol,* 50(4), pp. 251-260.

Trolove, S. N., Hedley, M. J., Kirk, G. J. D., Bolan, N. S. & Loganathan, P. (2003). Progress in selected areas of rhizosphere research on P acquisition. *Soil Research,* 41(3), pp. 471-499.

Trond, M., Shahab, S., Solveig, L., Even, H. & Alexander, H. R. (2015). Coaggregation between *Rhodococcus* and *Acinetobacter* strains isolated from the food industry. *Canadian Journal of Microbiology,* 61(7), pp. 503-512.

Tschech, A. & Pfennig, N. (1984). Growth yield increase linked to caffeate reduction in *Acetobacterium woodii*. *Archives of Microbiology,* 137(2), pp. 163-167.

Uchida, R. (2000). Essential nutrients for plant growth: nutrient functions and deficiency symptoms. *Plant Nutrient Management In Hawaii's Soils,* 4, pp. 31-55.

United Nations-Department of Economic and Social Affairs-Population Division. (2019). *World Population Prospects 2019: Highlights (ST/ESA/SER.A/423* [Online]. Available: https://population.un.org/wpp/Publications/Files/WPP2019_Highlights.pdf [Accessed 9 September 2021].

USDA. (2021). *World agricultural production* [Online]. USA: Office of Global Analysis, Foreign Agricultural Service. Available: https://www.fas.usda.gov/data/world-agricultural-production [Accessed 15 September 2021].

Vaidya, B. P., Hagmann, D. F., Haramuniz, J., Krumins, J. A. & Goodey, N. M. (2022). Artificial root exudates restore microbial functioning in a metal contaminated, barren, inactive soil. *Environmental Pollution,* 312, pp. 120007.

VanEtten, H. D., Mansfield, J. W., Bailey, J. A. & Farmer, E. E. (1994). Two classes of plant antibiotics: phytoalexins versus" phytoanticipins". *The Plant Cell,* 6(9), pp. 1191-1192.

Vassilev, N., Vassileva, M. & Nikolaeva, I. (2006). Simultaneous P-solubilizing and biocontrol activity of microorganisms: potentials and future trends. *Applied Microbiology and Biotechnology,* 71(2)**,** pp. 137-144.

Ventura, M., Canchaya, C., Tauch, A., Chandra, G., Fitzgerald, G. F., Chater, K. F. & van Sinderen, D. (2007). Genomics of Actinobacteria: tracing the evolutionary history of an ancient phylum. *Microbiology and Molecular Biology Reviews,* 71(3)**,** pp. 495-548.

Vera-Gargallo, B., Hernández, M., Dumont, M. G. & Ventosa, A. (2023). Thrive or survive: prokaryotic life in hypersaline soils. *Environ Microbiome,* 18(1)**,** pp. 17.

Vessey, J. K. (2003). Plant growth promoting rhizobacteria as biofertilizers. *Plant and Soil,* 255(2)**,** pp. 571-586.

Vierheilig, H., Coughlan, A. P., Wyss, U. & Piché, Y. (1998). Ink and vinegar, a simple staining technique for arbuscular-mycorrhizal fungi. *Applied and Environmental Microbiology,* 64(12)**,** pp. 5004-5007.

Vives-Peris, V., de Ollas, C., Gómez-Cadenas, A. & Pérez-Clemente, R. M. (2020). Root exudates: from plant to rhizosphere and beyond. *Plant Cell Reports,* 39(1)**,** pp. 3-17.

Von Braun, J. (2007). *The World Food Situtation: New Driving Forces and Required Actions,* Washington, DC, International Food Policy Research Institute.

Wairich, A., Aung, M. S., Ricachenevsky, F. K. & Masuda, H. (2024). You can't always get as much iron as you want: how rice plants deal with excess of an essential nutrient. *Frontiers in Plant Science,* 15**,** pp. 1-14.

Wakelin, S. A., Warren, R. A., Harvey, P. R. & Ryder, M. H. (2004). Phosphate solubilization by *Penicillium spp.* closely associated with wheat roots. *Biology and Fertility of Soils,* 40(1)**,** pp. 36-43.

Wang, F. (2014). *Mechanisms of microbe-mediated soil organic phosphorus turnover in the hyphosphere.* Ph.D. Thesis, China Agricultural University , Beijing.

Wang, F. & Feng, G. (2021). Arbuscular mycorrhizal fungi interactions in the rhizosphere. *In:* Gupta, V. V. S. R. & Sharma, A. K. (eds.) *Rhizosphere Biology: Interactions Between Microbes and Plants.* Singapore: Springer, Singapore

Wang, F., Jiang, R., Kertesz, M. A., Zhang, F. & Feng, G. (2013). Arbuscular mycorrhizal fungal hyphae mediating acidification can promote phytate mineralization in the hyphosphere of maize (*Zea mays* L.). *Soil Biology and Biochemistry,* 65**,** pp. 69-74.

Wang, F., Zhang, L., Zhou, J., Rengel, Z., George, T. S. & Feng, G. (2022). Exploring the secrets of hyphosphere of arbuscular mycorrhizal fungi: processes and ecological functions. *Plant and Soil,* 481(1)**,** pp. 1-22.

Wang, P., Bi, S., Wang, S. & Ding, Q. (2006). Variation of wheat root exudates under aluminum stress. *Journal of Agricultural and Food Chemistry,* 54(26)**,** pp. 10040-10046.

Wang, Q., Garrity, G. M., Tiedje, J. M. & Cole, J. R. (2007). Naive Bayesian classifier for rapid assignment of rRNA sequences into the new bacterial taxonomy. *Appl Environ Microbiol,* 73(16)**,** pp. 5261-5267.

Wang, Y.-N. & Wang, R. (2019). Chapter 1 - Reverse osmosis membrane separation technology. *In:* Ismail, A. F., Rahman, M. A., Othman, M. H. D. & Matsuura, T. (eds.) *Membrane Separation Principles and Applications*. Elsevier.

Wang, Z., Lu, K., Liu, X., Zhu, Y. & Liu, C. (2023). Comparative functional genome analysis reveals the habitat adaptation and biocontrol characteristics of plant growth-promoting bacteria in NCBI databases. *Microbiology Spectrum,* 11(3)**,** pp. e05007-05022.

Warcup, J. H. (1951). The ecology of soil fungi. *Transactions of the British Mycological Society,* 34(3)**,** pp. 376-399.

Waseem, R., Zhong , W., Alexandre , J., Qirong , S. & Ville-Petri , F. (2021). Extended plant metarhizobiome: understanding volatile organic compound signaling in plant-microbe metapopulation networks. *mSystems,* 6(4)**,** pp. 10.1128/msystems.00849-00821.

Watson, S. B. & Jüttner, F. (2023). Isopropylthiol emission by bloom-forming Microcystis: Biochemistry, ecophysiology and semiochemistry of a volatile organosulfur compound. *Harmful Algae,* 130**,** pp. 102527.

Wei, W., Ma, M., Jiang, X., Meng, F., Cao, F., Chen, H., Guan, D., Li, L. & Li, J. (2024). Soil P-stimulating bacterial communities: response and effect assessment of long-term fertilizer and rhizobium inoculant application. *Environmental Microbiome,* 19**,** pp. 86.

Weidner, S., Koller, R., Latz, E., Kowalchuk, G., Bonkowski, M., Scheu, S. & Jousset, A. (2015). Bacterial diversity amplifies nutrient-based plant–soil feedbacks. *Functional Ecology,* 29(10)**,** pp. 1341-1349.

Weisskopf, L., Schulz, S. & Garbeva, P. (2021). Microbial volatile organic compounds in intra-kingdom and inter-kingdom interactions. *Nature Reviews Microbiology,* 19(6)**,** pp. 391-404.

Welc, M., Ravnskov, S., Kieliszewska-Rokicka, B. & Larsen, J. (2010). Suppression of other soil microorganisms by mycelium of arbuscular mycorrhizal fungi in root-free soil. *Soil Biology and Biochemistry,* 42(9)**,** pp. 1534-1540.

Weller, D. M. & Thomashow, L. S. (1994). Current challenges in introducing beneficial microorganisms into the rhizosphere. *In:* O'Gara, F., Dowling, D. N. & Boesten, B. (eds.)

Molecular Ecology of Rhizosphere Microorganisms. Weinheim: VCH Verlagsgesellschaft.

Werdin-Pfisterer, N. R., Kielland, K. & Boone, R. D. (2012). Buried organic horizons represent amino acid reservoirs in boreal forest soils. *Soil Biology and Biochemistry,* 55**,** pp. 122-131.

Wewer, V., Brands, M. & Dörmann, P. (2014). Fatty acid synthesis and lipid metabolism in the obligate biotrophic fungus *Rhizophagus irregularis* during mycorrhization of *Lotus japonicus*. *The Plant Journal,* 79**,** pp. 398-412.

Whipps, J. & Lynch, J. (1985). Energy losses by the plant in rhizodeposition. *Annual Proceedings of the Phytochemical Society of Europe,* 26**,** pp. 59-71.

Whipps, J. M. (2001). Microbial interactions and biocontrol in the rhizosphere. *Journal of Experimental Botany,* 52(suppl_1)**,** pp. 487-511.

White, P. J. & Broadley, M. R. (2003). Calcium in plants. *Annals of botany,* 92(4)**,** pp. 487-511.

Whitelaw, M. A., Harden, T. J. & Helyar, K. R. (1999). Phosphate solubilisation in solution culture by the soil fungus *Penicillium radicum*. *Soil Biology and Biochemistry,* 31(5)**,** pp. 655-665.

Widdel, F. & Pfennig, N. (1981). Studies on dissimilatory sulfate-reducing bacteria that decompose fatty acids. I. Isolation of new sulfate-reducing bacteria enriched with acetate from saline environments. Description of Desulfobacter postgatei gen. nov., sp. nov. *Arch Microbiol,* 129(5)**,** pp. 395-400.

Wilkes, T. I., Warner, D. J., Edmonds-Brown, V., Davies, K. G. & Denholm, I. (2020). A comparison of methodologies for the staining and quantification of intracellular components of arbuscular mycorrhizal fungi in the root cortex of two varieties of winter wheat. *Access Microbiology,* 2(2)**,** pp. 1-6.

Williams, A., Langridge, H., Straathof, A. L., Fox, G., Muhammadali, H., Hollywood, K. A., Xu, Y., Goodacre, R. & de Vries, F. T. (2021). Comparing root exudate collection techniques: An improved hybrid method. *Soil Biology and Biochemistry,* 161**,** pp. 108391.

Wu, Y.-W., Simmons, B. A. & Singer, S. W. (2015). MaxBin 2.0: an automated binning algorithm to recover genomes from multiple metagenomic datasets. *Bioinformatics,* 32(4)**,** pp. 605-607.

Yahya, M., Islam, E. u., Rasul, M., Farooq, I., Mahreen, N., Tawab, A., Irfan, M., Rajput, L., Amin, I. & Yasmin, S. (2021). Differential root exudation and architecture for improved growth of wheat mediated by phosphate solubilizing bacteria. *Frontiers in Microbiology,* 12 pp. 744094.

Yang, R., Liu, G., Chen, T., Li, S., An, L., Zhang, G., Li, G., Chang, S., Zhang, W., Chen, X., Wu, X. & Zhang, B. (2019). Characterization of the genome of a Nocardia strain isolated from soils in the Qinghai-Tibetan Plateau that specifically degrades crude oil and of this biodegradation. *Genomics,* 111(3)**,** pp. 356-366.

Yang, S., White, B., Regan, F., Kent, N., Hall, R. L. & Daly, K. (2024). Integrating soil phosphorus sorption capacity with agronomic indices to improve sustainable P use in agriculture. *Journal of Soils and Sediments***,** pp. 1-11.

Yi, Y., Huang, W. & Ge, Y. (2008). Exopolysaccharide: a novel important factor in the microbial dissolution of tricalcium phosphate. *World Journal of Microbiology and Biotechnology,* 24(7)**,** pp. 1059-1065.

Young, M., Artsatbanov, V., Beller, H. R., Chandra, G., Chater, K. F., Dover, L. G., Goh, E.-B., Kahan, T., Kaprelyants, A. S., Kyrpides, N., Lapidus, A., Lowry, S. R., Lykidis, A., Mahillon, J., Markowitz, V., Mavromatis, K., Mukamolova, G. V., Oren, A., Rokem, J. S., Smith, M. C. M., Young, D. I. & Greenblatt, C. L. (2010). Genome sequence of the fleming strain of *Micrococcus luteus*, a simple free-living Actinobacterium. *Journal of Bacteriology,* 192(3)**,** pp. 841-860.

Yruela, I. (2005). Copper in plants. *Brazilian Journal of Plant Physiology,* 17(1)**,** pp. 145-156.

Yu, C., Lv, J. & Xu, H. (2024). Plant growth-promoting fungi and rhizobacteria control *Fusarium* damping-off in Mason pine seedlings by impacting rhizosphere microbes and altering plant physiological pathways. *Plant and Soil,* 499(1)**,** pp. 503-519.

Yu, Y., Gui, Y., Li, Z., Jiang, C., Guo, J. & Niu, D. (2022). Induced systemic resistance for improving plant immunity by beneficial microbes. *Plants,* 11(3)**,** pp. 386.

Yu, Z., Liang, K., Huang, G., Wang, X., Lin, M., Chen, Y. & Zhou, Z. (2021). Soil bacterial community shifts are driven by soil nutrient availability along a teak plantation chronosequence in tropical forests in china. *Biology,* 10(12)**,** pp. 1329.

Zaheer, A., Mirza, B. S., McLean, J. E., Yasmin, S., Shah, T. M., Malik, K. A. & Mirza, M. S. (2016). Association of plant growth-promoting *Serratia* spp. with the root nodules of chickpea. *Research in Microbiology,* 167(6)**,** pp. 510-520.

Zahran, H. H. (2001). Rhizobia from wild legumes: diversity, taxonomy, ecology, nitrogen fixation and biotechnology. *Journal of Biotechnology,* 91(2)**,** pp. 143-153.

Zhang, K., Zheng, D., Gu, Y., Xu, J., Wang, M., Mu, B., Wen, S., Tang, T., Rengel, Z. & Shen, J. (2024a). Utilizing soil organic phosphorus for sustainable crop production: insights into the rhizosphere. *Plant and Soil,* 498(1)**,** pp. 57-75.

Zhang, L., Fan, J., Ding, X., He, X., Zhang, F. & Feng, G. (2014). Hyphosphere interactions between an arbuscular mycorrhizal fungus and a phosphate solubilizing bacterium promote phytate mineralization in soil. *Soil Biology and Biochemistry,* 74**,** pp. 177-183.

Zhang, L., Feng, G. & Declerck, S. (2018). Signal beyond nutrient, fructose, exuded by an arbuscular mycorrhizal fungus triggers phytate mineralization by a phosphate solubilizing bacterium. *The ISME Journal,* 12(10)**,** pp. 2339-2351.

Zhang, L., Song, X., Shao, X., Wu, Y., Zhang, X., Wang, S., Pan, J., Hu, S. & Li, Z. (2019). Lead immobilization assisted by fungal decomposition of organophosphate under various pH values. *Scientific Reports,* 9(1)**,** pp. 13353.

Zhang, W.-P., Surigaoge, S., Yang, H., Yu, R.-P., Wu, J.-P., Xing, Y., Chen, Y. & Li, L. (2024b). Diversified cropping systems with complementary root growth strategies improve crop adaptation to and remediation of hostile soils. *Plant and Soil***,** pp. 1-24.

Zhang, X., Huang, Z., Zhong, Z., Li, Q., Bian, F. & Yang, C. (2022). Metagenomic insights into the characteristics of soil microbial communities in the decomposing biomass of Moso bamboo forests under different management practices. *Frontiers in Microbiology,* 13**,** pp. 1-11.

Zhao, M., Zhao, J., Yuan, J., Hale, L., Wen, T., Huang, Q., Vivanco, J. M., Zhou, J., Kowalchuk, G. A. & Shen, Q. (2021a). Root exudates drive soil-microbe-nutrient feedbacks in response to plant growth. *Plant, Cell & Environment,* 44(2)**,** pp. 613-628.

Zhao, X., Lyu, Y., Jin, K., Lambers, H. & Shen, J. (2021b). Leaf phosphorus concentration regulates the development of cluster roots and exudation of carboxylates in *Macadamia integrifolia*. *Frontiers in Plant Science,* 11**,** pp. 610591.

Zhou, X., Zhang, J., Shi, J., Khashi u Rahman, M., Liu, H., Wei, Z., Wu, F. & Dini-Andreote, F. (2024). Volatile-mediated interspecific plant interaction promotes root colonization by beneficial bacteria via induced shifts in root exudation. *Microbiome,* 12**,** pp. 207.

Zhou, Y., Neuhäuser, B., Neumann, G. & Ludewig, U. (2020). LaALMT1 mediates malate release from phosphorus-deficient white lupin root tips and metal root to shoot translocation. *Plant, Cell & Environment,* 43(7)**,** pp. 1691-1706.